The Effect of Cracks on Unsaturated Flow and Volume Change Properties of Expansive Clays and Impacts on Foundation Performance

by

Mohammad Abbaszadeh

A Dissertation Presented in Partial Fulfillment
of the Requirements for the Degree
Doctor of Philosophy

Approved October 2011 by the
Graduate Supervisory Committee:

Sandra Houston, Co-Chair
Claudia Zapata, Co-Chair
Bruno Welfert
William Houston

ARIZONA STATE UNIVERSITY

December 2011

ABSTRACT

The primary objective of this study is to understand the effect of soil cracking on foundation performance for expansive soil profiles. Two major effects of cracks were studied to assess the effect of cracks on foundation performance. First, the effect of cracks on soil volume change response was studied. Second, the effect of cracks on unsaturated flow properties and extent and degree of wetting were evaluated. Multiple oedometer-type pressure plate tests were conducted to evaluate the effect of cracks on soil properties commonly used in volume change (heave) analyses, such as swell pressure, soil water characteristic curve (SWCC), and swell potential. Additionally, the effect of cracks on saturated and unsaturated hydraulic conductivity was studied experimentally to assess the impact of cracks on properties critical to evaluation of extent and degree of wetting. Laboratory experiments were performed on both intact and cracked specimen so that the effect of cracks on behavior could be benchmarked against intact soil response. Based on laboratory observations, the SWCC of a cracked soil is bimodal. However, this bimodal behavior is only observed in the very low suction ranges. Because the bimodal nature of the SWCC of cracked clays is only distinguishable at extremely low suctions, the bimodal behavior is unlikely to have engineering significance when soils remain unsaturated.

A “lumped mass” parameter approach has been studied as a practical approach for modeling of cracked soils for both fluid flow and volume change determination. Laboratory unsaturated flow experiments were simulated using a

saturated-unsaturated flow finite element code, SVFlux, to back-analyze unsaturated hydraulic conductivity functions for the subject soils. These back-analyzed results were compared to the results from traditionally-applied analyses of the laboratory instantaneous profile tests on intact and cracked specimens. Based on this comparison, empirical adjustments were suggested for modeling "lumped mass" cracked soil behavior in numerical codes for fluid flow through cracked soils. Using the empirically adjusted flow parameters for unsaturated flow modeling, example analyses were performed for slab-on-grade problems to demonstrate the impact of cracks on degree and extent of wetting under unsaturated and saturated flow conditions for different surface flux boundary conditions.

DEDICATION

This doctoral dissertation is dedicated to my wonderful family, particularly my lovely wife, Elham, for her purest love, patience, and support. Also to my dear parents, Reza and Fershteh Abbaszadeh, who have always encouraged and supported my dreams of pursuing higher education.

ACKNOWLEDGMENTS

My sincerest gratitude goes to my advisers Dr. Sandra Houston and Dr. Claudia Zapata. I will be indebted forever to Dr. Zapata for encouraging me, believing in me, and leading me through the greatest research opportunities at Arizona State University. I am also very much grateful to Dr. Sandra Houston for her exceptional inspiration, insightful ideas, and all the valuable time she spent with me to make this a better project. It would have been impossible to complete this research work without the guidance of both my advisers.

I would also like to sincerely acknowledge Dr. Welfert for his patience in explaining the numerical concepts and his valuable inputs throughout the numerical analyses and modeling part of this work. Additionally, I am very grateful to Dr. Bill Houston for all his help at different stages of my research, from the laboratory experimental setups to theoretical and conceptual discussions. Last but not least, I would like to thank Mr. Peter Goguen, our laboratory manager, for teaching me many laboratory skills and also for his priceless effort to make the equipments available when we needed them.

This study was supported by the National Science Foundation (NSF) under grant number CMMI-0825089. The opinions, conclusions, and interpretations expressed in this dissertation are those of the authors, and not necessarily of NSF.

TABLE OF CONTENTS

Page

CHAPTER Page

CHAPTER Page

CHAPTER Page

CHAPTER Page

CHAPTER Page

APPENDIX Page

LIST OF TABLES

Table Page

Table Page

LIST OF FIGURES

Figure Page

Figure Page

Figure Page

Figure Page

Figure Page

Figure Page

Figure Page

Figure Page

Figure Page

Chapter 1

INTRODUCTION

The importance of soil-crack formation and its effect on the soil-water regime was recognized early in the fifties (Stirk (1954)). Soil cracking is a complex process that influences soil properties, plant growth, and the migration of water and solutes in soil (Bandyopadbyay et al. (2003); Xiong et al. (2006)). Generally, non-homogeneous characteristics of soils have made them one of the most unpredictable materials to work with, and the existence of cracks further complicates the situation.

One of the major damages from soil cracks is landslides. A number of landslides in unsaturated soils were triggered by rainfall infiltration during wet seasons (Zhan et al. (2006)). Zhan et al. believe that the field performance of an expansive soil slope may be significantly different from that of a residual soil. An expansive soil with active clay minerals exhibits significant swelling/shrinkage upon wetting/drying, and has an abundance of cracks and fissures in the field. The rainfall infiltration into such a crack-rich expansive soil is a complex hydrological process (Flury et al. (1994)).

In addition to slope stability problems, cracks can also affect the performance of foundations. Initially, it might sound reasonable to assume that cracks create worse performance; however, cracks can be beneficial to foundation performance as associated to their potential to eliminate or decrease heave during wet seasons by crack healing. The process of crack healing may reduce the amount of actual heave by absorbing some of the volume change potential.

Although a significant amount of research has been conducted during the last two decades on the topic of cracked soils, there are limited studies to evaluate the effect of cracks for engineering applications such as their effect on foundations or slope stability. In this dissertation, the effect of cracks on performance of foundations on expansive soils was emphasized. The effect of cracking was studied by conducting numerous laboratory experiments and these results were compared against the non-cracked (intact) identical experiments to evaluate how the existence of cracks would change the soil behavior. There are two aspects of cracks which affect foundation performance the most. First, the volume change behavior of cracked soil can have a significant effect on the performance of the foundations, either positively or negatively. Second, the water infiltration through the cracks, or in some cases the "capillary break" effect of cracks, can affect the foundation performance significantly, again, either positively or negatively. To study these aspects, an extensive laboratory study was conducted. Additionally, two sample problems were simulated in SVFlux using laboratory-determined cracked clay properties to evaluate the impact of cracking on foundation performance. Finally recommendations were made for modifications to existing heave models to better account for the presence of cracks in estimating movements of foundations for expansive soil profiles.

1.1. Significance of the study in engineering problems

In geotechnical engineering, there are many cases in which cracks play an important role. For instance, cracking due to shrinkage affects the stability of embankments and earth dams (Lau (1987)). Cracks may also evolve into piping

leaks, leading to dam failures as in the cases of the Stockton and Wister dams (Sherard (1973)). Similarly, facilities that are constructed using fine-grained soils such as waste containment facilities and mine tailings dams can be affected by hydraulic changes resulting from cracking (Yesiller et al. (2000)). In addition, the presence of tension cracks can affect slope stability computation and analysis in a number of ways (Spencer, (1968); Baker (1981); Bagge (1985); Silvestri et al. (1992)). For example, cracks may reduce the length of a potential slip surface over which the shear strength can be mobilized, or when they are filled with water it can exert an additional driving force which may result in slope failure. Furthermore, the existence of cracks can decrease the shear strength of clays along the direction of cracks (Stapledon (1970)). Throne (1984) mentioned that the available shear strength of a cracked soil depends on the relationship between the orientation of cracks and the orientation of the major principal stress direction. In addition, desiccation cracking of clay barriers is an important issue in landfill design, construction and long-term integrity of containment systems (Philip et al. (2002); Corser and Cranston (1991); Hewitt and Philip (1999); Melchoir (1997); Savadis and Mallwitz (1997); Miller et al. (1998); Tay et al. (2001)). For instance, Albrecht and Benson (2001) reported that cracks in clay liner material can increase the hydraulic conductivity of the liner up to 500 times than that of the intact material. From another perspective, Zein El Abedine and Robinson (1971) reported some of the effects of soil cracking such as the formation of gilgai micro-relief, slickensides, a churning or mixing of the upper part of the soil profile; and in some instances, the increase of the amount and depth of water penetration.

Silvestri et al. (1992) reported that crack presence can negatively impact the bearing capacity of foundations.

As mentioned earlier, the significance of cracks is different from one discipline to another. For example, in Agricultural engineering, crop growth and production heavily depends on the irrigation and water movement through the soil. . Because cracks can control the velocity and rate of water, and solutes and micro-organisms transport, cracks may have a significant impact on agricultural production (Bronswijk et al. (1995); Kelly and Poems (1998)). For instance, Rayhani et al. (2007) found that cracking increased the hydraulic conductivity by 12 to 34 times, depending on the plasticity of the soils. Same observation was reported by other researchers (Yuen et al. (1998); Ritchie et al. (1972)).

Cracks can substantially increase the retention volume of soils and infiltration intensity to prevent surface outflow (Novak (1999)). Therefore, under certain circumstances cracks may transfer water and solutes quickly through the unsaturated zone to the groundwater, which can affect the groundwater quality (Bouma (1981); Beven and German (1982); Jarvis et al. (1991)). Although cracking has received considerable amount of attention in the literature during the past two decades, the treatment is largely behavioral and qualitative (Morris et al. (1992); Kodikara et al. (2000)).

1.2. Research objectives and scope

The major objective of this research study is to evaluate the effect of cracks on performance of foundations on expansive clays. Two key aspects must be assessed to determine the effect of cracking on foundation performance: (1)

effect of cracks on volume change (heave), and (2) effect of cracks on fluid flow (extent and depth of wetting). Once these behaviors are better understood from a fundamental perspective, practical methods for inclusion of effects of cracking on the prediction of fluid flow and computation of heave associated with placement of foundations on expansive soils can be better explored.

The objectives of this dissertation are as following:

1. To study the effect of cracks on volume change (swell potential).
2. To study the effect of cracks on swell pressure.
3. To study the effect of cracks on unsaturated flow related properties: the soil-water characteristic curve and the unsaturated hydraulic conductivity.
4. To study the effect of cracks on unsaturated flow for purposes of evaluating the extent and degree of wetting.
5. To understand the effect of cracks on foundation performance.
6. Make recommendations for modeling cracked soils that are linked to more easily obtained flow/deformation properties of intact clay specimens (e.g. empirical adjustments to intact clay properties to account for cracking).
7. Make recommendations for modifications to existing heave models for inclusion of cracks in the prediction of heave.

1.3. Scope of the study

The scope of this study can be divided into laboratory experiments and numerical modeling.

1.3.1. Laboratory experiments

1.3.1.1. Laboratory SWCC tests

The Soil Water Characteristic Curve (SWCC) tests were performed in an oedometer-type pressure plate apparatus capable of controlling the matric suction and net normal stress, and measuring volume change during the test. The matric suction varied from 0.1 kPa to 1,420 kPa for the SWCC determination. For lower suction ranges, the hanging manometer technique was employed whereas for suctions greater than 5 kPa, the axis translation technique was used. To accelerate the equilibrium time, ceramic stones with different air-entry values (from 1 bar to 15 bars) were used. Both drying and wetting tests were performed to capture the differences associated with hysteresis. Cracked and intact samples were prepared by compaction to reduce specimen variability. The soil was compacted at 18% water content (slightly above the optimum) and 98% of maximum standard Proctor dry density. Cracks were manually introduced into the compacted specimens using shims to achieve crack patterns and volumes consistent with field observed cracks.

1.3.1.2. Saturated hydraulic conductivity tests

A conventional triaxial machine was used to conduct series of saturated conductivity tests in order to assess the effect of cracking on the saturated conductivity of the soil. The triaxial device allows controlling the cell pressure as well as the top and bottom pore water pressures of the sample. Specimens were compacted similar to the SWCC samples except that instead of using a brass ring, a cylindrical split mold was used for their preparation. The advantage of a

cylindrical mold is that after sample preparation process is completed, the sample can be removed by splitting the mold. The back pressure technique was applied gradually to saturate the sample. After the sample reached a degree of saturation greater than 90%, a pressure gradient of 30 kPa was applied to the specimen to induce flow through the soil specimen. As the water started to flow from the top of the sample to the bottom, the flow rate was recorded using a Volume Change Device (VCD). The saturated hydraulic conductivity was then calculated using Darcy's law. Alternatively, as an indirect hydraulic conductivity measurement technique, a set of conventional consolidation tests were performed for cracked and intact specimens to estimate the saturated hydraulic conductivity (k_{sat}) by measuring the coefficient of consolidation, c_v, and then adjusting the conductivity for lower stresses assuming that k_{sat} is proportional to $e^3/(e+1)$ when e is the void ratio of the soil at corresponding stresses.

1.3.1.3. Unsaturated hydraulic conductivity tests

As one of the most challenging laboratory experiments, unsaturated hydraulic conductivity of cracked soil were measured and compared with that of the intact soil. Typically, conducting a laboratory experiment for determination of unsaturated hydraulic conductivity of an expansive soil can be heavily time consuming as a result of the slow and sophisticated movement of water through the unsaturated zone. It is believed that at high suction ranges, the water flow occurs by vapor transport rather than by free-water movement through the soil. This is believed to be a primary factor that explains why the water movement occurs at such low rates in very dry situations. To overcome this issue, several

procedures and test designs were developed and executed, in an iterative process, in order to optimize the testing period without sacrificing the accuracy of the results. These experiments were primarily based on proper manipulation of the column test and instantaneous profile concept. All the tests were performed in a temperature-controlled environment.

1.3.1.4. Swell pressure tests

Swell pressure tests were performed using a computer-controlled consolidometer device. Axial deformations can be controlled and recorded by a Linear Variable Differential Transformer (LVDT) attached to the loading piston. Both, constant volume swell pressure and "free" swell pressure tests subjected to field overburden pressures, were conducted to determine the best estimate of swell pressure for cracked and intact specimens.

1.3.2. Numerical modeling

Based on laboratory results obtained from water retention curves, saturated and unsaturated conductivities, and swell pressure, the unsaturated hydraulic conductivity functions were evaluated through back-analysis of laboratory conductivity tests using the commercial finite element code SVFlux. The lumped parameter approach was used to model the cracked soil behavior using the SWCC and K_{unsat} function of cracked soils obtained from the laboratory investigations of this study. Two field condition cases of foundations placed on expansive soils (cracked and intact) were modeled to illustrate the effect of soil cracking on the extent and degree of wetting and the resulting foundation heave.

1.4. Layout of the dissertation

The organization of the research is outlined briefly below:

CHAPTER 1 (INTRODUCTION): This chapter outlines the framework of the work and briefly describes the objectives of this research.

CHAPTER 2 (BACKGROUND AND THE IMPORTANCE OF THE RESEARCH): This chapter starts with the review of the existing related research and emphasizes the importance of/need for the current research. This chapter is divided into three main parts. The first part presents a summary of the literature research on crack formation processes and modeling of the crack development process, including but not limited to: crack pattern, orientation and dimension, and volume change and crack formation modeling approaches. In the second part, existing laboratory techniques to measure hydraulic conductivity of saturated and unsaturated soils are reviewed. Finally, the last part presents the review of the retention and conductivity functions of fractured material with focus on soils.

CHAPTER 3 (EFFECT OF CRACKS ON VOLUME CHANGE AND SWELL PRESSURE): This chapter includes all the laboratory experiments conducted to evaluate the effect of cracks on volume change. Results and data interpretation are included.

CHAPTER 4 (EFFECT OF CRACKS ON UNSATURATED FLOW PROPERTIES): In this chapter, the experiments designed to evaluate the effect of crack on hydraulic conductivity (a function of soil suction) and SWCC are presented. The unsaturated hydraulic conductivity function will also be evaluated

through back-analysis of instantaneous profile laboratory hydraulic conductivity tests using the finite element code SVFlux.

CHAPTER 5 (NUMERICAL MODELING OF UNSATURATED FLOW AND IMPACT OF CRACKS ON EXTENT AND DEGREE OF WETTING FOR FIELD CONDITIONS): This chapter introduces the unsaturated flow modeling performed using the SVFlux software which solves the governing partial differential equations for fluid and vapor flow through saturated/unsaturated soils. Emphasis will be on modeling cracked soils using a lumped parameter approach and using soil properties of cracked soils obtained from the laboratory investigations of this study. The cracked soil properties required for the unsaturated flow modeling include SWCC and the K_{unsat} function. The intent of these numerical simulations is to model two field conditions of foundations placed on expansive soils (cracked and intact) and to show the effect of soil cracking on the extent and degree of wetting and the resulting foundation heave.

CHAPTER 6 (SUMMARY AND RESULTS): This chapter summarizes the findings of the present work. Recommendations for future work are also included in this chapter.

Chapter 2

BACKGROUND AND THE IMPORTANCE OF THE RESEARCH

2.1. Introduction

Cracked soils tend to be highly heterogeneous, which makes every crack study somewhat unique. In particular, soil cracks can vary in size, geometry, and behavior. Their formation process and sources of crack initiation may differ from site to site, resulting in no single "morphology" for cracked soil profiles. However, cracked clays (e.g. cracked from desiccation) are often associated with the vadose zone (unsaturated zone).

Since 1925 when Terzaghi presented his effective stress theory for saturated soils, it has been widely used in engineering designs. However, in the real world, there are only few cases where the soils are completely saturated. In practice, assuming saturated conditions will often lead to a highly conservative and somewhat more expensive design. Hence, it is quite reasonable to search for a better/more economical solution to the geotechnical problems that will eventually benefit the entire construction industry. Fortunately, during the last few decades, the importance of unsaturated soil mechanics has been understood, and more scientists are encouraged to conduct research in this field. The rapid growth of sustainability concept during the last few years has also forced civil engineers, from all disciplines, to look for more sustainable solutions for their specialty problems. Particularly in geotechnical engineering, to transit to the next level of engineering solutions to our problems, it is about the time to start applying the unsaturated soil mechanic principals into the practice.

Moving from saturated to unsaturated soil mechanics, many principals and theories change such as: stress state variables and formulations, volume change theories, and transport of flow. As now, we are probably in a "transition era" from saturated to unsaturated soil mechanics. Before being able to move to the next era which will be the "unsaturated soil mechanics era", every aspect of the unsaturated soil mechanics should be well studied and developed. There are some aspects which have developed well during the past decades, including volume change, water retention characteristics, stress state principals, etc. However, there are still some other aspects of unsaturated soils which need more attention. One such case relates to the effect of crack formation on soil response; the subject of cracked soils has not been thoroughly studied although it can be substantially important to foundation performance. Cracks can significantly increase the surface flux when positive pore water pressures exist, and this can create problems with moisture sensitive soils such as expansive and collapsible soils. Cracks can also affect total and differential settlements, which is an important factor in foundation designs. Clearly, not all aspects of cracks and the crack effects can be studied in this research, but this study can serve to illustrate important soil responses of cracked clays that have a direct impact on foundations and structures.

In this chapter, the existing studies are summarized in three parts. First, crack formation process and geometry is presented and followed by the crack modeling approaches and methods. The second part reviews the volume change

effects of soil cracking and the last part presents a review of the existing methods and models to predict flows in cracked soil.

2.2. Crack morphology and modeling

2.2.1. Crack classification

Crack study is an interdisciplinary area, so there is no single classification which reflects all different opinions and investigations precisely. For instance, cracks in soils can be classified into different types based on the formation process, induced origin, sizes, etc. Certainly, however, one of the most commonly used methods to classify different types of soil cracking is to directly refer to the sources which caused to cracks to form such as: desiccation and shrinkage, freezing and thawing, synaeresis, differential settlement, and penetration by plant roots (Johnston and Hill (1944); Johnson (1962); Fox (1964); Yesiller et al. (2000); Yoshida and Adachi (2004); LI Jinhui (2009)).

Chertkov (2002) conducted a study to model cracking stages, and he classifies growing cracks into two categories. The first includes fairly isolated cracks with negligible influence from other cracks. However, cracks of the second type develop by interacting strongly with other neighbor cracks. According to Chertkov, most cracks of the first type eventually develop into the second type.

Some researchers defined pores (cracks) in swelling soils as one of the following three types (Fox (1964); Dolezal and Kutilek (1972)):

1) Micropores inside the soil structure
2) Macropores formed by fauna and plant roots
3) Cracks caused during the evapotranspiration drying of the soils surface

2.2.1.1. Desiccation/Shrinkage cracks

Desiccation cracks are the cracks occurring due to the loss of water in clayey soils. Hu et al. (2006) defined desiccation cracking as the consequence of an excess of tensile stresses induced by shrinkage of the drying body with a constrained kinematics.

In geotechnical engineering field, desiccation cracking is indeed the most common type of cracks. Numerous studies have been conducted to explore different aspects of soil's desiccation cracking, and in a broad classification most of these studies are fall into three major categories; namely, cracking evolution and patterns (e.g. Nahlawi and Kodikara (2006); Tang et al. (2010)), numerical analysis and modeling of cracks, and hydraulic characteristics of cracks (Boynton and Daniel (1985); De Dreuzy et al. (2001); Chertkov and Ravina (2001, 2002); Rayhani et al. (2007)). Clearly, there is currently a lack of information about how the desiccation cracking may interface with different elements of a structure, and particularly with foundations. However, some notable contributions have been made by several researchers (Corete and Higashi (1960); Lau (1987)).

Shrinkage cracking, on the other hand, forms within muddy sediments in response to tensions produced as a result of volumetric changes (decrease) within the sediments, according to Plummer and Gostin (1981).

2.2.1.2. Freezing and thawing cracks

The cracks formed as a result of number of seasonal freezing and thawing cycles are called freezing and thawing cracks. When the water-phase inside the

soil freezes during the cold seasons, tension is built up inside the soil matrix which causes these types of cracks, which are typically wedge-shaped.

2.2.1.3. Synaeresis cracks

Synaeresis cracks are very similar to desiccation cracks. Plummer and Gostin (1981) reviewed shrinkage cracks and compared desiccation versus synaresis cracks. The authors mentioned that there are many different factors influencing the crack morphology such as sediment composition, bed thickness, and bed surface configuration. Additionally, the rate of initial drying, total exposure time, depth of the groundwater table, and direction of surface drainage are other factors controlling shrinkage cracks. Authors pointed out that as a result of the high level of complexity of these factors interplay, it is hard to differentiate between desiccation and synaeresis cracks origin.

2.2.1.4. Differential settlement cracks

An uneven vertical deformation of soil may result in building some tension inside the soil which can lead to the creation of this type of cracks. These cracks typically occur in regions with moisture sensitive soils such as expansive or collapsible soils in which differential settlement/heave may occur.

2.2.1.5. Penetration by plant roots

2.2.2. Crack creation process

Different types of cracks may form differently based on the initial forces originating the cracks. Hence, there are different explanations of crack formation in the literature. Raats (1984) mentioned that cracks originate in soil when the strain energy imposed by shrinking and swelling or tillage is sufficient to break

interparticle bonds. Chertkov and Ravina (1998) postulated that cracking can initiate in wet ductile soils as a means to relieve the strain imposed by shrinking clays. Kodikara et al. (2000) explained that desiccating clay soils crack when the tensile stress developed in the soil due to the matric soil suction exceeds the tensile strength of the soil. Tensile stresses develop only when the soils is restrained in some way against shrinkage. The authors also mentioned that the restraints can be external (e.g. rough layer interface) or internal (e.g. sections for soils undergoing non-uniform drying). Hu et al. (2006) pointed out the same concept; that the constraints may result from the external boundary conditions, kinematic compatibility, moisture content gradients, and internal boundary conditions resulting from the multi-phase structure of soil.

Miller et al. (1998) carried out a laboratory experimental investigation to study the occurrence and extent of desiccation cracking on a scaled model of a landfill liner. Unlike the previous studies which had suggested insignificant desiccation cracking for low plasticity soils or for soils compacted dry of the optimum moisture content (e.g. Daniel (1991)), Miller et al. found a significant crack formation for the conducted laboratory experiments. The authors reported cracks with widths of 10mm in the first drying cycle, and crack penetration through the entire 16 cm thickness of the clay. Another interesting finding of this particular study was the fact that nearly 90 percent of the crack development occurred during the first 19 hours of the experiment, while the experiment total duration was 170 hours. Based on the laboratory results presented in the article, cracking commenced at suction 6 bar (~600 kPa). They also found that adding

more moisture to soil sample, after cracking process was completed, resulted in partial closing of the surface of the cracks.

Weinberger (1999) carried out a research on initiation and growth of desiccation cracks of muddy sediments. He postulated that the mud cracks nucleated at or near the bottom of the crack polygons and propagated vertically upward and laterally outward. It was mentioned that the reason for this behavior is the tendency of mud cracks to be initiated at flaws such as grain boundaries, and small dimples or holes are more likely located at depth due to the natural sorting of grains in mud.

Velde (2001) studied the surface cracking and aggregate formation using a 2-D image analyses. Cracks were formed using a single cycle of wetting and drying of a prepared soil in the field. Based on this study, surface cracks develop in a two-stage process. On the first stage, crack network extends while on the second stage the widths of the previously formed cracks start to increase. Figure 2.1 shows the evolvement process of a crack network.

Hallett and Newson (2005) used the elastic-plastic fracture mechanics to describe the crack formation process in soils. They used a deep-notch (modified four-point) bend test to crack the specimen. The device was equipped to measure the crack-tip opening angle (CTOA). CTOA can be used as a powerful tool to assess soil cracking because it can be induced by soil shrinkage. The soil samples were formed by consolidating soil slurry one-dimensionally with a 120-kPa vertical effective stress. The authors studied the effect of three factors on the cracking process: 1) the direction of the applied consolidation stress, 2) clay

content, and 3) pore water salinity using 0.5 mole of NaCl. According to the experimental results of this study, it was found that the direction of the applied consolidation stress did not affect the crack formation considerably. However, the soil clay content affected the soil cracking significantly indicating that less strain is required to induce a crack when the clay content is less. Same behavior was observed with salinity and when the salt was added to the sample, a crack could be induced easier and with less strain.

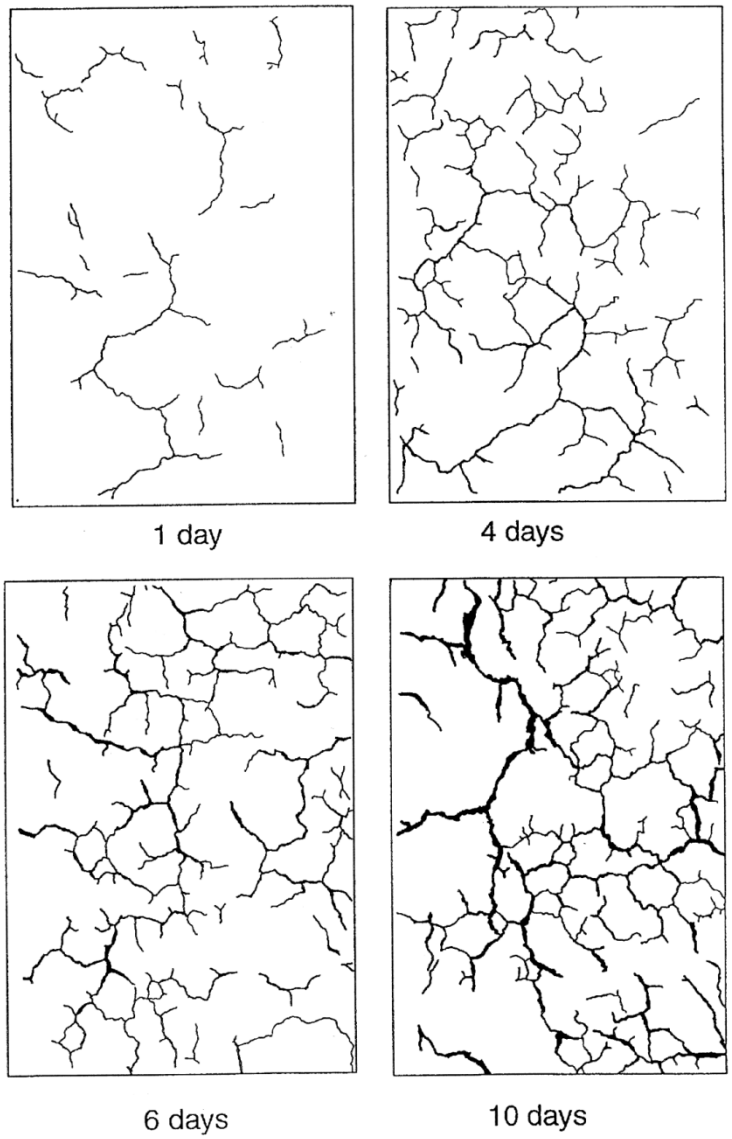

Figure 2.1. Surface crack formation process (from Velde (2001))

2.2.3. Crack geometry and pattern

In most studies related to soil cracking, the crack geometry is required prior to crack modeling or infiltration estimations. Nevertheless, crack geometry has been a mysterious phenomenon for scientists for a long time. Despite a considerable amount of research, crack pattern is not well understood yet. While most of the studies have been focused on laboratory created cracks, only few researchers have conducted field studies (Corte and Higasih (1960); Lau (1987); Morris et al. (1992); Kodikara et al. (2000)).

Lachenbruch (1962) mentioned that there are two possible crack systems that can be generated as a result of shrinkage, depending on the homogeneity and plasticity of the medium. For an inhomogeneous plastic media, an "orthogonal system" of cracking is expected. In this system, cracks intersect at 90º and form at loci of low strength. In homogeneous, relatively non-plastic media, "non-orthogonal systems" develops with cracks propagating laterally. Unlike the orthogonal system, all elements of non-orthogonal intersections are generated simultaneously.

Zein El Abedine and Robinson (1971) conducted a field study to measure the crack dimensions of some vetisols at Sudan. They used a V-shape plate to read the width of crack and employed some flexible graduated metal probes to measure the crack depth. The authors found that the widths of the cracks are affected by the duration of drying period, the soil type and the clay content. It was also proposed that the crack depths are inversely proportional to the irrigation sequences. The authors also measured the crack volumes and concluded that

irrigation reduces the volume of cracks to one-third or one-fourth of the original value.

Another field study was carried out by Dasog and Shashidhara (1993) which was similar, in methodology, with the previous work by Zein El Abedin and Robinson (1971). However, in this study, the crack dimensions were investigated in a vertisol soil from India under a different crop covers. Crack volume per unit area was used as an index to represent the cracking intensity because it reflects the three-dimensional properties of cracks rather than only one-dimensional. The authors used two methods to measure the crack volume. The first method involved measurements of the actual crack dimensions while in the second method, the cracks were filled with sand and with measuring the amount of sand that was poured into the cracks, the crack volume was calculated. The results suggested the same accuracy for both measurement methods were.

Elias et al. (2000) also conducted the field measurements similar to what Zein El Abedine and Robinson (1971) did. The same methodology was implemented to measure the crack depth, width and length as well as distances between the cracks at the end of the dry season. It was concluded that the intensity of cracking was increased by increasing the clay content. This is consisted with what Zein El Abedin and Robinson reported.

Scott et al. (1986) studied two main properties of the crack network; namely the density and orientation. The density of a crack pattern was assumed to be a function of the distances between the cracks. A statistical analysis was performed, based on some assumptions on the crack distances. The critical

assumption was that the cracks were planar. For measuring the density, the authors placed a probe through a finite volume of soil and measured the distances of neighboring cracks which were intersected by the probe. By ranking these distances, the cumulative distribution of the cracks were plotted. Figure 2.2 shows an example of the plots shown in this study.

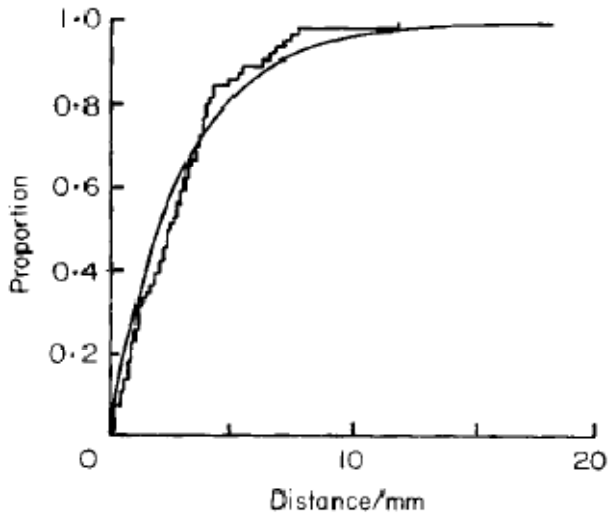

Figure 2.2. An example of cumulative distributions of inter-crack spacings (From Scott et al. (1986))

Preston et al. (1997) used the fractal geometry to quantify the complex geometry of the soil cracking patterns. To provide an adequate description of the soil cracks, mass fractal dimension, D_M (which provides a measure of crack heterogeneity) and the spectral dimension, d (which provides a measure of crack connectivity) were measured. The authors suggested that as the clay content increased, so did the D_M and d.

Weinberger (1999) studied the crack initiation and growth in muddy sediments and concluded that the dominant lateral components of cracks are more

likely generating the polygonal pattern. It was postulated that the intersection of the cracks at right angle forms T-junction, as depicted in figure 2.3.

Whilst discussing about cracks may usually be preceded by a primary assumption that cracks are vertical, it should be mentioned that horizontal cracks may also exist in some circumstances. Chertkov and Ravina (1999) explained the horizontal shrinkage cracks as: "Thin drying soil layers along walls of vertical crack (Fig. 2.4) tend to contract but the moister soil matrix prevents that. As a consequence, the thin drying layers are subject to tensile stresses that bring about the development of horizontal or almost horizontal cracks starting at the walls of vertical cracks. Additional evaporation from surfaces of horizontal cracks causes them to grow and broaden. The large number of vertical cracks, their statistically homogeneous distribution at the soil surface, and the distribution of their depths from zero to the maximum crack depth, z_m, imply that, on the average, distributions of volume and width of the developed horizontal cracks will be similar for any vertical profile."

Figure 2.3. Square shows a T-junction that formed in a muddy sediment in Israel. Geological hammer indicated by an arrow provides a scale (from Weinberger (1999)).

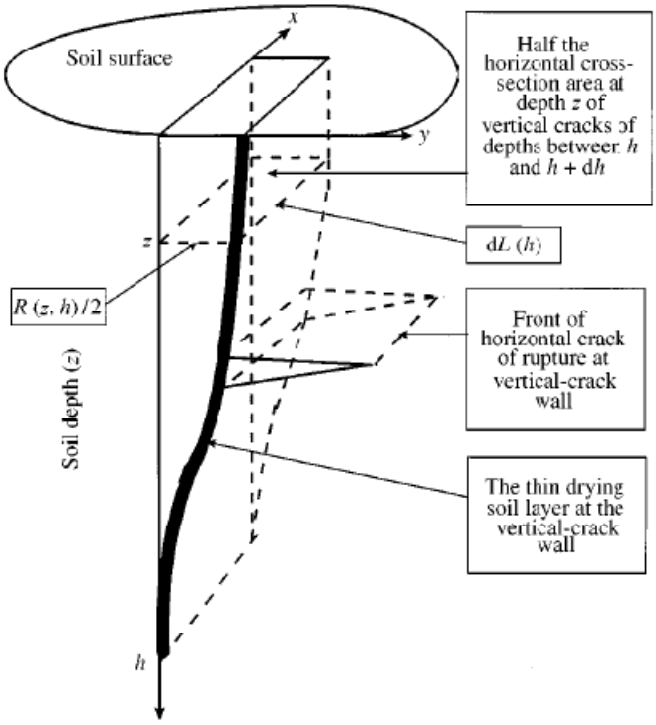

Figure 2.4. Three dimensional sketch showing vertical and horizontal cracks (from Chertkov and Ravina (1999))

Zhan et al. (2007) conducted a field study to measure the infiltration rates in an unsaturated slope. A 16m by 28m slope area from China was studied, and actual crack depths were reported. It was found that the upper soil layer with a thickness varying from 1.0 to 1.5 m was rich in cracks and fissures, particularly at the upper part of the overall slope. It was also noted that the maximum depth of the cracks was estimated to be approximately about 1.2 m while the maximum width was reported to be close to 10 cm. Figure 2.5 shows the dimensions of the cracks and fissures observed on the wall of a two-step excavation pit located near the monitoring area.

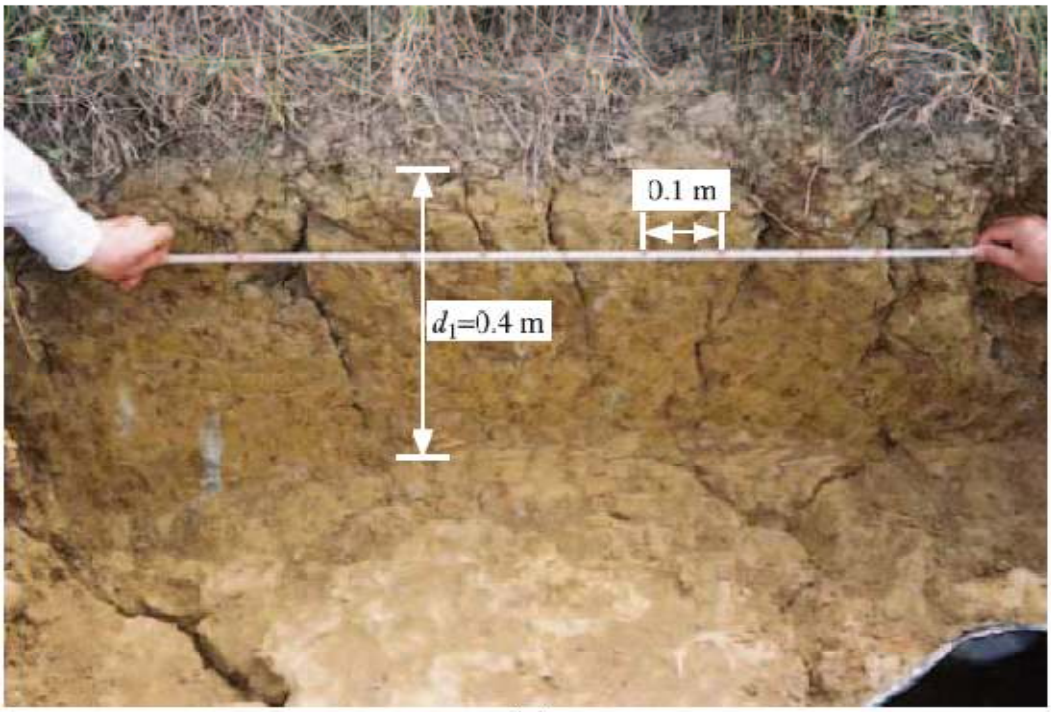

(*a*)

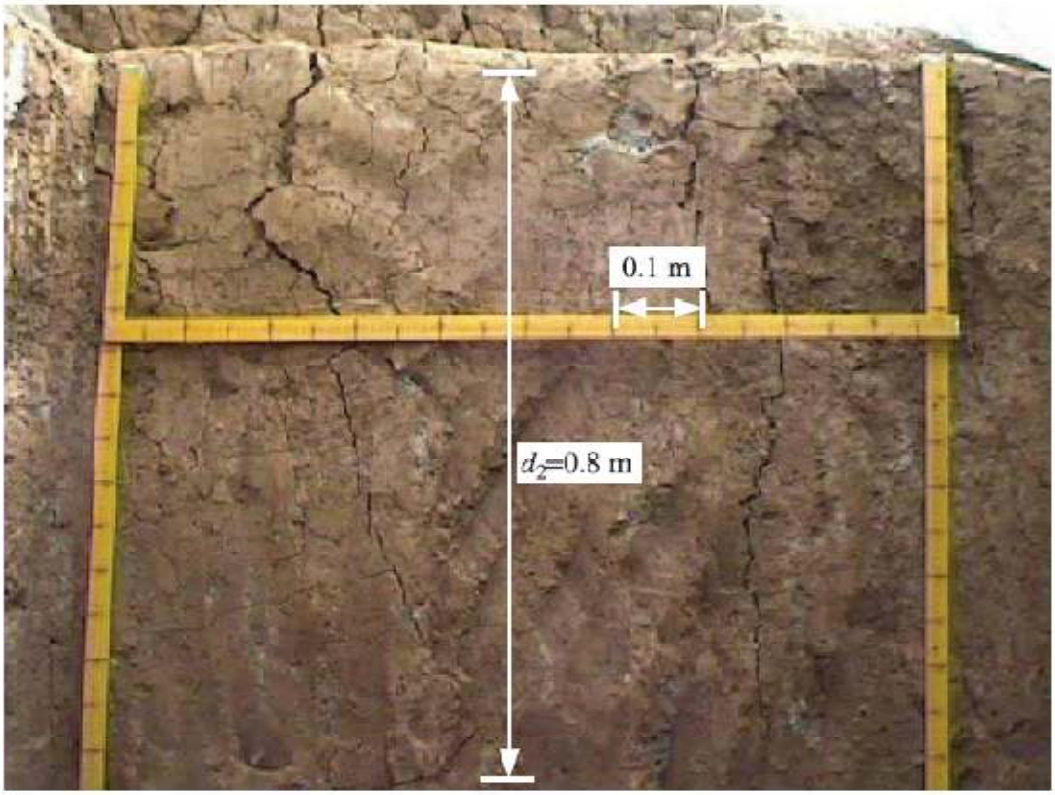

Figure 2.5. Cracks and fissures with the maximum depth of cracks ≈ d1 + d2 = 1.2 m (from Zhan et al. (2007).

Kishne et al. (2009) analyzed a 10-yr data set of Laewest clay to investigate the microtopography distribution of cracks, find a relationship between depth and width of the cracks, and study hysteresis and moisture effects on surface cracking. The authors concluded that crack development started dominantly and developed more extensively in microhighs. It was also found that, through different cycles of wetting and drying which led to different cycles of crack opening and healing, the crack openings were more or less occurred at the same location. However, the authors declared that the variations in the crack locations may happen as a result of temporal and spatial variability of rain pattern and water redistribution. A linear relationship between the crack width and depth was also proposed, with R^2=0.5, which is shown in figure 2.6. Figure 2.6 also illustrates the correlation between the vertical crack depth and surface crack width for different microtopographies.

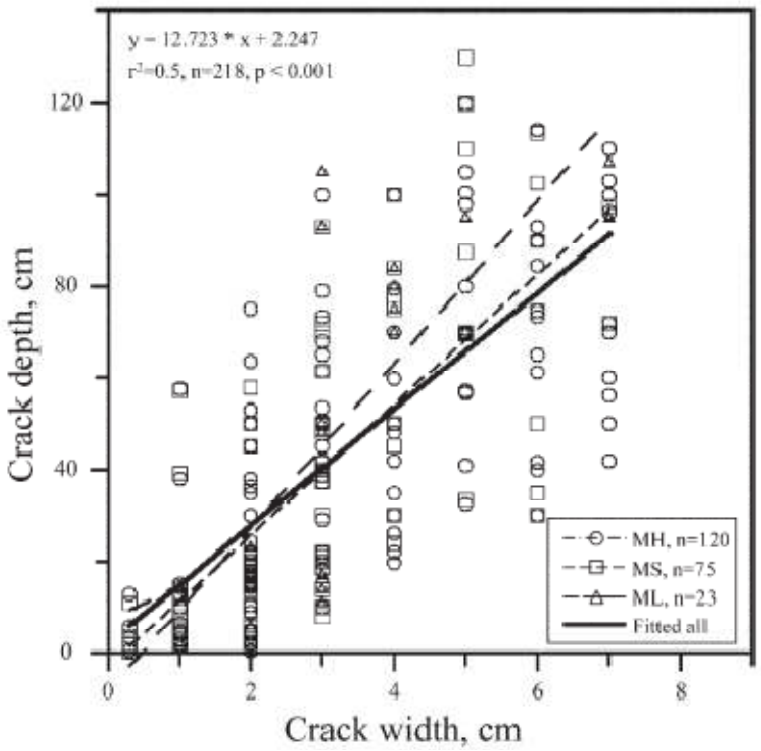

Figure 2.6. Linear correlation between vertical crack depth and surface crack width based on measurements taken on microhighs (MH), and microslopes (MS), microlows (ML) (from Kishne et al. (2009)).

Sun et al. (2009) introduced secondary cracks which are the cracks that appear after primary cracks as evaporation continues. They formulated the secondary crack spacing using stress analyses, and verified the equation using some field data. Figure 2.7 depicts the concept of primary and secondary cracks propagation.

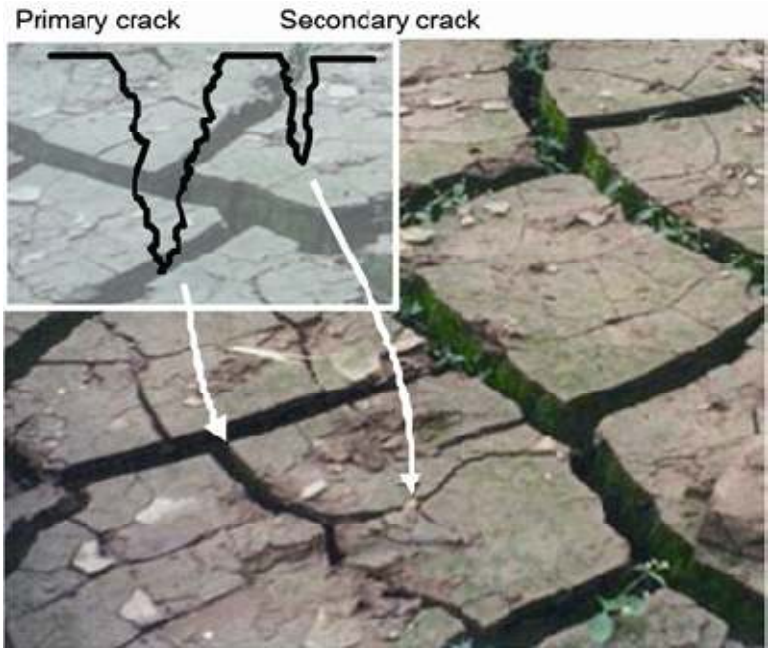

Figure 2.7. Illustration of primary and secondary cracks (From Sun et al. (2009)

2.3. Volume change effects of cracks

Volume change responses of soils to moisture changes have been studying for many years. From the geotechnical engineering point of view, the soil volume changes can significantly affect the foundation performances. It can change the foundation equilibriums by changing the applied forces. Also, it can influence the structural deformations, and if not been accounted for during the design, it might lead to the failure or a significant damage of the structure. While the current literature is flooded by numerous studies, models, and experimental procedures to identify and measure the soil deformation (heave/swell/shrinkage), there is a lack on identifying the effect of cracks on the soil volume changes during the wet/dry seasons. The main reason that this topic is remained unknown is probably the high degree of uncertainties associated with the soil cracks. This section reviews the

related literature related to the effect of soil cracking on the volume change perspectives of the soils.

2.3.1. Swell/Shrink potential of soil cracks

Arnold et al. (2005) studied the crack volume change by monitoring the crack data for a soil from central Texas for a period of two years (from 1998 to 2000). Soil movements were monitored bi-weekly beginning in January 1998. Figure 2.8 illustrates the relative movements of soil anchors at different depths below the ground surface relative to the deep borros point monument at 4.5 m. The authors indicated that over 70% of the cracks occurred in the upper 1.5 m layer of the soil. Crack volume per unit area was estimated from changes in layer thickness after Bronswijk (1991) and Bauer et al. (1993) and then summed for the entire soil profile. Measured and simulated total crack volume is presented in figure 2.9. The authors also related the crack volume change to the estimated soils waster content and potential evaporation rate (PET) which are shown in figures 2.10 and 2.11 respectively. From figure 2.10, it can be noted that the volume of cracks is inversely proportional to the moisture content of the soil, which can be related to the healing process of soil cracks. Also, from figure 2.11, it can be clearly seen that the crack volume and the potential evaporation are in direct relationship, yet with some amount of lag.

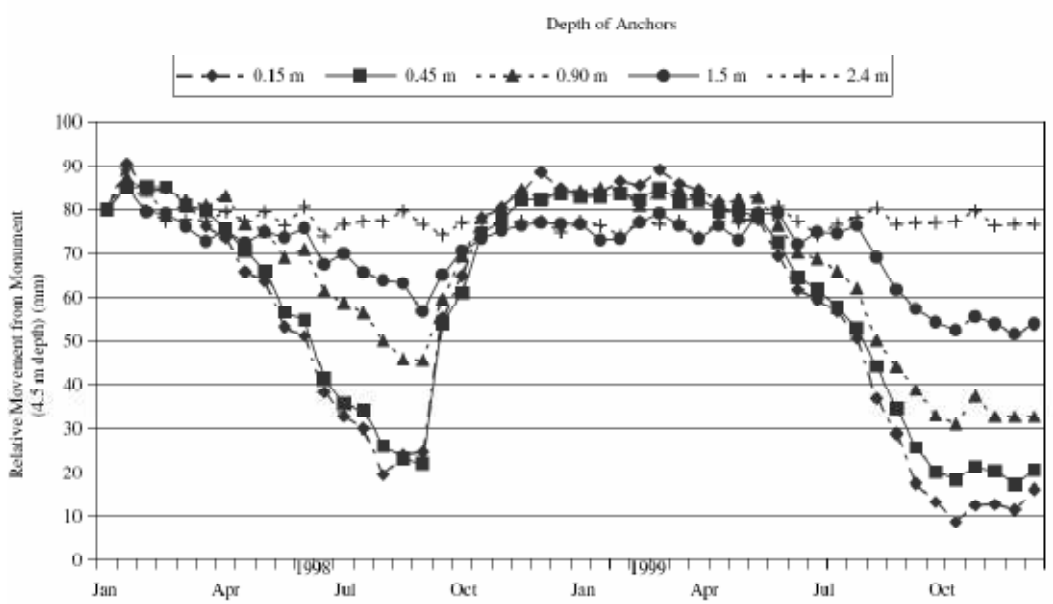

Figure 2.8. Movement of the mounted borros anchors relative to the monument at 4.5 m depth (From Arnold et al. (2001))

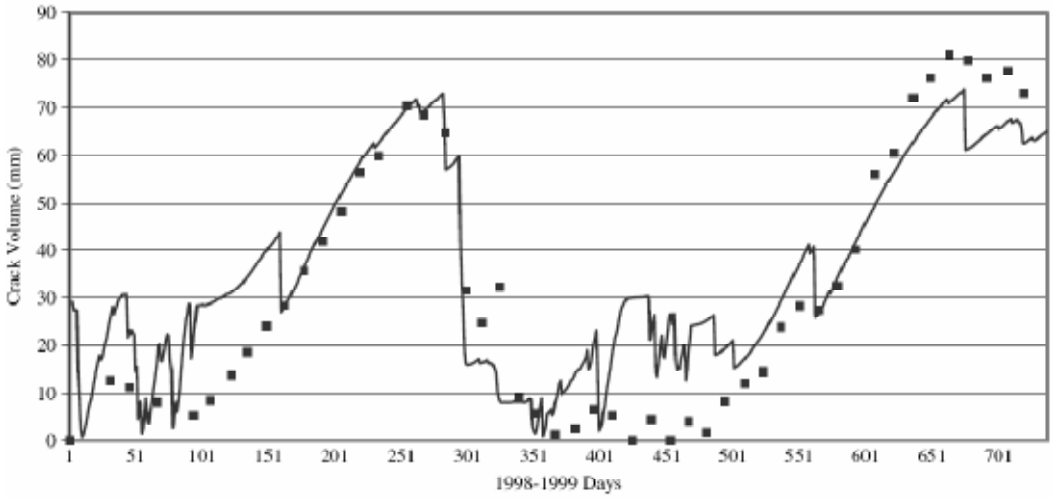

Figure 2.9. Measured and simulated total crack volumes for 1998–1999 (From Arnold et al. (2001))

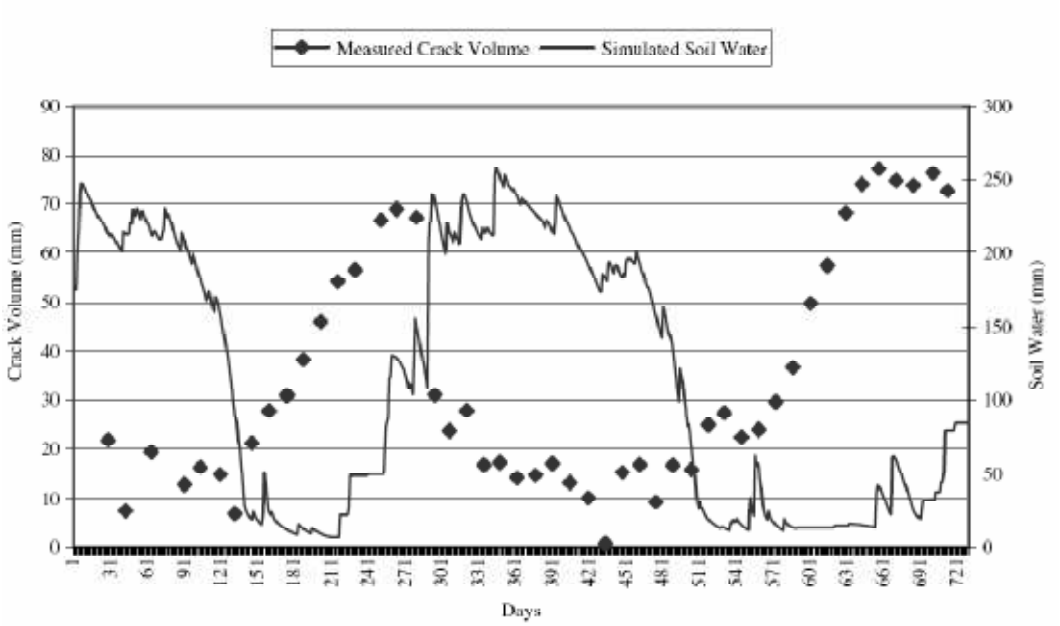

Figure 2.10. Relationship between crack volume and simulated soil water (From Arnold et al. (2001))

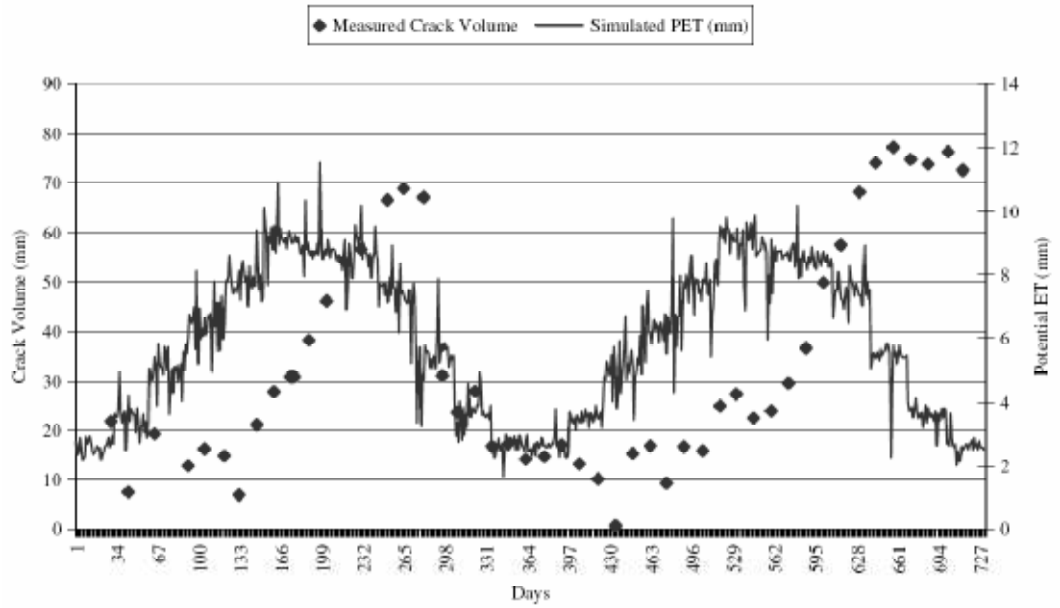

Figure 2.11. Relationship between crack volume and simulated potential evapotranspiration (From Arnold et al. (2001))

2.3.2. Healing potential of cracks

One of the main questions that often arise about the cracks is whether or not they heal after a certain amount of permeation or after an application of the

final effective stress. Ruy et al. (1999) reported that the crack width ranges from 0 for a saturated soil to several centimeters at the end of the dry season.

Albrecht and Benson (2001) studied the effect of desiccation on compacted natural clays. Specimens were compacted from eight natural clayey soils used for clay liners and covers and subjected to cycles of drying and wetting. The authors also studied the potential healing of the specimen by permeating two cracked specimen (from Houston Red and Sauk County soils) for about one year or subjected to different effective stresses. Results of these tests are illustrated in Figure 2.12. They summarized their findings for healing potential as follows: "Healing of damage caused by desiccation is unlikely to occur during extended periods of hydration unless the effective stress is increased considerably. No significant decrease in hydraulic conductivity was observed in specimens permeated for a period of 350 days, suggesting that even under extended periods of hydration desiccation cracks will not close. Tests at various effective stresses showed that an effective stress of at least 60 kPa was needed to close desiccation cracks so that the hydraulic conductivity is $\leq 10^{-7}$ cm/s. This effective stress is higher than that found in most cover applications, suggesting that desiccation damage to covers will be permanent."

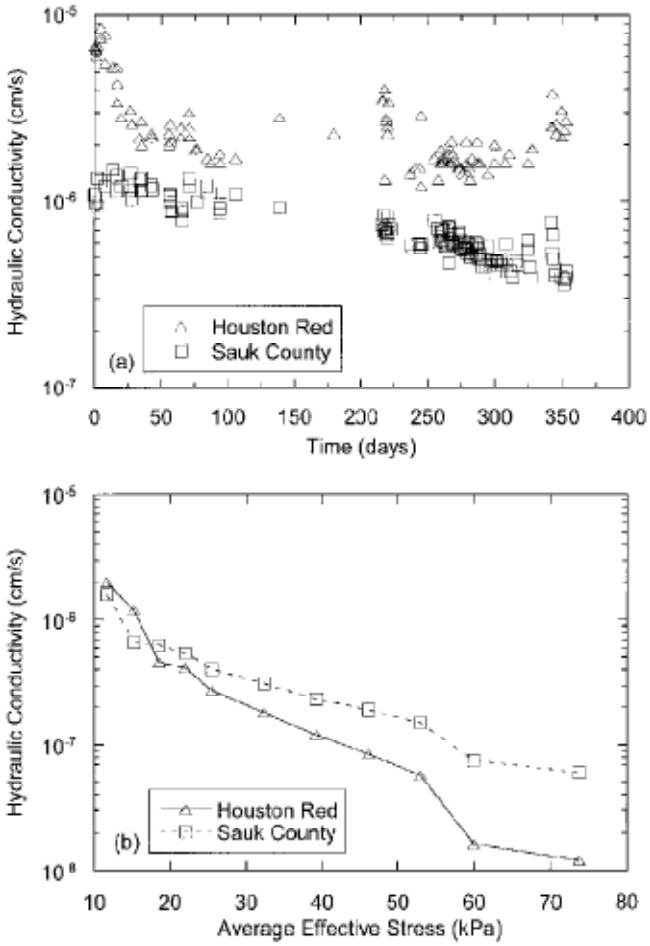

Figure 2.12. Hydraulic Conductivity versus (a) Time and (b) Effective Stress (From Albrecht and Benson (2001))

2.3.3 Heave estimation methods and cracking effects

Heave is the vertical swelling of soil and, according to Zhang (2004), it can cause structural damages in cases that it is not uniform because differential settlements can cause stress concentration in structures. Previous heave prediction methods are summarized in tables 2.1.

Table 2.1. Heave prediction methods based on oedometer test results (from Singhal (2010))

Name of the Method	Country of Origin	Reference
1. Double Oedometer method	South Africa	Jennings and Knight (1957); Burland (1962); Jennings (1969)
2. Salas and Serratosa method	Spain	Salas and Serratosa (1957)
3. Volumemeter method	South Africa	de Bruijn (1961)
4. Mississippi method	U.S.	Clisby (1962); Teng et al. (1972); Teng et al. (1973); Teng and Clisby (1975)
5. Sampson, Shuster, and Budge's method	U.S.	Sampson et al. (1965)
6. Noble method	Canada	Noble (1966)
7. Sullivan and McClelland method	U.S.	Sullivan and McClelland (1969)
8. Komornik, Wiseman, and Ben-Yacob method	Israel	Komornik et al. (1969)
9. Holtz method	U.S.	Holtz (1970)
10. Navy method (Direct Method)	U.S.	NAVFAC (1971)
11. Wong and Yong	U.K.	Wong and Yong (1973)
12. U.S.B.R. method	U.S.	Gibbs (1973)
13. Simple Oedometer method	South Africa	Jennings et al. (1973)
14. PVR Method (Texas Highway Department)	U.S.	Smith (1973)
15. Controlled strain test	U.S.	Porter and Nelson (1980)
16. Heave index method	U.S. (Denver)	Nelson et al. (1998)
17. Fredlund, Hasan and Filson's method	Canada	Fredlund et al. (1980)

As can be seen from the summarized methods, there are only two methods (Lytton (1977b); McKeen (1981)) which take the crack effect into consideration. McKeen postulated that the rate of swell is primarily related to the permeability of the soil. Therefore, an initially dry, fissured soil swells rapidly at first as water moves through the existing shrinkage cracks. As these passages are closed by swelling, the permeability is drastically reduced and a much slower rate of swell results. Lytton accounted for the effect of cracks in his heave prediction method by simply introducing the cracking fabric factor, f, which varies from 1/3 for heavily cracked soil to 1 for tight soil with high lateral restraint. All other methods have simply ignored the cracks effect in heave predictions while cracks may significantly affect the heave estimations.

2.4. Water movement through cracked soils

Estimating the ground surface flux is one of great interdisciplinary interest for disciplines including soil science, geology, geotechnical engineering, environmental engineering, environmental ecology, hydrology, water resources, landscape architecture, agricultural engineering, and forestry. While surface flux is related to number of factors including but not limited to soil type, soil topography, climate conditions, depth of ground water table, and vegetation, cracks can also have a significant effect on the surface flux as well. Seasonal cracking of the soil matrix results in poor estimates of runoff and infiltration due to the changing soil storage conditions (Arnold et al. (2005). In general, the problem of estimating the ground surface flux is a complicated problem to solve even for an intact soil, but the existence of cracks makes the problem even more sophisticated due to the numerous uncertainties associated with cracks. Many studies have been conducted for evaluation of water movement in cracked soils. In a general classification, the related studies can be divided into three major types of theoretical, experimental and modeling. Here, the literature is reviewed and presented with respect to these three categories.

2.4.1. Theoretical investigations

Novak et al. (2000) presented the physical basis for simulating the infiltration of precipitation/irrigation water into relatively dry, cracked, fine-textured soils. They considered that the infiltration into the soil matrix would be either vertical infiltration through the soil surface or lateral infiltration via soil cracks. The authors used 1-D Richards equation to describe and solve the first

component while Green-Ampt approach was used to calculate the horizontal infiltration from soil cracks into the soil matrix.

Li et al. (2009) investigated the development of a permeability tensor and a representative elementary volume (REV) for saturated cracked soils using a random crack generation technology. They found that the permeability anisotropy of a cracked soils can be explained using the permeability tensor. Based on this research, an REV is harder to establish for sparse crack network in clays than in homogeneous sands. In fact, the permeability of the cracked clay mainly comes from the crack network while, in contrast, the contribution of the crack network is more or less negligible when the soil matrix is made of sand.

2.4.2. Experimental investigations

One of the methods that was used commonly to study the preferential flow paths in a cracked soil is to employ dyes into the soil matrix with which the flow paths can be traced (Aubertin (1971); Kissel et al. (1973); Anderson and Bouma (1973); Ehlers (1975); Saffigna et al. (1976); Bouma et al. (1977); Ghodrati et al. (1990); Flury et al. (1994)). This method allows to stain the flow paths of water in soils. For instance, Bouma and Dekker (1978) determined the infiltration pattern into four different clays as a function of infiltration rate and quantity using "Methylene Blue" as a tracer (dye). The authors used term "short-circuiting" referring to quick downward water flow through the large pores (cracks) that are initially filled with air. In other words, water bypasses the soils matrix by moving through these pores. Their experiments showed that water will only flow into open larger pores (forming stains) if the upper surface of the fine porous peds

cannot conduct all the applied water. The authors also found that water penetration depth can vary with soil type, water infiltration rates and quantities, but in general they found it to be around 1 meter for the types of clay soils used in the experiments.

Flury et al. (1994) also tested the susceptibility of 14 different soils, from field sites in Switzerland, to preferential flow and the results showed different degrees of wetting for different soils. The authors postulated that in most soils tested in this study, water bypassed a portion of the soil matrix, but the extent of the bypassing differed. They referred to occurrence of the preferential flow as a rule rather than an exception.

Topp and Davis (1981) conducted a field study in Canada, and applied a simulated rainfall to a cracked clayey soil and used time-domain reflectometry (TDR) to identify the water content of different profiles of the soil within different distances from the cracks. The authors concluded that at a depth of 10 to 30 cm the rate of wetting of soil immediately adjacent to the cracks was more rapid than that of the soil at some distance from the cracks. They also found that more than 1 cm of rainfall is contributed to the cracks for rainfall rates greater than 0.1 cm/h. The authors also reported a low depth of wetting for soils with some distance from the cracks as opposed to a much higher depth of wetting for soils adjacent or within the cracks.

Bouma and Wosten (1984) carried out a research to characterize the ponded infiltration into a dry cracked soil. They used physical and morphological techniques to evaluate the water infiltration in two large blocks of cracked soil

carved out in situ. The upper surface area of the blocks was around 1500 cm^2 and the height of blocks was 23 and 40 cm. In addition to infiltration rates into the blocks and into the subsoil during the shallow ponding, they also measured the water content profile with diffusivity of the block as well as the depth and degree of wetting for the soils adjacent to the cracks. Figure 2.13 below shows the distribution of moisture content with time throughout different horizontal distances from the ponding region. The authors neglected the swelling effect of soil by restricting their experiments only to the first 10 minutes of the infiltration.

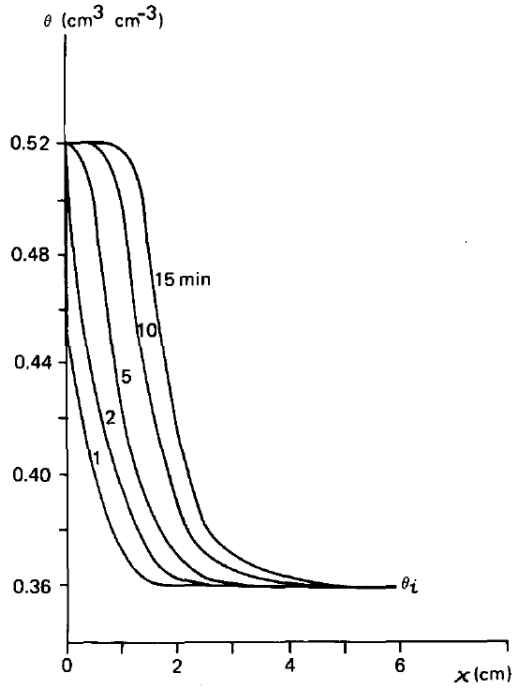

Figure 2.13. Moisture distribution as a function of time and distance for horizontal infiltration in a dry clay soils per unit surface area (from Bouma and Wosten (1984))

Favre et al. (1997) conducted a field study in Senegal to investigate the water movement and soil swelling characteristics in a dry, cracked Vertisol. The subject cracks of this study were 0.01 to 0.02 m in width and about 0.3 m in depth. The authors reported that surface irrigation and simulated rainfall resulted

in complete crack closure after 4.5 hours meaning that the preferential flow only occurred during that first phase of precipitation. It was also reported that as the soils saturated, the cracks started to close from top layers of soil and this process continued downward until the entire crack network is more or less closed. The authors suggested that soil swelling was heterogeneous and can be separated into two components: (1) soil islands (2) cracks. This concept is illustrated in figure 2.14 below. It was reported that the swelling of the soils islands continued after crack closure, but the contribution of that to crack closure did not exceed 30% after one day.

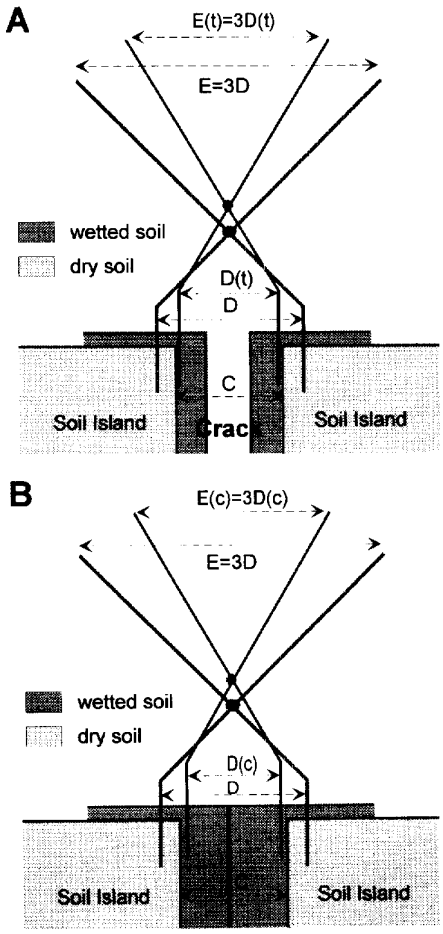

Figure 2.14. Lateral movement measurement of soil islands A) before crack closure B) after crack closure. (from Favre et al. (1997))

Albrecht and Benson (2001) evaluated the effect of desiccation on compacted natural clays. Specimens were compacted from eight natural clayey soils used for clay liners and covers and subjected to cycles of drying wetting. Hydraulic conductivity tests were performed for the samples which experienced cracks after drying-wetting cycles. The results of conductivity tests showed that cracking of the specimens resulted in an increase in hydraulic conductivity, sometimes as large as three orders of magnitude. The authors also assessed the effect of different cycles of drying-wetting and it was proposed that the most significant increase in hydraulic conductivity took place after the first drying cycle, because the first drying cycle produced cracks in the specimens. Figure 2.15 below illustrates the effect of drying cycles on the conductivity of the cracked specimen.

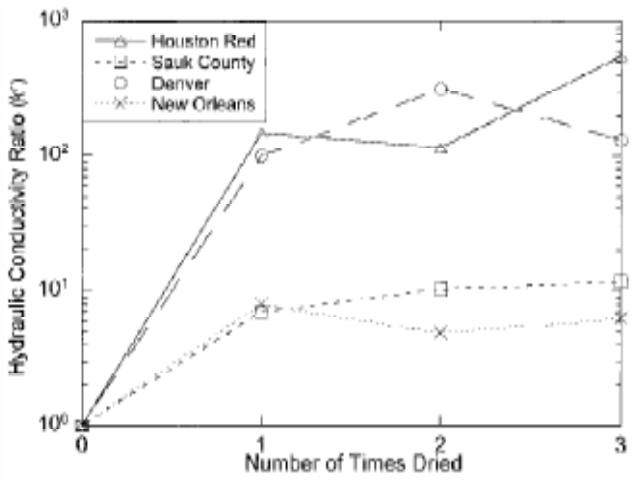

Figure 2.15. Hydraulic Conductivity ratio vs. Number of Drying Cycles for Different Specimens (from Albrecht and Benson (2001))

Liu et al. (2003) conducted number of laboratory soil column experiments to investigate the factors influencing the water infiltration in cracked paddy field. After studying various factors such as soil texture, fracture apertures, flooded

water depth, etc., it was concluded that swelling and cultivation of soil have the most impact in water infiltration rates. The authors postulated that the macro pores increased the initial conductivity of soils but as the soils started to saturate, the conductivity was decreased due to the swelling effect. This is consistent with Favre et al. (1997) findings. They also noted that sometimes the final conductivity of an initially cracked soil can be even lower than that of an intact soil due to the swelling effect which closes the cracks and results in a denser soil matrix.

Zhan et al. (2007) carried out a field study of rainfall infiltration into an unsaturated slope, and they found interesting results regarding the effect of cracks. The authors tested two different parts of the slope, one with cracks and the other without cracks. It was found that the infiltration occurs faster for the cracked slope than the intact slope. This field study suggested that for the first few hours the conductivity was very high for the cracked soil due to the preferential flow and openings which have made the water flow much easier. However, after about 4 to 5 hours, the infiltration rate became lower and tended to reach to a constant value which was very close to the initial infiltration rate of the intact soil (See Figure 2.16). Primarily, the decrease in infiltration rate was related to the swelling of the soil after suction was decreased which caused the crack and fissure openings to close. Secondarily, lower infiltration rates could also occur as a result of the lower suction gradient after the soil suction is decreased due to the wetting. In general, the authors suggested that a greater depth of wetting should be expected for the cracked soil as a result of an extensive network of cracks existing in the unsaturated expansive soil.

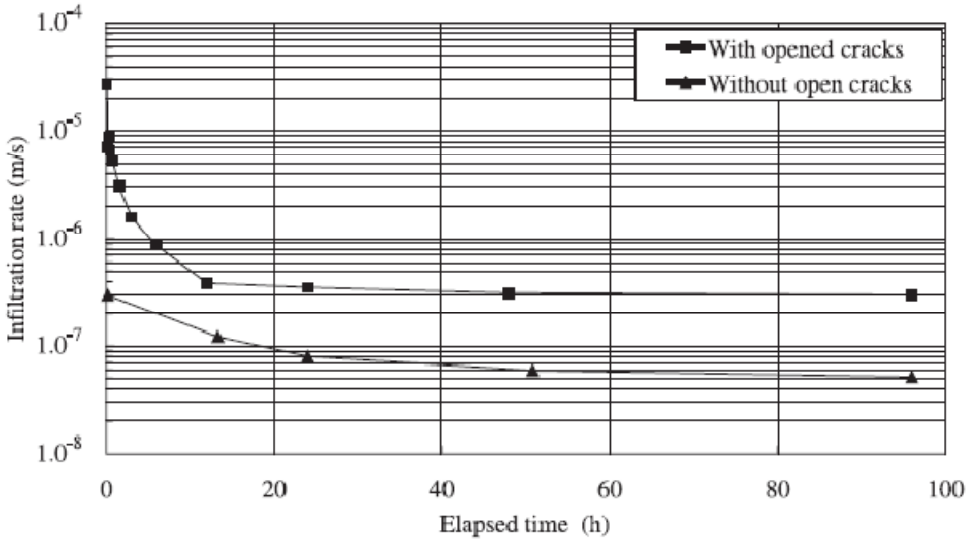

Figure 2.16. Changes of infiltration rates with time from the double-ring infiltration test (From Zhan et al. (2007))

Reyhani et al. (2007) conducted a set of saturated laboratory hydraulic conductivity experiments on different types of cracked clays from Iran. The results showed that cracking increased the conductivity by 12 to 34 times depending on the plasticity of the soil. However, it was reported that by increasing the saturation time the hydraulic conductivity decreased which can be as a result of the healing process of the initial cracks.

Greve et al. (2010) investigated the process of soil crack formation and preferential flow using a cracking clay soil in a weighting lysimeter. A weighing lysimeter is a device that was created by placing a fiberglass barrel, with inner diameter of 1.3 m and depth of 0.78 m, on a scale, with measurement range of 0 to 3000 kg and resolution of 0.1 kg. To allow drainage, the lysimeter was tilted at an angle of 3.5º and had a 28 mm diameter drainage opening cut into the lowest point of its side wall. A total of 6 irrigation events (5 rains and 1 flood) were applied and followed by a drying period. This 5 year research resulted in some

valuable findings regarding the preferential flow in cracked soils which are summarized below:

1) Lateral infiltration from the macropores into the soil significantly affects the water flow and should be included in water flow simulations of dry cracking soils.

2) Macropores remain pathways for preferential flow even after they seem to be healed at the surface.

3) Location of surface cracks depends on the water application type. For instance, flood irrigation is favoring reappearance of cracks at previous crack locations, while rainfall results in shifting crack locations.

Figure 2.17 illustrates the conceptual model of crack formation and infiltration processes, where different figures show the lysimeter at different stages such as: (a) before drying period; (b) after drying period with primary crack network; (c) during irrigations 1–3; surface runoff, which is carrying dissolved NaCl is infiltrating laterally into the soil matrix adjacent the cracks; (d) before irrigation 4; the primary crack network is closed at the surface, new surface cracks have formed at new locations; (e) during irrigation 4; water from the moist top layer is entering the traces of the primary crack network once the field capacity in the top of the profile is exceeded; preferential flow occurs and contributes to the drainage; (f) during irrigation 5; added water fills up soil moisture deficit caused by evaporation in previous drying period; no drainage occurs; and (g) during irrigation 6; drainage occurs but data indicating occurrence or lack of preferential flow is not conclusive.

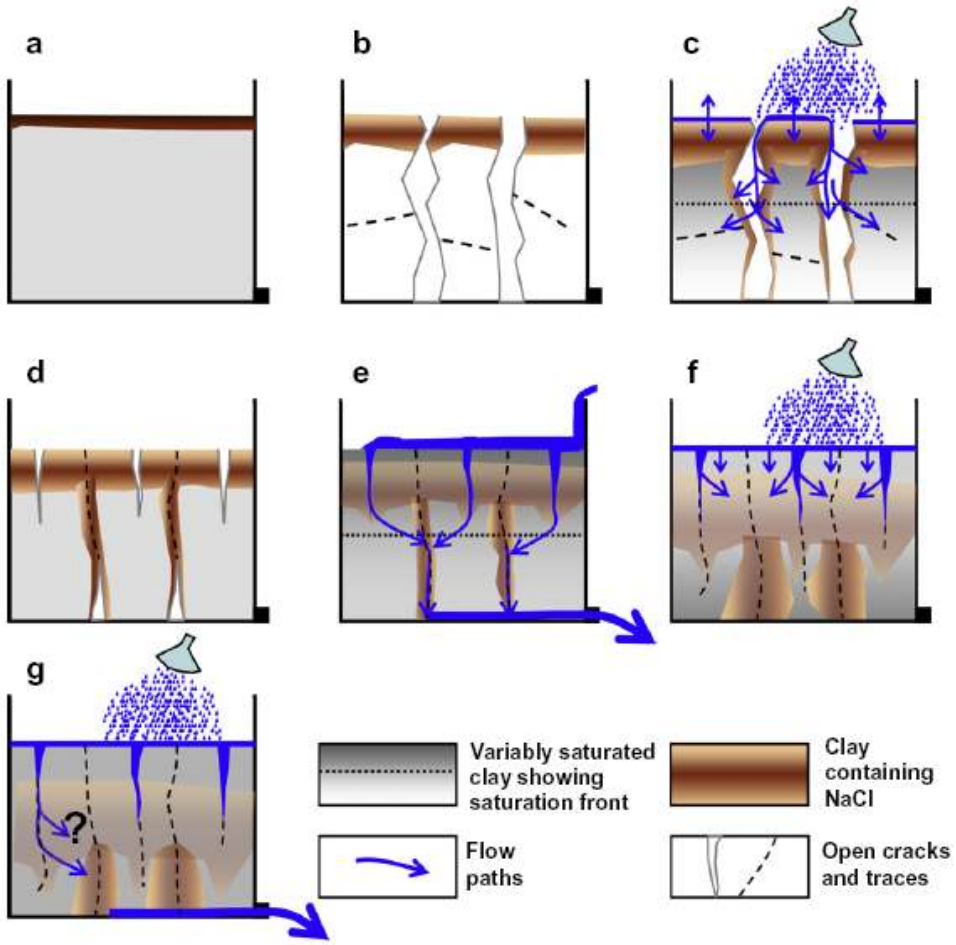

Figure 2.17. Conceptual model of flow processes into a cracked soil and volume change behavior (from Greve et al. (2010))

2.4.3 Simulation and modeling investigations

Davidson (1985) numerically calculated the infiltration of a cracked soil using a finite difference numerical solution of the saturated-unsaturated flow equations for selected soil hydraulic characteristics. The author made some simplifying assumptions to solve the problem. First, it was assumed that all cracks are equally spaced from each other and filled with water during the analysis. Furthermore, it was assumed that the cracks remain open from the beginning to the end of the analysis. In other words, the swelling effect of the soils was neglected.

Bronswijk (1988) introduced the shrinkage characteristics into the modeling of water balance, cracking and subsidence of clay soils. This allowed direct calculation of volume change in response to the moisture transport. The rainfall was dynamically partitioned in soil matrix and crack infiltration as shown in Figure 2.18. Then to modify the presented model, one of the previous models, FLOWEX, was modified into a version compatible with clay soils, FLOCR, and computations with that were in agreement with field observations.

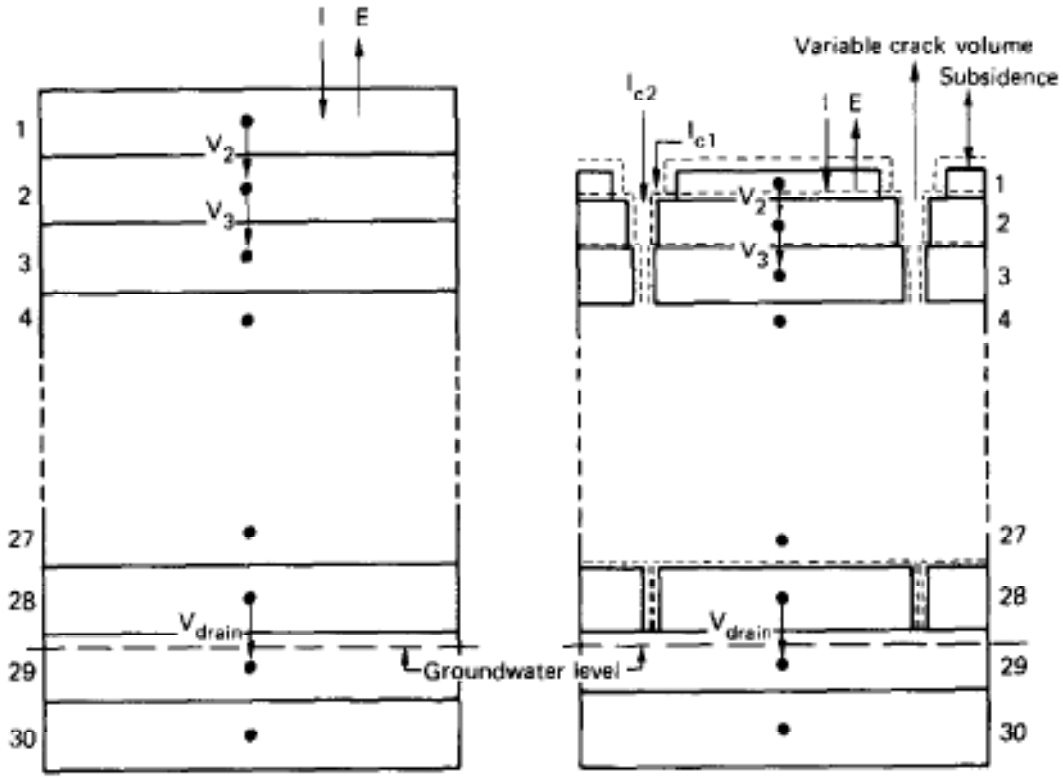

Figure 2.18. A schematic representation of a simulation model, left, and its adapted version, right. (from Bronswijk (1988))

where in figure 2.18: I = infiltration rate in soil matrix (m/s); I_{c1} = part of total crack infiltration caused by rainfall intensity exceeding maximum infiltration rate of soil matrix (m/s); I_{c2} = part of total crack infiltration caused by rainfall directly into the cracks (m/s); E = actual evapotranspiration (ms-1); V = Darcy

flux between two nodal points (m/s); V_{drain} = drain discharge (m/s). Matrix-crack system at time T is indicated by a solid line, matrix-crack system at time T + ΔT is indicated by a broken line.

Perrier et al. (1995) developed a computer model to study the relationship between the hydraulic properties and structural properties of soils. In this study, the authors introduced a two-dimensional method to construct the soil structure including both soil particles and fractures. The presented method is based on consecutive fragmentation process that leads to different levels of aggregation. Figure 2.19 below illustrates the construction of soil structure on one level of fragmentation.

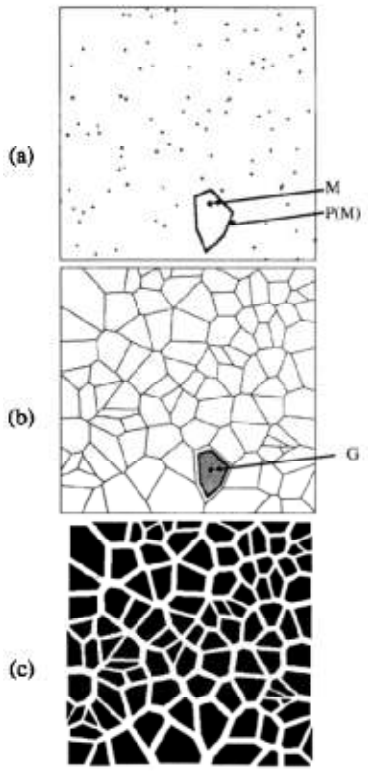

Figure 2.19. Illustration of consecutive fragmentation process (from Perrier et al. (1995))

Lehmann and Ackerer (1998) compared two of the most common iterative methods (Picard and Newton method) which are being used to solve the Richards equation to improve the previous solutions. The authors used two examples to evaluate the numerical performance of different forms of 1-D vertical Richards equation and different iterative solution schemes. Based on their findings, a combination of the modified Picard and Newton methods was found to be more efficient than either method being used individually.

Ruy et al. (1999) developed a mechanistic model for infiltration of water into the vertisol with consideration of the volume change. This model accounts for the three components of porosity of this soil (matric, structural and macro-cracks). Inputs of the model are the shrinkage curve, the retention curve and the hydraulic conductivity of the matric porosity which should be measured in laboratory. The problem with the developed model is that the parameters used in this model are highly sensitive to the soil-type and should be determined separately each time a different soil is being used.

Askar and Jin (2000) developed a mathematical description of water flow through unsaturated swelling soil based on Richards equation. Then the relationship between the soil volume change and corresponding water changes were investigated which is presented as the following equation:

$$\frac{1}{1+e}\frac{\partial}{\partial t}[(1+e)\theta] = \frac{\partial}{\partial z}\left(D\frac{\partial \theta}{\partial z}\right) - \frac{\partial K(\theta)}{\partial z} + S \qquad (2.1)$$

where θ is the volumetric moisture content; t is the time of flow; K is the hydraulic conductivity; D is the water diffusivity function; D (θ) = K (θ) ($\partial\psi/\partial\theta$);

ψ is the matric suction; z is the soil depth, positive downward with the ground surface taken as the datum level; S is source/sink term; and e is the void ratio. After developing the abovementioned equitation, it was applied to Regina clay to validate the presented numerical model and results were found to be satisfactory.

Diiwu et al. (2001) used a field data to propose a transfer function model through a macroporous soil. The model is based on the difference between the hydraulic characteristics of macroporous and microporous. The authors used mixed probability distribution to characterize drainage and solute transfer into the soil for both macroporous and microporous domains. The lognormal distribution was found the best distribution for drainage while the two-parameter gamma distribution was found the best for solute transport for both domains. One of the drawbacks of this model is that the presented parameters are field dependent so from one field to another, the parameters are required to be calibrated which may require a lot of effort.

Romkens and Prasad (2006) suggested that the water flow through an expansive cracked soil, for field application scales, can be modeled combining Darcian matrix flow for the soil medium and Hortonian flow on the walls of the cracks. Figure 2.20 sketches the concept of the model developed by the authors. In this model, it was assumed that the excess rain flows along the vertical walls of the crack with lateral imbibitions into the soil. However, the authors postulated that this assumption may not be valid during the heavy storms when the cracks are filled from bottom up. Two years after this study, Khalili (2006) developed a fully

coupled formulation for two-phase fluid flow through a deformable fractured porous media.

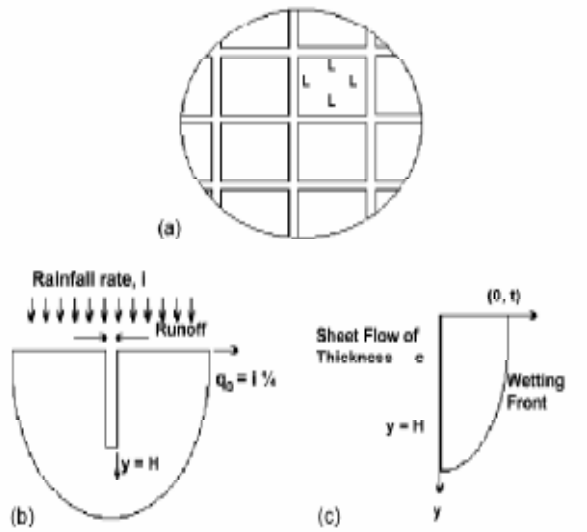

Figure 2.20. A geometric representation of the infiltration model and different views of cracked profile (from Romkens and Prasad (2006)).

Chertkov and Ravina (2002) attempted to generalize their earlier model for estimating the hydraulic conductivity of swelling clay soils by combining the effect of interblock and interaggregate capillary cracks together. The authors used the lysimeter experiment data from Bronswijk (1991). In this research, similar to their previous work, for estimating the contribution of a clay matrix to the hydraulic conductivity, approach of van Genuchten (1980) and Mualem (1976) were used which predicts the relative conductivity function of a soil matrix based on its water retention curve. Although the total contribution of interaggregate and interblock capillary cracks to water retention of the soil stays negligible, at sufficiently small pressure heads the contribution of capillary cracks of both types to the hydraulic conductivity of the clay soil can prevail (See Figure 2.21).

Results from the modeling were in agreement with the data from Bronswijk's lysimeter experiment.

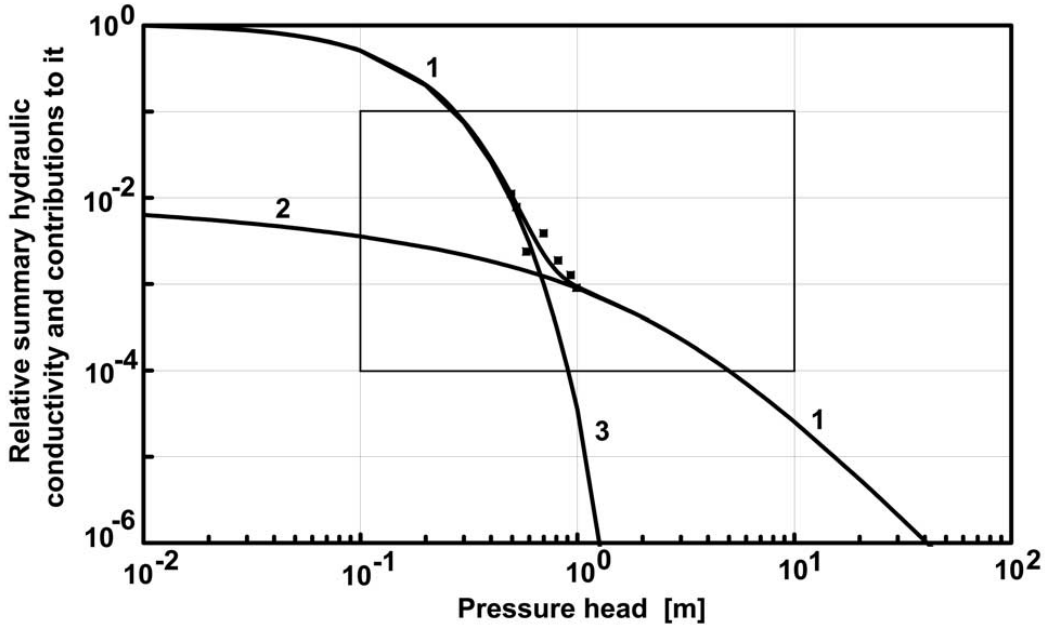

Figure 2.21. The relative summary hydraulic conductivity for 1) the overall cracked soil, 2) predicted contribution of the soil matrix, and 3) predicted contribution of the cracks (from Chertkov and Ravina (2002))

Lie et al. (2004) studied the extent and depth of wetting for a cracked paddy field soil. The modeling and field experimental investigations were performed and compared to evaluate the effect of crack depth on the extent of wetting. The authors used Hasegawa and Sato (1985) soil-crack model, which was originally used to model the upward water evaporation movement through cracks, to simulate the downward infiltration into the cracked paddy fields. It should be noted that the swelling behavior of cracks during the infiltration was neglected in this model. Based on the experimental investigations of this study, cracked paddy has a high water infiltration rate of about 16 cm/day. Simulation results revealed that infiltration rate increases as the crack depth increases. More

specifically, infiltration rates for cracks with depths of 80, 60, and 27 cm were respectively 19, 14.5, and 8 time higher than that of a 20 cm deep crack.

Romkens and Prasad (2006) developed a model for predicting the water infiltration through the cracked expansive soil. The authors used the same approach as Kutilek (1996) but the following two assumptions were made to simplify the problem: (1) No vertical infiltration takes place due to the sealed surface condition (except inside the cracks). (2) The geometry is represented by a prismatic column structure with cracks between the columns. For filed scale estimations of rainfall infiltration through highly expansive soils, the authors suggested to consider the process based predictive relationships of two interactive domains, namely, matrix flow into the soil and macro-flow into cracks. Experimental evidences of this study showed that at early stages of the rain, the water infiltrates from the uppers parts of the crack wall into the soil matrix and as the rain continues and the lower parts of the cracks walls become wet, the lower layers of the soil matrix starts to become wetter. However, this process can be reversed in cases when the precipitation rate is high such as in rainstorms.

Li et al. (2009) presented a mathematical model to establish the permeability tensor and representative elementary volume (REV). The authors used a random crack generation method based on statistical parameters of crack geometry. By modeling the water flow through the created cracks the permeability tensor and REV were studied. It should be noted that the crack volume change effects were not taken into account in this model. The following cubic law equation, which was first presented by Snow (1969), were used for

water flow through a single planar crack with width of b and length of l. Then the same equation was applied to all of the cracks.

$$q = \frac{gb^3}{12\mu} J \tag{2.2}$$

where q is the rate of flow through a unit depth of fracture (m^2/s), g is the gravitational acceleration (m/s^2), m is the kinematic viscosity of water (m^2/s), and J is the hydraulic gradient in the crack. Based on this study, it was found that the permeability anisotropy of cracked soils can be explained by permeability tensor. Also, it was reported that REV can be defined simply for the cases when the crack network is relatively dense, like in sands, whereas for the cases that the crack network is sparse, like in clays, defining REV would be difficult.

2.5. Current state of the knowledge

Although cracking has received a considerable amount of attention in the literature during the past two decades, the treatment is largely behavioral and qualitative (Morris et al. (1992); Kodikara et al. (2000)). Very little data is available in the literature for unsaturated hydraulic conductivity functions for intact unsaturated soils, and almost always, the volume change of soils has been neglected. Because the existence of cracks further complicates the problem, a thorough literature review failed to reveal data for unsaturated hydraulic conductivity functions for cracked unsaturated soils. Although cracked soils are expected to exhibit bimodal behavior, due to dramatic crack-related pore size variability, no experimental evidence can be found in the literature in support of the bimodal unsaturated hydraulic conductivity and SWCC behavior of cracked

soil. This is likely because of the challenging and time-consuming nature of these types of experiments. Although there have been broad investigations to identify the important engineering properties of cracked soils, such as geometry, conductivity, and volume changes, no study can be found in the literature that compares the properties of intact clay to cracked clay. One thing that makes this study unique is the fact that all of the laboratory investigations and numerical modeling have been replicated for cracked and intact soil wherein the clay matrix of the cracked soil is "identical" to the intact clay specimens. Therefore, a rational comparison of crack and intact soils can be made and the effect of the existence of cracks can be explored more thoroughly. Most importantly, very limited information can be found in the literature regarding the effect of cracks on the performance of foundations. The vast majority of heave prediction methods have neglected the effect of cracks on the calculations of heave, and analyses that have taken cracks into consideration are limited and largely judgment-based.

Chapter 3

EFFECT OF CRACKS ON VOLUME CHANGE AND SWELL PRESSURE

3.1. Abstract

The volume change properties of soils are important design parameters for both Geotechnical and Structural Engineers. In typical practice, the actual 3-D volume change problems are simplified to 1-D problems by considering only the one-dimensional heave or settlement. This is a reasonable approach for many engineering applications where loads are applied over a relatively large area and when the ground surface is not sloped. However, this simplification of the 3-D problem to a 1-D problem is not adequate to render most problems of heave and settlement estimation of soils solvable. In fact, despite numerous research attempts during the past four decades and various protocols and procedures that have been developed to estimate the volume change of soils, this remains one of the most challenging subject areas in geotechnical engineering, particularly the estimation of heave (and shrinkage) of expansive soils. Fredlund and Rahardjo (1993) have listed thirteen oedometer-based heave prediction methods. In 2010, Singhal (2010) extended that list to seventeen methods. The variety of heave estimation methods goes even further as other methods are introduced (e.g., suction-based methods). This wide range of heave prediction methods make it difficult for practicing engineers to choose a consistent and reliable approach to estimate the volume change of an expansive soil. Since each method has its own merits, no single method has yet been widely accepted amongst the professional, and many empirically-based methods or empirical adjustments are made that are

only regionally applicable. This lack of agreement of approach, even to testing of expansive soils, can be vividly noticed. For example, in 2003, the ASTM Standard D4546-03, which presents the test procedures for Measurement of One-Dimensional Swell or Collapse of Cohesive Soils, presented three different methods. One of the methods was method C, the Constant Volume (CV) test, in which the specimen is maintained at constant height during the course of the experiment by adjusting the normal load as the sample is saturating (and presumably exhibiting some swell). This laboratory test, though challenging to perform, has been used widely and considered to be one of the most reliable methods for determination of swell pressure. Nevertheless, about five years later, when ASTM released an updated version of D4546-08, the CV test method was removed from the new standard. This was probably due to the difficult and somewhat impossible restrictions for CV test such as controlling the vertical deformation by 0.005-0.01 mm, which requires computer control and also careful adjustments for apparatus compliance. Also it could be as a result of the highly sensitive nature of the results to the compressibility of the apparatus.

Aside from the problems and difficulties associated with heave/shrinkage predictions, it is critically important to estimate these movements because they can result in drastic and costly damages to infrastructure, including residential, commercial, and public systems. In the United States alone, the damage from expansive soils is estimated between 7 to 15 billion dollars per year (Nuhfer et al. (1993); Wray and Meyer (2004); Krohn and Slosson (1980)). This is greater than the combined damages from natural disasters such as floods, hurricanes,

earthquakes, and tornadoes annually in the United States ((Jones and Holtz (1973); Jones and Jones (1987); Handy (1995)).

While the above-mentioned difficulties and problems are associated with all expansive soils, whether intact or cracked, the introduction of cracks further complicates the problem. After a thorough literature review, only very limited information was found regarding the effect of cracks on the performance of foundations. The vast majority of heave prediction methods have neglected the effect of cracks on the calculations of heave, and analyses that have taken cracks into consideration are limited and largely empirically-based (e.g. Lytton (1994)).

In this chapter, first a history of swell (heave)/collapse (settlement) measurement techniques is outlined, followed by a presentation of laboratory investigations from this research study wherein volume change and swell pressure measurements of cracked and intact expansive soils were made and compared.

3.2. Introduction

A reliable estimation of heave is a prerequisite for the selection of treatment alternatives to minimize the volume change or preparation of a foundation design to accommodate the volume change (Erzin and Erol (2007)). In the literature, numerous techniques related to measuring the swelling properties and methods of heave prediction can be found, but there are very limited studies that included the effect of soil cracking; most have simply neglected the effect of cracks. Even in the studies that have taken the soil cracking into account, the method of inclusion of cracked soil into the problem is not very clear. Thus,

studying the volume change effects of cracks appears to be a largely untouched field which needs more attention.

Generally, one may presume that heave of an expansive soil with cracks may be more than that of a non-cracked soil because cracks would function as preferential paths and allow more water to infiltrate into the soil which eventually may lead to greater volume change; and, to some extent, that is the case. However, at the same time, the crack network in an expansive soil may also function as swell-absorbent media (void spaces within the soil) which can reduce the total amount of swell that the soil would experience. Hence, it is critically important to investigate the effect of cracks on volume change of expansive soils. In this study, an extensive laboratory investigation was carried out in order to quantitatively evaluate the volume change effect of cracks in expansive soils and also understand how soil cracks would affect the swelling properties of soils such as swell potential and swelling pressure.

3.3. Background

As reported by Erzin and Erol (2007), heave problems account for more economic loss than all other soil problems combined. As previously discussed, in the United States alone, the damage from expansive soils is estimated between 7 to 15 billion dollars per year (Nuhfer et al. (1993); Wray and Meyer (2004); Krohn and Slosson (1980)). This is two times more than the damage caused by the combination of all other annual natural hazards in the United States such as earthquake, tornados and floods, etc. ((Jones and Holtz (1973); Jones and Jones (1987); Handy (1995); Rollings and Rollings (1996); Montgomery (1997)). Due

to the severe extent of damage that expansive soils can potentially cause, this field has received a vast attention by geotechnical engineering researchers. One of the most challenging tasks is to predict the volumetric deformation of these expansive soils that can be a threat to stability of structures and foundations. Thus, significant amount of effort has been made for determination of swelling properties of expansive soils, such as swell pressure and swell potential.

By definition, swell pressure is the vertical pressure required for maintaining the same volume (no swell or compression) upon submergence (full soaking) of the expansive soil. Swell potential is the water-induced vertical strain of the soil when the soil is given free access to water under a specific net normal stress. In general, the studies related to determination of swelling properties can be divided into the two categories of direct and indirect methods. In direct methods, experimental program would be used to measure the swelling properties of soil directly from experiments, while in indirect methods typically an analytical or empirical solution would be employed to determine the swelling properties of soil, commonly using soil index properties such as Atterberg limits and gradation. In the following section, an overview of each method is presented.

3.3.1 Direct methods

Direct methods refer to any experimental attempt to directly measure the swelling properties of an expansive soil. Typically, an oedometer type device is used to measure the swelling properties of a soil, although other devices such as triaxial or modified pressure-plate devices have been used. Despite the variety of swell pressure measurement techniques and equipment, it is still believed by most

geotechnical engineers that the one-dimensional consolidometer test is the most practical and applicable test to be performed in evaluating soil swelling pressure (Attom and Barakat (2000)).

The most common swell tests are Free Swell (FS) test, Load-Back (LB) test, and Constant Volume (CV) test. In Free Swell test, the specimen is inundated while only a token load (seating pressure ≈ 1 to 7 kPa) is applied and vertical deformations are recorded; a common modification to the FS test is to apply the field overburden plus structural load stress (or some other stress, e.g. 1000 psf) to the specimen and then to inundate and observe swell. A Load-Back test is a FS test, except that after the free swell is observed and recorded the specimen is loaded back to its original height to obtain a Load-Back swell pressure value. In the Constant Volume (CV) method no volume change is allowed during the course of the experiment. After inundating the sample, vertical load is elevated periodically as the specimen swells, to prevent the specimen from experiencing any normal deformation. This technique is often considered to be the most reliable and accurate technique of measuring the swell pressure. At the same time, it is one of the most difficult and cumbersome methods of measuring the swell pressure. High level of difficulty in performing the CV test adhering to the volume change restrictions of ASTM 4546-03 has lead to elimination of this method from the revised version of ASTM 4546-08.

In the latest version of ASTM 4546 which was published in 2008, three methods of swell potential measurement were presented. The first method (method A) is called “wetting after loading test on multiple specimens”. This

method can be used to measure swell or collapse potential of both natural (in situ) and compacted soils. For this test, four or more identical specimens are required. Each sample is tested under a different constant vertical load and given free access to water. After the process of primary swell or collapse is completed, the final swell or collapse is recorded and plotted on a vertical strain percentage (swell (+) and collapse (-)) versus vertical stress plot as shown in Figure 3.1. In addition to "swell pressure" this method can also be used to measure "free swell" and one-dimensional settlement or heave.

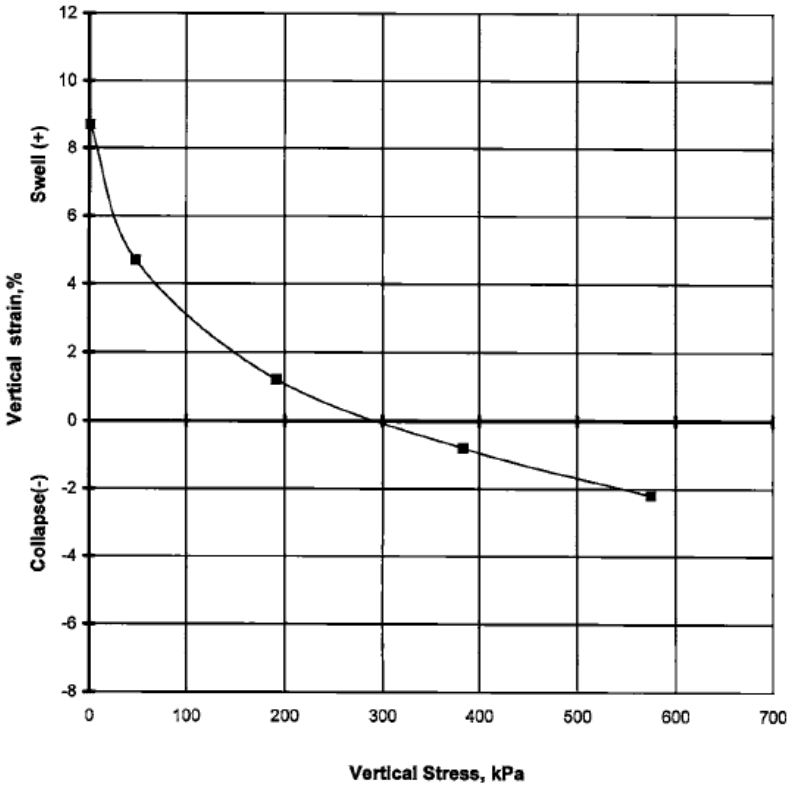

Figure 3.1. Vertical stress versus wetting induced vertical strain – Method A (from ASTM 4546-08)

Method B, which is referred to as "single point wetting-after-loading test on a single specimen" can also be used to measure wetting-induced one-

dimensional swell (or collapse) for a natural soil (undisturbed) or a compacted soil. Test procedure is similar to method A, except that only a single specimen is tested. Typically, a vertical load corresponding to the in-situ overburden stress is used as constant normal load, or if the free swell strain is required, only a token load (e.g. 1kPa to 7 kPa) is applied. An example of test result from method B is shown in Figure 3.2.

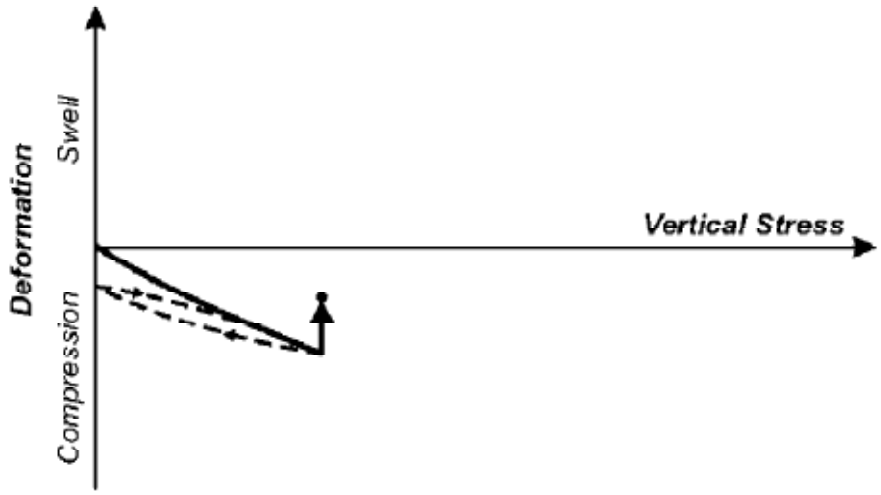

Figure 3.2. Vertical stress versus deformation – Method B (from ASTM 4546-08)

Method C is referred to as "loading-after-wetting test" because it measures load-induced deformations after wetting induced swell or collapse deformations have occurred. This method is applicable to situations where an extra load is applied to the soil that has gone through wetting-induced deformations before. Figure 3.3 illustrates an example of this method. This is also referred to as the Load-back method.

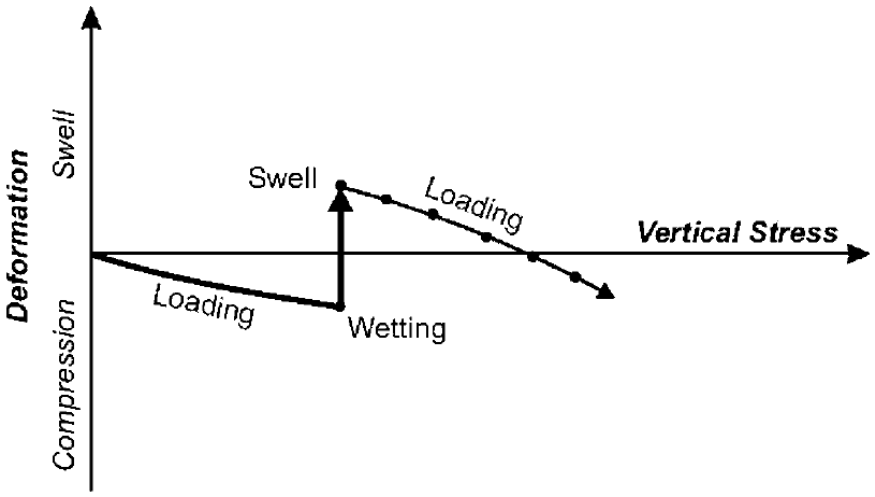

Figure 3.3. Vertical stress versus deformation for loading-after-wetting test – Method C (from ASTM 4546-08)

The abovementioned ASTM methods are currently being used widely among practicing engineers in order to determine the swelling properties of expansive soils. These techniques, along with several other direct methods have been used broadly by many researchers in order to study different aspects of swelling response of expansive soils. For instance, Al-Homoud et al. (1995) studied the effect of cyclic wetting and drying on the swell potential and swell pressure of some expansive soils. They carried out a number of CV and FS tests and found that upon repeated wetting and drying, soils showed signs of fatigue resulting in decreased swelling abilities. Similar results were found in other studies (Tripathy et al. (2002); Tripathy and Rao (2009)). According to Sridharan and Gurtug (2004) both swell pressure and swell potential are significantly influenced by the compaction energy. The load-back method was used to measure the swell pressure and swell potential of multiple samples compacted at different energy levels and the results were found to vary depending on the energy of the compactive effort applied during specimen preparation.

Many studies have reported that swelling property measurements are highly sensitive to the test method. In fact, there are some evidences that showed that a swell pressures on the same soil obtained from one test method was 10 times greater than that determined from another method test method (Kayabali and Demir (2011)). Many studies can be found in the literature that attempted to expose and explain these discrepancies by comparing various direct methods. As an example, Sridharan et al. (1986) conducted laboratory experiments to assess the effect of test method on the swell pressure measurements. Three of the most common methods have been used in this study, namely Load-back FS, CV, and "Swell under load" methods. The latter method is equivalent to method A, "wetting-after- loading test on multiple specimens" in the ASTM 4546-08 standard. They showed that the Load-back FS test gives the maximum swell pressure value while Method A in the ASTM 4546-08 gives the minimum value for swell pressure. The swell pressures values determined from the CV method were in between the other two methods. It was also reported that the swell pressure is highly sensitive to the initial dry unit weight (void ratio) while the initial moisture content, in the tested range of 0 to 18%, was found by these researchers to have less effect.

Similarly, Attom and Barakat (2000) compared three of the most common direct methods of swell pressure determination. They used six types of clayey soils from northern Jordan and measured the swell pressure using the Load-back FS, CV, and "Different Pressure" method. The latter method corresponds to method A in the ASTM 4546-08 standard. Based on their experimental data, the

Load-back FS method provided the highest swell pressure value and the "Different Pressure" method provided the lowest swell pressure.

Recently, Nagaraj et al. (2009) carried out an experimental investigation to evaluate the sources of variability of test results for two of the most popular swelling property measurement techniques: CV and Load-back methods (Load-back FS). According to the earlier studies, the Load-back technique always yields the highest swell potential and highest swell pressure. This is primarily due to the fact that in the Load-Back method the sample is allowed to expand, which allows the specimen to imbibe more water than in CV method.

Probably, the most recent published study of this comparative nature is the one from Kayabali and Demir (2011). They employed various direct testing methods to measure the swell pressure. Although they had referred to only one of their testing methods as direct, referring to other testing methods as indirect, based on the definition presented earlier in this chapter, all of their methods these authors used should be considered as direct methods. First, they assumed that CV test is the most reliable method to measure swell pressure. Then, they compared the results form CV test with the swell pressure values calculated from other methods including double oedometer, swell-consolidation, zero swell and restricted swell methods. Based on the results from CV test, they concluded that some methods underestimate the swell pressure such as the restricted swell tests whereas others, such as zero swell test and swell-consolidation test, may overestimate the swell pressure. Kayabali and Demir showed that the swell

pressure data from CV test correlated reasonably well with FS data and suggested the following relationship:

$$SP=93.3FS - 53.4 \quad (3.1)$$

Where SP is the swell pressure (σ_{zrw}) in kPa, and FS is the percent swell (swelling potential, S_{Po}) determined from the token load FS test.

3.3.2 Indirect methods

Indirect methods use empirical methods to predict the swelling properties of the soil. Rao et al. (2011) summarized a good number of the empirical-based studies for determination of swelling properties, as presented in Table 3.1. In addition to the following studies, Zapata et al. (2006) found that the Expansion Index (EI) correlates poorly with PI and percent passing US sieve number 200, when considered separately. However, the authors found that the product of these two parameters, wPI, improves the correlation drastically.

Table 3.1. Summary of indirect techniques for determination of swelling properties

Relationship	Reference
$S = kA_c^{2.44}C^{3.44}$	Seed et al. (1962)
$S = kM\text{PI}^{2.44}$	Seed et al. (1962)
$S = m_1\text{SI}^{2.67}$	Ranganatham and Satyanarayan (1965)
$S = 4.57 \times 10^{-5}[\text{SI}/(C - 13)]^{2.67}C^{3.44}$	Ranganatham and Satyanarayan (1965)
$S = 4.113 \times 10^{-4}[\text{SI}/(C - 13)]^{2.67}C^{3.44}$	Ranganatham and Satyanarayan (1965)
$\text{Log}(S_p) = 2.132 + 0.0208\text{LL} + 0.000665\gamma_d - 0.0269w$	Komornik and David (1969)
$S_p = 3.5817 \times 10^{-2}\text{PI}^{1.12}(C^2/w_i^2) + 3.7912$	Nayak and Christensen (1971)
$S_p = 2.29 \times 10^{-2}\text{PI}^{1.43}(C^2/w_i) + 6.38$	Nayak and Christensen (1971)
$\text{Log}(S) = (1/12)(0.4\text{LL} - w_n + 5.5)$	Vijayvergiya and Ghazzally (1973)
$\text{Log}(S) = (1/19.5)(6.242\gamma_d + 0.65\text{LL} - 130.5)$	Vijayvergiya and Ghazzally (1973)
$\text{Log}(S_p) = 0.9\text{-}(\text{PI}/w_0) - 1.19$	Schneider and Poor (1974)
$S = 7.5 - 0.8w + 0.203\text{CL}$	McCormack and Wilding (1975)
$\text{Log}(S_p) = -2.89 - 7w + 6.65\text{CL}$	McCormack and Wilding (1975)
$S = 2.77 + 0.131\text{LL} - 0.27w_0$	O'Neil and Ghazzally (1977)
$\text{Log}(S) = 0.036\text{LL} - 0.0833w_0 + 0.458$	Johnson and Snethen (1978)
For $\text{PI} \geq 40$, $S_p = 23.82 + 0.7346\text{PI} - 0.1458H - 1.7\ w_0 + 0.0025\text{PI}w_0 - 0.00884\text{PI}H$	Johnson (1978)
For $\text{PI} \leq 40$, $S_p = -9.18 + 1.5546\text{PI} + 0.08424H + 0.1w_0 - 0.0432\text{PI}w_0 - 0.01215\text{PI}H$	Johnson (1978)
$S_p = 0.0446\text{LL} - 1.572$	Nayak (1979)
$S_p = 0.057\text{PI} - 0.566$	Nayak (1979)
$S = 0.000195\text{LL}^{4.17}w^{-2.33}$	Weston (1980)
$S = 0.0000114A_c^{2.558}\text{CL}^{3.44}$	Bandyopadhyay (1981)
$S = 0.2558e^{0.0838\text{PI}}$	Chen (1988)
$S = 41.161A_c + 0.6236$	Cokca (2002)
$S = 0.0763\psi_i - 339.03$	Cokca (2002)
$\text{Log}(S_p) = -4.812 + 0.01405\text{PI} + 2.394\gamma_d - 0.0163w_i$	Erzin and Erol (2004)
$\text{Log}(S_p) = -5.197 + 0.01405\text{PI} + 2.408\gamma_d - 0.819I_L$	Erzin and Erol (2004)
$\text{Log}(S_p) = -5.020 + 0.01383\text{PI} + 2.356\gamma_d$	Erzin and Erol (2004)
$S_p = 63.78e^{0.1528S}$	Sridharan and Gurtug (2004)
$S_p = 12.5(0.001\psi)^{0.25}$	Thakur and Singh (2005)
$S_p = 25(0.001\psi)^{0.25}$	Thakur and Singh (2005)
$S_p = -8.04 + 0.0177\text{PI} + 4.390\gamma_d + 0.540\log\psi$	Erzin and Erol (2007)

Where the symbols used in table 3.1 are:

A_c: activity

C, CL: clay content

G_s: specific gravity of solid

H: depth of soil

I_L: liquidity index

K, m1, M: constants

LL: liquid limit

PI: plasticity index

PL: plastic limit

S, SP, S_{Po}: percentage swelling, swelling potential

FSI: free swell index

SI: shrinkage index

LI: liquidity index

e_0: initial void ratio

q_i: initial surcharge (kPa)

w: moisture content (%)

w_i, w0: initial moisture content (%)

w_n: natural moisture content (%)

σ_{zrw}: swell pressure, sigma zero response to wetting

γ_d: dry unit weight

γ_{di}: initial dry unit weight (kN/m^3)

ψ_i: initial soil suction

ψ: total suction

Yilmaz (2009) carried out an experimental investigation to determine the empirical relationship between liquidity index (LI) and swelling potential (S_{Po}) of clay samples selected from five areas in Turkey. The correlation coefficient of 0.87 was reported for the following equation:

$$S_{Po} = 2.0981e^{(-1.7169LI)} \quad (3.2)$$

Rao et al. (2004) proposed relationships to predict swelling properties of remolded and compacted expansive soils using the Free Swell Index (FSI). Their study was based on experimental data for soil samples from 10 different locations. Following equations were developed by performing multiple linear regression

analysis on the entire experimental dataset for predicting swell potential (S_{Po}) and swell pressure (σ_{zrw}):

$$S_{Po} = 4.24\gamma_{di} - 0.47w_i - 0.14q_i + 0.06\ (FSI) - 55 \quad (3.3)$$

$$\text{Log}\ \sigma_{zrw} = 0.30\ \gamma_{di} - 0.02w_i + 0.005\ (FSI) - 3 \quad (3.4)$$

Johnson and Snethen (1978) proposed the following relationship to calculate the swell pressure from total soil suction measured using a psychrometer:

$$\text{Log}\ \sigma_{zrw} = A-((100B\times e_0)/G_s) \quad (3.5)$$

Where A and B are the intercept and slope of the logarithm of suction versus water content plot respectively.

Cokca (2000) performed a similar investigation and measured the suction for different samples with wide range of plasticity and water contents. Then the swell pressure was measured in accordance with CV test procedure and the swell pressure was plotted versus the log of suction. Results suggested the following linear relationship between the logarithm of initial suction and CV swell pressure measured in the oedometer:

$$\sigma_{zrw} = -4610+2975\log\psi \quad (3.6)$$

Where σ_{zrw} is the swell pressure (kPa) and ψ is the total soil suction (kPa). Cokca indicated that the relationship recommended earlier by Johnson and Snethen (1978) overestimates the ultimate swell pressure to some extent.

3.3.3 Heave prediction methods

Many heave prediction methods make use of one dimensional oedometer test results. A list of various methods utilizing the oedometer test results is

presented in Table 3.2. Among these methods, the direct model method (The Texas Highway Department Method TEX-124-E) and the Jennings and Knight "Double Oedometer Method" are the most common methods used by practicing engineers due to their simplicity yet applicability to the field conditions. Nonetheless, Abdullah (2002) postulates that these methods overestimate the heave for conditions in field that are not one dimensional. Thus, he introduced a "Heave Reduction Factor", R_f, to account for lower observed field heave. Abdullah's experimental investigations showed that R_f decreases significantly as the footing pressure increases. For example, for the direct method (Texas Highway Department Method TEX-124-E), R_f reduced from 0.92 to 0.62 as the footing pressure increased from 25 kPa to 50 kPa. In his laboratory testing program, he compacted a clayey soil inside a metal box container and placed a model footing at the center of the soil surface to be able to apply different pressures (25 and 50 kPa). Then he gave the soil free access to water and monitored the surface deformations (swell/heave), using pre-installed dial gauges, until no more deformation has occurred. Abdullah considered the results from this test as the actual values for heave and compared it against the values estimated from two of the most common heave prediction methods, namely double oedometer method (Jennings and Knight (1957)) and the direct method (Texas Highway Department Method TEX-124-E). Both of these methods are based on one-dimensional oedometer test results but double oedometer method allows the soil specimen to swell under a token load (≈1kPa) while the direct method requires a field stress level to be applied on the soil specimen before it is allowed

to swell. In general, Abdullah considered the direct method to be a more accurate method than the double oedometer method.

Table 3.2. Various Heave prediction methods utilizing oedometer test results (from Singhal (2010) which was edited from Fredlund and Rahardjo (1993))

Name of the Method	Country of Origin	Reference
1. Double Oedometer method	South Africa	Jennings and Knight (1957); Burland (1962); Jennings (1969)
2. Salas and Serratosa method	Spain	Salas and Serratosa (1957)
3. Volumemeter method	South Africa	de Bruijn (1961)
4. Mississippi method	U.S.	Clisby (1962); Teng et al. (1972); Teng et al. (1973); Teng and Clisby (1975)
5. Sampson, Shuster, and Budge's method	U.S.	Sampson et al. (1965)
6. Noble method	Canada	Noble (1966)
7. Sullivan and McClelland method	U.S.	Sullivan and McClelland (1969)
8. Komornik, Wiseman, and Ben-Yacob method	Israel	Komornik et al. (1969)
9. Holtz method	U.S.	Holtz (1970)
10. Navy method (Direct Method)	U.S.	NAVFAC (1971)
11. Wong and Yong	U.K.	Wong and Yong (1973)
12. U.S.B.R. method	U.S.	Gibbs (1973)
13. Simple Oedometer method	South Africa	Jennings et al. (1973)
14. PVR Method (Texas Highway Department)	U.S.	Smith (1973)
15. Controlled strain test	U.S.	Porter and Nelson (1980)
16. Heave index method	U.S. (Denver)	Nelson et al. (1998)
17. Fredlund, Hasan and Filson's method	Canada	Fredlund et al. (1980)

After reviewing the most common heave prediction methods, it was found that the effect of soil cracks has been neglected in almost all of the methods. Only Lytton (1994) introduced the crack effects into his model. He suggested that volumetric strain, $\Delta V/V$, is linearly related to the logarithm of total stress and matric suction. Then he introduced *f*, crack fabric factor, to compute vertical strain, $\Delta H/H$, using previously calculated volumetric strain ($\Delta V/V$) for intact specimens, as illustrated in equation 3.7. Back-calculated from field observations of heave and shrinkage, he proposed crack fabric factors of 0.5 and 0.8 for drying and wetting conditions, respectively.

$$\frac{\Delta H}{H} = f \frac{\Delta V}{V} \tag{3.7}$$

It was found, from the literature review, that the effect of soil cracking on the swelling response of expansive soils has not yet been fully understood or investigated. In this study, a laboratory investigation was performed to study the effect of soil cracking on swell pressure and swell potential of an expansive soil, and to gain insight into possible approaches for inclusion of soil cracking in making heave estimates for field conditions.

3.4. Experimental investigations

Various direct measurement techniques were employed to determine and compare the swelling response (swell pressure and percent swell) of cracked and intact soils. As pointed out earlier in this chapter, there are several methods for measurement of the swell pressure of an expansive soil. Preliminary experiments were conducted using the most common direct methods including: constant volume (CV), Load-Back FS, and wetting-after-loading tests on multiple specimens (Method A). After examination of these three methods, it was concluded that Method A gives the most reproducible results in the absence of computer control CV testing equipment. Errors in swell pressure introduced due to specimen variability were minimal because only compacted specimens were used for this study.

The tests were performed utilizing an oedometer-type device. A 1,000 lb load cell with 0.05 lb resolution was calibrated and used to monitor and control the vertical load, and an LVDT (Linear Variable Differential Transformer) with

0.0005 mm (0.00002 in) resolution was employed to monitor the vertical deformations.

3.4.1 Materials

The soil used in this study was Otay Clay obtained from a site near San Diego, California (from now on the soil will be referred to as San Diego soil). The reason behind selecting a clayey soil was that these types of soils are susceptible to desiccation cracking and they also exhibit some volume change during the wetting/drying seasons. Basic index and soil characterization tests were performed, in accordance with current ASTM standards, as shown in Table 3.3. The test results are shown in Table 3.4, Figure 3.4 (gradation plot for this soil, including hydrometer), and Figure 3.5 (Standard Proctor curve). The San Diego soil is classified as a Sandy Lean Clay (CL).

Table 3.3. Summary of the basic tests performed

Soil Test	ASTM Specification
Sieve Analysis and Hydrometer	ASTM D 422-63: Standard Test Method for Particle Size Analysis of Soils
Atterberg Limits	ASTM D 4318-00: Standard Test Methods for Liquid Limits, Plastic Limit, and Plasticity Index of Soils
Specific Gravity	ASTM D 854-02: Standard Test Methods for Specific Gravity of Soil Solids by Water Pycnometer
Standard Proctor Compaction Test	ASTM D 698-00: Standard Test Methods for Laboratory Compaction Characteristics of Soil Using Standard Effort
Expansion Index	ASTM D 4829-03: Standard Test Method for Expansion Index of Soils
Swell	ASTM D 4546-03: Standard Test Methods for One Dimensional Swell or Settlement Potential of Cohesive Soils
Consolidation	ASTM D 2435-04: Standard Test Methods for One Dimensional Consolidation Properties of Soils Using Incremental Loading
USCS Classification	ASTM D 2487-00: Standard Practive for Classification of Sloils for Engineering Purposes (USCS)

Table 3.4. Basic index properties of San Diego Soil

Specific Gravity		2.72
Particle Size Analysis	% Sand	63
	% Silt	30
	% Clay	7
Unified Classification System		SC
Atterberg Limits	LL	41
	PL	17
	PI	24
Standard Proctor Test	Optimum water content	18%
	Max Dry Density (g/cm3)	1.74
Expansion Index (ASTM)		115

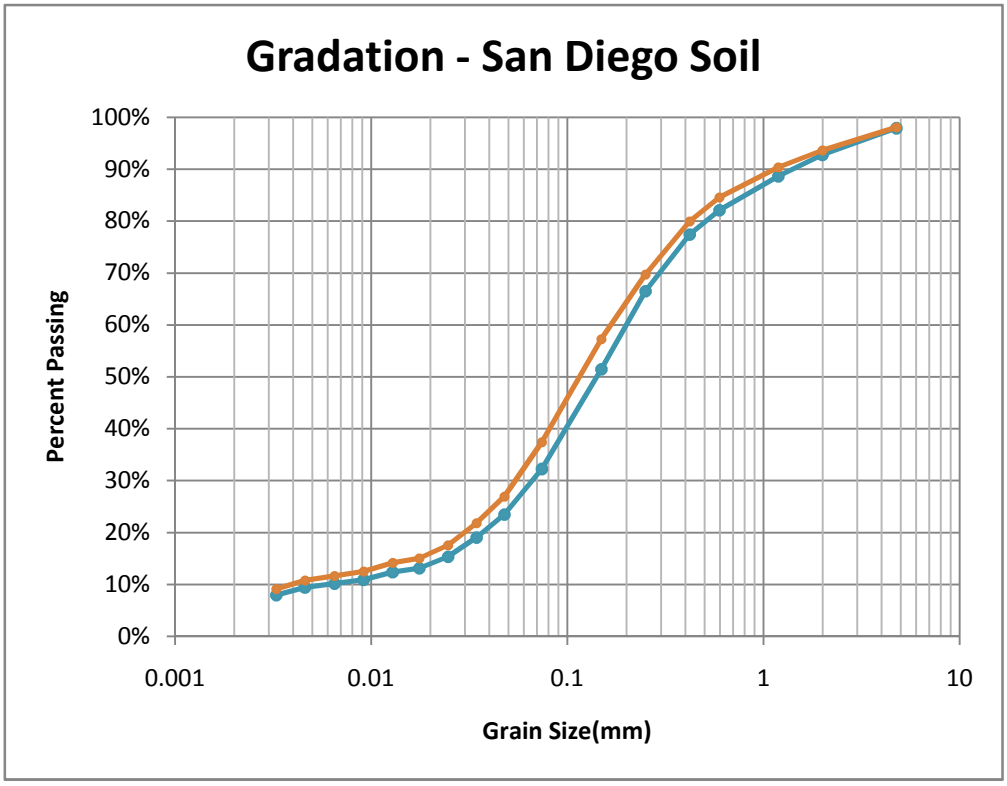

Figure 3.4. Gradation results for San Diego Soil

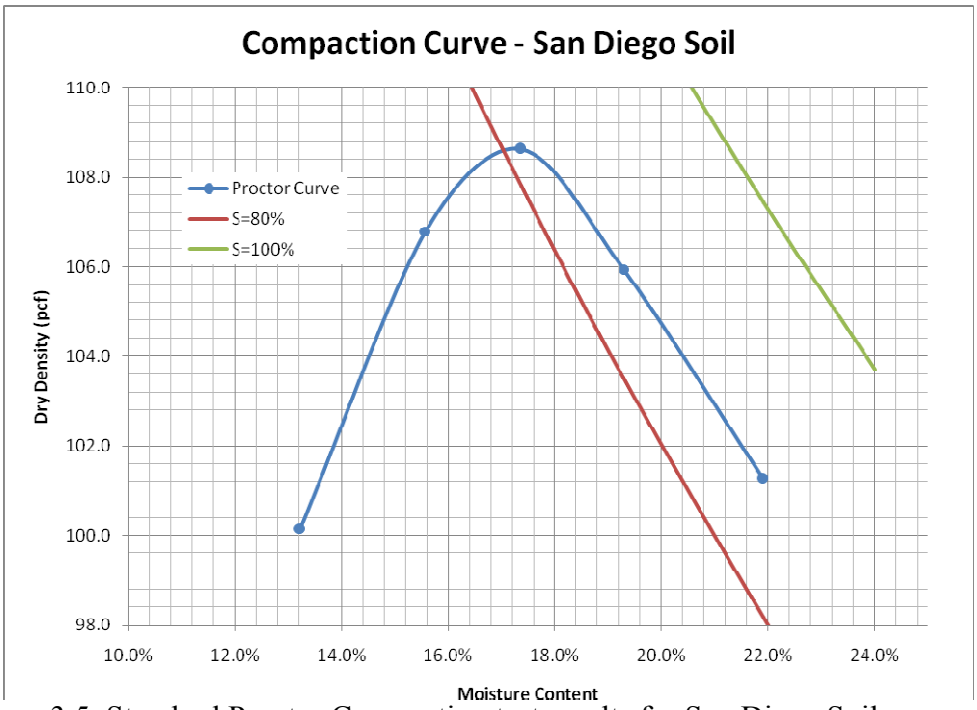

Figure 3.5. Standard Proctor Compaction test results for San Diego Soil

3.4.2 Test procedures

A step by step procedure for conducting swell pressure measurement using method A from ASTM 4546-08 is presented here. As reported in many studies, swell potential and swell pressure measurements are sensitive to the test method used. This is due to the many different factors that can affect the test results. For example, initial moisture content, density, system compressibility/compliance, temperature, relative humidity, identical degree of saturation of the specimen, to name a few factors, can have a significant effect on the swell potential and swell pressure of a specimen. Therefore, to measure swell pressure or swell potential (percent swell) of a sample, it is important to carefully follow test procedure (e.g. ASTM) and to report specimen conditions prior to initiation of the swell test. Consistency and accuracy of the test procedure is the key to generating reliable

and reproducible test results. This section is divided into two parts. First, the sample preparation method is discussed in detail for both intact and cracked specimens and next the experimental set up and testing method is explained.

3.4.2.1 Sample preparation method

Prior to embarking on the specimen preparation, a large quantity of San Diego clay was thoroughly broken up and mixed to ensure as much uniformity of material batches as possible. In this process, first a large heavy-duty plastic sheet was placed over a relatively flat surface. Then the San Diego soils from different batches (buckets) were damped on the plastic sheet for breaking and mixing the soil using a shovel. After obtaining a desired homogeneity, the San Diego soil was poured back into the buckets. To provide the best uniformity and consistency between different buckets, all of them should be refilled simultaneously. This means that instead of filling one bucket first before going to the next bucket, all of the buckets should be filled gradually and together.

All of the samples were compacted in three equal layers inside brass ring of 25 mm height and 61 mm diameter to 98% of standard proctor maximum dry density (1.74 g/cm^3) at optimum water content (18%). Soil was first passed through a #4 (4.76 mm) sieve, and then enough water was added to reach to the optimum water content of 18%. Then the soil was left inside a sealed plastic bag for at least 48 hours before starting the sample compaction. This "curing" process is to allow the water inside the soil to equilibrate throughout the soil, so that the moisture would distribute uniformly. After the compaction of each layer is completed and just before starting the compaction of the next layer, the top

surface of the preceding layer was scarified using a sharp tool. This is to generate a better contact between the two layers and produce a more uniform compacted specimen. During the compaction of the last (third) layer, care was taken not to over-compact the specimen. In a perfect compaction, the top soil layer should be leveled with the top part of the ring; however, if some small amount of soil extended above the top of the ring, the specimen surface was trimmed and leveled and any minor adjustments to dry density were made. After the last layer is compacted, the sample was weighed and it was ready for the test. Specimens were placed as immediately as possible into the oedometer device, and were protected against drying prior to placement. Figure 3.6 shows an example of an intact specimen.

Figure 3.6. An example of an Intact compacted specimen

To create a cracked specimen, first an intact specimen was prepared according to the procedure indicated above. Afterwards, aluminum shims of 0.025" thickness were used to create the cracks. After reviewing many different field and laboratory crack patterns through a combination of a literature and

laboratory study, it was concluded that the hexagon pattern was most appropriate because it was most consistent with the actual crack patterns. An example of a cracked specimen is shown in figure 3.7 below.

While preparing a cracked specimen for conducting a swell pressure test, it is very important to check the level of the top of the soil sample after the crack creation process is completed. Sometimes during the crack creation process, especially while removing the shim upward, the soil layer is slightly heaved. This can cause some errors later while conducting a swell pressure test. To overcome this problem, after all the cracks were created, the cracked surface was slightly compacted back to the same level as the top of the ring.

Figure 3.7. An example of different stages of creating a cracked specimen

3.4.2.2 Swell pressure measurement test set up

The main purpose of these experiments was to study the effect of cracks on swelling response of the subject soil. Cracked and non-cracked (intact) specimens were prepared and tested to capture the influence of cracking on the swelling properties of the soil. An oedometer type device was utilized to conduct the swell pressure measurement test using method A in accordance with ASTM Standard 4546-08. In this method, multiple identical specimens are prepared and

each is tested under a different vertical load (net normal stress). Typically the testing sequence starts with the lowest normal stress (≈2 to 7 kPa in this study) and the next stress level is chosen based on the results (the magnitude of swell or collapse). The normal pressure should not be allowed to exceed the target value during test set up. The step by step procedure of the swell pressure measurement test is as follows:

Step 1- Check the load cell and the LVDT for an accurate reading. Also, before starting the test, one should be aware of the load ranges being used through the whole testing program, so that an appropriate load cell and LVDT can be employed.

Step 2 – The load cell should be pulled all the way up for ease of access while centering the sample in place.

Step 3 – the consolidometer or the device in which the specimen is placed should be checked to ensure that water circulation paths are clean and clear so that the inundation process takes place efficiently. Regardless of the method being used, the results are highly sensitive to the final degree of saturation of the sample. Consequently, if the sample does not have free access to water due to any reason, results will not be satisfactory.

Step 4 – Two previously boiled and air-dried porous stones are required to keep sample safe from erosion during the saturation process and also to prevent direct contact between the load cell and the soil surface. The top porous stone diameter should be 0.2 to 0.5 mm smaller than that of the ring as recommended by ASTM 2435-04.

Note 1 – Filter paper is not required between soil and porous stones due to its high compressibility.

Step 5 – After placing the porous stones and the specimen, they should be centered under the load cell to prevent any eccentricity during the loading process.

Step 6 – The load cell reading value should be reset to zero and then it should be pulled down carefully until it contacts the sample and creates the token stress level (e.g. 1 to 7 kPa).

Step 7 – Normal deformation reading value should be reset to zero mm.

Step 8 – Should the swell test be the for token load stress, go to step 12.

Step 9 – Normal load should be gradually increased to the target value (stress) at which the percent swell (compression) is to be determined, but to prevent sample from drying, the total loading time should not exceed 1 hours according to ASTM 4546-08.

Once again, care should be taken not to exceed the desired load (stress). If the target stress is exceeded, the specimen is not suitable and a new specimen must be prepared.

Step 10 – After the desired load (stress) is achieved, some time is required for the load to settle on the specimen (equilibration time). Typically, 10 minutes is adequate.

Step 11 – Normal deformation should be recorded and the LVDT re-zeroed after the load is settled.

Step 12 – The test specimen is now inundated and given free access to water. Test duration is dependent on the soil type and soil condition (e.g. density). Typically 24-72 hours is enough for most of the soil types because the primary swell would occur during this period. For this study, 24-36 hours was found to be sufficient. For high plasticity clays longer equilibration times are required.

The testing system used in this study is depicted in Figure 3.8. Also, Figure 3.9 illustrates the main steps of test set up for the Method A, ASTM 4546-08 experiment.

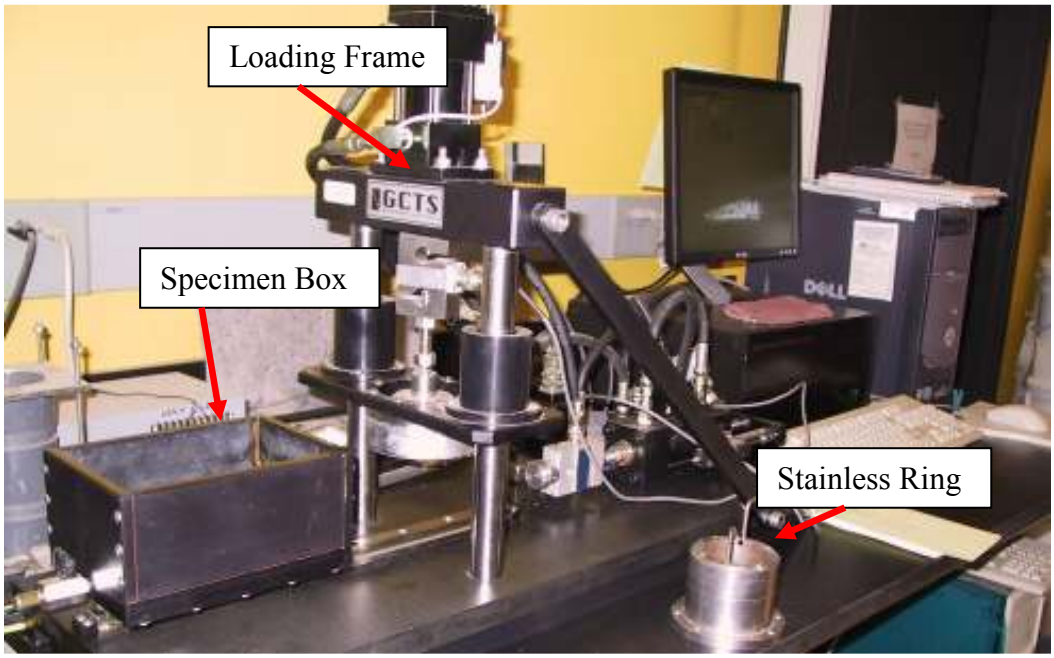

Figure 3.8. General view of the machine used in performance of swell tests

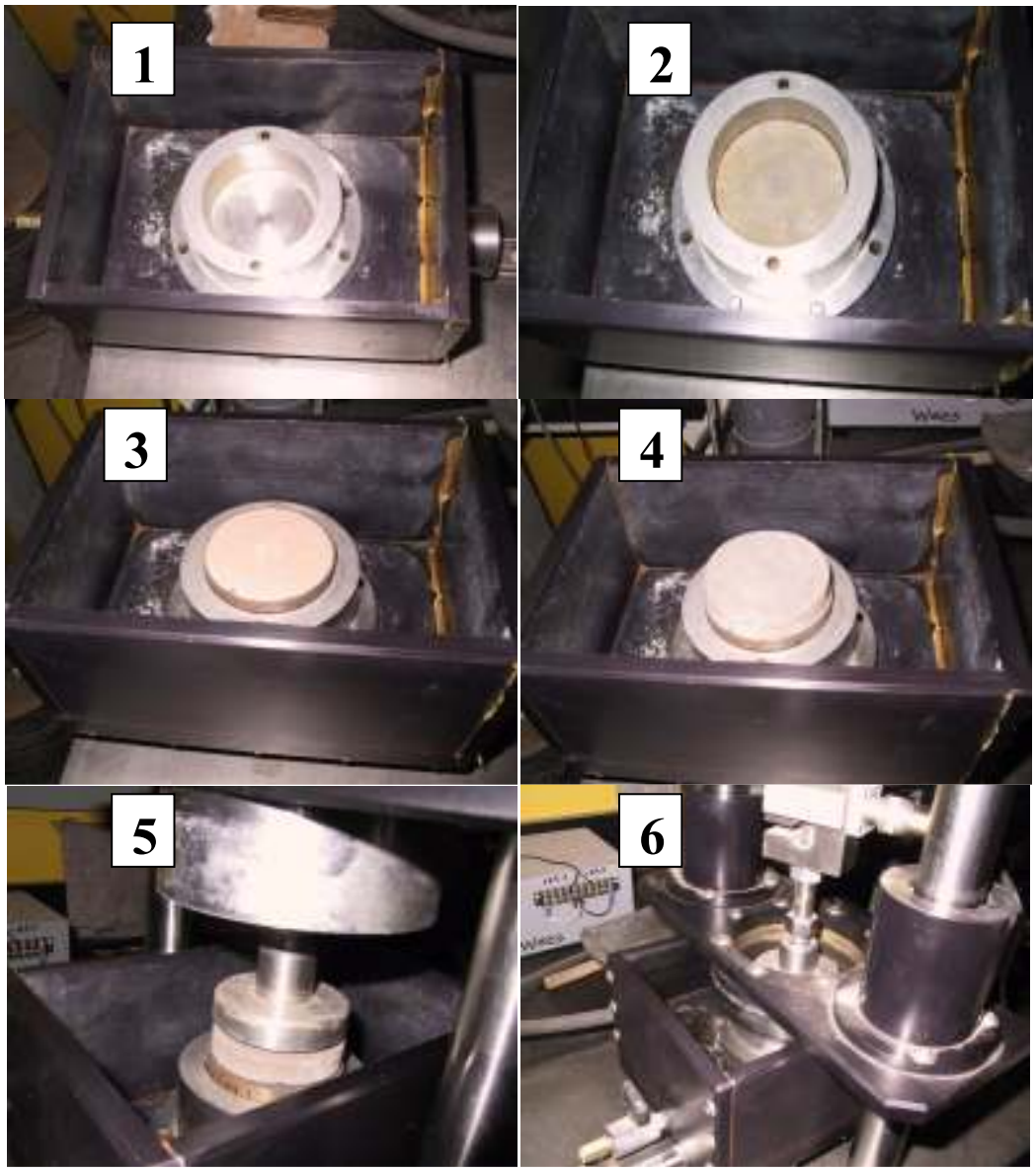

Figure 3.9. Test setup for conducting the Method A, ASTM 4546-08, swell pressure measurement test

3.4.3 Results and discussions

An experimental investigation was performed to study the effect of soil cracking on swelling and volume change properties of the subject soil. Among various test methods used to evaluate the swelling properties of soil, method A, wetting-after-loading test on multiple specimens, in accordance with ASTM 4546-08 was selected for this study, because preliminary investigations showed a

better correlation and consistency for this method. Comparison of results for intact and cracked specimens was used in order to assess the effect of soil cracks in swell pressure measurements. First, the swell pressure was measured for multiple intact (non-cracked). All of the specimens were prepared identically and the only difference was the initial vertical load that was applied to the specimens prior to inundating the sample. Once the swell pressure of the intact samples was determined, swell pressure for the cracked specimens were obtained. To be consistent with the entire research program, which included many elements of study of cracked San Diego clay, the same hexagonal patterns were used for all of the cracked samples. To investigate the effect of crack density (volume of cracks) on swelling pressure and swell potential, two types of cracked specimens were prepared with different crack volumes of 3% and 1.5% respectively. The crack pattern was the same for both types, as well as the crack widths which was around 1.0 mm. The crack depth was varied to achieve the crack volume percentages of 3% and 1.5%. The crack depth was decreased from 12.0 mm for 3.0% volume cracked volume specimen and 6.0 mm for the 1.5% crack volume specimen.

First, swell pressure was determined for intact (non-cracked) specimens, followed by swell pressure of 3.0% volume cracked and 1.5% volume cracked samples. The test results from these tests not only demonstrate the differences between the cracked and intact swell pressures, but they can also be used to evaluate the effect of crack density on percent swell.

The results for swell pressure of the intact specimens are given in figure 3.10. Test method A, wetting-after-loading test on multiple specimens, was

performed in accordance with the ASTM 4546-08 standard. Two sets of tests were performed to examine the reproducibility of the experiment. As can be seen in figure 3.10, results from the two tests, intact-01 and intact-02, are well agreed with each other, and the percent swell values at each stress level were averaged for comparison to the cracked specimens.

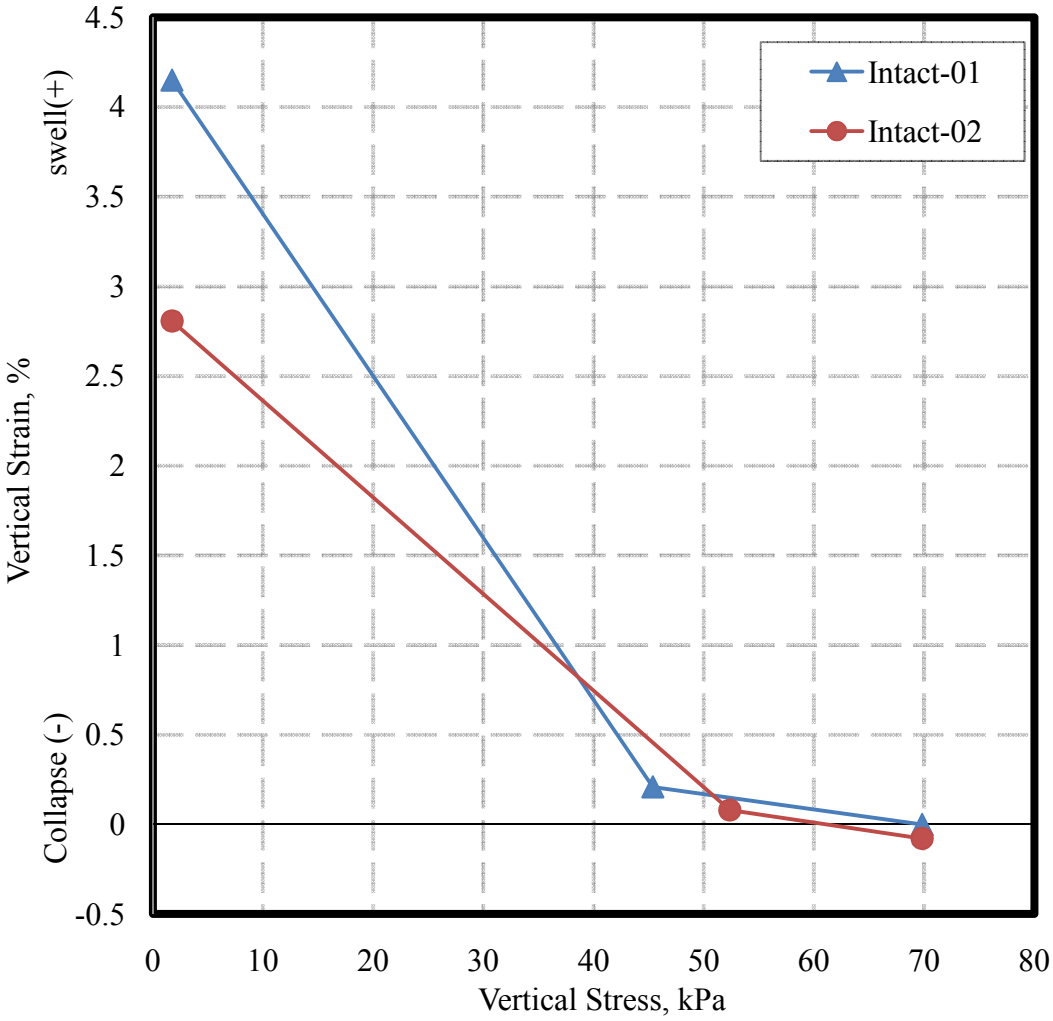

Figure 3.10. Vertical Stress vs. Wetting-Induced Swell/Collapse Strain for Intact Specimens

To evaluate the effect of soil cracks on swell pressure, similar experiments were conducted for multiple cracked specimens with different initial crack

volumes. Previous laboratory investigations suggested that the volume of desiccation cracks for San Diego soil after cycles of wetting and drying is somewhat between 1% and 4% of the total volume of the soil sample. Hence, two cases of 1.5% and 3.0% volume cracked specimens were considered to be studied for the volume change evaluation. Figure 3.11 shows the results for both 1.5% and 3.0% volume cracked and specimens.

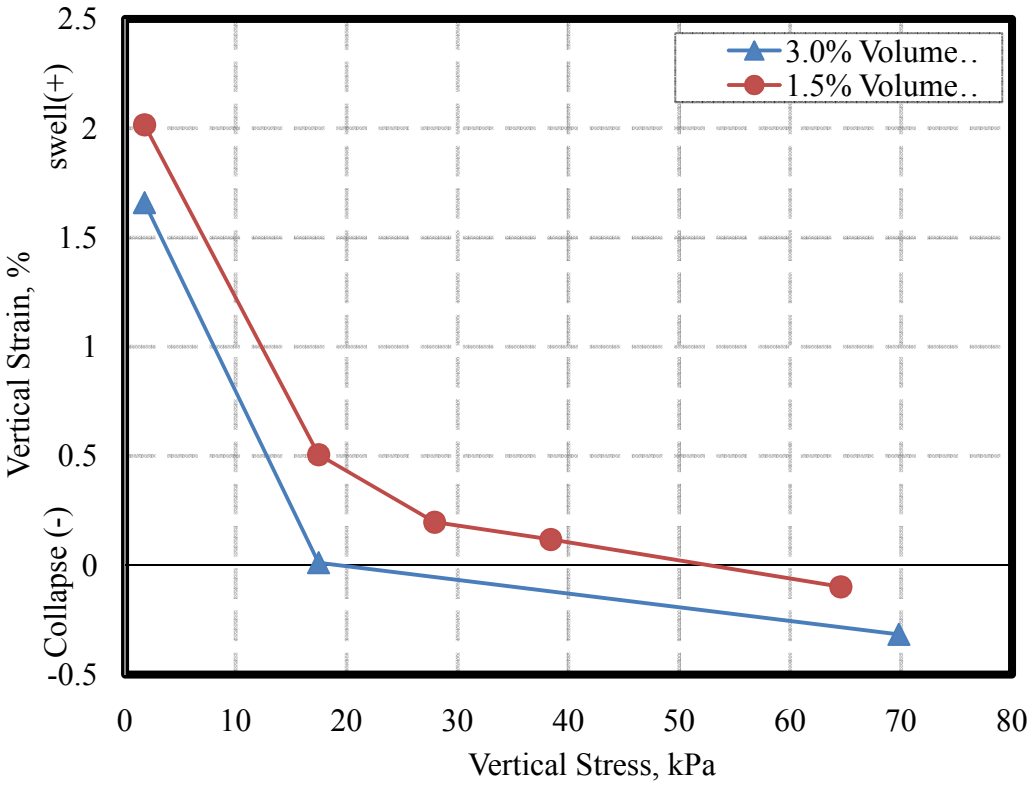

Figure 3.11. Vertical Stress vs. Wetting-Induced Swell/Collapse Strain for Cracked Specimens

According to figures 3.10 and 3.11, the shape of the stress-strain curves appear to be somewhat exponential, which is consistent with the literature (See figure 3.1) and the typical finding that percent swell versus log of net normal stress is approximately linear over a wide range of stress. Additionally, these experimental results suggest that the swell pressure of the intact (non-cracked)

soil is greater than that of the cracked soil. This is because the cracked soils have more void spaces and these spaces can accommodate the swell of the soil partially or completely, depending on the volume of the cracks. This also explains why the swell pressure for 1.5% volume cracked specimen was higher than that for 3.0% volume cracked specimen. Theoretically, there should be a crack density (volume) for each soil for which zero swell pressure is realized; although it is likely that the configuration of cracks (spacing of cracks) has some impact as well and if cracks are very widely spaced some heave would be anticipated between cracks. This question of effect of crack spacing was not addressed in this study and remains a research question for future studies.

Swell pressure prediction is an essence for all the heave prediction methods as well as for foundation design purposes (Al-Shamrani & Al-Mhaidib (1999); Nagaraj et al. (2009); Rao et al. (2004); Das and Samui (2010); Windal and Shahrour (2002); etc.) As can be noticed from conducted laboratory results, there is always some degree of variability associated with these types of tests which makes it difficult to obtain a precise swell pressure.

It is a common practice to plot the stress vs. strain relationships on a semi-log plot (figures 3.12 and 3.13).

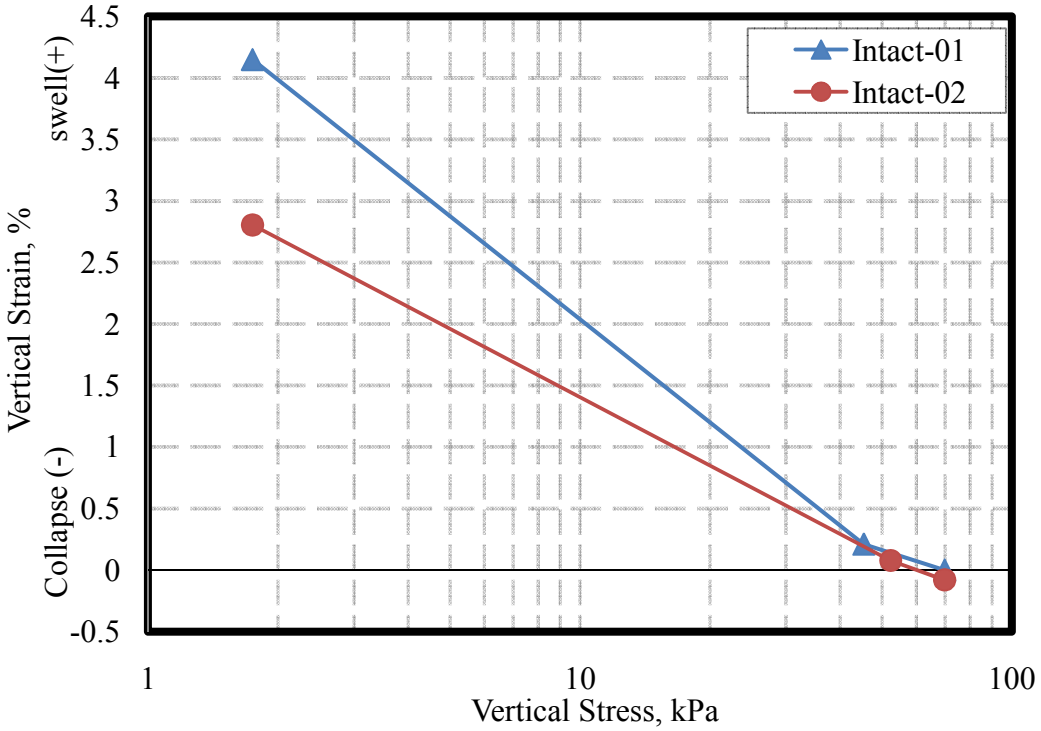

Figure 3.12. Vertical Stress vs. Wetting-Induced Swell/Collapse Strain for Intact Specimens (Semi-log plot)

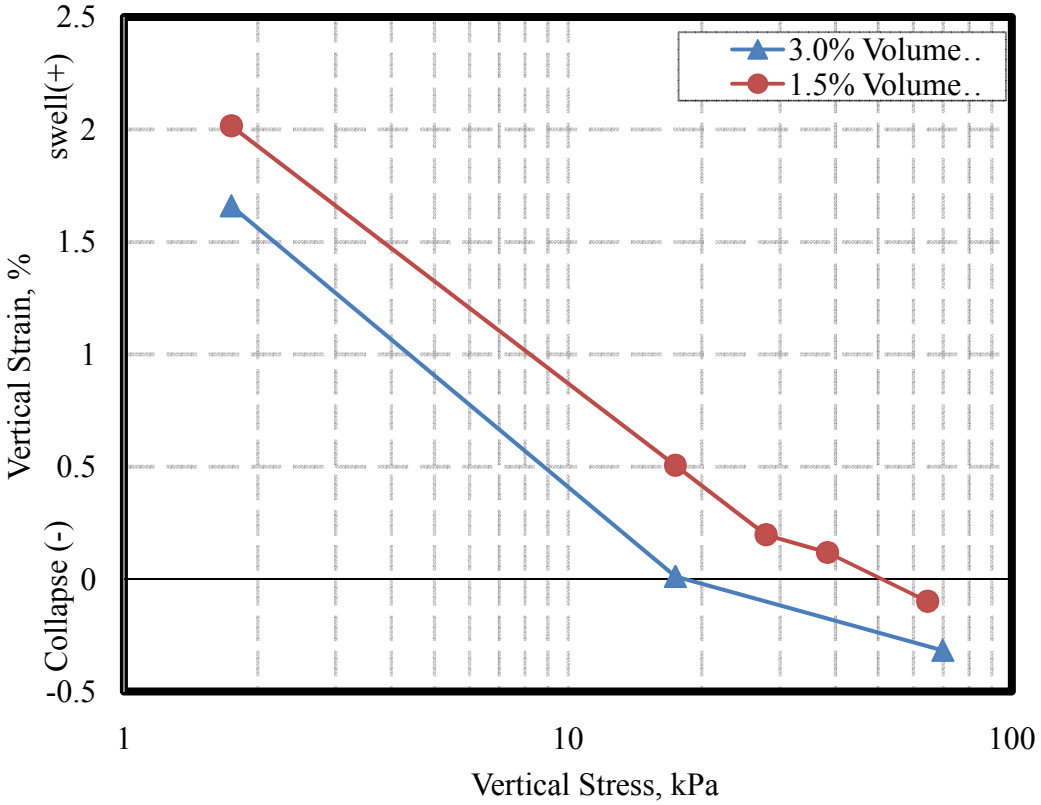

Figure 3.13. Vertical Stress vs. Wetting-Induced Swell/Collapse Strain for Cracked Specimens (Semi-log plot)

In the semi-log plots, the stress-strain relationship can be approximated by a straight line over a wide range of stress for most soils. Many studies have shown percent swell versus log of normal stress as approximately linear (e.g. Borgesson (1985), Alshamrani and Al-Mhaidib (1999) and Abdullah (2002)). Results for each test are presented individually in Figures 3.14 to 3.17 including the trend-line and its position relative to the actual laboratory data. Figure 3.18 is plotted only for comparison purposes so that one can understand how all the four test results would compare against each other.

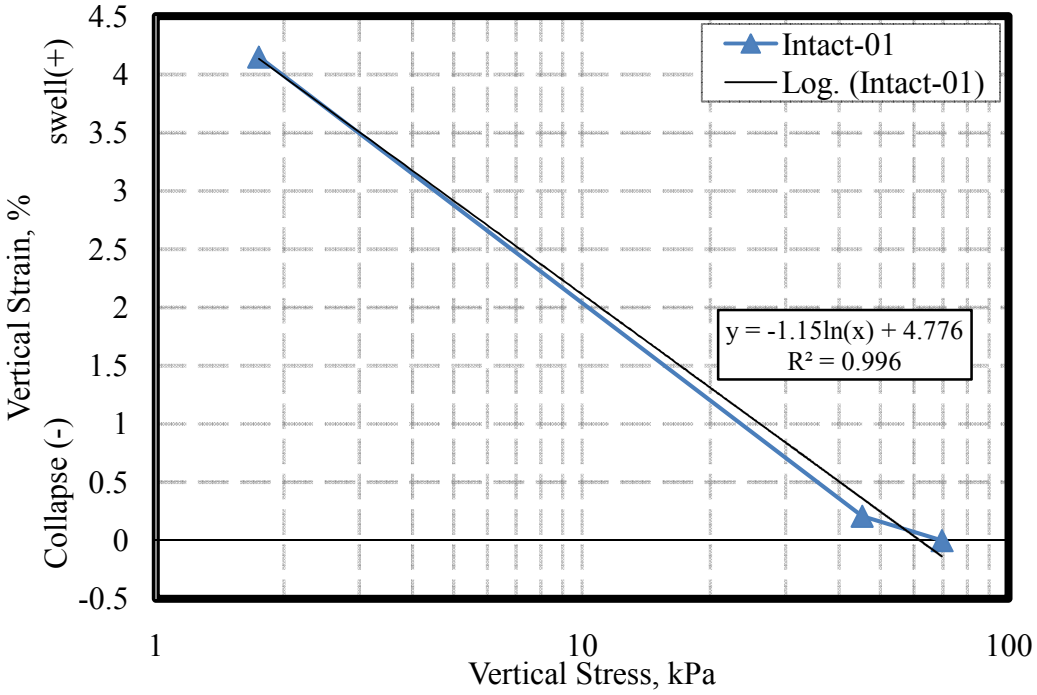

Figure 3.14. Stress vs. Strain correlation for the first intact test

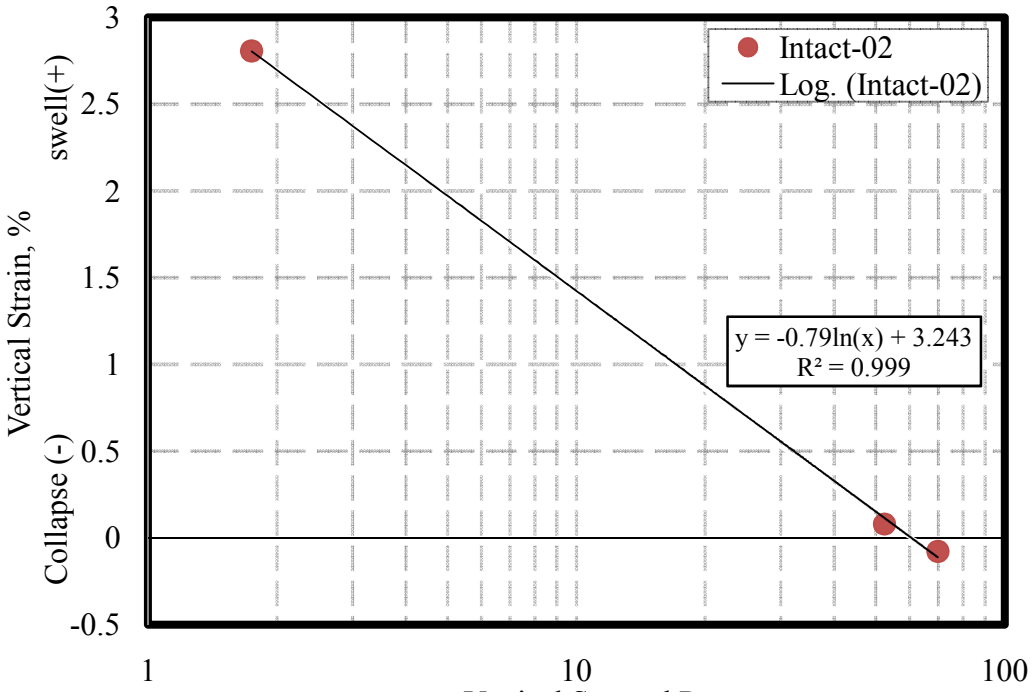

Figure 3.15. Stress vs. Strain correlation for the second intact test

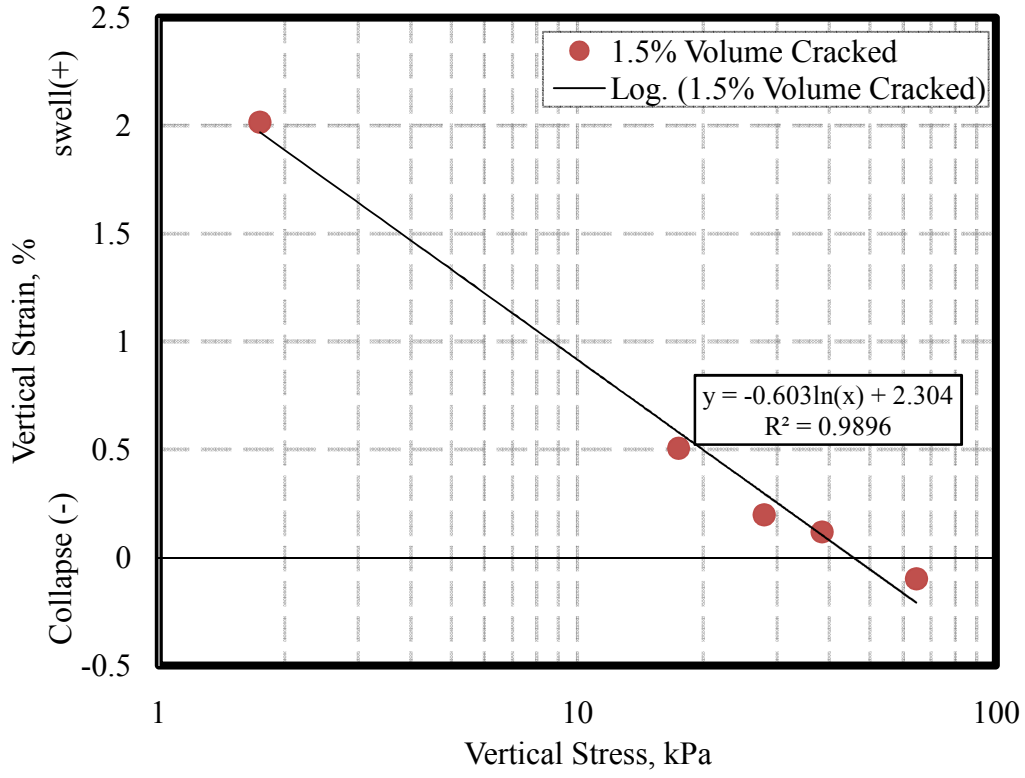

Figure 3.16. Stress vs. Strain correlation for the 1.5% volume cracked test

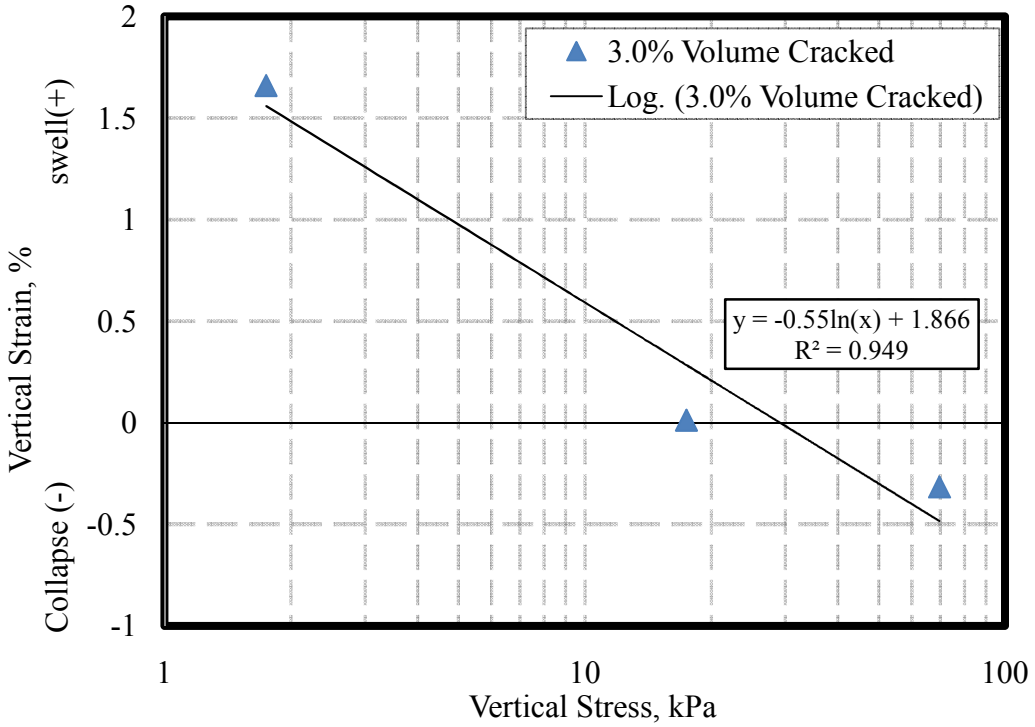

Figure 3.17. Stress vs. Strain correlation for the 3.0% volume cracked test

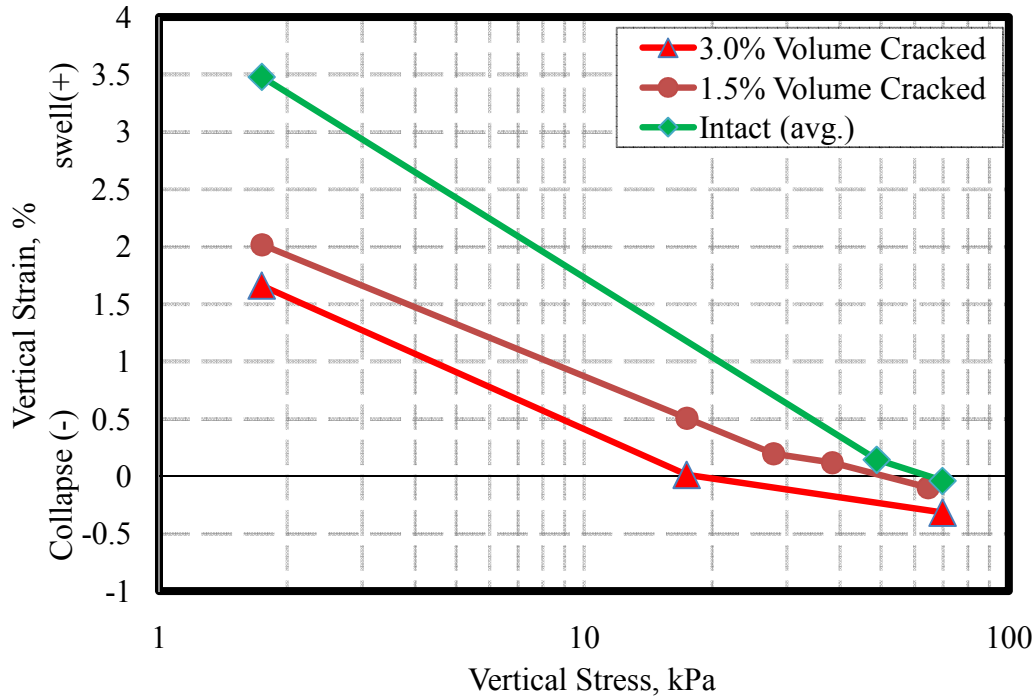

Figure 3.18. Summary plot of all the intact and cracked specimen stress-strain relationship

3.5 Analysis of data

The volume change behavior of cracks was addressed in this chapter and the influence of soil cracking on the swelling properties such as swell pressure (σ_{zrw}) and swell percentage (swell potential, S_{Po}) was also explored through experimental programs. In general, the results from laboratory investigations revealed the fact that the swell pressure reduces as cracks are introduced into the soil. Also, it was found that as the crack volume increases, the swell pressure decreases. It is valuable to study the relationship between the swell pressure and the crack volume as a percentage of the total volume. This relationship is given in figure 3.19 based on the conducted laboratory experiment results.

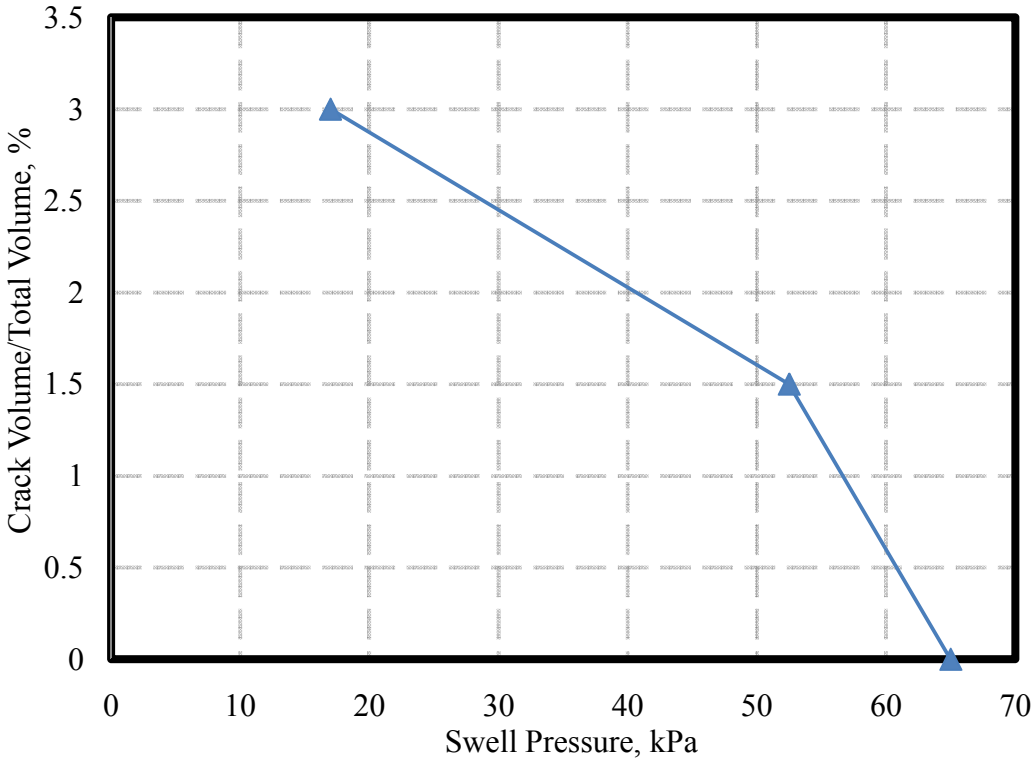

Figure 3.19. Swell Pressure relationship with Crack Volume

From another perspective, it is also important to evaluate the volume change of cracks while swelling occurs. In other words, it is critical whether or

not the cracks are closed after completion of swelling. The volume change comparison between cracked and intact specimens is intended to assess the overall volume change effect of soil cracking. As described earlier, when considering two identically prepared cracked and intact samples, the main reason that the cracked specimen has a lower swell pressure than the intact specimen is because the crack network performs as a swell-absorbent medium. In other words, for a cracked soil, some amount of the total volume change is consumed to closure of the cracks while some part of the volume change (swell) is that creating the swell pressure. This explains why the swell percentage (swell potential) of a cracked specimen is lower than that of an identical intact specimen.

Table 3.5 compares the two cracked cases with the average of the two intact cases. This quantitative comparison is based on the assumption that the swell potential for the intact matrix of both cracked and uncracked samples are more or less the same. The calculations shown in table 3.5 suggest that the cracks were closed completely after swelling for the case with 1.5% cracks but only closed by 60% for the case with 3.0% cracks. However, based on the visual observations, the cracks were closed at the end of the swelling for both cases, so it is certain that the void ratio of the material inside the visually closed cracks was increased relative to the surrounding intact matrix. That explains why the preferential flow still remains even after the visually complete crack closure. It is also possible that when the crack volume is small comparing to the swell potential, the cracks will almost completely heal, but if the crack volume is large

comparing to the swell potential, then the cracks will not completely heal which causes the preferential flow to occur.

Table 3.5. Volume change calculation for cracked and intact specimens

	Intact (avg.)	Cracked 1.5%	Cracked 3.0%
Vertical Volume Change $(cm)^3$	2.60	1.51	1.24
Initial Volume of the cracks $(cm)^3$	0.00	1.06	2.28
Intact vertical volume change minus observed vertical volume change $(cm)^3$	n/a	1.09	1.36
Percentage crack closure (%), assuming void ratio of the intact matrix is with the same as the intact specimen	n/a	100%	60%

3.6 Summary and conclusions

One of the main objectives of this study was to evaluate the effect of soil cracking on the volume change behavior of an expansive soil. The swelling properties of both cracked and intact specimens were studied utilizing a one-dimensional oedometer-type device. The results from laboratory experiments showed that introducing cracks into the soil reduces both the swell pressure (σ_{zrw}) and swell potential (S_{po}, or % swell) of the soil. Most likely, the reason behind that is the fact that the crack network can behave as a swell-absorbent medium inside the soil. It was also concluded that as the volume of the cracks increase, the more swell pressure and swell potential reduction should be expected.

At the end of each swell test, the cracks were assessed visually to estimate the degree of crack closure during the inundation and after completion of the swell process. Results showed that regardless of the initial crack volume and the applied pressure, cracks were entirely closed (visually) at the end of the test.

However, the degree of crack closure due to the wetting depends very much on various factors such as the type of soil being tested, the crack pattern, crack creation process, and the initial crack dimensions and volume. Furthermore, the visual observation is only limited to the top portions of the soil cracks and does not necessarily reveal the behavior of the cracks at deeper levels. Thus, it is wrong to assume that all of the cracks behave similar to the ones studied here and more investigation is required before any generalization can be made.

Additionally, quantitative analysis was performed to compare the initial volume of the cracks with the total volumetric swell of the specimen after completion of the swell. The main assumption for this comparison was that the swell potential for the intact matrix of both cracked and uncracked specimens are more or less the same. In this analysis, the actual measured vertical volume changes were compared against the initial volume of the cracks for each case. This analysis suggested that the cracks were completely closed only for the case with 1.5% cracks while for the case with 3.0% cracks the cracks were only 60% of the cracks were closed after completion of the swelling. Nonetheless, the visual observations of this study showed that the cracks were closed at the end of the experiments, which suggests that the void ratio of material inside the cracks were higher than that of the intact soil matrix. Furthermore, from this analysis, it can be concluded that when the crack volume is small comparing to the swell potential, the cracks will more or less heal, but if the crack volume is large then the cracks will not completely heal, resulting preferential flow through cracks even after some swell occurs.

Chapter 4

EFFECT OF CRACKS ON SATURATED AND UNSATURATED FLOW PROPERTIES

4.1 Abstract

Water, as one of the main phases of both saturated and unsaturated soils, can significantly affect the engineering behavior of most soils, especially expansive and other moisture sensitive soils. A wide range of Geotechnical problems may arise from the change in surface and ground water regime. Rainfall-induced landslides and slope stability problems and foundation heave/settlement are some common costly examples. Damage from unsaturated expansive clays alone is estimated between $11 to 15 billion per year (Nuhfer et al. (1993); Wray and Meyer (2004)). Sometimes geotechnical problems associated with changes in moisture conditions can be life-threatening. According to Spike and Gori (2003), 25 to 50 people die each year as a result of rainfall-induced landslides. While all of these catastrophic damages can occur for an intact (uncracked) soil, as the soil transitions from intact to cracked, more problems may arise. For instance, the functionality of facilities that are constructed using fine-grained soils such as waste containment facilities and mine tailing dams can be affected by hydraulic changes resulting from cracking (Yesiller et al. (2000)). Also, cracks can affect the slope stability analysis in a number of ways (Spencer, (1968); Baker (1981); Bagge (1985); Silvestri et al. (1992)). Although numerous studies can be found for measurement and estimation of flow properties of an intact soil, the effect of cracks on the flow

properties of soils has not been thoroughly understood, particularly for unsaturated flow conditions.

In this study, an extensive laboratory investigation has been conducted to better understand the effects of soil cracking on saturated and unsaturated flow properties (soil-water characteristic curve, storage function, and hydraulic conductivity). The subject soil is an expansive clay from San Diego, CA. Direct laboratory techniques have been employed to quantitatively study the effect of soil cracking on the saturated and unsaturated hydraulic conductivities and water storage properties. An instantaneous profile method (column method) was used in this study to determine the unsaturated hydraulic conductivity of both cracked and intact soils. In addition, saturated hydraulic conductivity for cracked and intact soils specimens were determined using constant head permeability tests performed in a conventional triaxial machine. Finally, an oedometer-type device (Fredlund SWCC cell) was employed to determine the Soil Water Characteristic Curve (SWCC) and associated Storage Function for the subject soil for both cracked and intact conditions.

This chapter starts with the review of the literature to detail the current state of knowledge regarding the effect of soil cracking on flow properties of soils. Following is a presentation and discussion of the extensive laboratory investigations conducted on the San Diego clay. Finally, results of the laboratory investigation are presented and discussed.

4.2 Introduction

Cracks are developed in clayey soils as the matric suction increases, particularly when confining stress is relatively low. Crack propagation always starts from the soil surface, where less confining pressure exists, and progresses downward until the confining pressure becomes large enough to prevent the cracks from forming (Fredlund et al. (2010)). There are several sources of soil cracking, but the most interesting ones for geotechnical engineers are usually desiccation and freeze and thaw cracks. When cracks are developed in a soil, they can affect the saturated/unsaturated flow properties of the soil dramatically. As one of the most common effects, numerous studies have shown that cracks increase the saturated hydraulic conductivity of soils. For example, Albrecht and Benson (2001) showed that cracks in clay liner material can increase the hydraulic conductivity of the liner up to 500 times higher than its original value. Likewise, Rayhani et al. (2007) reported that soil cracking increased the hydraulic conductivity by 12-34 times, depending on the plasticity of the soils. Similar observations have been reported by other researchers (Ritchie et al. (1972); Yuen et al. (1998); Novak et al. (2000)), although these studies are focused on saturated soils and saturated hydraulic conductivity. The focus of this particular study is unsaturated flow and unsaturated hydraulic conductivity.

4.3 Background

For the past three decades, numerous experimental investigations have been made by many researchers around the world to understand the effect of soil fissures (cracks) on hydraulic properties of expansive soils. Some of these studies

are based on field measurements while the others are based on laboratory measurements. Essentially, field experiments may be preferable to laboratory investigations because they may better reflect the actual, though complex, boundary conditions that govern the flow process in the prototype, and unlike laboratory investigations, sample disturbance does not affect the results of a field study. However, field experiments are usually large scale tests which require advanced equipment and usually cost more comparing to laboratory studies. Furthermore, laboratory measurements often allow more control on the environment and conditions and boundary conditions for the test. Some examples of field and laboratory investigations related to the effect of soil cracking on the hydraulic properties of soils are discussed below.

Arnold et al. (2005) carried out a field study at a site located in Riesel, Texas to determine the nature of soil cracking and its effects on surface runoff. In this study, the crack volume as well as the surface water runoff were physically measured and compared with the simulated values from some models previously developed by the authors. Soil anchors were placed at multiple depths to allow for measurement of the soil movement. These measurements were used by the researchers to estimate crack volume assuming an isotropic shrinkage of the soil. The comparison of actual measurements to simulations showed good agreement. The relationship between the measured crack volumes and the simulated runoff is shown in figure 4.1. It can be clearly seen that the runoff will not occur while the crack volume is high. Essentially, during the rainfall events more water infiltrates through the soil which creates some soil expansion (swell) and eventually

decreases the volume of cracks. The critical calculations of this study, however, are based on the saturated filed conditions.

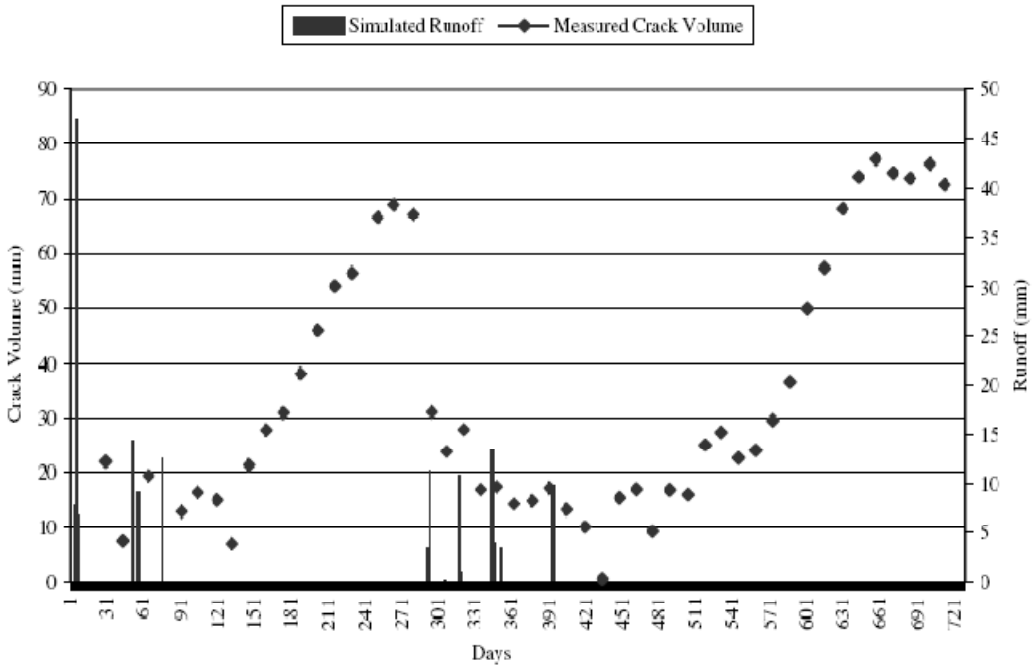

Figure 4.1. Relationship between crack volume and surface runoff (From Arnold et al. (2005))

Bouma (1980) studied the movement of water through swelling clays soils. Undisturbed large soil columns with diameter of 30 cm and height of up to 40 cm which were incased in gypsum were used and the saturated hydraulic conductivity (k_{sat}) was measured using an infiltrometer. The condition of the tested soil was nearly saturated prior to infiltration. Results from around 80 measurements of k_{sat} for soils between 30 to 70 cm below the surface ranged from 1 cm/day for the soil that had been allowed to swell (thus with reduced crack widths) to 5m/day for some initially dry soils with large cracks. Bouma also mentioned that the infiltration rate into the cracked soil changes with time as shown in figure 4.2. For a high intensity rainfall, such as i_1, water absorption is

allowed for a short period of time (t_1) and after that the exceeded water runs off and will not enter into the cracked soil. For a low intensity rainfall, such as i_2, water absorption is allowed for a longer period of time (t_2), but continued rain entirely cannot be accepted by the cracked soil if the application rate exceeds the infiltration rate.

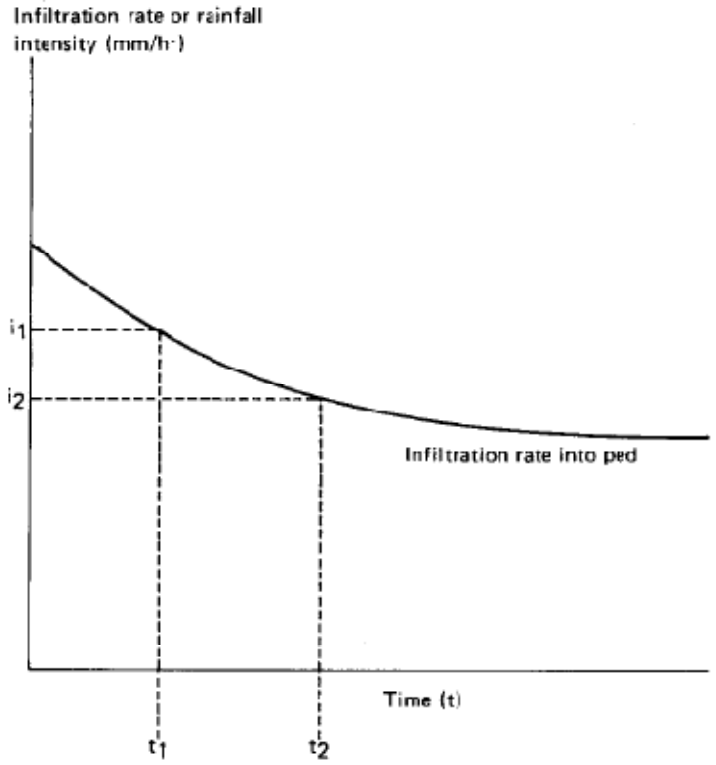

Figure 4.2. An infiltration curve showing the decrease of the infiltration rate into an initially dry cracked soil as a function of time (From Bouma (1980))

In a full-scale (16 m wide by 28 m long) field study in China, Zhan et al. (2007) Simulated rainfall infiltration into an unsaturated expansive soil slope and addressed the effect of cracks on water infiltration. The top 1.0 to 1.5 m layer of soil was reported as highly cracked. The maximum depth and width of the open cracks were approximated to be 1.2 m and 10 cm respectively. The researchers found the hydraulic conductivity of the soil with open cracks to be very high (10-

4 m/s) during the first 1-2 hours of the simulated rain. However, with time, the infiltration rate decreased dramatically. The authors believed that the sharp decrease in infiltration rate was primarily related to the water storage capacity of open crack channels. But after cracks are fully filled with water, the authors postulated that they tend to close with time because of soil swelling upon wetting. Nevertheless, as shown subsequently in this chapter, it is also possible that the reduced rate of infiltration was a result of the lower hydraulic conductivity of the unsaturated clay matrix surrounding the cracks. Comparing to the cracked soil, the infiltration rate for the non-cracked soil was found to be distinctly lower (10^{-7} m/s). Figure 4.3 shows the difference between the measured infiltration rates for cracked and non-cracked soils.

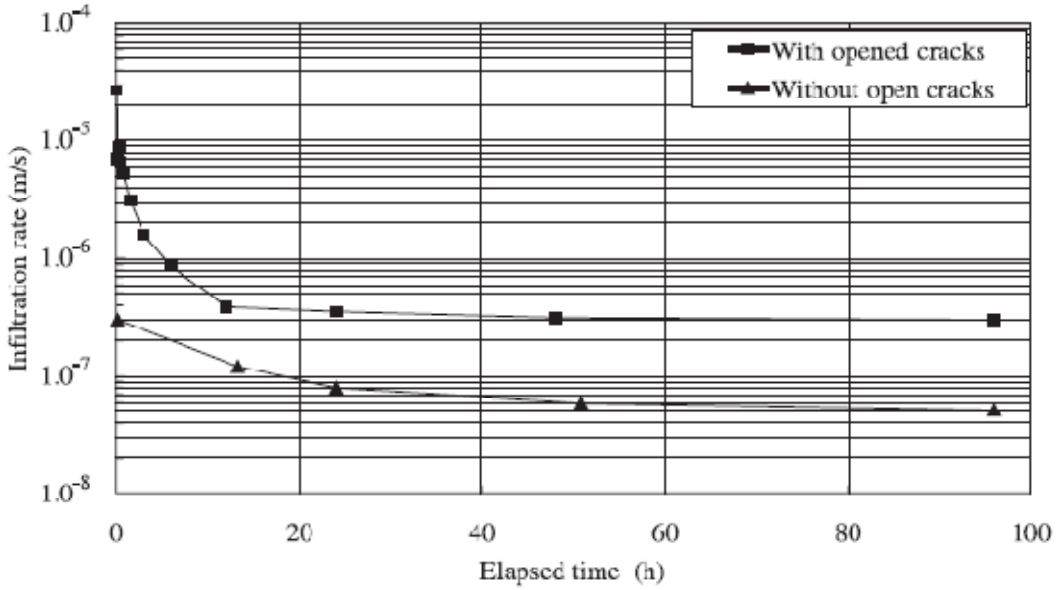

Figure 4.3. Comparison of infiltration rates for cracked and intact soils (From Zhan et al. (2007))

As an example of laboratory studies related to the effect of soil cracking on flow properties of soils, Greve et al. (2010) investigated the process of soil crack formation and preferential flow on infiltration into an expansive clay that

was placed inside a weighting lysimeter. The lysimeter was created by placing a fiberglass barrel of 1.3 m diameter and 0.78 m height on a 3 ton capacity scale. To allow drainage, the lysimeter was tilted 3.5º and had a 28 mm diameter drainage opening cut into the lowest point of its side wall. Six irrigation events (5 rains and 1 flood) were applied and followed by a drying period. The main conclusions from this 5 year research program are twofold:

1) Lateral infiltration from the macropores into the soil can significantly affect the water flow and should be included in water flow simulations of dry cracking soils.

2) Macropores remain pathways for preferential flow even after they seem to be healed at the surface.

Another example of laboratory investigation is a study carried out by Rayhani et al. (2007). The authors studied the effect of desiccation-induced cracking on saturated hydraulic conductivity of four different clayey soils from Iran. Each soil was compacted into sample tubes, and the soils were placed at 95% of the maximum dry density and 2% above the optimum moisture content for standard Proctor conditions. The samples were cycled through drying and wetting conditions and then subjected to the saturated hydraulic conductivity testing using the falling head method. Based on their laboratory findings, the hydraulic conductivity of soil was increased by 12 to 32 times, as the cycles of wetting and drying increase. However, the rate of infiltration into the cracked soil decreased with time, which was attributed by the authors to self-healing of desiccation cracks after absorbing water.

In addition to the field and laboratory experiments to study the influence of cracks on the hydraulic properties of soils, many researchers have attempted to develop new models to simulate water flow through the cracked soil. According to Fredlund et al (2010), prior to the 1990s, most studies had only considered the flow of water through the fracture system, and most of these studies were on fractured rocks rather than unsaturated expansive clay. However, after the 1990s, researchers have started to consider the flow of water through the soil matrix in addition to the flow through the fractures. Apart from the mathematical details associated with different models, the main problem for modeling the water transport through a fractured medium is how to handle the fracture-matrix interaction under different conditions which involves multiple phase flow. Wu and Pruess (2005) categorized the most commonly used mathematical methods as: (1) an explicit discrete-fracture and matrix model (e.g., Snow (1969); Stothoff and Or (2000)), (2) the dual-continuum method, including double- and multi-porosity, dual-permeability, or the more general "multiple interacting continua"' (MINC) method (e.g., Barenblatt et al., (1960); Warren and Root, (1963); Kazemi, (1969); Pruess and Narasimhan, (1985)), and (3) the effective-continuum method (ECM) (e.g., Wu, (2000)).

Discrete fracture models have been developed to study groundwater flow through cracked rock, and in this model the fractured rock is assumed to consist of two components, namely, the fracture network and a porous rock matrix. The main groundwater flow occurs through the fractured network. This discrete fracture model is not as commonly used as the dual-continuum model due to the

computational intensity involved, as well as the lack of detailed knowledge of fracture and matrix geometric properties and their associated spatial distributions at a given site. On the other hand, the dual-continuum approach has been perhaps the most widely used method in petroleum and geothermal engineering and groundwater hydrology, because of its computational efficiency and to match many types of laboratory or field-measured data which capture a "lumped" media response (e.g. Kazemi (1979); Wu et al. (1999)).

Generally, the measurement of unsaturated hydraulic conductivity of a soil is a challenging task, but as cracks are introduced into the soil it becomes extremely difficult. For an intact soil, most of the estimation models developed to-date use the SWCC and k_{sat} to compute the unsaturated hydraulic conductivity. More often than not, these models are based on a continuum mechanics approach. Some researchers have attempted a continuum approach for modeling flow through a fractured network. For example, in an article titled "A continuum model for water movement in unsaturated fractured rock mass", Peters and Klavetter (1988) proposed a continuum mechanics model for water flow through a fractured rock mass. The major assumption in this development was that the pressure heads in the fractures and the matrix are identical in the direction perpendicular to flow. Simulations of small-scale problems that explicitly incorporate the fractures and an analytical model of matrix recharge from partially saturated fractures showed that this assumption was reasonable for the studied site. Evaluation of the coefficient in the fluid continuity equation using both macroscopic and

microscopic approaches yields similar results. Figure 4.4 clearly explains the approach that the authors used in derivation of the composite conductivity.

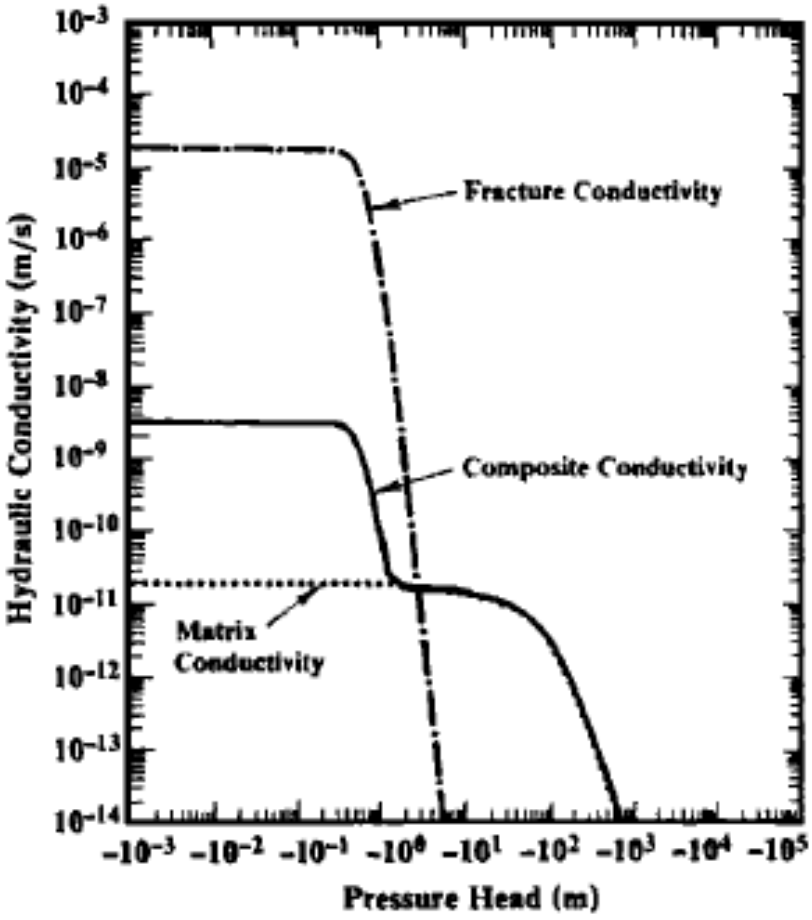

Figure 4.4. Derivation of the bimodal (composite) conductivity from matrix and fracture conductivities (From Peter and Klavetter (1988))

Since the 1990s, attempts have been made to incorporate multimodal hydraulic conductivity functions to characterize a heterogeneous soil. Mallant et al. (1997) and Kohne et al. (2002) used unimodal and multimodal SWCC equations (Van Genuchten (1980)) along with the Mualem (1976) model for determination of saturated and unsaturated hydraulic conductivities of soils. According to these studies, it was found that the multimodal SWCC performed better than the unimodal SWCC.

Despite the variety of the proposed models to estimate the saturated and unsaturated conductivity of fractured medium, a thorough literature search failed to uncover any experimental determination of the SWCC for a cracked soil. However, there are a few theoretical approaches proposed in the literature. Zhang and Fredlund (2004) proposed the application of theories from rock mechanics studies for determination of the SWCC of a cracked material. The soil was assumed to be non-swelling and the SWCC was based on the pore size distribution curve of the soil. It was assumed that the intact soil and cracks combine together to form a continuum with a continuous function that contains saturated-unsaturated soil parameters. The SWCC computed for the continuum is presented in figure 4.5. This figure suggests that the SWCC for a cracked soil may also be assumed to take on a bimodal behavior. There are also several other mathematical models that considered the SWCC to be bimodal for fractured material (e.g. Durner (1994); Burger and Shackelford (2001); and Gitirana and Fredlund (2004)). However, there is no experimental evidence, to-date, to support or criticize this hypothesis, other than the studies presented as a part of this study (Abbaszadeh et al. (2011)). In this study, it is attempted to address this lack of information by conducting extensive laboratory tests to measure the SWCC for the cracked soil.

As a brief overview, this chapter can be divided into four sections. In the first section, the saturated hydraulic conductivity experiments for both intact and cracked samples prepared from San Diego clay are presented, including the test procedures and results. Second, the unsaturated hydraulic conductivity

experimental result and analyses are explained and the results for intact and cracked soils are compared and discussed. The experimental design for this part has been performed collaboratively with Sean Jacquemin but the analyses of the data from these experiments were solely conducted by Sean Jacquemin as a part of his MS thesis work at Arizona State University (Jacquemin (2011)). The results of these analyses are summarized herein for completeness. The third part of this chapter includes the methods and procedures involving the laboratory determination of the SWCC for the cracked and intact soil, and is followed by the results and comparison between the intact and cracked soil SWCCs. Finally, the effect of soil cracking on the flow properties of saturated and unsaturated soils is summarized, with emphasis on the effect of cracking on unsaturated flow.

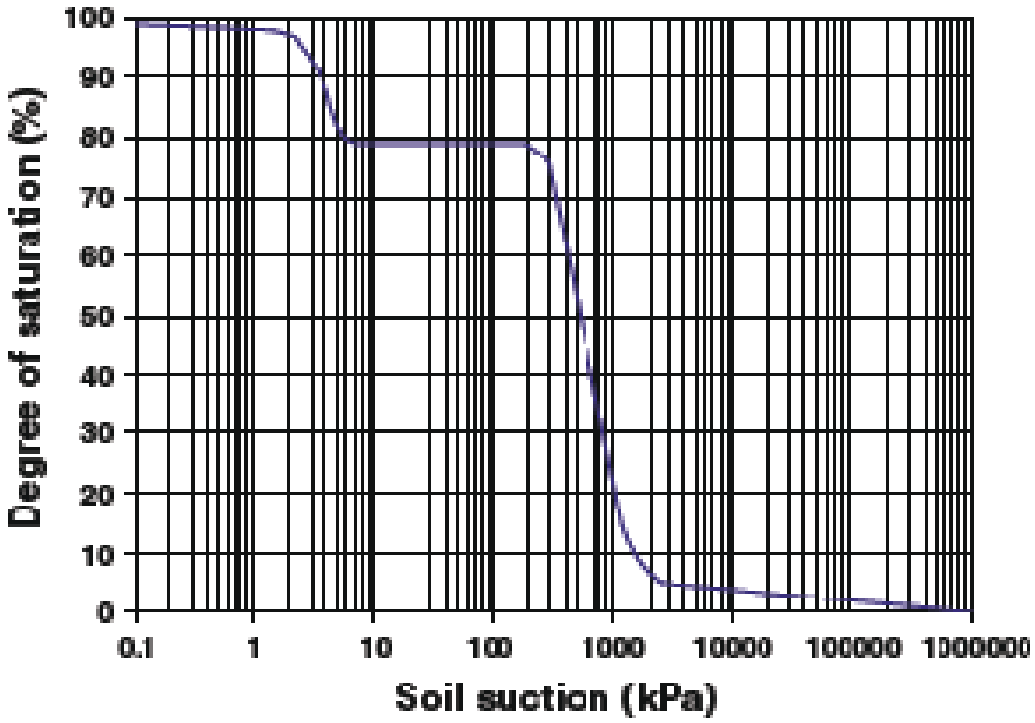

Figure 4.5. SWCC for a fractured rock (From Zhang and Fredlund (2004))

4.4 Effect of soil cracking on saturated hydraulic conductivity

To study the effect of cracks on saturated hydraulic conductivity of soils, two approaches have been used in this research; namely, direct and indirect methods. In the direct method, the saturated hydraulic conductivity of both intact and cracked San Diego soils were directly measured using a flexible wall constant head permeability test. For the indirect method, the saturated hydraulic conductivity was back-calculated from conventional consolidation test results for cracked and intact specimens. Details regarding each method are presented below.

4.4.1 Direct method

Typically, designing a conductivity test for soils is a challenging task due to the low degree of reproducibility associated with these types of experiments. Specifically, the results of a conductivity test are sensitive to many different factors such as initial density, compaction moisture content, compaction energy, swelling potential, etc. These factors make the hydraulic conductivity test results some of the most variable soil property in the field of soil mechanics. To overcome this issue of variability, the effort has been made to eliminate as much variability as possible while designing the experiment and more than one specimen has been tested in each case to evaluate, to some extent, reproducibility.

After studying various alternatives based on the available equipments at the Arizona State University advanced geotechnical laboratory, it was found most suitable to conduct the saturated hydraulic conductivity tests utilizing the conventional triaxial device, modified for flexible wall constant head permeability testing. A schematic of this device is shown in figure 4.6. As mentioned earlier, in

this method (direct method) the k_{sat} is determined by applying a constant head gradient to the specimen, after the soil is saturated, and monitoring and recording the water discharge from the sample. From the discharge flow rate, the k_{sat} can be calculated by applying Darcy's law. A sample calculation of saturated hydraulic conductivity can be found in appendix A.

4.4.1.1. Step by step test procedure

Once again, it is crucially important to follow the procedure accurately in order to minimize the variability of the results. After a few trials and errors, a detailed test procedure was developed for direct k_{sat} measurement experiment with which the sources of variability in results were eliminated as much as possible. This procedure will lead to a more reliable and reproducible results for k_{sat}.

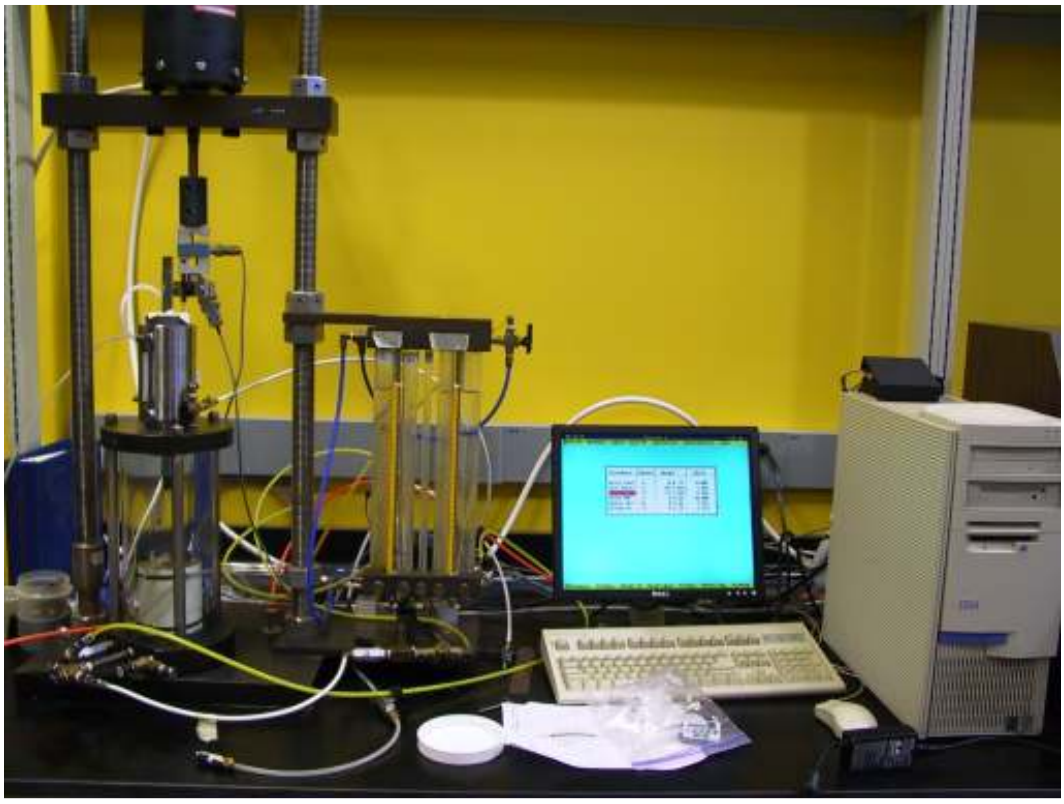

Figure 4.6. A schematic view of the triaxial apparatus used for direct k_{sat} measurement

The step by step procedure is presented below:

Step 1 (sample preparation) – The sample is compacted in a cylindrical split mold in three equal layers at 98% of a standard proctor test (See figure 4.7) and the optimum moisture content, 18%. The diameter of the mold is 2.8 inch and the thickness of the sample is 1.0 inch. After the compaction of each layer is completed and just before starting the compaction of the next layer, the top surface of the preceding layer should be scarified using a sharp tool. This is to generate a better contact between the two layers and produce a more uniform compacted specimen.

Figure 4.7. Illustration of different stages of sample preparation for direct ksat measurement test

Step 2 (preparation of the triaxial machine) – Before starting the test, one should check the o-rings to ensure that they are clean. Also, the water should be flushed through every hose in the system to release any entrapped air before starting the experiment. Figure 4.8 illustrates the process of filling the Volume Change Device (VCD). It is critically important to ensure that the water passage for both top and bottom platens are completely open and free of any clogs. Also it is highly recommended to place a small piece of filter paper over the bottom

platen's opening to prevent the small soil particles from traveling into the platen's pathway. After removing any entrapped air from the system, the sample can be placed over a porous stone which is located on top of the bottom platen. Two filter papers should be situated on both ends of the soil specimen before placing the soil sample on a porous stone. This will prevent the porous stones from getting plugged during the course of the test. However, care should be taken in selecting the filter paper and porous stone with high enough conductivities such that the flow of water through the soil during the experiment would not be impeded. Figure 4.9 shows a specimen placed appropriately inside the device. Afterwards, the latex membrane can be wrapped around the specimen and bottom platen, but before placing the top platen in position, the membrane should be sealed at the bottom platen using an o-ring. Figure 4.10 illustrates the procedure. Another o-ring should also used to seal the membrane against the top platen. At this stage, the cell is ready to be filled up with water.

Step 3 (filling the cell with water) – After the sample is properly located inside the cell and wrapped and sealed with the membrane, the triaxial cell should be closed and filled with water. It is likely that some air bubbles are formed inside the chamber while filling the triaxial cell with water. To remove the entrapped air, the triaxial cell should be tilted for a moment and turned back into the normal position. Figure 4.11 shows a filling process of a triaxial chamber.

Figure 4.8. Illustration of removing the entrapped air from the system and filling the Volume Change Device (VCD) tubes

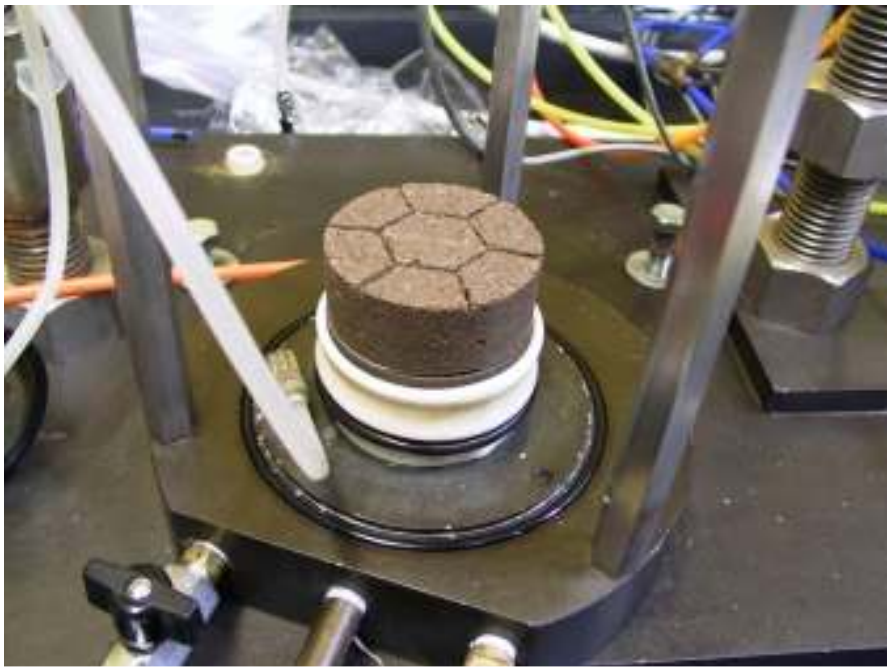

Figure 4.9. Illustration of placing a cracked soil sample on the bottom platen

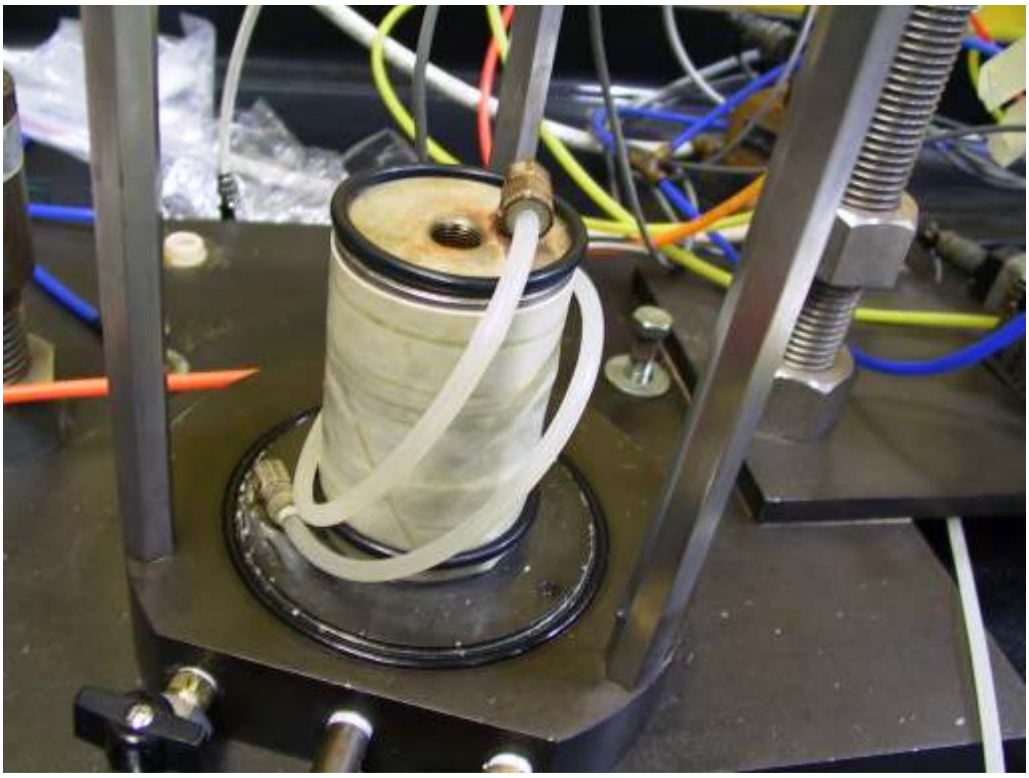

Figure 4.10. Illustration of placing the top platen while the membrane is sealed from the bottom

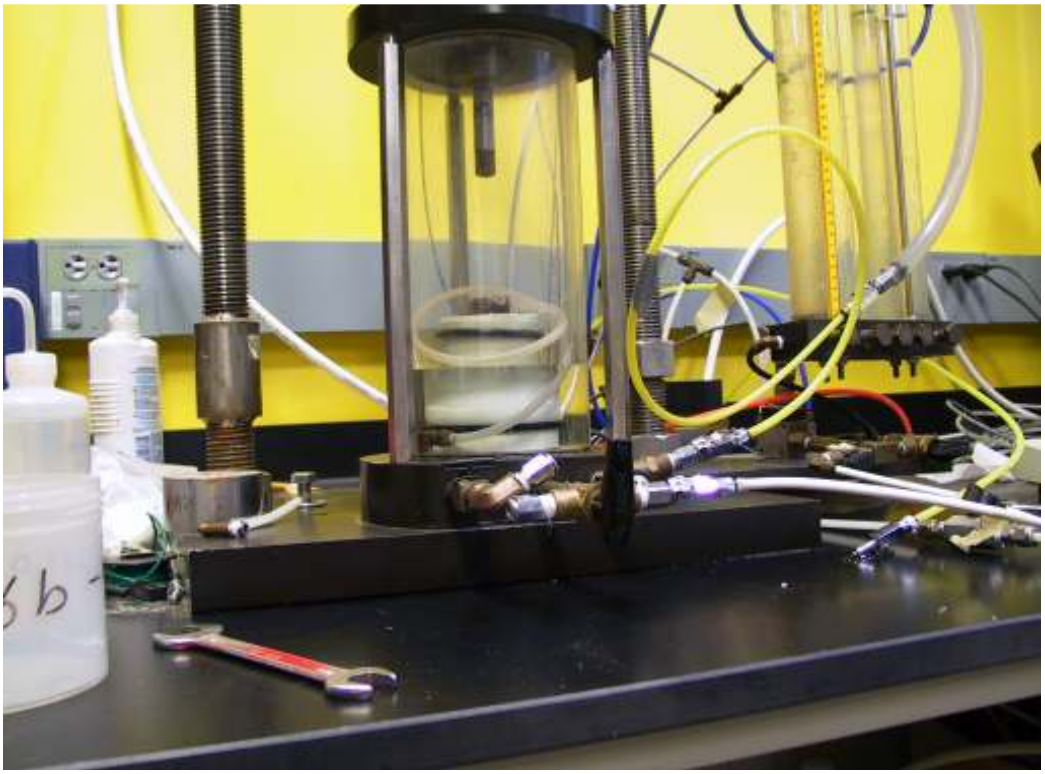

Figure 4.11. Filling a triaxial cell with water

Step 4 (sample saturation using back pressure technique) – before being able to run a k_{sat} test, the sample should be saturated. At this stage, the back pressure should be applied to the sample together with some cell pressure, to saturate the sample. Care should be taken to keep the effective stress between 15 to 20 kPa at all times during this step to avoid consolidation of the specimen. If the effective stress becomes too high during backpressure saturation, the specimen will become disturbed and non-representative. Both the cell pressure and the back pressure should be increased simultaneously such that the effective stress remains within the abovementioned range. The rate of increasing the pressure is also important. If the pressures are applied too fast, it may cause damage to the sample. Empirically, the following stress increment program is found to be practical for the subject soil.

- Cell pressure should be started from 50 kPa and be increased to 200 kPa in three equal steps. For each step, it is recommended to wait for at least 30 minutes.
- Beyond 200 kPa of cell pressure, 100 kPa increments can be used with a minimum of 60 minutes between each increment.
- When the cell pressure is reached to 500 kPa, it is recommended to wait for at least 90 minutes and then increase the cell pressure to 650 kPa. This is the final pressure and after that the soil should be allowed to saturate for at least 24 hours. Then the B-value test should be performed to check the degree of saturation.
- In the B-value test, the pressure valves for top and bottom pressures are closed and the cell pressure will be increased by a fixed amount, X. Ideally, if the

sample is 100% saturated, the effective stress should not be increased because all of the applied confining pressure is expected to be transferred to the water. However, it is almost impossible to completely saturate a clayey soil, so the effective stress will be usually increased to some amount, Y. The B-value, which relates to the degree of saturation, is equal to:

$$B(\%) = \frac{X - Y}{Y} \times 100 \qquad (4.1)$$

- Should the calculated degree of saturation from B-Value test is equal or greater than 90%, one can proceed to the next step.

Step 5 (starting the conductivity measurement test) – After the sample is well saturated, the k_{sat} measurement test can be started. For this study, a pressure gradient of 30 kPa was applied from top of the specimen to the bottom so that the water travels from top to the bottom. This is similar to the mostly vertical water transport path through the soil during a rainfall or irrigation. The applied pressure gradient corresponds to hydraulic gradient of 118. Using the Volume Change Device (VCD), the flow rate of the water that transports through the soil can be measured. Finally, the saturated hydraulic conductivity of soil can be calculated using Darcy's law:

$$k = \frac{QL}{hAt} \qquad (4.2)$$

Where k is the saturated hydraulic conductivity in m/s

Q is the total discharged volume in m^3 at the time t (s)

A is the cross sectional area of the sample in m^2

h is the applied head gradient in m, and

L is the sample thickness in m

4.4.1.2 Test results for cracked and intact specimens

Three types of specimen were prepared and tested for the saturated hydraulic conductivity measurement. First, three identical intact specimens were prepared and tested. Second, four cracked specimens with crack depth of ½" (3% crack by volume) were tested and finally, three cracked specimens all with crack depth of ¾" (4% crack by volume) were prepared for k_{sat} measurement test. The widths of the cracks were approximately 0.05" (~ 1 mm). For consistency purposes, the same hexagonal crack patterns were used as previously explained in chapter three for the swell pressure tests. These crack patterns were selected based on a literature research focusing on the natural formation of cracks and their sizes. Different crack depths were studied to understand the effect of the initial crack volume on the saturated hydraulic conductivity of soils. The results from the k_{sat} tests are summarized in table 4.1.

Table 4.1. Summary of k_{sat} results for different specimens

Test		K (m/s)	Average
Intact	intact 1	1.07 E 10-8	1.33 E 10-8
	intact 2	8.68 E 10-9	
	intact 3	2.07 E 10-8	
1/2" Deep Cracks (3%)	cracked 1	4.49 E 10-8	2.69 E 10 -8
	cracked 2	3.95 E 10-8	
	cracked 3	1.94 E 10-8	
	cracked 4	3.64 E 10-9	
3/4" Deep Cracks (4%)	cracked 5	3.2 E 10-8	3.87 E 10-8
	cracked 6	4.1 E 10-9	
	cracked 7	8.00 E 10-8	

As expected, the measured hydraulic conductivities for both types of cracked specimens are higher than that for the intact specimens. In fact, the

average k_{sat} for ½" deep cracked specimens is approximately twice, and for ¾" deep cracked specimens, k_{sat} is three times, that of the intact specimens. The calculations for the k_{sat} values shown above are based on the assumption that the flow path, L in equation 4.2, remains the same for all of the three cases. However, if the shorter drainage paths of ½" and ¼" would have been employed for the ½" deep and ¾" deep cracked cases, respectively, the calculated hydraulic conductivities for the cracked cases should have been ½ and ¼ times lower than the reported values in table 4.1 for the ½" deep and ¾" deep cracked specimens, respectively. If this assumption that the only effect of the crack is to shorten the flow path is applied, the final saturated hydraulic conductivities of all the cracked and intact specimens would be more or less within the same range. Thus, the difference in hydraulic conductivity of the cracked specimens appears to be primarily related to the decreased length of flow path created by introduction of the cracks. In other words, if the flow path length is adjusted downward to account for the length of the cracks, the saturated hydraulic conductivity of all specimens, cracked and uncracked, is essentially the same. This means that the flow was primarily being controlled by the intact portion, and that the flow went through the cracked segment of the specimen without being impeded (i.e. without significant head loss). Consequently, the measured k_{sat} values are for the intact portion of the matrix, rather than for the entire cracked soil. This suggests that the k_{sat} for cracked portion is dramatically higher than for the intact clay portion because the flow was apparently not significantly retarded before reaching to the intact portion of the soil matrix.

The assumption that the top cracked layer is bypassed during the water flow can be a reasonable assumption when the crack network is broad enough such that the water can move relatively quickly downward towards the lower intact portion of the matrix. Under high hydraulic gradients, such as the one used in this study, it can also be assumed that after water bypasses the top cracked portion of the soil and reaches to the lower intact portion, it moves laterally and that the use of the whole cross sectional area of the intact portion is appropriate for computation of conductivity.

Although the trend of the measured saturated hydraulic conductivities of the studied cracked and intact specimens seems reasonable, one may argue that this may not exactly reflect what happens is field.

Also, it should be remembered that these are saturated hydraulic conductivities, and not unsaturated conductivities. In other words, these numbers may not reflect what happens in field just after a rainfall starts in a very dry cracked soil, when the soil is still unsaturated, but they may very well represent what happens after a few days, weeks, or years of ponding on a cracked soil and when the cracks are all fully filled with water. The calculated saturated hydraulic conductivities for the cracked and intact soils in this study suggest that while the cracks are saturated and completely filled with water, the saturated hydraulic conductivities for cracked specimens are dramatically higher than that for intact soil such that the water bypasses the entire cracked region and it is only the intact portion of the specimen that governs the flow.

4.4.2 Indirect method

As an alternative method, the saturated hydraulic conductivity for intact and cracked specimens was back-calculated based on the results from the conventional consolidation experiments. The consolidation experiments were performed for cracked and intact specimens in accordance with ASTM standard D 2435 – 04: Standard Test Methods for One-Dimensional Properties of Soils Using Incremental Loading. The sample preparation and details are exactly similar to those presented in Chapter 3 for the swell pressure tests.

After performing the test and plotting the time-deformation curves, the coefficient of consolidation, c_v, should be computed using the following equation:

$$c_v = \frac{TH_{D_{50}}^{\ 2}}{t} \tag{4.3}$$

Where T = a dimensionless time factor $T_{50} = 0.197$

t = time corresponding to the particular degree of consolidation in sec or min. The value of $t=t_{50}$ is used in here.

H_{D50} = length of the drainage path at 50% consolidation, in cm or m for double-sided drainage. H_{D50} is the specimen height at the appropriate increment and for one-sided drainage, H_{D50} is the full specimen height.

The results for consolidation experiments are shown in figure 4.12 for cracked and intact samples.

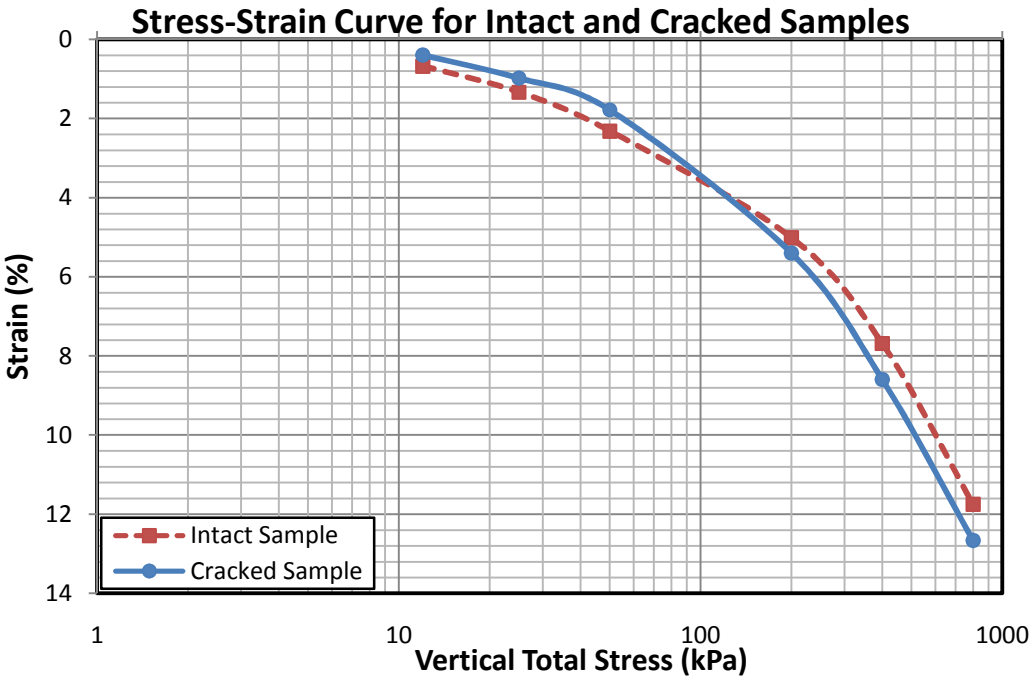

Figure 4.12. Conventional Consolidation results for intact and cracked specimens

After computing the coefficient of consolidation from equation 4.3, the hydraulic conductivity can be estimated from the following equation:

$$k = c_v m_v \gamma_w \qquad (4.4)$$

Where, k is the saturated hydraulic conductivity of the soil in the direction of the consolidation.

c_v is the coefficient of consolidation

m_v is the coefficient of volume change, and

γ_w is the specific weight of water (9.8 kN/m^3)

Table 4.2 summarizes the calculated Preconsolidation pressure (P_p), coefficient of consolidation (c_v), and saturated hydraulic conductivity (k_{sat}) for both cracked and intact soils. It should be noted that the back-calculated k_{sat} values shown in table 4.2 are based on tests at 800 kPa total stress, while in the

field, the stress level is generally lower where cracks are present and, consequently, the saturated hydraulic conductivity is expected to be higher. Taking this into consideration, an empirical relationship was used to adjust the calculated k_{sat} for the lower stress levels in field. This procedure is explained in the following paragraph.

Table 4.2. Summary of k_{sat} back-calculation at 800 kPa for intact and cracked soils

	P_p (kPa)	t_{50} (min)	c_v (cm^2/min)	k_{sat} (m/s) based on 800 kPa stress
Cracked	260	17	0.019	3.07×10^{-9}
Intact	325	20	0.0158	2.56×10^{-9}

Kozeny (1927) proposed an equation which relates the hydraulic conductivity to porosity (n), particle size, angularity of soil particles, specific surface area (A) and viscosity of water (η_w). Twelve years later, Carman (1939) modified Kozeny's equation and replaced porosity with void ratio, e. The equation is now known as Kozeny-Carman equation:

$$k = \frac{\rho_w g}{D\eta_w A^2}\frac{e^3}{1+e} \tag{4.4}$$

Where g is the acceleration due to gravity (9.81 m/s^2), ρ_w is the mass density of water (1Mg/m^2), and D is a shape factor (5 for spherical particles). Replacing all of the constants with C, equation 4.4 can be rewritten as equation 4.5:

$$k = C\frac{e^3}{1+e} \tag{4.5}$$

To estimate k at void ratios other than the test void ratio, it can be said that:

$$k_1 : k_2 = C_1 \frac{e_1^{\,3}}{1+e_1} : C2 \frac{e_2^{\,3}}{1+e_2} \tag{4.6}$$

For simplification purposes, C_1 and C_2 were assumed to be approximately equal. Then equation 4.6 can be written as equation 4.7:

$$k_1 : k_2 = \frac{e_1^{\,3}}{1+e_1} : \frac{e_2^{\,3}}{1+e_2} \tag{4.7}$$

Using equation 4.7, the back-calculated k_{sat} based on 800 kPa normal stress were adjusted for 50 kPa total stress. Table 4.3 summarizes the saturated hydraulic conductivity measurement results for both direct and indirect methods. It can be seen from Table 4.3 that the adjusted k_{sat} values are higher than the initially calculated k_{sat} values based on 800 kPa total stress.

Table 4.3. Summary of k_{sat} measurements for direct and indirect methods

	Sample description		K (m/s)	Average
Direct Method	Intact	intact 1	$1.07 E 10^{-8}$	$1.33 E 10^{-8}$
		intact 2	$8.68 E 10^{-9}$	
		intact 3	$2.07 E 10^{-8}$	
	1/2" Deep Cracks (3%)	cracked 1	$4.49 E 10^{-8}$	$2.69 E 10^{-8}$
		cracked 2	$3.95 E 10^{-8}$	
		cracked 3	$1.94 E 10^{-8}$	
		cracked 4	$3.64 E 10^{-9}$	
	3/4" Deep Cracks (4%)	cracked 5	$3.2 E 10^{-8}$	$3.87 E 10^{-8}$
		cracked 6	$4.1 E 10^{-9}$	
		cracked 7	$8.00 E 10^{-8}$	
Indirect Method	K_{sat} (m/s) based on 800 kPa stress	intact	3.07×10^{-9}	
		cracked	2.588×10^{-9}	
	Adjusted K_{sat} (m/s) for 50 kPa stress	intact	4.22×10^{-9}	
		cracked	3.77×10^{-9}	

The saturated hydraulic conductivity of the cracked and intact specimens was calculated using two different methods, namely direct and indirect methods. In direct method, a conventional triaxial device was employed in order to directly measure the k_{sat} for the compacted specimens using the flexible wall constant head permeability method. On the other hand, in indirect method, k_{sat} was back-calculated from the one-dimensional consolidation test and then adjusted for lower stress levels using the Kozeny-Carman equation (equation 4.7).

Comparing the measured saturated hydraulic conductivities for cracked and intact specimens revealed that the saturated conductivity of the cracked portion of samples were extremely higher than that of the intact portion of the samples and the intact specimens such that the cracks were not impeding the flow

and the cracked portion of the specimen did not impede the flow to the lower intact soil matrix. The intact clay part of the specimens was responsible for controlling the saturated hydraulic conductivity. As a matter of fact, the water must flow through the intact portion of the specimen, even if the flow through the cracks is relatively unimpeded. Although the cracks visually "heal" when the specimen is saturated, due to swelling of the clay, it is concluded that flow through these "healed" crack is still relatively unimpeded compared to flow through the intact clay matrix. It should be noted that the effect of confining pressure on the hydraulic conductivity of samples was not studied because the main purpose of this study was to compare the results for intact versus cracked samples; and since the test conditions were kept the same for both cases, the results are valid for comparison purposes.

4.5 Effect of soil cracking on unsaturated hydraulic conductivity

Numerous empirical models have been developed for estimation of the hydraulic conductivity function of an unsaturated soil. The majority of these models require the SWCC and k_{sat} of the soil in order to predict the unsaturated hydraulic conductivity function. While all of these models have been proposed for intact (non-cracked) soil, an approach for applying them for cracked soils is unclear because determination of SWCC and k_{sat} for a cracked soil is very difficult. Thus, the measurement of the hydraulic conductivity for an unsaturated, cracked soil is extremely complex. This section presents the experimental determination of the unsaturated hydraulic conductivity of cracked soil. A comparison has been made between the cracked and intact unsaturated hydraulic

conductivities of San Diego soil. As mentioned earlier, the majority of the test protocols were developed collaboratively with Sean Jacquemin and the data analysis was performed solely by Sean Jacquemin. To prevent repetition, only a brief summary of the test methods and procedures are presented in this document. For more details about test protocols and data analysis, the reader is encouraged to refer to Jacquemin (2011).

4.5.1 Techniques for measurement of unsaturated hydraulic conductivity

In a general categorization, k_{unsat} can be measured either directly from a test or indirectly from soil properties such as SWCC, grain size distribution, k_{sat}, etc. In this study, both methods have been used. Direct k_{unsat} measurement techniques include testing of soil either in the laboratory or in the field. In the laboratory, the soil sample can be disturbed or undisturbed. However, the field methods are conducted in situ such that the soil fabric and stress conditions are representative, yet often more difficult to quantify. Some of the direct methods are based on steady-state flow (e.g. constant-head method and centrifuge method) while the others are based on the transient flow such as horizontal infiltration method and instantaneous profile method. The latter method is modified and used for this research because it is one of the most commonly used methods to determine the unsaturated hydraulic conductivity of soils either in laboratory or in situ, and because of its relative ease of application. The instantaneous profile method often takes very long, especially for clayey soils, and therefore, some modifications have been made to facilitate the test pace.

In the following section, the instantaneous profile method is discussed in details. For more information about other techniques for measuring the unsaturated hydraulic conductivity of soils, the reader is encouraged to refer to Appendix B.

4.5.1.1. Instantaneous profile method (IPM)

This method is an unsteady state testing method applicable to either laboratory or field determination of the unsaturated hydraulic conductivity function. This technique uses a column of soil that is subjected to water flow from one end to the other end. During this transient flow, the profiles of water content and suction of soil are obtained for different periods of time. The initial boundary condition is always known and there are several variations on how to set up the initial boundary conditions. The one which is used in this study is to start with multiple moisture contents such that when moving from one end of the column to the other end, the water content of different sections of compacted soils are all increased or decreased. The volume of water which traveled from one side of the column to the other side can be computed by measuring the time-dependent changes in water content profile. Likewise, the hydraulic gradient which is creating the flow can be estimated by measuring the time-dependent changes in suction profile. Darcy's law can then be used to compute the hydraulic conductivity of the soil.

The decision to place the soil at different initial moisture contents was made because of the extremely long equilibration times required for the test soil, placed at optimum moisture content, to reach the values of suction of interest for

the full range of testing of unsaturated hydraulic conductivity. Recognizing that the soil fabric affects the hydraulic conductivity, studies were performed to assess the impact of compaction of the test soil at different water contents. This was done by measuring saturated hydraulic conductivity of the clay prepared at different compaction moisture contents. Results, shown subsequently in this chapter, revealed that for this particular clay, compaction moisture content, over the range used in specimen preparation of this study, did not significantly affect saturated hydraulic conductivity. However, it is quite likely that for other soils, particularly higher plasticity clays, that the differing fabric effects associated with differing compaction moisture content could become significant.

4.5.2 Design of experiments

A total of seven experiments were designed in order to measure the unsaturated hydraulic conductivity of San Diego soil for both cracked and intact specimens. All of these test protocols were developed based on the instantaneous profile method, with some modifications being applied. Table 4.4 summarizes the conducted experiments. The main differences between the experiments were aimed at either testing different ranges of suctions or studying various aspects of water infiltration through unsaturated cracked soil. To create different suction ranges, soils with different moisture contents were compacted on different sections of the instantaneous profile column. One may argue that, for a plastic soil, the soil fabric will be significantly different while compacting at different moisture contents. To evaluate the sensitivity of the subject soil's fabric to the compaction moisture content, two sets of k_{sat} measurement tests were carried out

for specimens with different moisture contents. It was decided to take one moisture content from the lower bound (8%) and one form the upper bound (20%) of the soils moisture content. The same testing technique was used for k_{sat} measurements as described earlier in this chapter (see 4.4.1.1). The results from these two tests are presented in table 4.5. It can be seen that the measured saturated hydraulic conductivities are very close and actually within the variability of a saturated hydraulic conductivity test. Consequently, it can be said that for the studied soil, the compaction moisture content does not affect the saturated hydraulic conductivity of the soil significantly.

In the following section, the setup for instantaneous profile method for intact soil is discussed followed by the description of different methods used to simulate the crack behavior and study the instantaneous profile method for cracked soil. Sections 4.5.2.1 and 4.5.2.2 are taken form Jacquemin (2011) with minor modifications.

Table 4.4. Summary of Instantaneous profile method experiments (From Jacquemin (2011))

Test Number	Intact or Cracked	Method	Column Length	Number of Soil Sections	Experiment Description
Test No. 1	Intact	Trial	36"	4	Volumetric moisture probes installed
Test No. 2	Intact	Trial	36"	4	Duplicate of Test No. 1
Test No. 3	Intact	Duplicate	9"	2	
Test No. 4	Cracked	Method B	9"	2	Two sets with different number of horizontal cracks
Test No. 5	Cracked	Method C	9"	2	Two sets of different crack widths
Test No. 6	Cracked and Intact	Method A	9"	1	
Test No. 7	Intact	Duplicate	9"	2	Lower suction range than Test No. 3

Table 4.5. Saturated hydraulic conductivity results for samples with different compaction moisture contents

Test	intact - 8% wc	intact - 20% wc
k_{sat} (m/s)	2.52×10^{-8}	2.1×10^{-8}

4.5.2.1 Instantaneous profile method for intact soil

4.5.2.1.1 Test Number 1

Test Number 1 (TN1) was an instantaneous profile experiment using a long soil column with four different sections at different initial water content. The water contents chosen gave suction values that varied over a broad range which was desired for this experiment. The test sample was placed in the horizontal position while the soil was allowed to equilibrate. The water content was measured over time by taking manual water content samples and from the volumetric moisture probes installed inside the soil column. The matric suction

was measured using filter paper method at the same locations for which manual water contents were taken.

4.5.2.1.2 Test Number 2

Test Number 2 (TN2) was a duplicate of TN1. Test conditions for TN2 were the same as TN1, including the sectional water contents, sampling methods, time periods, and test set up. The only difference in the TN2 experiment was that volumetric moisture probes were not used. The primary purpose of TN2 was for manipulation/reconfiguration of the experiments. At the beginning of this experiment, it was thought that if the flow in the samples was too slow, TN2 would be used to accelerate the infiltration process by introducing water into the sample. TN2 was also used to check the reproducibility of the results from the experiment.

4.5.2.1.3 Test Number 3

Observations from instantaneous profile experiments TN1 and TN2 revealed that these methods require some modification for better performance. The main problem with TN1 and TN2 were the extensive scatter found in the data and slow movement of water or change in water content for different sections of the soil column. To improve the accuracy and reliability of the results, a new test methodology was developed for TN3.

Test Number 3 was also based on the instantaneous profile experiment concept, but only used two soil sections of different water content. This allowed for improved control over the suction gradients. The tube used for TN3 was shorter than that used for TN1 and TN2 since only two soil sections were needed.

The methodology for TN3 involved creating 6 duplicate samples simultaneously with the same soil conditions and then completely destroying the sample specimens for sampling at different time periods. This duplicate method allowed for the sample specimens to be completely destroyed so the measurement of water content was more accurate and representative. In addition, the matric suction was measured using filter paper tests. Filter paper was placed in between soil compaction layers and were removed and measured during the sampling events. The sampling events were performed at various time periods with increasing time between sampling events. Typical sampling time intervals used were 25, 50, 75, 100, 150 and 300 days. The drawback of this method, however, was the difficulty associated with producing the identical specimens at the beginning of the experiment.

4.5.2.1.4 Test Number 7

Test Number 7(TN7) used the same test technology as that used for TN3. The only difference was that a lower suction range was used in TN7 comparing with TN3. This was done to gain a wider range of suction values for the hydraulic conductivity function for the intact condition. To gain conductivity values in a lower suction range, lower initial water contents were used for TN7 than those used in TN3.

4.5.2.2 Instantaneous profile method for cracked soil

The objective of the cracked instantaneous profile experiments was to measure the unsaturated coefficient of permeability for the cracked condition. These experiments differed from the intact experiments in that the samples were

prepared with cracks or air voids. Different methods were proposed to simulate and measure the infiltration of water through a cracked matrix. The determination of the cracked unsaturated hydraulic conductivity function may comprise of a combination of the cracked methods presented. Experiments include different test method that varied the orientation and direction of the cracks with respect to the soil profile. These experiments allowed for anisotropy and crack orientation effects to be considered. To analyze the aspects of how water flows through a soil sample as experienced in the field, three methods were considered to simulate the direction of the water flow with respect to the crack orientation. Figure 4.13 schematically illustrates the three methods and the moisture flow direction with respect to the cracks orientation.

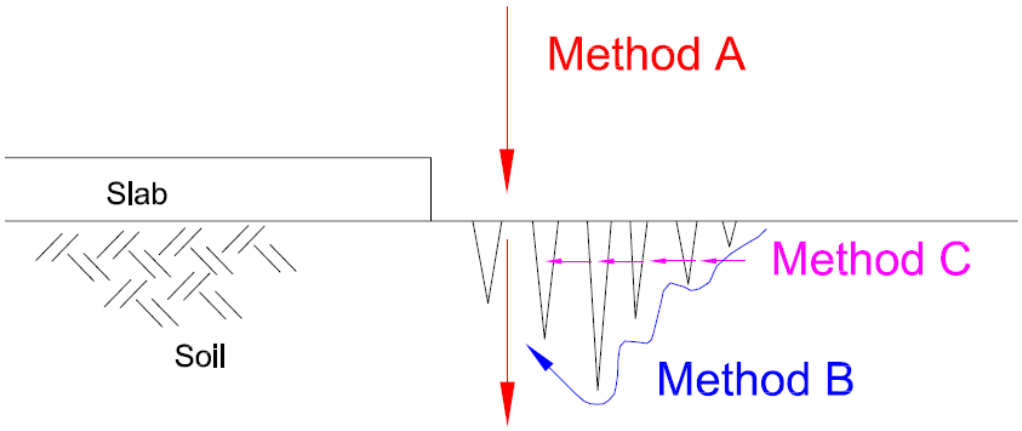

Figure 4.13. Different methods used to capture the effect of cracks on unsaturated hydraulic conductivity (From Jacquemin (2011))

4.5.2.2.1 Test Number 4

Test Number 4 (TN4) uses Method B whereas the crack orientation is perpendicular to the soil profile and the direction of the flow of water through the

sample (see figure 4.13). This experiment was designed to observe the possible tortuosity effects of having cracks that divert or render the water movement through the soil. To consider this effect and measure the hydraulic conductivity for this type of simulation, two experiments were conducted with a different number of perpendicular cracks aimed at creating different lengths in flow paths.

Similar to TN3, the sample was compacted into cylindrical tubes with two soil sections of different water content. The water contents were chosen to provide the desired suction range and hydraulic gradient. The matric suction was measured using filter paper tests. The sampling events were performed at various time periods with increasing time between sampling events. The cracks were cut into the soil profile using a circular saw after the soil was compacted in the apparatus tubes. Each sample was prepared so cracks extended from the side of the sample tube. The crack volume for each sample set was then calculated.

4.5.2.2.2 Test Number 5

Test Number 5 (TN5) used Method C for a condition in which a single crack existed horizontally in the middle of the soil profile (see figure 4.13). This method was used to analyze the interface of a single crack and the air-water-vapor transfer that occurs at this interface. The conductivity that is calculated over the air gap represents a lower limit of the hydraulic conductivity and may represent the conductivity due to evaporation transfer. A special procedure was used to create the crack (air-gap) in the middle of the tube. This procedure involves compacting a soil section into half of a sample tube. Soil plugs from two half tubes were then extruded into a sample tube from opposite ends. The soil plug

sections were carefully pushed together so that a small air gap remained in the middle of the tube at the desired width. Two sample sets, Set 3 and Set 4, with air gaps of 1/8" and 1/4" respectively were prepared.

Similar methodology as TN3 was used for this test. To avoid temperature effects, the sample tubes were stored in an environmental chamber.

4.5.2.2.3 Test Number 6

Test Number 6 (TN6) incorporated Method A representing the case where the water flows vertically into the cracks. In these experiments, water was added to the top of the tube where the cracks extended into the sample and provided a path for water to infiltrate into the sample. This method used a duplicate intact sample in order to compare results and observe the impact of the cracks on the hydraulic conductivity. All samples for TN6 were created in the same manner using the same procedure. For the cracked samples, the cracks were formed using the same cracked configuration (hexagonal pattern) used in previous testing related to this study, by driving a wedge into the soil. The sample specimen were prepared and compacted in layers at a single water content which was chosen to provide results within the desired suction range. The water content was the only parameter measured at two locations using volumetric moisture probes. The matrix suction was determined using the relationship from the SWCC for the soil.

4.5.3. Computations and discussions

A total of seven tests were carried out to measure the unsaturated hydraulic conductivity function for San Diego clay. These experiments were based on the instantaneous profile method concept. However, some modifications

were made to improve the accuracy and equilibration time of the tests. The unsaturated hydraulic conductivity of the specimens was calculated based on the manually measured gravimetric water content and matric suction. Filter paper method was used in accordance with ASTM D5298-03.

4.5.3.1. Instantaneous profile method computations

The first two tests conducted to measure the unsaturated hydraulic conductivity of the subject soil were based on the conventional instantaneous profile method which has been used by many researchers during the past decades. In this method, different sections of soils with different moisture contents are compacted along a long tube such that when moving from one end of the tube to the other end, the moisture content is decreased, or increased gradually. The difference in matric suctions between the adjacent soil sections acts as the driving force to transport water from the wetter side to the dryer end. Unfortunately, the results from the first two tests conducted based on this method were not satisfactory, primarily due to the soil disturbance during the moisture content and suction measurements as well as the confusion on determination of the actual direction of the flow. Jacquemin (2011) reported the deficiencies associated with this method in more details.

After experiencing some deficiencies associated with the conventional instantaneous profile method, the duplicate method was designed and used for measurement of unsaturated hydraulic conductivity. This method incorporates the same concept as the instantaneous profile method but only two soil sections with different initial moisture content is used. First, multiple samples, usually between

4 to 6 samples, are prepared simultaneously with the same conditions, and after a certain period of time, one of the samples is used for moisture content and matric suction measurements. Filter paper sandwiches can be installed at different locations throughout the tube for further suction measurements. In the duplicate method, each sample is used only once so the measured matric suction and moisture content is more representative. One may argue that it is impossible to compact the initial multiple samples exactly identical, so the soil fabric will be different for each specimen, which can significantly affect the saturated and unsaturated hydraulic conductivity of the soil. To overcome this issue, several k_{sat} measurements were conducted for specimens prepared with different initial conditions, and it was concluded that, for the studied San Diego clay, the effect of soil fabric was negligible (see table 4.5).

The parameters required to calculate the unsaturated hydraulic conductivity are the matric suction and volumetric water content between two points at two different times, the distance between the two points, and the time interval for which two water content and suction measurements are obtained. An example of computations required for unsaturated hydraulic conductivity measurement can be found in Jacquemin (2011).

4.5.3.2. Effect of soil cracking on unsaturated hydraulic conductivity of soil

A 2 year laboratory investigation was conducted to understand the effect of cracks on unsaturated hydraulic conductivity of soils. As described in previous section, various test protocols were designed and employed to capture the influence of soil cracks on the hydraulic conductivity of unsaturated soils.

Additionally, different crack patterns and orientations were introduced to the experiments to simulate and study different scenarios that may occur in the field. The analysis of the results from all the experiments, which were performed by Sean Jacquemin, revealed that there is no significant different between the unsaturated hydraulic conductivity of cracked and intact soils for the suction range tested of 200 to 8,000 kPa (see figure 4.14). This range is applicable for most of the geotechnical engineering problems. However, in the lower suction ranges, some differences can be seen. The finding of this study is consistent with what Zhang et al. (2011) suggested based on theoretical considerations. Zhang et al. found that there might be some variation between the unsaturated hydraulic conductivity of cracked and intact soils at very low suction ranges (i.e. suctions less than 1 kPa), but the unsaturated hydraulic conductivity is expected to be similar for both cracked and intact soils at higher values of suction, as shown in figure 4.15.

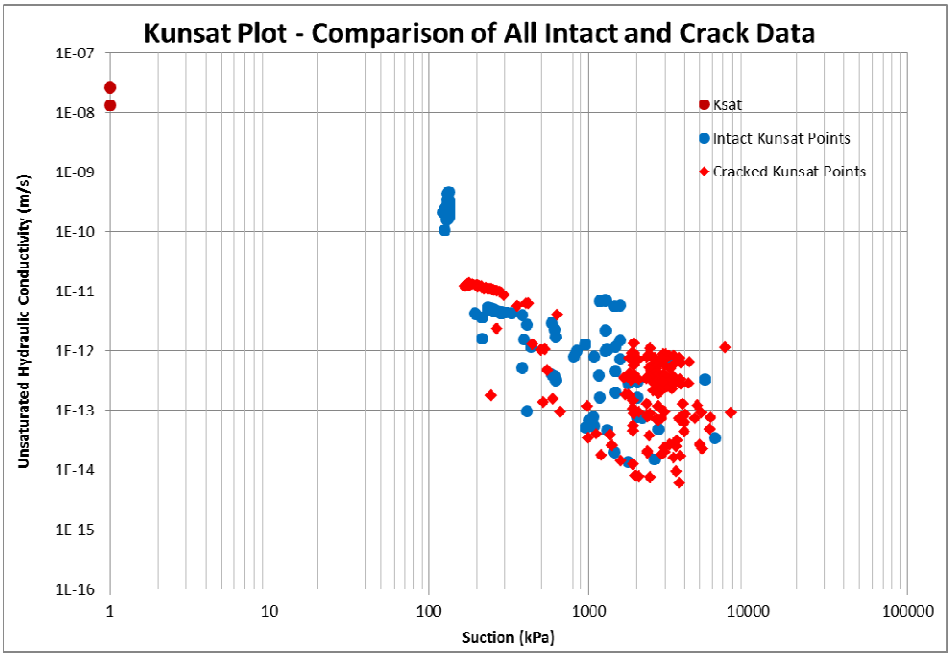

Figure 4.14. K_{unsat} data comparison for all intact and cracked data points (from Jacquemin (2011))

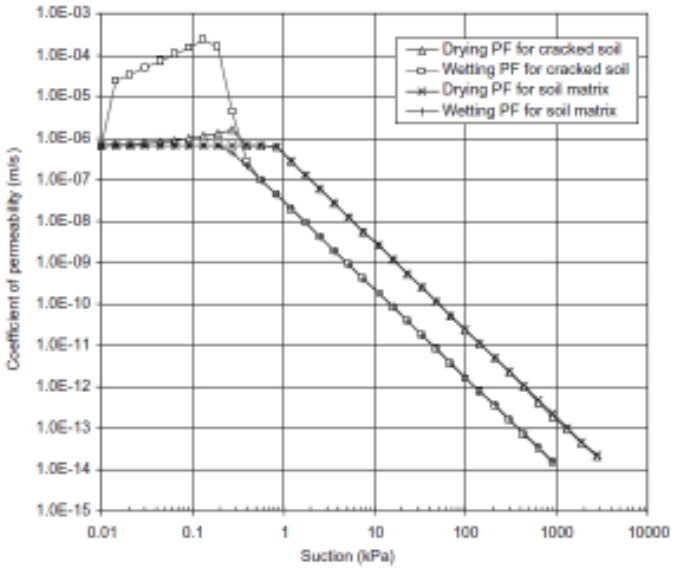

Figure 4.15. Permeability of cracked and intact soil (from Zhang et al. 2011).

After observing no significant variation between the unsaturated hydraulic conductivity values for the measured suction range, for intact and cracked soil, it was decided to only use the intact data for further analyses. There are numerous statistical or semi-empirical relationships in the literature that relates the

unsaturated hydraulic conductivity and the matric suction. However, only the most commonly used relationships including the Gardner (1958), the Kunze et al. (1968), van Genuchten-Mualem (1980), and Leong and Rahardjo (1997) models were used to fit the data determined from the laboratory experiments. Figure 4.16 shows the data for intact soil along with the most commonly used models from the literature.

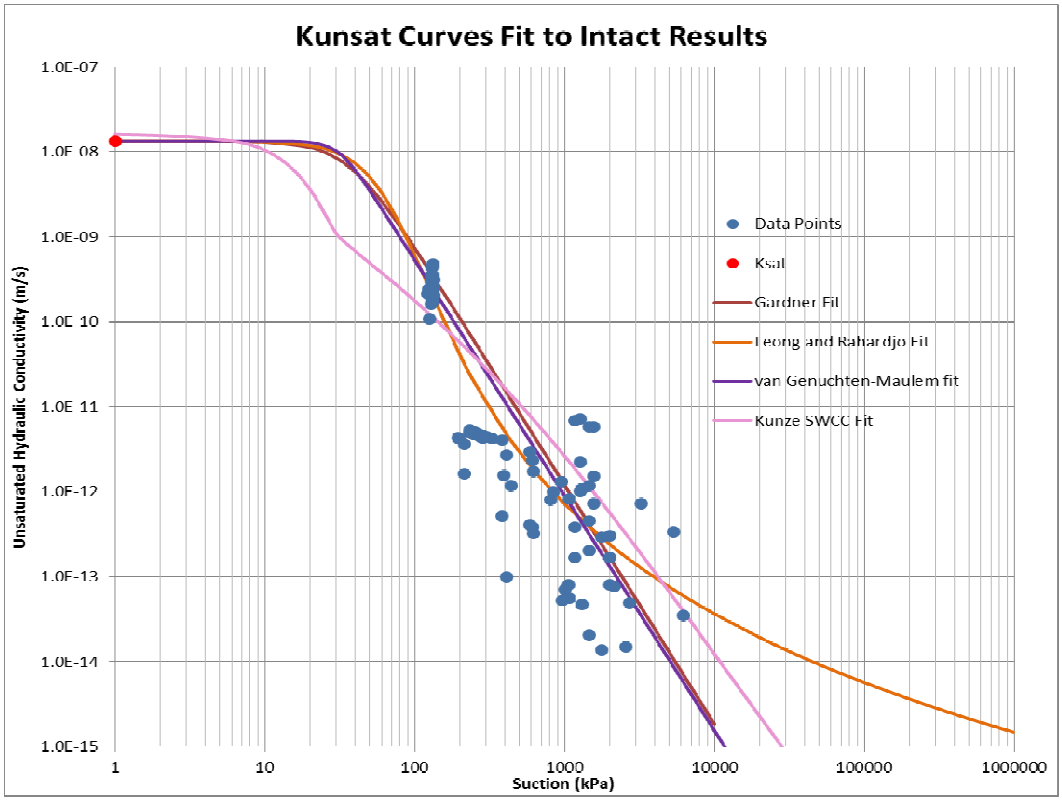

Figure 4.16. K_{unsat} curves fit to intact unsaturated conductivity data (from Jacquemin (2011))

As seen in figure 4.16, the Kunze et al. model, which is based on the drying SWCC of the material, does not fit with the data very well. According to Mitchell and Soga (2005), this method is most accurate for soils with relatively narrow pore size distribution such as sand. This, to some extent, explains why this relationship does not fit to the data well.

The other two methods shown in figure 4.16 are the Gardner and van Genuchten-Mualem models which fit the data well for the lower suctions but they do not accurately predict the conductivity behavior at higher suctions. A study by Ebrahimi et al. (2006) suggested that there is a lower limit for the water permeability coefficient ($\approx 1 \times 10^{-14}$ m/s). This minimum value agrees with the experimental data, but the limit is not implemented in Gardner and van Genuchten-Mualem models, so they can not represent very well what happens at higher suction ranges.

The Leong and Rahardjo model, shown in figure 4.16, probably fits better the experimental data, and reflects the true behavior of the unsaturated hydraulic conductivity for the San Diego soil. Sean Jacquemin developed a new model which was based on the consideration of soil-water-air-vapor phases and transitions between these phases. Jacquemin model is based on the experimental investigations and the considerations provided by Ebrahimi et al. (2006). According to Ebrahimi et al. (2006), the conductivity of a soil is at its highest value at suctions lower than the AEV, and starts to decline after the AEV as air starts to enter through the soil voids. As the soil reaches the residual condition, the conductivity of the soil is governed by the vapor conductivity. This suggests that, depending on the matric suction range, the conductivity function of a soil is a combination of both the soil-water and vapor conductivities. This fact is illustrated in figure 4.17 followed by Jacquemin's proposed model in figure 4.18.

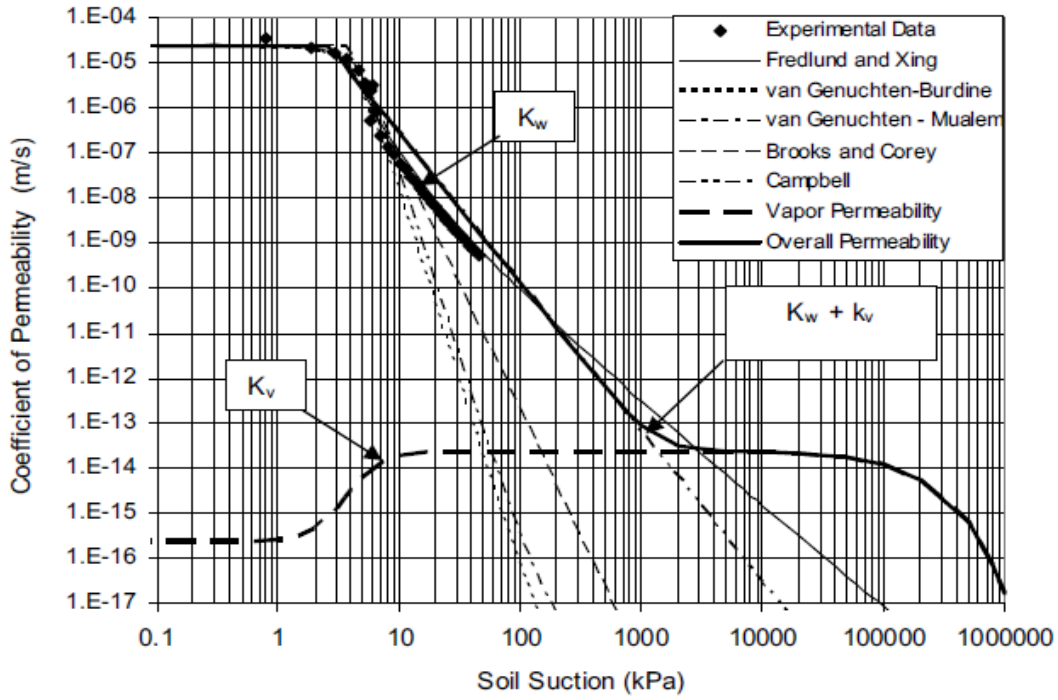

Figure 4.17. Estimation of the permeability function of a soil based on the combination of water and vapor permeability (from Fredlund (2006))

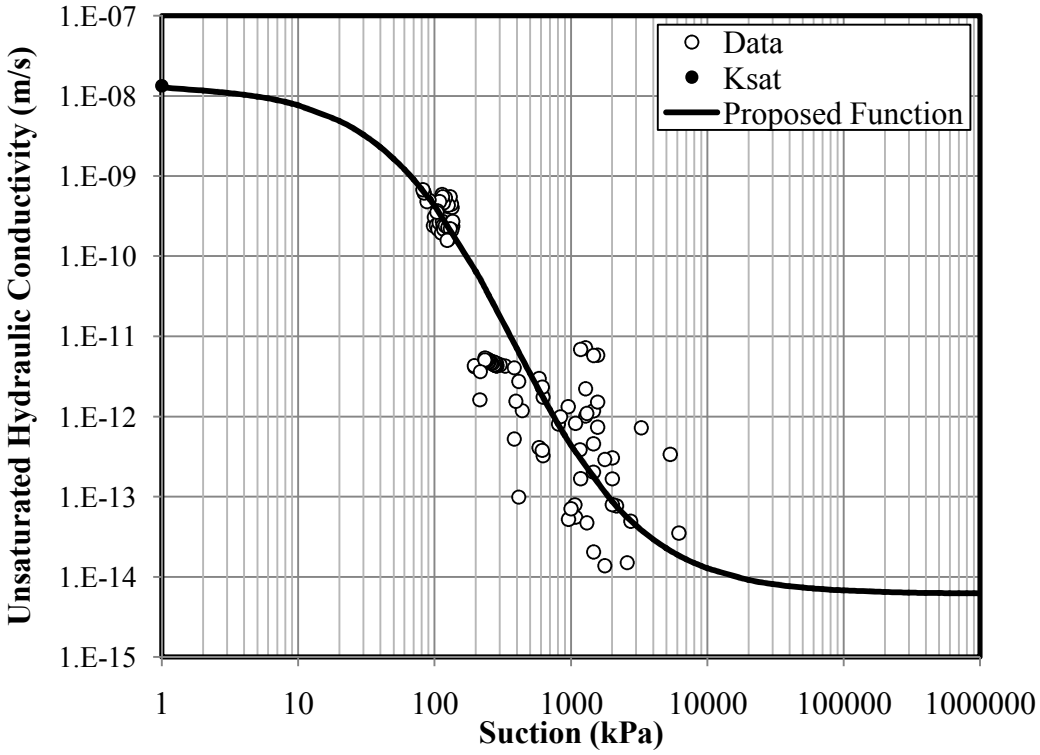

Figure 4.18. Proposed K_{unsat} function for unsaturated soils (Jacquemin (2011))

4.6 Effect of soil cracking on the soil water characteristic curve (SWCC)

A soil water characteristic curve (SWCC), also known as water retention curve, demonstrates the relationship between the matric suction of a soil and the amount of water that the soil can hold at that particular suction, which can be expressed in terms of moisture content, degree of saturation or any other index representing the amount of water inside the soil. Since the beginning of the postulation of unsaturated soil mechanics, the SWCC has played a vital role as one of the most important properties of soils. The SWCC has been used directly or indirectly by many soil scientists and geotechnical engineers around the world for various purposes such as numerical modeling of fluid flow through an unsaturated soil, prediction of unsaturated hydraulic conductivity, stress-deformation properties, and more.

Various methods and procedures have been developed for determination of the SWCC, both for field and laboratory. However, all of the presented methods and techniques have been used only for intact soil. Although there are a few theoretical models related to determination of the SWCC for cracked soil, there is a lack of experimental SWCC data to validate such models. In general, the SWCC determination for a cracked soil is extremely challenging because of the very low Air Entry Value (AEV) of the cracks. In this study, some techniques have been employed to determine the SWCC of cracked soil, and results are compared with SWCC of intact soil. In the following sections, various suction measurement methods are explained first. Second, the SWCC measurement method used in this study for intact soil is discussed. Third, the method used in

this study for SWCC determination of cracked soil is presented, and the challenges associated with SWCC determination for a cracked soil are outlined. Fourth, the laboratory SWCC results for the intact and cracked soils are compared, and an overview of the effect of soil cracking on the SWCC is presented.

4.6.1 Different suction measurement techniques

The matric suction is basically the air pore pressure, which is equal to atmospheric pressure in field, minus the negative pore water pressure (see equation 4.8). It can be measured either directly or indirectly.

$$\text{Matric suction} = u_a - u_w \tag{4.8}$$

Where u_a is the pore air pressure and u_w is the pore water pressure. The total suction, however, has two components; namely, matric suction and osmotic suction. Equation 4.9 shows the relationship between the three different suctions.

$$\psi = (u_a - u_w) + \pi \tag{4.9}$$

Where ψ is the total suction, $(u_a - u_w)$ is the matric suction and π is the osmotic suction. By definition, the decrease in relative humidity due to the presence of dissolved salts in the pore-water is referred to as the osmotic suction, π. Table 4.6 illustrates the most common devices used for measuring different suctions. In this study, the axis translation technique was employed which is explained below in the next section. Should a reader need further information about any of the other methods, detailed information can be found in Fredlund and Rahardjo (1994), Zapata (1999) or any other unsaturated soil mechanics textbook.

Table 4.6. Soil suction measurement devices (from Fredlund and Rahardjo (1994))

Name of device	Suction component measured	Range (kPa)	Comments
Psychrometer	Total	100[a]-8000	Constant temperature environment required
Filter paper	Total	Entire range	May measure matric suction when in good contact with moist soil
Tensiometers	Negative pore-water pressure or matric suction when pore-air pressure is atmospheric	0-90	Difficulties with cavitation and air diffusion through ceramic cup
Null-type pressure plate (axis translation)	Matric	0-1500	Range of measurement is a function of the air entry value of the ceramic disk
Thermal conductivity sensors	Matric	0-400	Indirect measurement using a variable pore size ceramic sensor
Pore fluid squeezer	Osmotic	Entire range	Used in conjunction with psychrometer or electrical conductivity measurement

[a] Controlled temperature environment to 0.001 ºC

4.6.1.1 Axis translation method

The direct measurement of the soil-water characteristic curve (SWCC) involves different experimental techniques that are used to provide a series of discrete data points comprising the relationship between soil suction and water content. These methods can be either applied for field or laboratory SWCC determination. As mentioned earlier, one of the most common direct methods to measure the matric suction is axis translation method. This method, which was

originally proposed by Hilf (1956), can be used in laboratory for testing disturbed or undisturbed specimens. The setup used by Hilf is illustrated schematically in figure 4.19. The general term axis translation refers to the practice of elevating pore air pressure in unsaturated soil while maintaining the pore water pressure at a measurable reference value, typically atmospheric (Lu and Likos (2004)). In this technique, the soil sample is placed inside an oedometer-type device over a ceramic stone or High Air Entry Disk (HAED). The HAED is designed in a manner that it allows water to infiltrate through the disk but it does not allow the air to pass through the disk. In this way, when the ceramic stone is saturated and the sample is in good contact with the stone, it can be said that the pore water pressure is almost equal to the atmospheric pressure, because the water underneath the stone is freely connected to the atmosphere. Thus, the matric suction of the soil would be equal to the value of the applied air pressure inside the cell. In other words, in axis translation method the negative pore pressure is translated into the higher range of atmospheric pressure so that the matric suction can be controlled by only applying a known value of air pressure inside the cell using a hydraulic pump. The implementation of this method is explained in more details in section 4.6.2.

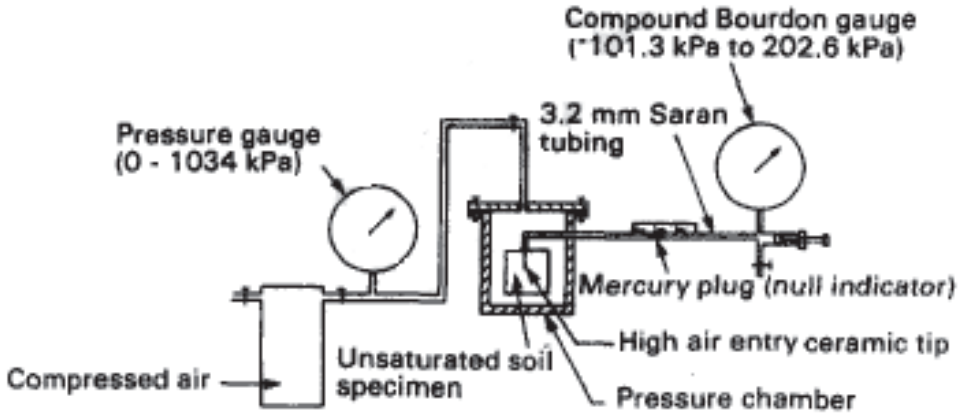

Figure 4.19. Original setup for the null-type, axis-translation device for measuring negative pore-water pressures (from Hilf (1956)).

4.6.2 SWCC determination for intact soil

Five SWCC tests were conducted for intact San Diego soil entailing both drying (3 tests) and wetting (2 tests) paths. These experiments were conducted either under zero or 20 kPa net normal stress. In cases where zero normal stress was applied, some token load (≈ 1kPa) was applied in order to maintain the specimen in good contact with the ceramic stone.

4.6.2.1 Apparatus

The Fredlund SWCC cell was used to conduct both the drying and wetting SWCC tests. A schematic of this device is shown in figure 4.20. This device is consisted of two main parts: one oedometer-type cell in which the specimen should be placed and one volume change device which is being used for measuring the amount of water released (in a drying test) or absorbed (in a wetting test) by the specimen. The oedometer-type cell has three main parts; namely the bottom plate, the cell wall(s), and the top plate which is tighten to the

bottom plate with the wall in between using four long bolts. There is often a loading ram mounted on top of the SWCC cell, which allows the application of the normal stress to the specimen and, if equipped with an LVDT, the vertical deformations can be measured during the course of the test. In the absence of the LVDT, a spring caliper or a dial gauge may be used to measure the movement of the load plate with respect to the top plate of the cell. To prevent the loading ram from moving during the application of the cell pressure, a pressure compensator is incorporated into the loading ram. The bottom plate (the base) is where the ceramic stone rests over a grooved surface, as shown in figure 4.21. The grooved channel is connected to the volume change device (volumetric tubes). The objective of the grooved channels is to maintain the ceramic stone saturated during the test as well as to facilitate the flushing of diffused air during the testing program. As illustrated previously in table 4.6, the suction range for this device depends directly on the type of the ceramic stone being used. Typical ceramic stone capacities are 1, 3, 5, and 15 bars. With knowing the maximum suction that will be applied to the specimen, an appropriate ceramic stone can be selected for use. It is very important not to exceed the capacity of the stone during testing. It is also possible to change the stones in the middle of a test; however it can only be achieved once the specimen is equilibrated at the previously applied suction, and care should be taken to prevent any water lost from the sample.

Figure 4.20. General view of Fredlund SWCC device (from www.gcts.com)


Figure 4.21. Fredlund cell bottom plate (base) with grooved channel

Multiple pressure regulators with proper pressure gauges were used depending on the range of the required pressure. For lower suction application, the pressure gauges with more accuracy were used while for higher suction ranges, higher capacity pressure gauges were employed. The laboratory temperature was kept nearly constant at 21 ºC (+/-1 ºC), and the evaporation rate during the whole period of testing program was recorded and the results were adjusted accordingly.

4.6.2.2 Sample preparation

To be consistent with other experimental study of this research, the same sandy clay (SC) San Diego soil was used for SWCC experiments. Full soil characterization information is provided in Chapter 3. "Identical" companion specimens were compacted by using the same methods as those explained in chapter 3 for preparation of the swell pressure test specimens. For drying tests, after sample preparation, specimens were saturated by completely soaking them under water. For wetting tests, however, it is more complicated to start the test. While performing a wetting test, it is very important to start the test with a soil which is within a close suction range as the desired initial suction. Otherwise, it will take a long time for the specimen to equilibrate, especially if the initial suction is higher than 700 kPa. Therefore, after compaction of the specimen is completed, the sample was allowed to dry naturally (air-dry) in laboratory environment until the desired water content (representing the estimated for the desired initial suction based on SWCC drying curves) was achieved. After that, the sample was sealed in a plastic bag to prevent any further moisture changes,

and left for internal moisture equilibration for 4 to 10 days. The purpose of wrapping the sample is to ensure that the moisture inside the specimen is equally distributed throughout the soil. It is believed that during the air-drying process, more water would evaporate from the soil surface, so the sample requires some time to reach to the internal moisture equilibration.

4.6.2.3 Testing procedure

A total of five SWCC tests were performed, three of which followed a drying path and the other two followed a wetting path. SWCC tests were performed with" zero" (nominal seating load) and 20 kPa of vertical stress. From the results of the wetting SWCC tests, it was concluded that the effect of overburden pressure on the SWCC results are negligible for the soil under study over the range considered. Therefore, it was decided to conduct the other two drying SWCC tests with nominal normal stress as the replicates for the first conducted SWCC drying test (performed under 20 kPa confinement).

After initial dimension and weight of each specimen was measured, the sample was placed on the High Air Entry Value (HAEV) ceramic disk which is seated on the bottom plate. The HAEV should be saturated prior to the test (soaked in distilled water for at least 24 hours), and the epoxy glue around the ceramic stone should be flawless. Also the O-ring and its container on the bottom plate should be clean of any soil particles before starting the test. Then the cell wall(s) should be placed over the bottom plate in direct contact with the O-ring. There is also another O-ring on top of the cell wall which should be cleaned before the top plate is positioned on the wall. The top and bottom plates can then

be secured by tightening the appropriate bolts to seal the cell. The volumetric tubes should be filled with distilled and de-aired water and the water needs to be flushed using any flushing device available to expel any trapped air in the groove of the bottom plate. While flushing, one should be careful not to introduce more air into the grooves located in the bottom plate and also not to spill any water from the top of the tubes. It is important to cover the top of the volumetric tubes after flushing to prevent water evaporation from the tubes. Placement of a thin film of oil on top of the water column has been shown to prevent evaporation. While no more air bubbles are observed during the flushing, the device is ready to use and the test can be started by applying the desired normal load and cell pressure (suction). If measurement of the soil volume change is required, an appropriate volume change monitoring device should be assembled such as LVDT, spring caliper, or a dial gauge. The water level at both tubes should be recorded and checked regularly until the sample reaches equilibrium. For the tested soil, the equilibrium was considered to be reached when the volume change reading did not change for 72 hours. At this point, the water content change from the previous stage can be determined by having the amount of water released/absorbed. After reaching equilibrium at a particular suction and before going further to the next suction level, the cell can be either disassembled for weight and volume change measurements or it can only be relied on the volumetric tubes readings and proceed to the next stage with no need to open the cell. In this study, for drying tests, the cell was disassembled after equilibrium was attained for each suction in order to measure the weight and volume change

of the sample. However, it was assumed that for wetting, the volume change only occurs vertically, which can be measured without need to open the cell. Thus, the cells were maintained closed throughout the wetting SWCC experiments. At the end of each test, the sample was weighted and volume changes were measured and recorded and the sample was left in the oven for 16 to 20 hours in order to calculate the final water content of the soil. The obtained data was used to compute the required properties such as volumetric water content, degree of saturation and void ratio. Table 4.7 shows some details about the conducted SWCC tests for intact specimens.

Table 4.7. Summary of SWCC tests for intact (non-cracked) specimens

Test ID	Test type	Applied air pressure (kPa)	Applied normal stress (kPa)
Intact-01	Drying	10, 90, 200, 450, 1240	0
Intact-02	Drying	25, 100, 200, 450, 1240	0
Intact-03	Drying	8, 50, 265, 480, 1240	0
Intact-04	Wetting	1320, 320, 140, 35	0
Intact-05	Wetting	1320, 320, 140, 35	20

4.6.2.4 Results of SWCC tests for intact (non-cracked) San Diego samples

A total of five SWCC experiments were conducted for intact specimens. Three of these tests were conducted following drying paths and the other two were conducted following wetting paths. The SWCC results for the drying and wetting tests on intact specimens of San Diego soil are summarized in figure 4.22.

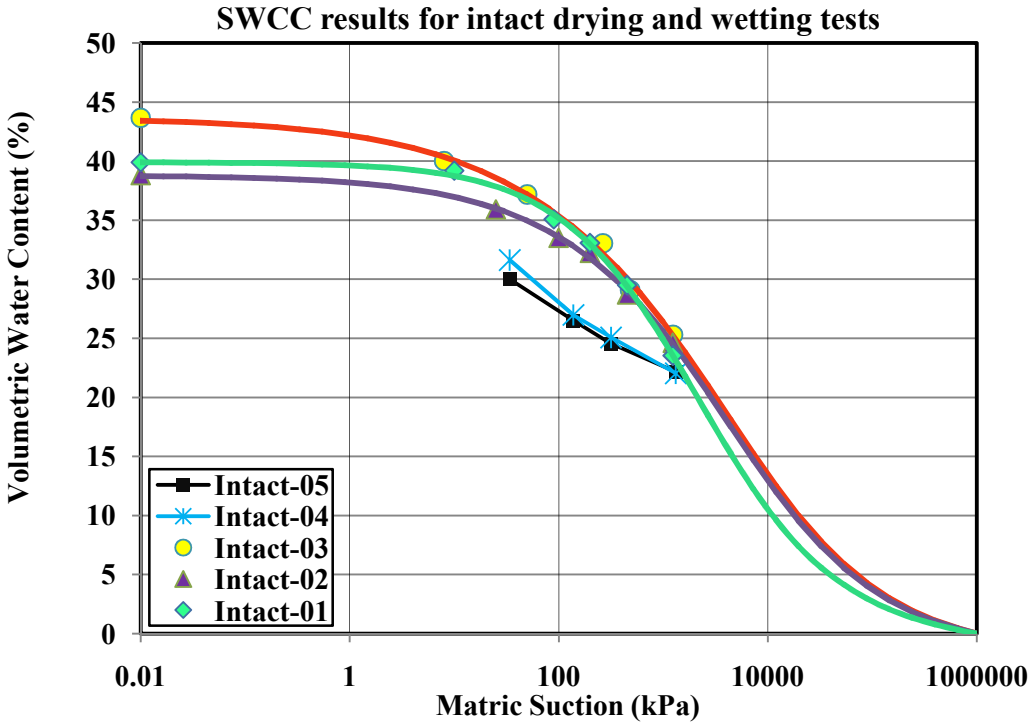

Figure 4.22. Summary of SWCC test results for intact drying and wetting tests

4.6.3 SWCC determination for cracked soil

Six SWCC tests were conducted for cracked San Diego soil, four of which were conducted following a drying path and two of them following a wetting path. Similar to SWCC tests for intact soil, the Fredlund SWCC cell was used to conduct the drying and wetting SWCC experiments. The cracked samples were initially prepared exactly as if preparing an intact specimen, but later an aluminum shim was used to create some artificially-introduced cracks inside the sample. The main challenge for SWCC determination of a cracked soil is to somehow apply and maintain an extremely low suction at the beginning of a drying test, because it is believed that the AEV of the created cracks is so low that by applying an initially high suction, the behavior of cracks cannot be studied

thoroughly. More details regarding the methods and techniques used for applying very low suctions are discussed in the following section.

4.6.3.1 Apparatus

The Fredlund SWCC cell was employed to perform four drying and two wetting experiments. Except one of the wetting tests that was conducted under 20 kPa of vertical stress, other experiments were performed with no overburden pressure (≈ 1kPa normal stress was applied only to keep the contact between the sample and the ceramic stone).

4.6.3.2 Sample preparation

As mentioned earlier, the sample preparation procedure was similar to the one for the intact specimen except after the sample was compacted inside the stainless steel ring, soil cracks were introduced into the soil matrix using an aluminum shim. The literature was studied thoroughly for finding a suggested crack pattern consistent with field crack observations. However, due to the extremely sophisticated process of soil cracking formation, it is impossible to generalize one crack pattern for all soils. After reviewing many different field and laboratory crack patterns through a combination of literature and laboratory studies, it was concluded that the hexagon pattern was the most appropriate pattern because it was relatively consistent with the actual crack patterns. Taking the hexagonal pattern is also consistent with the findings of Konard and Ayad (1997) that suggested a polygon crack pattern (shown in figure 4.23) during different stages of cracking as well as the observed field cracks (shown in figure 4.24) reported by Longwell (1928).

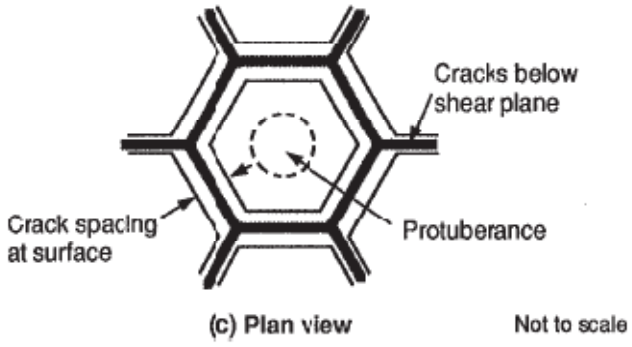

Figure 4.23. Potential crack polygon (from Konard and Ayad (1997))

Figure 4.24: Hexagonal mud crack pattern on a playa surface composed of very uniform (homogeneous) sediments, Nevada (from Longwell 1928, notes: the hammer and handle measured 330 mm; adopted from Kodikara et al. (1998)).

To create a cracked specimen, an intact specimen was prepared according to the procedure indicated above. Afterwards, aluminum shims of 0.025" thickness were used to create the cracks. Figure 4.25 illustrates the artificial crack creation process. For drying SWCC tests, the sample should be saturated by submerging the specimen inside a water tray while both ends of the soil sample are covered by one filter paper directly in contact with the soil surface and a porous stone which is only in direct contact with the filter paper. This process

prevents losing any soil during the swelling and saturation phase and also facilitates the infiltration of water through the porous stones. For wetting SWCC tests, however, the specimen is required to be air-dried until it reaches the water content range corresponding to the desired initial suction at which the test will be started.

Figure 4.25. An example of different stages of creating a cracked specimen for SWCC tests

4.6.3.3 Testing procedure

A hanging manometer technique was used to apply very low suction values. This method involves creating a negative pore water pressure (u_w), while keeping the pore air pressure (u_a) constant and equal to atmospheric pressure. This will result in matric suction (u_a-u_w) being equal to the value of the negative pore water pressure. As the water elevation inside the water tubes is positioned lower than the base elevation of the oedometer, the sample experiences a suction equal to -u_w. For instance, to apply 0.1 kPa, one has to create the elevation difference equal to 1.0 cm between the water level in the tubes and the cell base (where the sample sits). Figure 4.26 shows a hanging manometer technique being applied to create very low suction values.

One of the major difficulties associated with setting a fixed low suction value is the continuous elevation change of the water that occurs inside the tube as the specimen seeks equilibration with the applied suction. Thus, the applied suction changes as the water elevation of the tube changes, and to keep the small applied suction constant, close monitoring is required on regular basis, becoming cumbersome considering the lengthy test times required for equilibration, especially for highly plastic soils. Another fact which makes tests at low suctions challenging is that it is not possible to fully saturate the intact portion of the specimen because back-pressure saturation techniques are not easily employed in pressure plate testing. It was observed, at some very low suction stages of the SWCC test, that even after the specimen (likely the cracks in the specimen) released water at a prior, lower suction stages, the sample would tend to absorb water from the tube as the suction was increased (though still quite low). It is believed that this behavior is a result of the intact matrix part of the soil not having been fully saturated, even when the cracks were filled with water and extensive time for saturation of the specimen under submergence conditions had preceded the SWCC test. In other words, at early stages of the test, when the cracks are still full of water, the fractured phase of the soil dominates the behavior, while at later, higher suction stages, as the cracks dewatered, the intact soil matrix (not 100% saturated) governs the response. Table 4.8 summarizes the SWCC tests that were conducted for cracked specimens.

Figure 4.26. Illustration of hanging manometer technique for determination of SWCC for cracked soil

Table 4.8. Summary of SWCC tests for cracked specimens

Test ID	Test type	Applied air pressure (kPa)	Applied normal stress (kPa)
Cracked-01	Drying	0.1, 1.0, 25, 90, 200, 485, 1240	0
Cracked-02	Drying	0.075, 1.035, 8.0, 30, 90, 345, 1240	0
Cracked-03	Drying	0.075, 0.555, 1.46, 10, 25, 90, 565, 1240	0
Cracked-04	Drying	0.09, 0.78, 10, 45, 100, 200, 425, 1260	0
Cracked-05	Wetting	1255, 290, 100, 35	0
Cracked-06	Wetting	1255, 290, 100, 36	20

4.6.3.4 Results of SWCC tests for cracked soil

Total of six SWCC tests were conducted for cracked specimens prepared by compaction of San Diego soil. Four of these tests were conducted following drying paths and the other two were conducted following wetting paths. To apply very low suctions, hanging manometer technique was used. The SWCC test results of the cracked specimens are summarized in figure 4.26 including both wetting and drying curves. It should be noted that experiments cracked-05 and cracked-06 are wetting curves while the rest of the tests represent drying curves. Although it is difficult to draw a single curve representing the entire data set, the

curve shown in figure 4.27 clearly demonstrates the bimodal behavior of the SWCC for the cracked samples. It should be noted that sample cracked-04 exhibited an abnormal behavior throughout the course of the test so for the sake of consistency, the results for cracked-04 are not included herein. It was found that the main reason for observing unrealistic results for test cracked-04 was that the sample was not completely saturated prior to the test commencement. The effect of overburden stress, for the limited stress range considered here, seems negligible for the wetting experiments. More variability or scatter is observed in the SWCC of cracked soils in comparison with the SWCC for intact soils. It is believed that the scatter is due to the complex behavior of the soil cracks that will bring more uncertainties and unknowns into the picture. In other words, while the cracks are introduced into the soil, although one may try to create identical specimens, cracks will make it more or less impossible for two similarly prepared specimens to be truly identical.

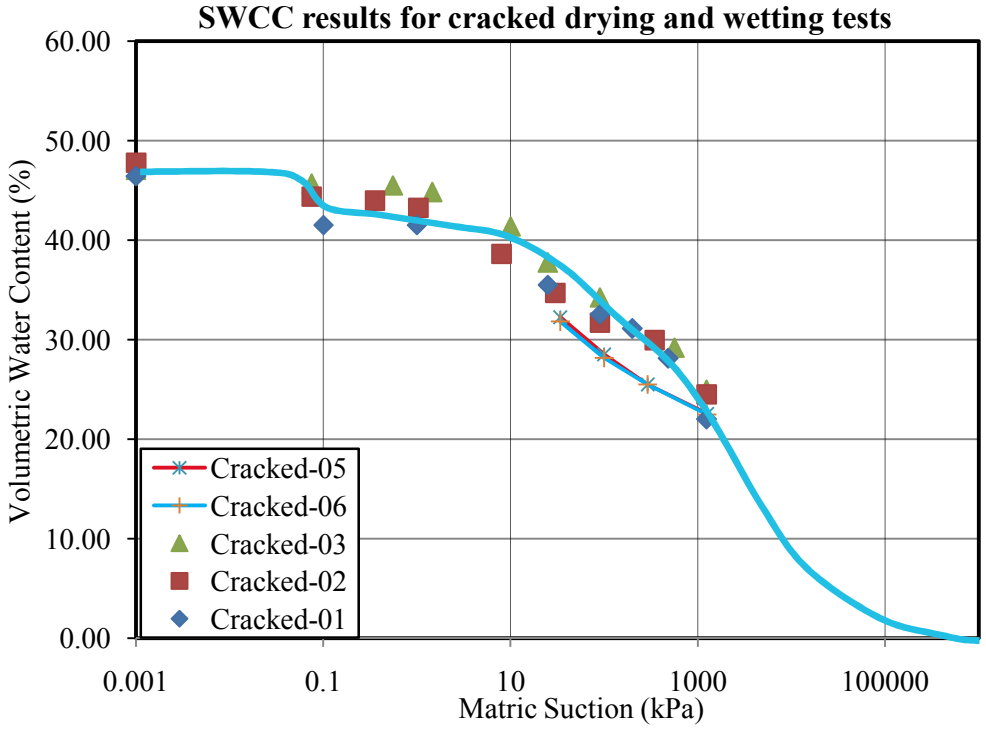

Figure 4.27. Summary of SWCC results for drying and wetting tests on cracked soils

4.6.4 Effect of soil cracking on SWCC

The purpose of conducting over 10 different SWCC tests for intact and cracked compacted specimens, prepared identically from San Diego soil, was to compare the results for intact and cracked samples which eventually enable us to better understand the effect of soil cracking on the SWCC. By looking at figure 4.27, it can be said that the cracked soil has a bimodal behavior while the first AEV belongs to the cracks and the second AEV is related the soil matrix. The AEV of subject cracks of this study was found to be around 0.1-0.2 kPa. This is consistent with the theoretical calculations obtained by Abbaszadeh et al. (2010), which is also presented in Appendix C to explain the relationship between width of crack and capillary rise in a crack. Additionally, this AEV range for the

cracked soils tested in this study is also consistent with the author's visual observations while conducting the SWCC experiments. The visual observations showed that the dewatering of the cracks occurs at matric suction higher than 0.07 kPa and lower than 1.0 kPa. Figure 4.28 below compares the SWCC test results for intact and cracked specimens.

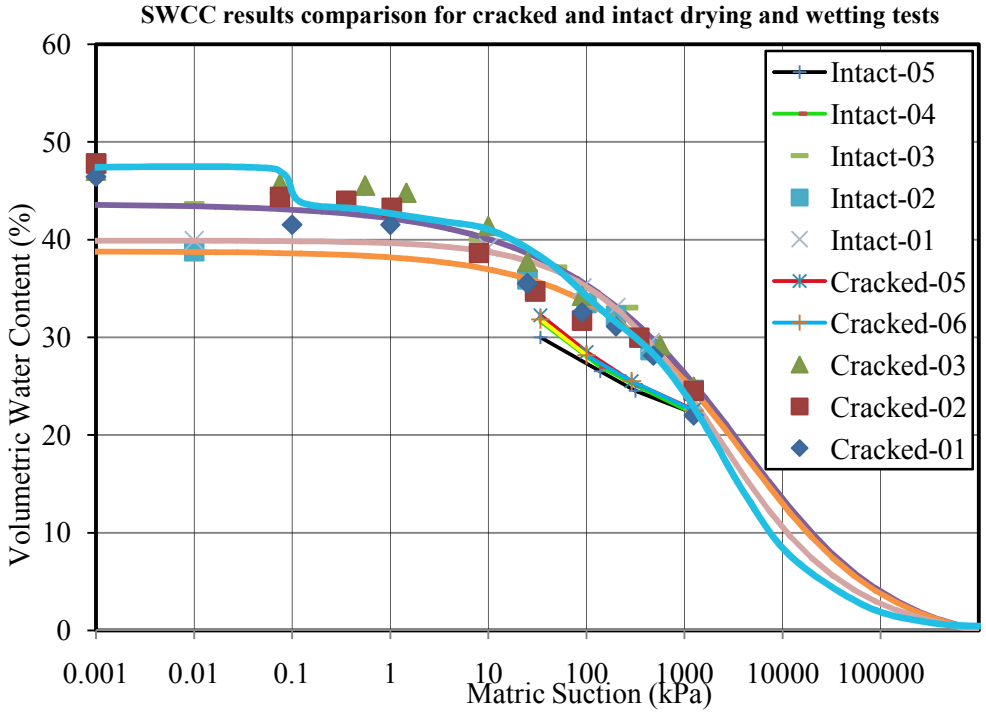

Figure 4.28. Comparison of all the measured SWCC tests for cracked and intact specimens

From the above plot, it can be concluded that the SWCC for cracked soil is only different from the intact soil at very low suction values. Theoretically, the cracked soil is expected to exhibit bimodal behavior. This phenomenon can be explained by the pore space distribution disparity that the cracks will create in the matrix structure of the soil. In other words, the cracks will dewater easier than the soil's internal matrix voids. However, at higher suctions the SWCC is not affected by the presence of cracks. This means that after a certain matric suction range, the

water storage capacity of the intact and cracked soils tend to merge. The range of suction where the curves merge depends entirely on the crack dimensions such that the smaller cracks would have larger AEV and larger cracks would have smaller AEV. This finding is a significant contribution to geotechnical engineering field because many unsaturated soils problems of a practical nature involve unsaturated conditions when the soil suction is much higher than the crack's AEV range. Furthermore, the studied crack sizes in this research represent the lower range of field cracks in term of dimensions. Consequently, for most of the unsaturated field applications, it would be rational and convenient to treat a cracked soil as an intact and use the intact properties for further property predictions or for modeling purposes.

Additionally, the wetting SWCC results for cracked and intact soils showed no significant difference in the suction range of interest for most unsaturated soil problems. Also, it was concluded that the normal stress does not have a considerable impact on neither wetting nor drying SWCC tests. It should be noted that although the unsaturated soil SWCC for cracked and intact specimens is essentially the same over a wide range of suction of interest for unsaturated soil mechanics problems, saturated flow properties of cracked and intact specimens may be quite different, and volume change properties may be quite different, particularly for swelling soils where the presence of cracks provides a cavity for expansion that reduces vertical heave and swell pressure. These aspects of cracked versus intact behavior are discussed in other section of this dissertation.

4.6.5 Total and available storage capacity for intact and cracked unsaturated soils

The storage capacity of a soil corresponds to the amount of water that a soil can embrace while given a free access to the water. Some soils are able to absorb and hold more water than others. The storage function has a significant impact on the infiltration rate of a soil. In the case where a soil has a high storage capacity, it is also important to recognize how much of that capacity is truly available for the water. Sometimes, the storage capacity is not completely available for the water. Note that when the total storage capacity of a soil is used, the soil can be considered as a saturated soil and the saturated hydraulic conductivity can be used. However, often times, an unsaturated soil remains unsaturated after the rainfall or irrigation event, because the duration of the water infiltration has not been enough so that the entire storage capacity of the soil can be mobilized. Particularly in a soil with open cracks, the initial water will flow relatively fast through the cracks and fill them out, but after the entire crack network is filled with water, it is difficult for the water to infiltrate through the somewhat impermeable unsaturated soil matrix. The speed of the latter flow will be governed by the unsaturated hydraulic conductivity of the soil surrounding the cracks which is drastically lower than the saturated hydraulic conductivity of the soil. Thus, although the experimental investigations of this chapter suggest that a cracked soil has a higher storage capacity than the intact soil, more than often this capacity is only partially available for the water, and as soon as the available storage capacity is exceeded, water runs off. Only after a sustained steady state saturated flow is the total storage available. This is considered to be a significant

contribution to geotechnical engineering field because it illuminates the water-soil interaction in the field in a more realistic fashion.

For many years now, numerous experimental and field studies have reported the same behavior of cracked soils as they are introduced to water. It has been found by many researchers that the infiltration rate through a cracked soil is initially very high but after a certain period of time (usually in the orders of hours), the infiltration rate drops drastically (e.g. Bouma (1980); Zhan et al. (2007)). Almost all of the researchers have related this reduction in infiltration rate to the healing of the cracks. Nevertheless, after the abovementioned discussion regarding the storage capacity, it can be also said that the dramatic drop in the infiltration rate is due to the fact that the available storage capacity of the soil matrix is used during the first few hours of the raining event. For more water to enter into the soil, the water can only flow into the unsaturated region, which occurs extremely slowly because of the very low unsaturated hydraulic conductivity values.

These important aspects of storage capacity are needed to be considered while attempting to model the unsaturated cracked and intact soils. More discussion regarding how the storage capacity should be addressed for modeling purposes is presented in Chapter 5.

4.7 Summary and conclusion

The main objective of this chapter was to study the effect of soil cracking on the saturated and unsaturated flow properties of soil. In order to achieve this objective, three main laboratory tasks were accomplished. First, the saturated

hydraulic conductivity of cracked soil was measured utilizing a conventional triaxial apparatus, and compared against the measured k_{sat} for the intact soil. Second, the unsaturated hydraulic conductivity of cracked soil was measured and compared with that for intact soil. The instantaneous profile method was used to measure the unsaturated hydraulic conductivity of cracked and intact soils. Finally, the effect of soil cracking on the SWCC of soil was investigated. Both wetting and drying curves were studied. The effect of normal stress on the conducted SWCC experiments was also considered.

The measured saturated hydraulic conductivities for the cracked samples were found to be primarily governed by the intact portion of the soil matrix. This means that the conductivity of the cracked soil is extremely high such that the flow is not retarded by the cracked portion. This finding is consistent with what have been reported repeatedly in the literature and referred to as preferential flow. In fact, the existence of the cracks facilitates the bypassing of the top cracked soil layer during the water flow. Most of the cracked soils are very plastic and moisture sensitive, often expansive, soils. As such, whenever the water in introduced to these soils, they swell and the cracks will tend to heal (close). After the cracks are closed, the preferential flows will be visually disappeared, but it is likely that these "healed" cracks still represent a relatively unimpeded flow path, as evidenced by the saturated hydraulic conductivity tests performed as a part of this study. Furthermore, conventional consolidation tests were used as an alternative method to determine the saturated hydraulic conductivity. This method underestimated the k_{sat} values, and that is largely because of the fact that the

sample was overconsolidated. Furthermore, the relationship which was used to adjust the initially computed k_{sat} values for a lower void ratio is not precisely applicable for clayey soils.

Seven experiments were designed and performed in order to measure the unsaturated hydraulic conductivity of cracked and intact soils. Different crack orientations were studied to simulate the direction of flow with respect to the crack orientation or direction. Different methods and setup are explained in 4.5.2.1 and 4.5.2.2. The results suggested that the unsaturated hydraulic conductivity of a soil is not significantly affected by the soil cracks within the matric suction range of the experiments (200-8000 kPa). This finding is a significant contribution to geotechnical engineering, because it can help engineers to design and model cracked soil as an intact when they need to predict the unsaturated hydraulic conductivity of a cracked soil.

Additionally, laboratory determination of SWCC for both cracked and intact soils were conducted. Both drying and wetting curves were studied as well as the effect of normal stress on SWCC tests. The hexagonal crack pattern was accepted from a combination of literature and laboratory research. Cracks were introduced artificially by using a shim. Hanging manometer technique was implemented in order to apply and maintain extremely low matric suctions during the course of the SWCC determination for cracked samples. Experimental results showed that the SWCC for a cracked soil can be represented by a bimodal curve. However, the AEV of the cracks is very low, even for the relatively small width cracks considered in the laboratory study. Dewatering of larger field cracks

would be expected to occur at extremely low suction values, and perhaps to dewater under gravity alone. SWCC results at higher suctions were very similar for cracked and intact specimens which may strengthen the thought of considering a cracked soil as a continuum.

Finally, some important aspects of the storage function were discussed. It was proposed that the secondary slow infiltration rates for cracked soils might be associated with the almost impermeable unsaturated soils surrounding the cracks. While many studies have suggested that the healing of the cracks act as the main reason for the dramatic drop of the infiltration rate after a few hours, it is believed that the unavailable storage capacity of the intact portion of the soil matrix can also be an important factor, or maybe the major factor, in slowing the water penetration through the soil. These discussions about the total and available storage capacity of a soil are also important for the modeling of an unsaturated soil in general, and a cracked soil in particular, which is addressed in Chapter 5.

Chapter 5

NUMERICAL MODELING OF UNSATURATED FLOW AND IMPACT OF CRACKS ON EXTENT AND DEGREE OF WETTING FOR FIELD CONDITIONS

5.1. Abstract

One of the keys to perform a successful numerical modeling of unsaturated flow is to properly describe the unsaturated soil properties. There are always some degrees of variability associated with the unsaturated properties of soils such as SWCC and unsaturated hydraulic conductivity, which can impact the numerical modeling solution. For instance, the hysteresis effect and the degree of reproducibility of the SWCC experiments are some sources of variability associated with the SWCC. Furthermore, the variability of the unsaturated hydraulic conductivity functions, to some extent, can also be explained by the variability of the SWCC because most of the available models in the literature use the SWCC for prediction of the unsaturated hydraulic conductivity function. In addition, for direct experimental measurements of k_{unsat}, as already shown in chapter 4, the variability is attributed to the challenges of reproducibility of the experiments.

One and two-dimensional modeling of unsaturated flow of intact and cracked soil were performed to: 1) understand the impact of variability associated with the unsaturated soil properties on the numerical solutions and modeling outputs; 2) Back-analyze unsaturated hydraulic conductivity functions for the subject soil and make comparison to the results from the laboratory instantaneous

profile tests; 3) Suggest empirical adjustments for modeling "lumped mass" cracked soil behavior in numerical codes for fluid flow through cracked soils; and 4) Perform example analyses, using the empirically adjusted flow parameters, for slab-on-grade foundation problems to demonstrate the impact of cracks on degree and extent of wetting under unsaturated and flow conditions with a surface flux boundary condition corresponding to Arizona climatic conditions.

5.2. Introduction

The problem of water flow through the vadose zone is a multidisciplinary topic which has been addressed extensively in the literature by different specialties including soil scientists, hydrologists, agricultural engineers, environmental and geo-environmental engineers, and geotechnical engineers. Richards equation has been used widely by many scientists to analyze the unsaturated flow. The pressure head-based formulation of this equation is:

$$\frac{\partial}{\partial x}(k(h)\frac{\partial h}{\partial x}) = \gamma_w m_{2w}\frac{\partial h}{\partial t} \tag{5.1}$$

Where k(h) or k_{unsat} is the unsaturated hydraulic conductivity as a function of h (m/s), x is the elevation (m), h is the total head (m), t is the time, γ_w is the specific weight of water (9.81 kN/m^3), m_{2w} is the storage capacity of soil that can be represented by the slope of the SWCC (m^2/kN), and t is the time (s). Various analytical and mathematical methods have been developed to solve Richards equation which is a nonlinear, parabolic, advection-diffusion partial deferential equation. Also, there are many commercial and public domain software available to solve this equation. In this study, SVFlux (part of the SVOffice software suite)

is used to obtain a numerical approximation. SVFlux is a finite element program based on a FlexPDE kernel which is a general tool for solving PDE systems.

From equation 5.1, it can be postulated that the solution of Richards equation is sensitive to both SWCC (slope of SWCC) and k_{unsat} functions of the soil. On the other hand, it is quite impossible, for a particular soil, to define the SWCC and/or unsaturated hydraulic conductivity function precisely. There is always some degree of variability associated with these unsaturated soil properties. Hence, it is always necessary to examine the influence of the uncertainties associated with these unsaturated soil properties on the numerical models. Dye et al. (2011a) carried out a study to investigate the impact of unsaturated soil properties variability on moisture flow modeling. The authors postulated that small variations in the unsaturated soil hydraulic conductivity function have significantly changed the outputs, while substantial changes in SWCC alone had little effect on the solution. Dye et al. proposed that a range of potential unsaturated hydraulic conductivity functions should be considered to determine the range of possible soil responses to unsaturated flow. This is consistent with the findings of this study, which will be discussed later in section 5.3.1.

5.3. Instantaneous profile (1-D) modeling and the impact of uncertainties associated with unsaturated properties of soil on the numerical solution

The commercial finite element-based software, SVFlux (part of the SVOffice software suite), was chosen for the unsaturated flow modeling of this study. To simulate the instantaneous profile laboratory experiments, one-

dimensional analyses was performed. The purpose of this modeling was to: 1) evaluate the sensitivity of the results from the unsaturated flow models to the variability of the unsaturated soil properties; and 2) compare the results from numerical analyses to the results obtained from the instantaneous profile laboratory experiments. In the following sections, first the influence of the SWCC and k_{unsat} variability on moisture flow is investigated. Then, the results from different numerical modeling scenarios are compared with the instantaneous profile laboratory experiments. Based on this comparison, some minor empirical adjustments to directly measured k_{unsat} functions are proposed for further 2-D numerical modeling. For purposes of this study, the instantaneous profile test number 3 was simulated using a simplified 1-D numerical modeling approach.

5.3.1. Sensitivity of the numerical analyses of unsaturated flow to SWCC and unsaturated hydraulic conductivity function, k (h)

The variability of the SWCC is attributed to different factors such as hysteresis, various test techniques, different test procedures, operator error, and dry density (Zapata (1999)). Hence, for the SWCC of a soil, it is more realistic to consider a band for SWCC rather than a single curve. Figure 5.1, developed by Zapata (1999), shows the uncertainty associated with the SWCC for a clayey soil.

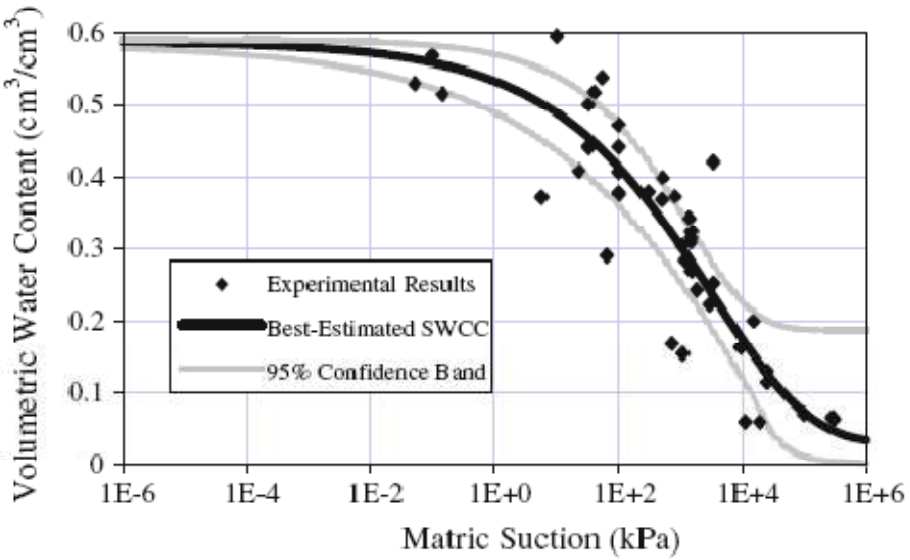

Figure 5.1. Uncertainty of the SWCC for a clayey soil from Arizona (from Zapata (1999))

For the unsaturated hydraulic conductivity function, the variability expected is even higher than for the SWCC, because the kunsat function is often times estimated based on soil properties such as the SWCC and saturated hydraulic conductivity. It was shown in Chapter 4 that even with the most advanced experimental techniques the scatter in kunsat results is inevitable. Numerical analyses were performed, using SVFlux software, to investigate the influence of the above-mentioned uncertainties on the unsaturated flow of intact soils. To be consistent with the entire experimental program of this study, the same soil from San Diego was used for numerical modeling purposes. Moreover, instantaneous profile experiment number 3 was chosen for simulation. In this test, two sections of soil with different initial moisture contents were compacted inside a 9.0" long tube with 2.75" inner diameter. Figure 5.2 depicts the test set-up and initial conditions. Further details regarding test number 3 can be found in section 4.5.2.1.3.

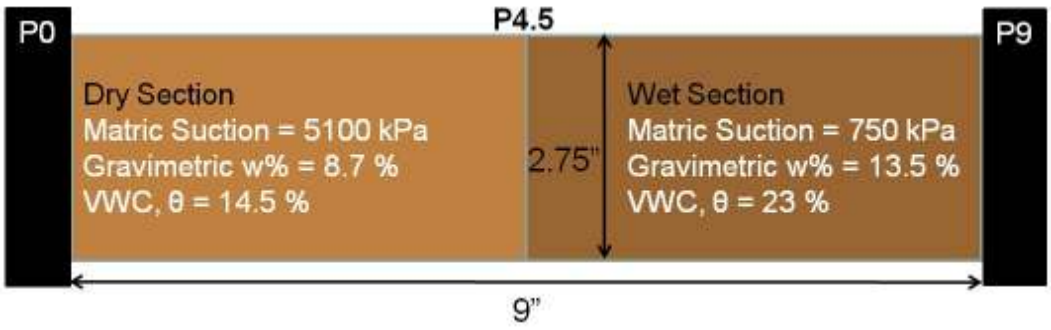

Figure 5.2. Illustration of test No. 3 set-up and initial conditions

Several one-dimensional analyses were performed to simulate the unsaturated flow conditions for instantaneous profile test number 3. Table 5.1 summarizes the different scenarios used in modeling, which are illustrated graphically in figures 5.3 and 5.4.

Table 5.1. Summary of different SVFlux modeling scenarios

Case number	SWCC	k_{unsat}	Equilibration time (days)
1	Upper band	Best fit	800
2	Lower band	Best fit	600
3	Best fit	Best fit	1000
4	Best fit	Upper band	20
5	Best fit	Lower band	6000

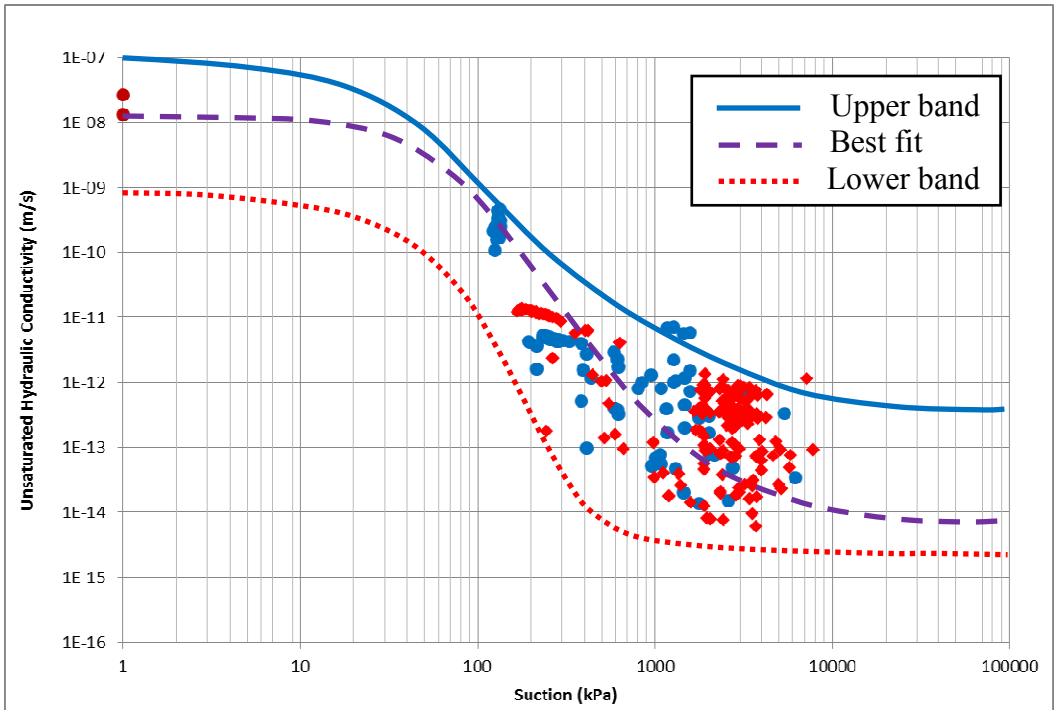

Figure 5.3. Studying possible k_{unsat} bands for modeling purposes

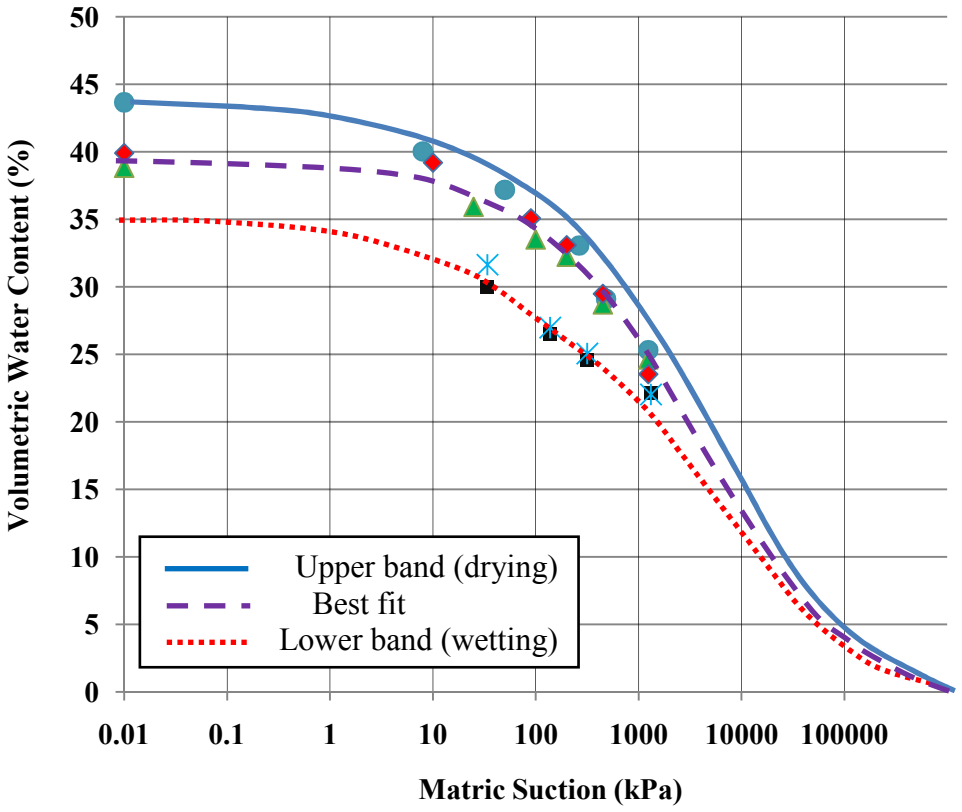

Figure 5.4. Studying upper and lower SWCC bands for modeling purposes

Figure 5.5 shows the geometry of the implemented model in SVFlux environment.

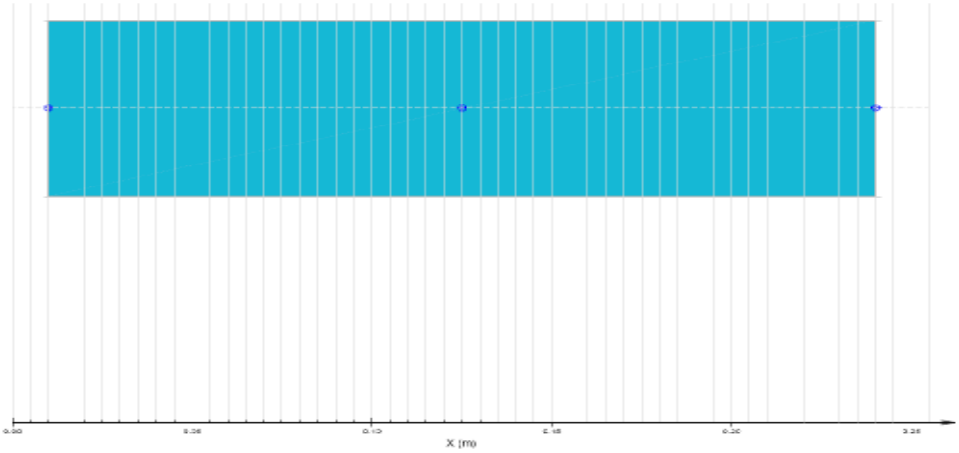

Figure 5.5. 1-Dimensional Instantaneous Profile Test (IPT) model geometry in SVFlux

The horizontal 1-D analysis was selected for the Instantaneous Profile Test (IPT) model. No-flux boundary condition was chosen for the left and right end boundaries. Similar to the laboratory test number 3, the left-half section of the tube corresponded to the dry condition while the right-half corresponded to the wet condition. This distinction was incorporated into the software by applying different initial pore water pressures for the left-half and right-half of the model. Then, by changing only one parameter at a time, the influence of the unsaturated properties of soils was examined in accordance with Table 5.1.

In case number 1, the upper band SWCC is used together with the best fit k_{unsat} function. As illustrated in figure 5.2, the initial suction is 5,090 kPa and 750 kPa for the left and right sections, respectively. After running the program for a simulated period of 1,000 days, the suction profile was monitored and recorded for three points inside the column corresponding the dry end, middle, and wet end

segments (P0, P4.5, and P9 in figure 5.2). Based on the SVFlux outputs, equilibration time was varied from 20 days to 6,000 days for different scenarios. Figures 5.6 through 5.10 show the suction profile results for cases 1 through 5.

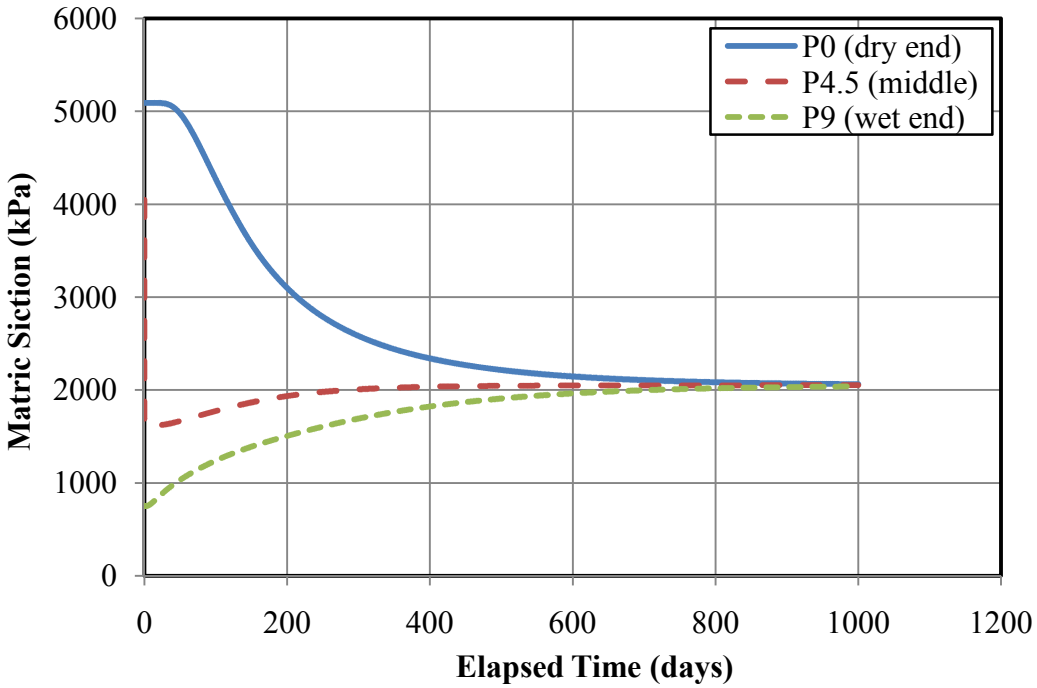

Figure 5.6. Suction profile results for Case number 1 (Upper band SWCC-Best fit k_{unsat})

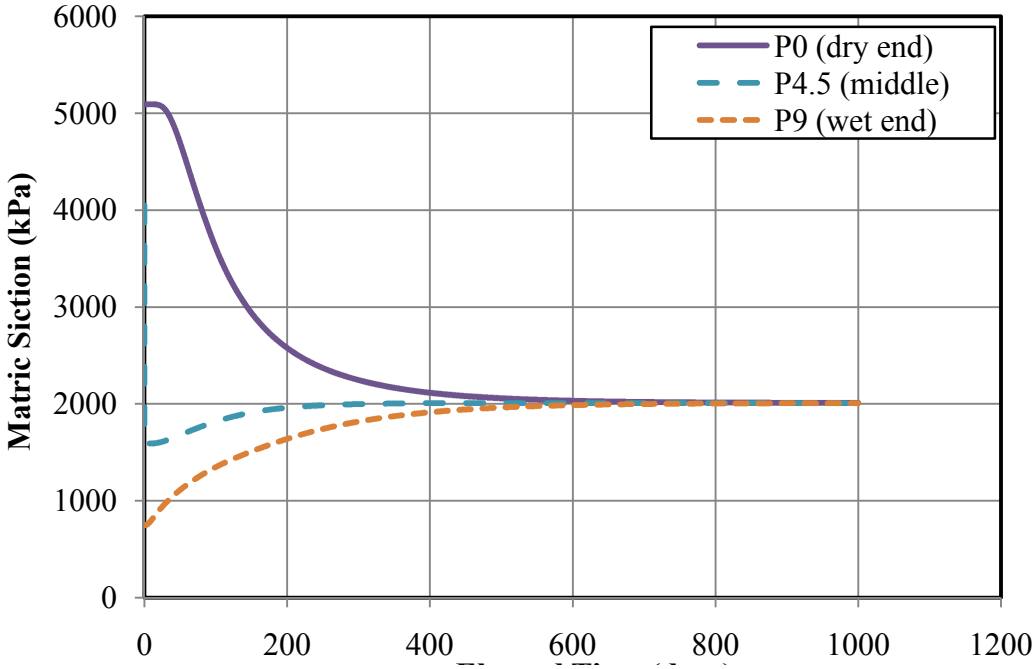

Figure 5.7. Suction profile results for Case number 2 (Lower band SWCC-Best fit k_{unsat})

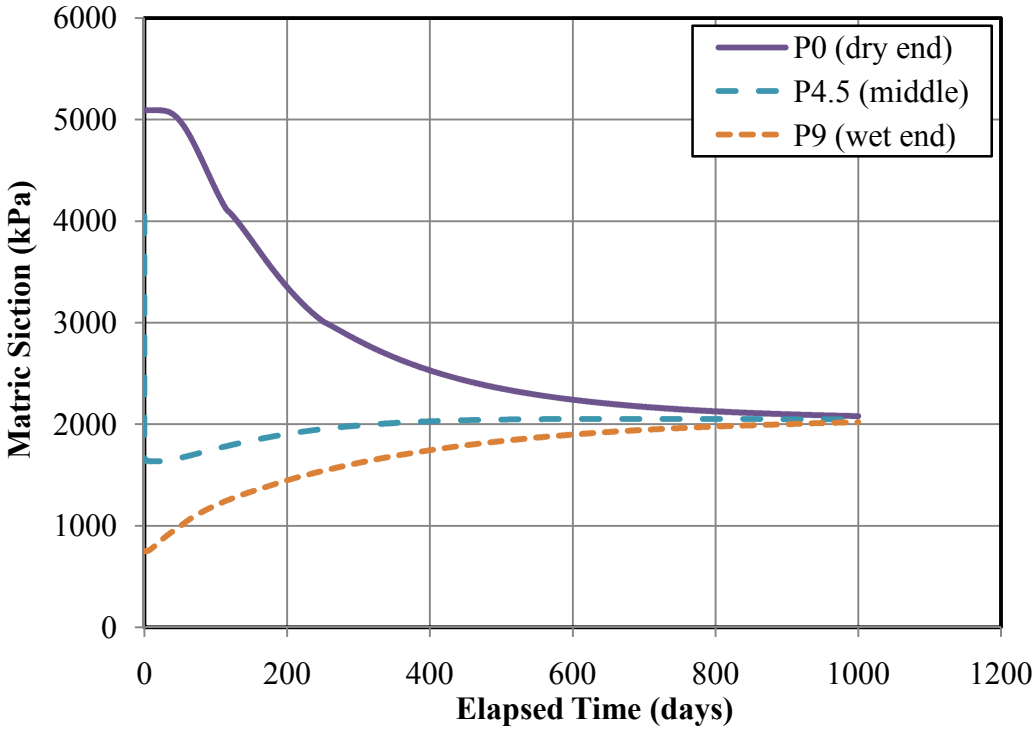

Figure 5.8. Suction profile results for Case number 3 (Best fit SWCC-Best fit k_{unsat})

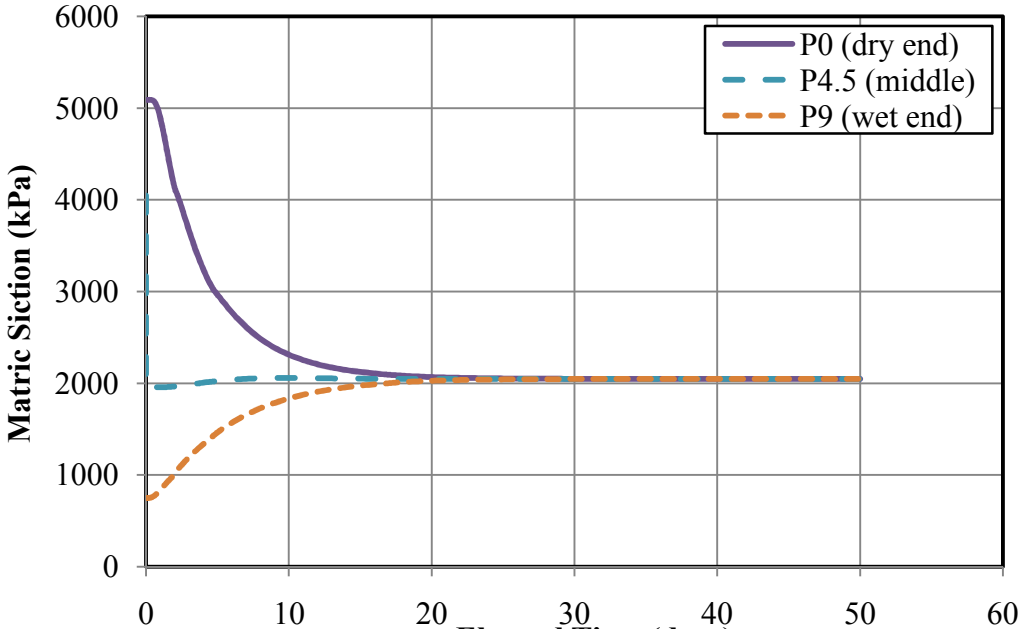

Figure 5.9. Suction profile results for Case number 4 (Best fit SWCC-Upper band k_{unsat})

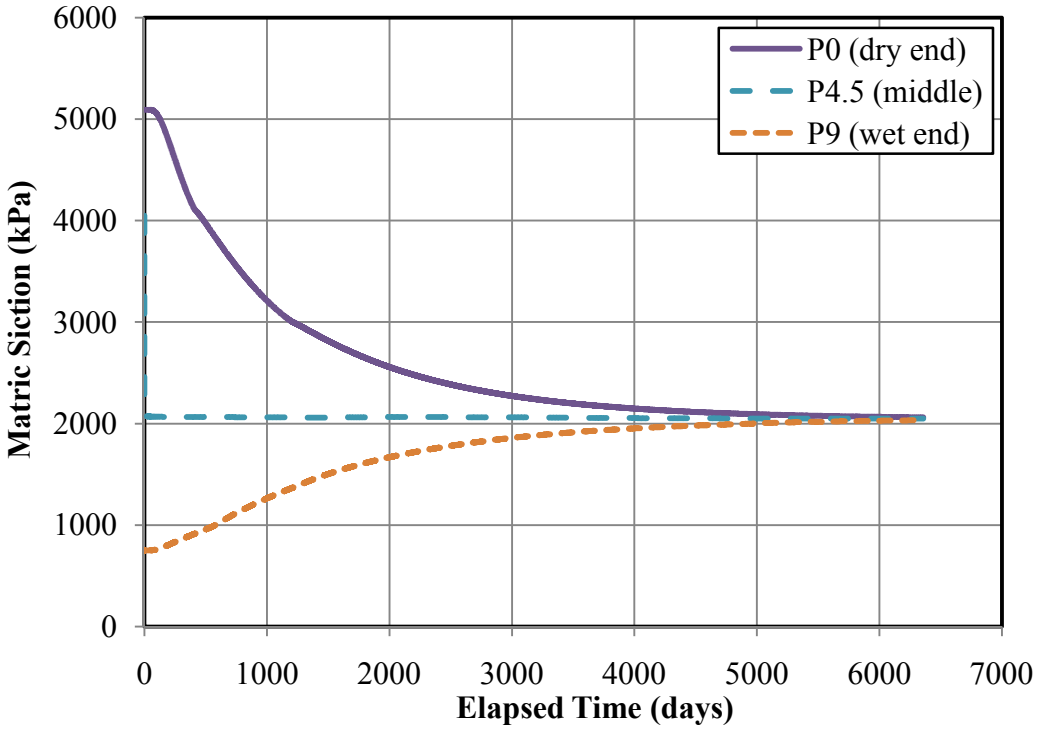

Figure 5.10. Suction profile results for Case number 5 (Best fit SWCC-Lower band k_{unsat})

The effect of SWCC on the numerical solutions can be studied by looking at cases 1 through 3 in which the k_{unsat} function is kept constant while different SWCC functions were tested. Regarding the effect of the SWCC on the numerical solutions, it can be postulated that the main effect takes place as a result of differences between the storage functions. However, for the tested conditions, it does not seem that the SWCC significantly impacts the numerical solutions. Furthermore, figures 5.6 to 5.10 imply the fact that if the time would have been rescaled, we should have gotten the similar results. In other words, if we had non-dimentionalization of the problem with appropriate time scales, the same results would be expected for the different runs.

On the other hand, the effect of k_{unsat} function on the numerical solutions can be studied by considering cases 3 through 5 in which the SWCC is kept constant while various k_{unsat} functions were examined. From the results shown in figures 5.8 through 5.10 it can be concluded that the equilibration time is extremely sensitive to the selected k_{unsat} function. This is consistent with the findings of Dye et al. (2011), and as expected given the Darcy's law model incorporated into Richards' equation.

5.3.2. Comparison of the 1-D numerical models to the laboratory experiment results

The results obtained from the laboratory investigations of this study for the instantaneous profile test number 3 are presented in figure 5.11.

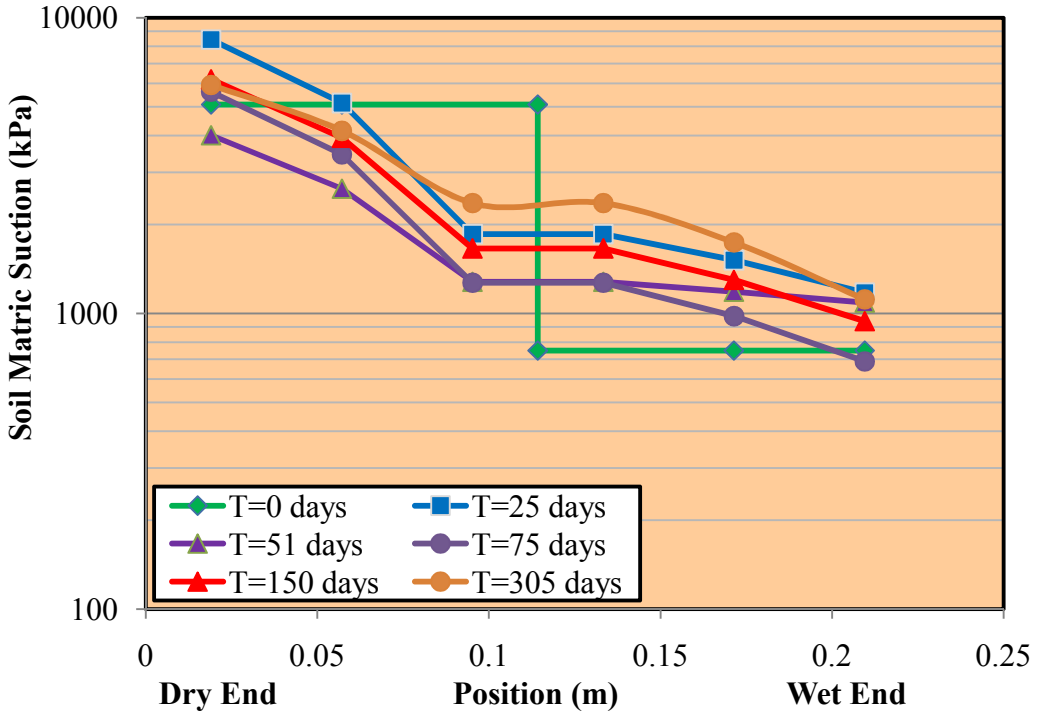

Figure 5.11. Actual laboratory results for instantaneous profile test number 3 (from Jacquemin (2011))

Although the laboratory experiments only feature the first 305 days of the equilibration process, it is still valid to compare the projected equilibration suction and duration from the numerical models to the measured values from the experimental program at different stages of the test. From this comparison, it appears that the projected equilibration suction from the numerical modeling is consistent with the trend of suction variations from laboratory investigations. For instance, it can be seen from figure 5.11 that after 305 days, the suction is around 2200 kPa for the mid-point of the profile (P4.5). It should also be noted that the laboratory results for mid-point is considered to be the most accurate results throughout the entire tested profile due to the minimal influence of the imposed boundary conditions in this region of the test specimen. After comparing the

results from the numerical modeling and the laboratory experiments, it appears that case 3 which uses the best fits for both SWCC and K_{unsat} provides the closest results to the ones form the actual laboratory experiments. Thus, it was decided to use case 3 for further 2-D slab-on-grade analyses. Additionally, since the numerical and laboratory experimental results were in good agreement, it is not recommended to use a more sophisticated model other than Richards equation for the subject problem of this study.

5.4. Slab-on-grade (2-D) modeling and effect of cracks on performance of foundations

After understanding the effect of unsaturated soil properties on the 1-D numerical analyses and selecting the appropriate SWCC and k_{unsat} function consistent with laboratory investigations, a number of 2-D models were developed to simulate the slab-on-grade foundations on an expansive soil. These 2-D models incorporate cracked conditions by using lumped parameter properties obtained from experimental instantaneous profile tests on cracked soils, and the results are compared to the un-cracked conditions in order to capture the effect of cracks on the performance of foundations.

5.4.1. The problem statement

The slab-on-grade foundation is simulated using 2-D modeling with the SVFlux software. Figure 5.12 illustrates the geometry and imposed boundary conditions for the model. It should be noted that, as shown in figure 5.12, only half of the entire problem is simulated and, due the symmetry about the centerline beneath the center of the slab, the results will be identical for the other half.

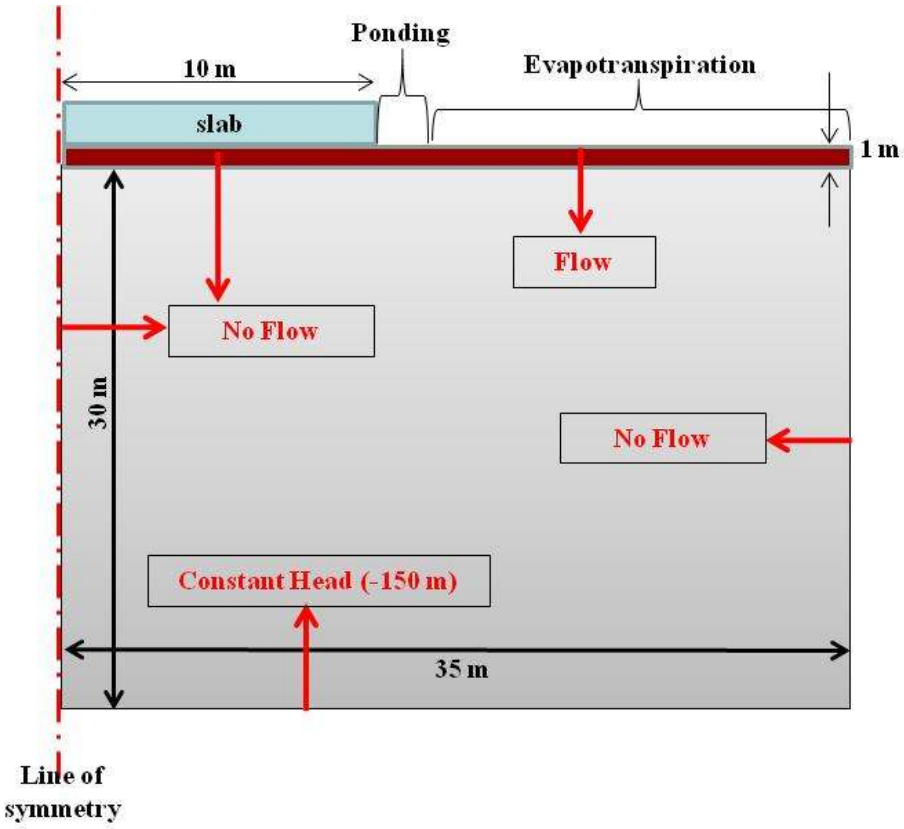

Figure 5.12. Slab-on-grade foundation used in 2-D SVFlux modeling

To impose the ponding and evapotranspiration climatic conditions, average reported Arizona precipitation and evaporation were used from Dye (2008). Rainfall on the roof area was ponded next to the slab following a rainfall event, but any ponding resulting in a pond height of more than 0.15 m was allowed to run-off rather than infiltrate. Outside of the slab and pond areas, natural climatic precipitation and evapotranspiration were applied. These conditions are summarized in figures 5.13 below.

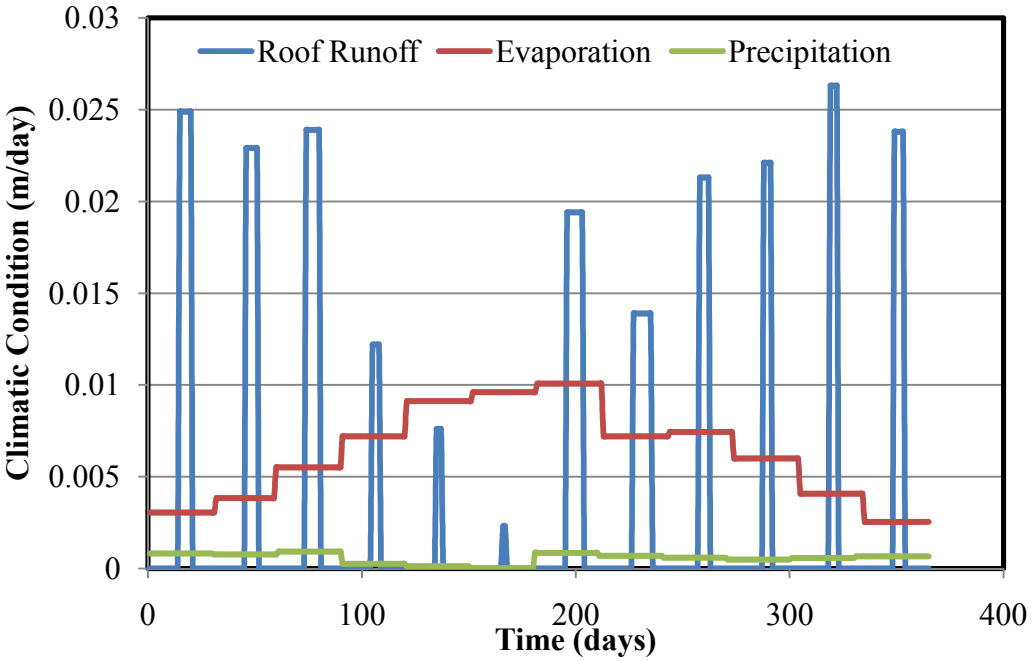

Figure 5.13. Average precipitation/evaporation data in Arizona used as the boundary conditions for the ground surface

The evaporation and precipitation were averaged throughout each month. However, for ponding, Dye (2008) found that it is reasonable to multiply the total evaporation of each month by 6 to estimate the total ponding for that particular month. Then the total ponding for each month should be divided by total days of rain for that month to estimate the rate of ponding per day for those particular raining days of the month. In this study, for simplification purposes, it was assumed that rainfall starts in the middle of each month.

5.4.2. Establishing the initial condition

Establishing a suitable initial condition for the problem was found to be one of the most challenging tasks to reach a stable numerical solution. A steady state analyses were performed and used as the first initial condition for the transient analyses and followed by an iterative process of using the final results

from each transient analyses as the initial condition for the next analyses until a desired stable solution is attained.

For the initial steady-state analyses, it is important to use the same boundary conditions and mesh size distribution as will be used for further transient analyses. If a transient solution failed during the effort for reaching a stable solution, the last reliable data saved on the system can be used as the initial condition for the next transient analyses. For the subject study, it was found that it usually takes from 6 to 10 iterations to reach to a stable solution.

5.4.3. Unsaturated soil properties for cracked and intact material

The results from 1-D modeling revealed the fact that the numerical solution is sensitive to the unsaturated soil properties used for the analyses. Furthermore, the comparison between the results from actual laboratory experiments and different modeling scenarios showed that using the best fit SWCC and k_{unsat} function provides the best solution for the unsaturated flow problems of this study. Hence, the remaining challenge is how to implement the effect of soil cracks into the numerical analyses.

The results from laboratory investigations of this study have been used to differentiate between cracked and intact soils in numerical models. Essentially, the SWCC experiments showed similarities between intact and cracked soils at suction values above the crack's AEV, which was found to be very low for the studied crack dimensions. Moreover, even though the cracked soil exhibited bimodal behavior considering suction levels lower than the AEV of the cracks, the difference between soil water characteristic curves for intact and cracked soils

were found to be very small for suction values in excess of the AEV of the cracks. Consequently, for most field applications of unsaturated soil mechanics, it is reasonable to use the same SWCC for cracked and intact soils because the suction value corresponding to the AEV of the cracks is so small as to be of little engineering significance for unsaturated flow applications. Thus, one SWCC was used for cracked and intact soils in the numerical modeling investigations of this study. Figure 5.14 shows the SWCC used to model both intact and cracked soils. Likewise, the unsaturated hydraulic conductivity of the tested soil was not considerably influenced by the cracks because the k_{unsat} functions for the cracked and intact clay are essentially the same at suction values greater than the AEV of the cracks. Nevertheless, the saturated hydraulic conductivity tests showed that the k_{sat} is extremely higher for a cracked soil compared to an intact one. Therefore, for the suction ranges lower than the AEV of the cracks, the hydraulic conductivity is expected to be dramatically higher for cracked soils. From the modeling perspective, this fact is implemented by defining a bimodal hydraulic conductivity function for cracked material. Figure 5.15 and 5.16 illustrate the inclusion of this bimodal hydraulic conductivity function for modeling purposes. It should be kept in mind that this study uses a "lumped-mass" approach in which the cracked material is considered to behave as a continuum, as opposed to the "discrete" approach in which the cracks and intact media are considered/modeled separately. It is also should be noted that employing the "lumped-mass" approach has its own limitations and restrictions.

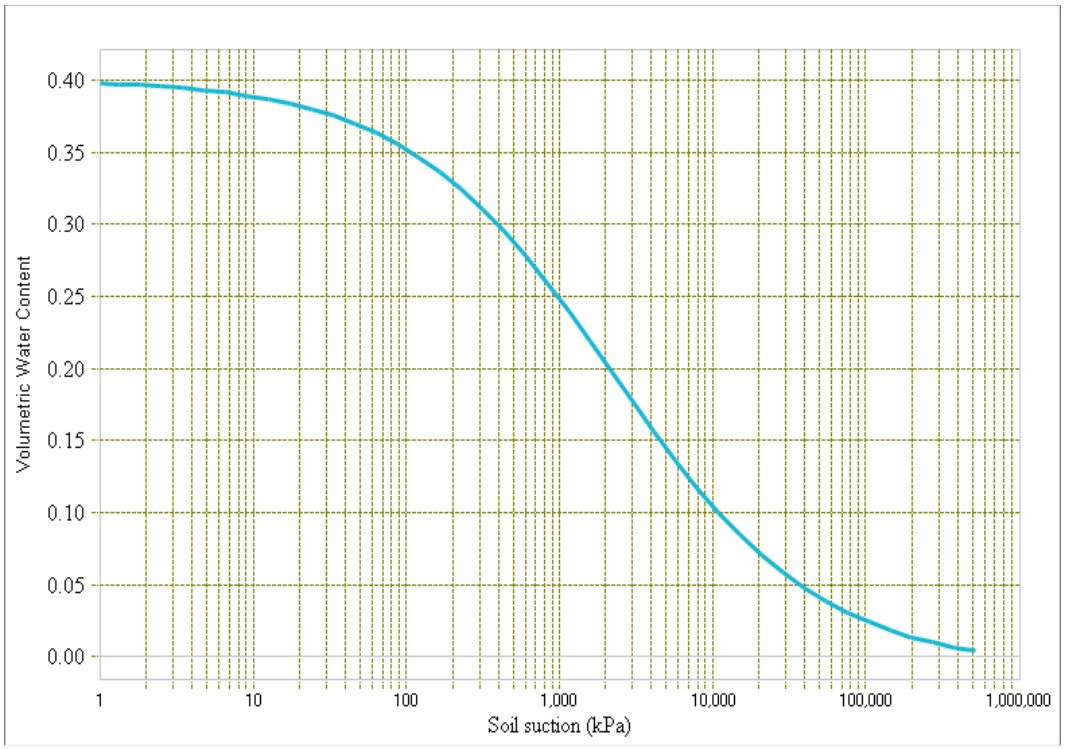

Figure 5.14. SWCC used for modeling of cracked and intact San Diego soil

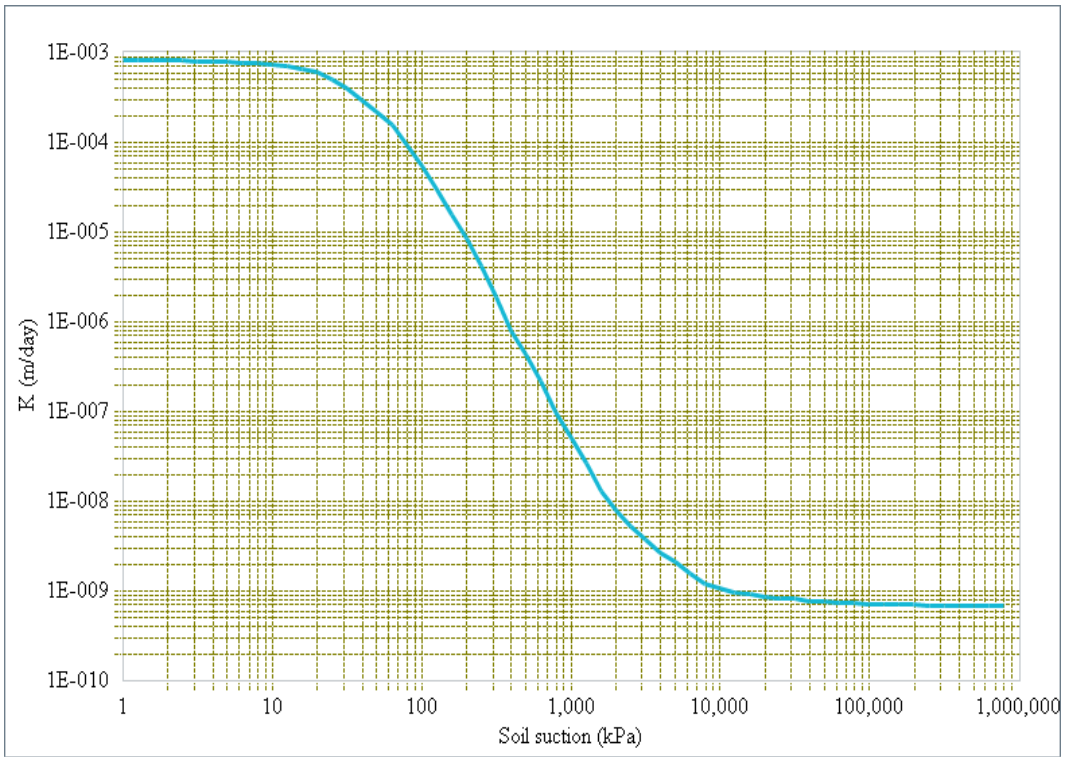

Figure 5.15. K_{unsat} used for modeling of intact San Diego soil

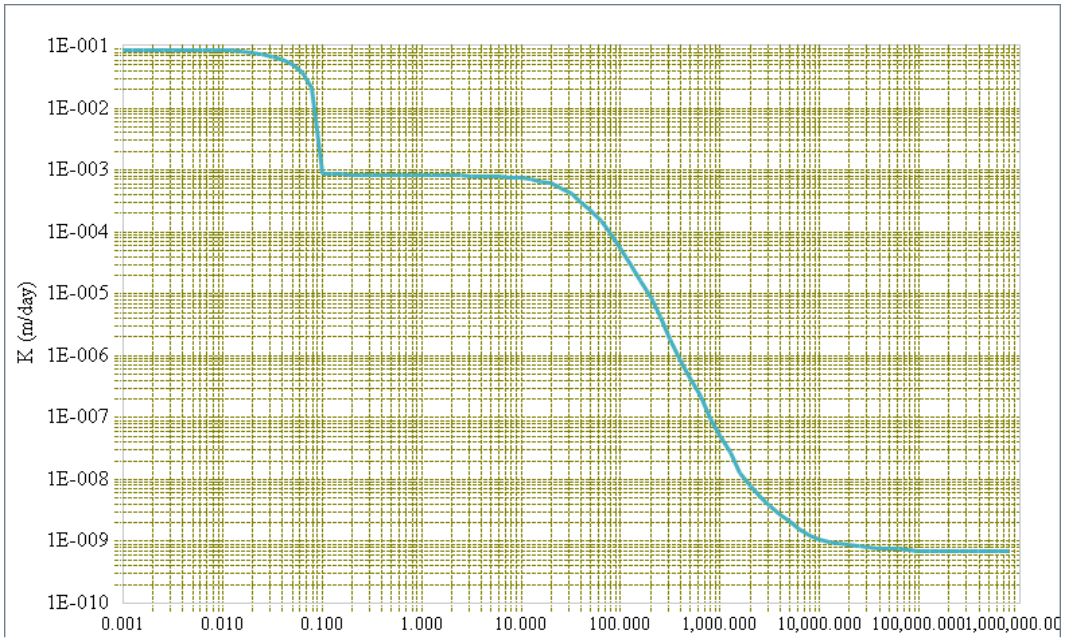

Figure 5.16. K_{unsat} used for modeling of cracked San Diego soil

For this study, different k_{sat} values for the cracked soil were considered and tested but eventually it was decided to use the k_{sat} which was 2 orders of magnitude higher than the measured k_{sat} for the intact material (as shown in figure 5.16). This value is also consistent with field-measured values of saturated hydraulic conductivity for cracked soil reported in the literature (e.g. Zhan et al. (2007)). This magnitude increase in k_{sat} provided the most stable numerical solution while remaining consistent with field observations of k_{sat} for cracked and intact clays.

5.4.4. Modeling with SVFlux

2-D modeling was performed using SVFlux software, part of SVOffice software suite. SVFlux is commercial software for modeling seepage and groundwater problems of saturated and unsaturated soils. The relatively simple CAD-based user interface can be used to create the models effectively. The

created model is then translated automatically to a math scripting language so that it can be used explicitly by FlexPDE kernel to solve the numerical model. The primary steps to create and analyze a model using SVFlux is as follows:

Step 1: Create model geometry – CAD-based user interface can be used to create the model geometry in SVFlux.

Step 2: Define initial condition – As mentioned earlier, an appropriately defined initial condition facilitates reaching to a stable solution faster. In this study, a steady-state analysis was performed in which a constant head of -150m (approximately 1500 kPa suction) was applied to the entire model as the initial condition. The results from this steady-state analysis were then used as the initial condition for the next transient analysis. Likewise, the final profile of each preceding run was used as the initial condition for the succeeded run. This procedure was continued until a stable solution was reached.

Step 3: Define boundary conditions – The boundary conditions are required to be defined properly. Figure 5.12 shows the boundary conditions used in this study. In cases where no boundary condition is required for an element, "No BC" option is to be selected.

Step 4: Define material properties: Saturated/Unsaturated soil properties such as SWCC, k_{unsat} function, k_{sat}, and specific gravity must be specified for materials assigned to different regions throughout the model. Figures 5.14 through 5.16 are some examples of well-defined material properties.

Step 5: Define the desired plots and outputs: Before starting to analyze the problem, the required plots and outputs should be defined properly.

Step 6: Define mesh size and time steps: SVFlux is capable of automatically refining the mesh size based on the concurrent boundary conditions. Defining the mesh size appropriately results in a more reliable numerical solution. Also, it is important to define the time steps properly to generate rational results. In this study, mesh size of 0.2 m was used for sensitive regions while the maximum allowable mesh size was used for the rest of the model. Time steps of 0.1 and 0.2 were used consistently throughout the whole modeling program. Several studies, not shown herein, on mesh size and time step sensitivity were performed in arriving at these values for this particular problem. Mesh size and time step evaluations must be performed on a case by case basis to ensure stable and convergent numerical results for the problem at hand.

Step 7: Analyze the model: Once the problem has been defined properly, by running the program, a descriptor file will be created by SVFlux and used by the FlexPDE solver to analyze and solve the problem. If the problem has not been defined completely, the solver may not run and an error message may be displayed.

5.4.5. Modeling results and discussions

Two cases were studied using the 2-D numerical modeling. On the first case, the entire model was considered to be intact (non-cracked) San Diego soil, while on the second case, the top 1-meter soil layer was considered to be cracked San Diego soil. Other than the material properties for cracked and intact soils, the remaining factors such as boundary conditions were kept the same for both cases. Both models were analyzed for a simulated period of one year. For the studied problems, it was found that the behavior of intact and cracked cases were nearly identical. Total of sixteen points were considered at two different depths for comparison between the results from the two cases. Figure 5.17 shows the position of the selected points within the top two layers.

Figure 5.17. Different points selected for studying the extent of wetting

As shown in figure 5.17, points “a” through “h” are located at depth 0.5 meter and points “i” through “p” are located at depth 1.0 meter below the ground surface. The results for both cracked and intact cases are summarized in figures 5.18 through 5.29. Both cracked and intact cases exhibited the same behavior for the imposed boundary conditions. For example, considering point b beneath the edge of the slab at 0.5 m depth, the suction at 100 days for the intact case is approximately 200 kPa (Figure 5.18) and the suction at point b at 100 days is also about 200 kPa for the case in which a cracked clay layer is simulated (Figure

5.19). It should be noted that the soil remained unsaturated throughout the whole modeling process, with suction values above the AEV of the cracks. Consequently, it can be postulated that soil cracks do not significantly affect the water flow regimes only if the soil remains unsaturated. Otherwise, for severe wetting conditions (such as continuous ponding resulting in extremely low suction or positive pore water pressure), it is expected to observe excessive wetting under the cracked soil as a result of its extremely high saturated hydraulic conductivity.

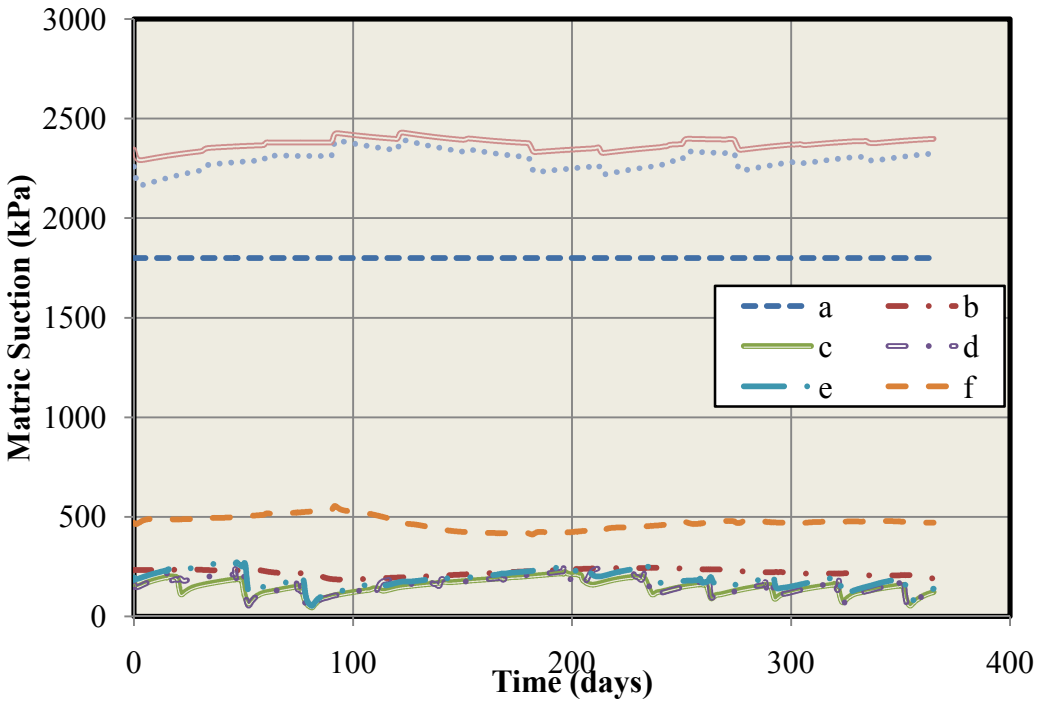

Figure 5.18. Matric suction profile for different points located at 0.5 m depth for intact case

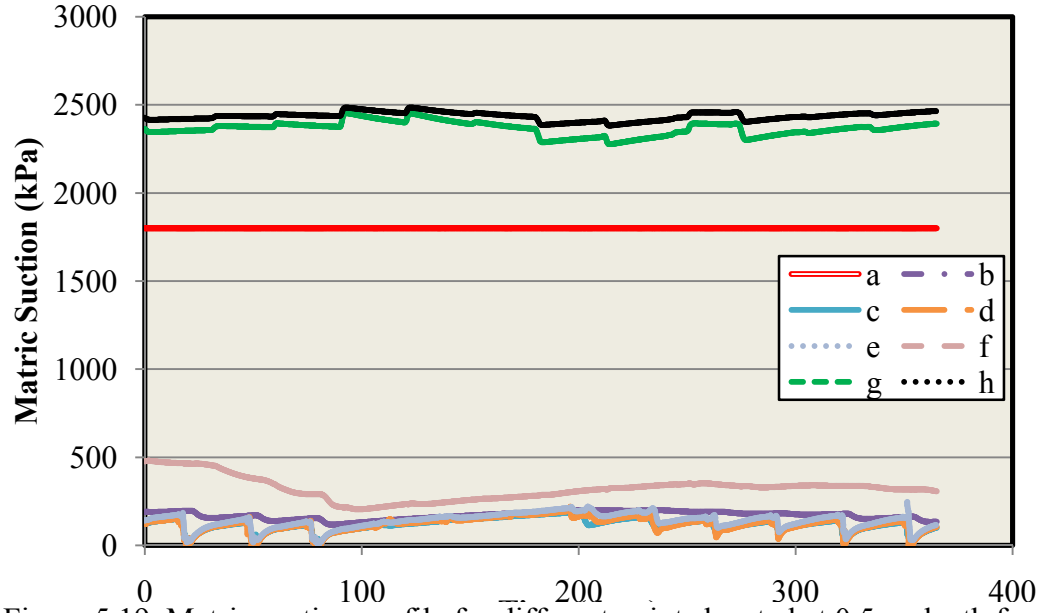

Figure 5.19. Matric suction profile for different points located at 0.5 m depth for cracked case

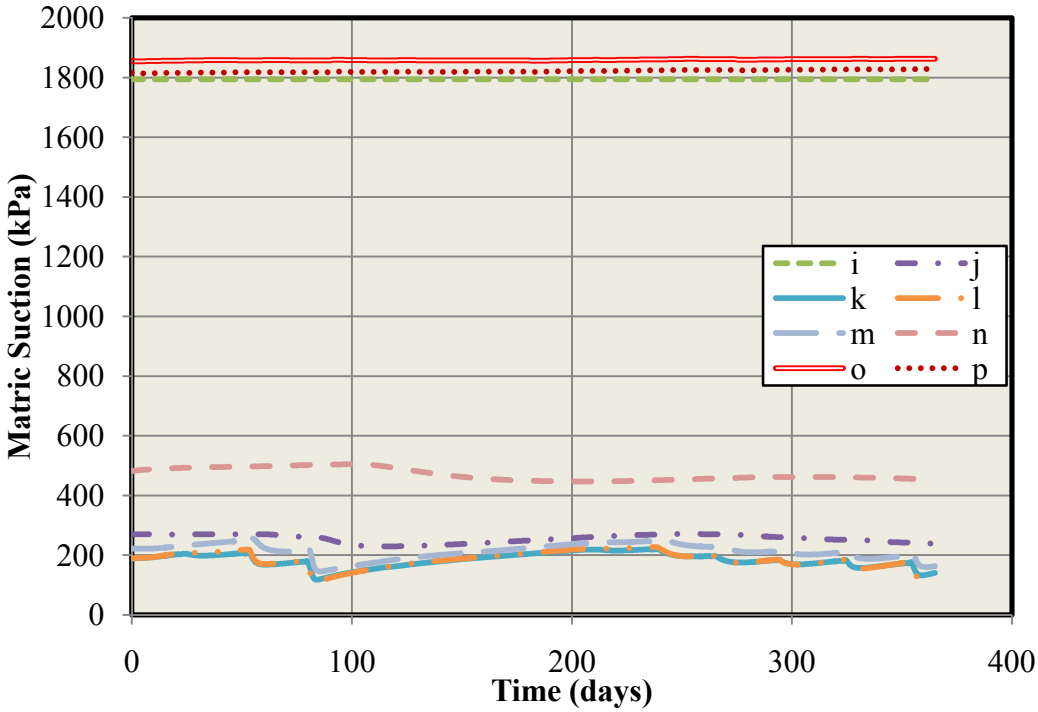

Figure 5.20. Matric suction profile for different points located at 1.0 m depth for intact case

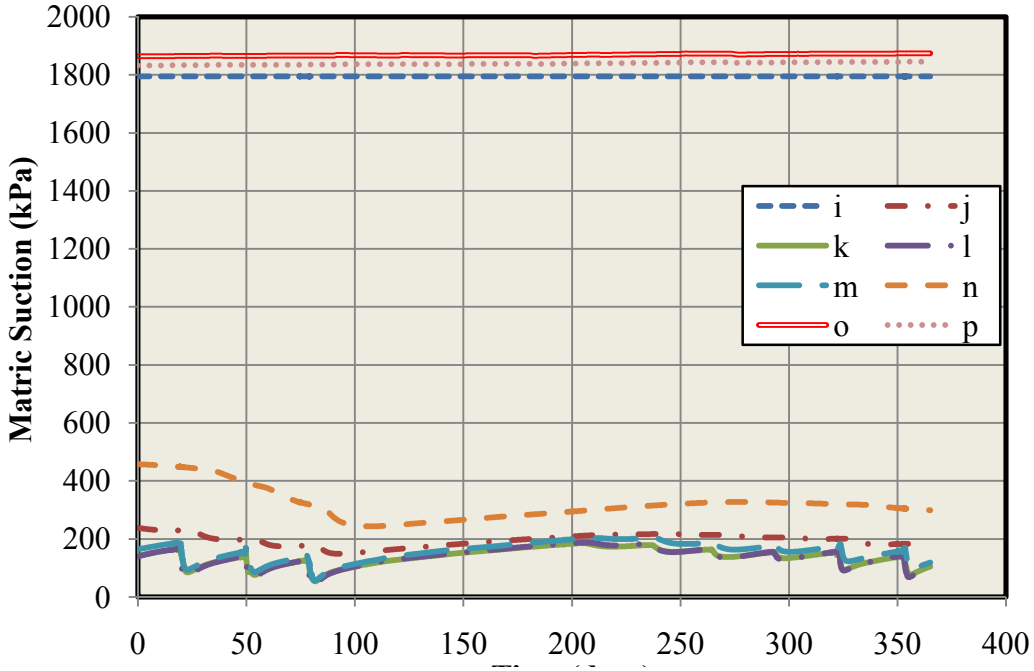

Figure 5.21. Matric suction profile for different points located at 1.0 m depth for cracked case

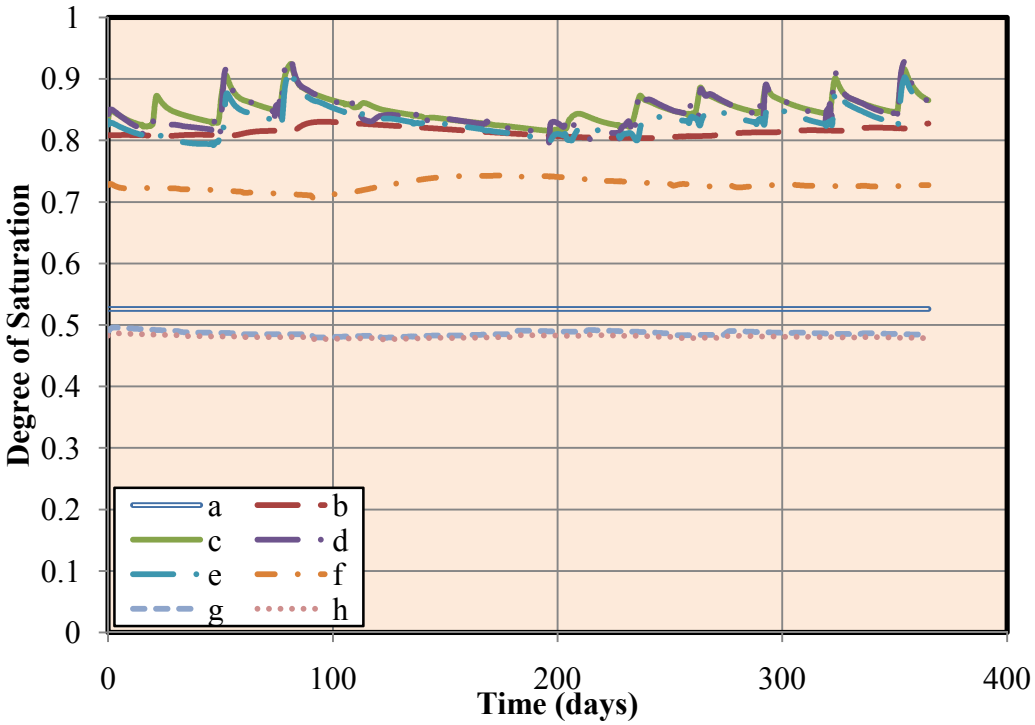

Figure 5.22. Degree of saturation history for different points located at 0.5 m depth for intact case

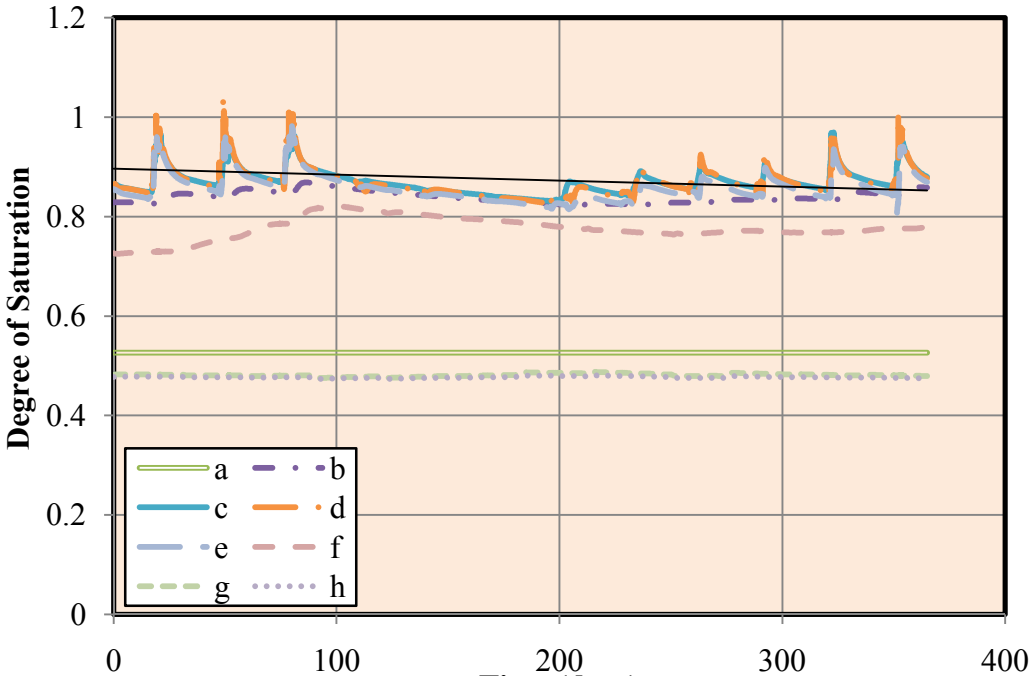

Figure 5.23. Degree of saturation history for different points located at 0.5 m depth for cracked case

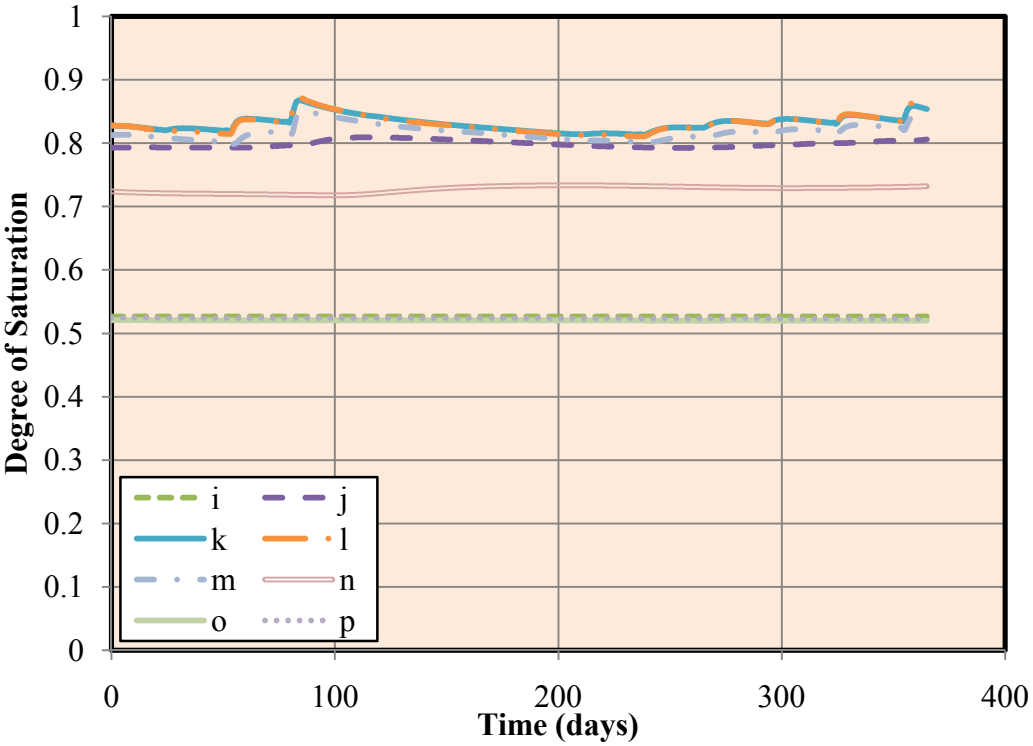

Figure 5.24. Degree of saturation history for different points located at 1.0 m depth for intact case

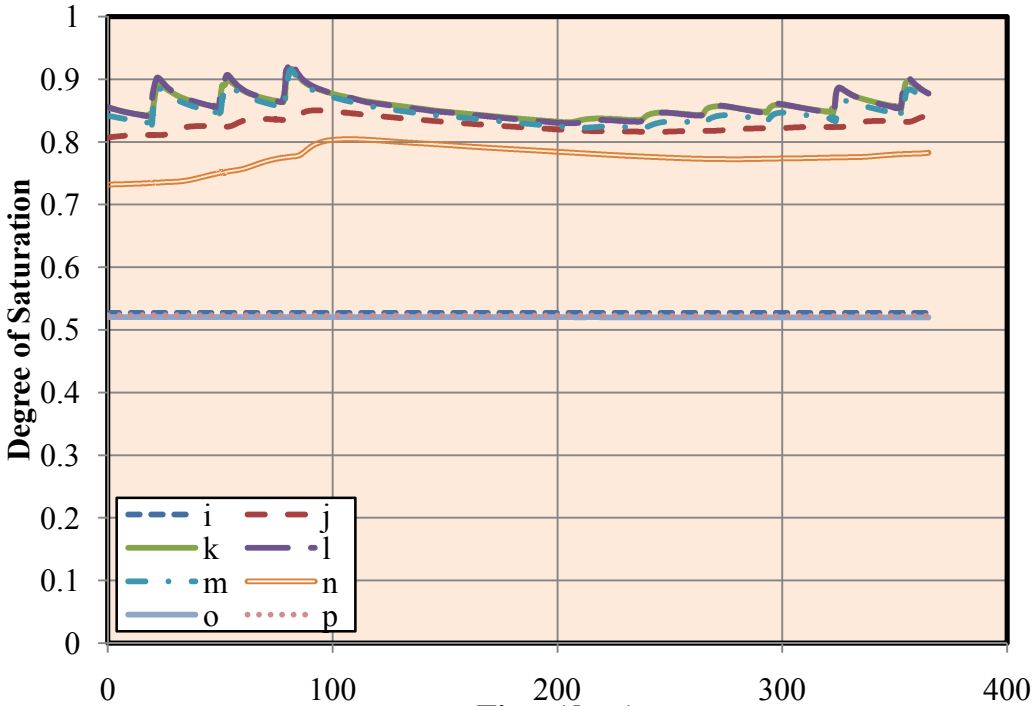

Figure 5.25. Degree of saturation history for different points located at 1.0 m depth for cracked case

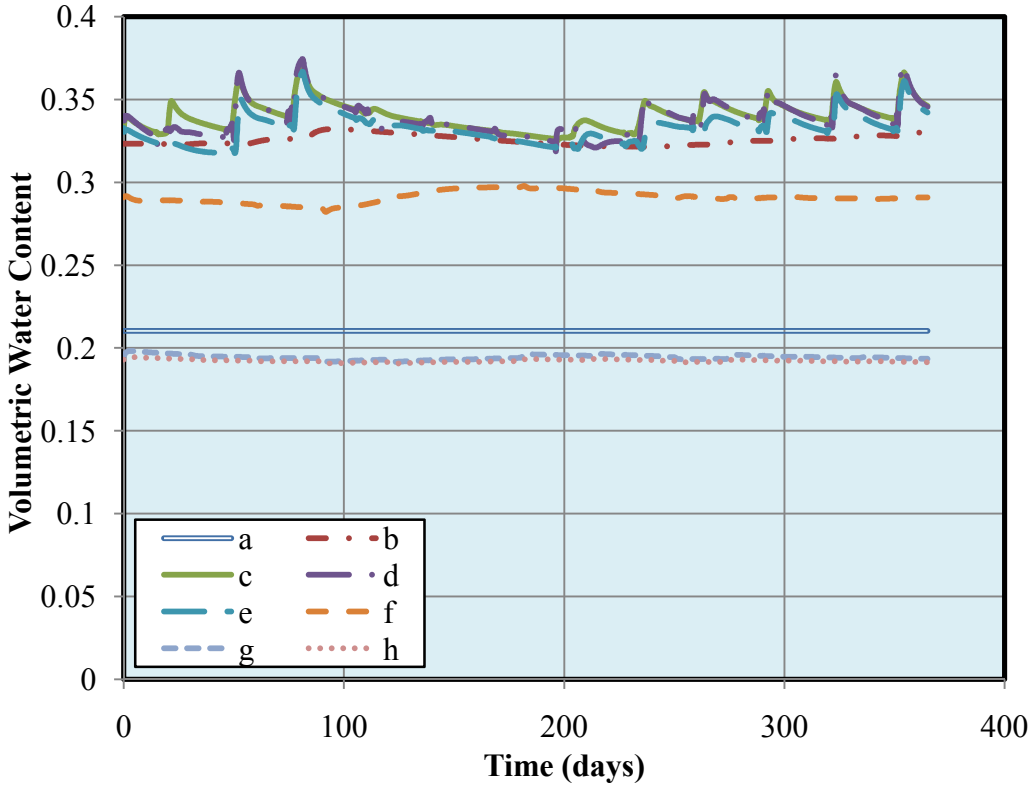

Figure 5.26. Volumetric water content (VWC) change with time for different points located at 0.5 m depth for intact case

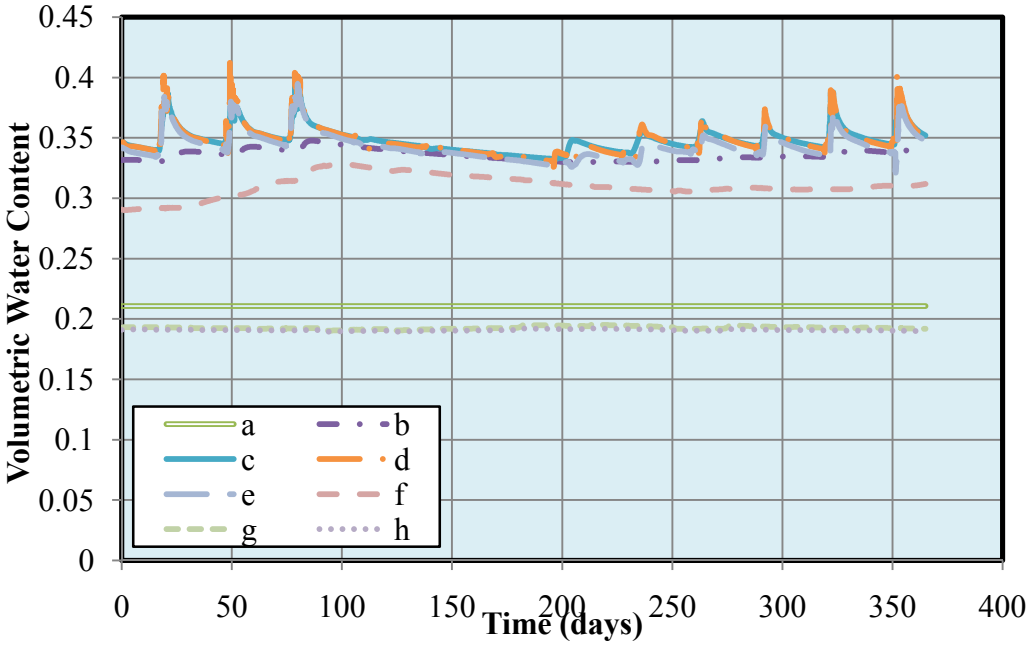

Figure 5.27. Volumetric water content (VWC) change with time for different points located at 0.5 m depth for cracked case

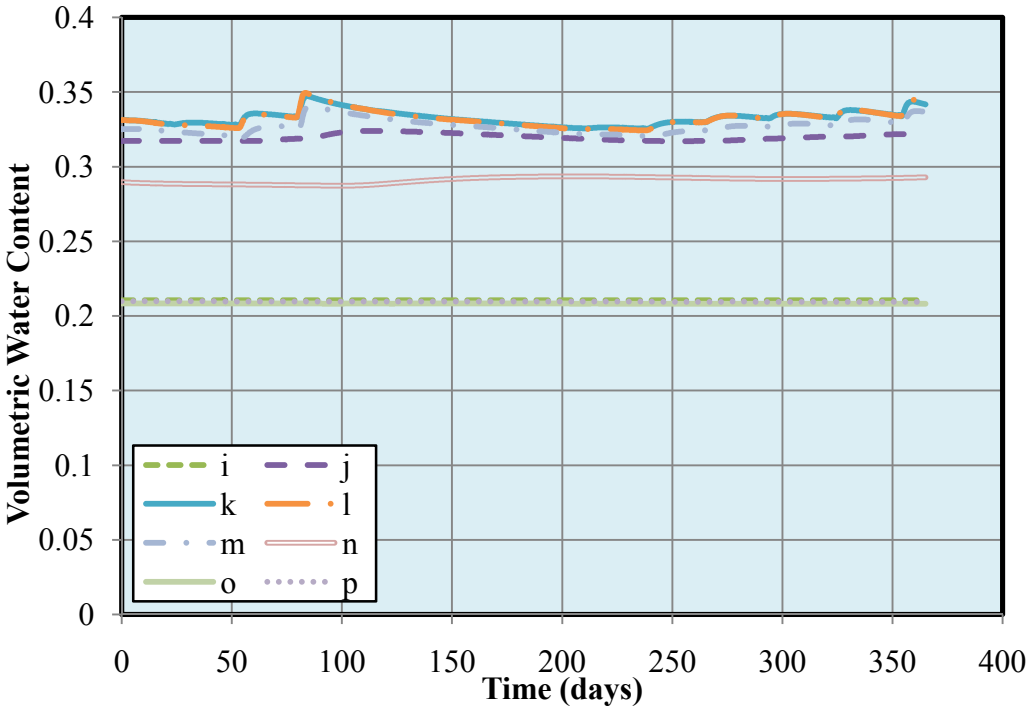

Figure 5.28. Volumetric water content (VWC) change with time for different points located at 1.0 m depth for intact case

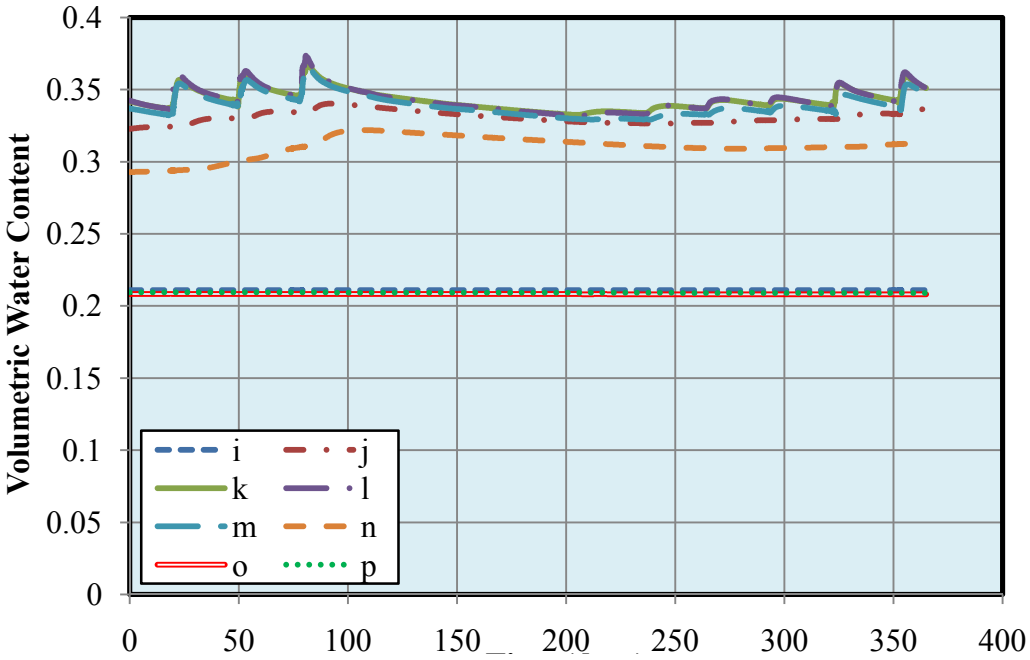

Figure 5.29. Volumetric water content (VWC) change with time for different points located at 1.0 m depth for cracked case

5.5. Summary and conclusion

A systematic approach was used to model the unsaturated flow through cracked and intact clay. The primary objective of the conducted numerical modeling was to investigate the impact of soil cracking on the extent and degree of wetting of soils under field conditions. To address this main objective, a two step modeling process was required. First, a number of 1-dimentional models were developed in which the instantaneous profile experiments were simulated with SVFlux software. The purpose of the 1-D modeling was to evaluate the effect of unsaturated properties of soils on the numerical solutions. Different scenarios were considered and the best scenario was selected based on the comparison between the results from the numerical models and actual laboratory test results. After determination of the required unsaturated properties from 1-D

modeling, several slab-on-grade foundation models (2-D) were developed and analyzed to assess the effect of soil cracking on the extent and degree of wetting. Figure 5.30 outlines the relationship between the numerical modeling and the experimental investigations of this study.

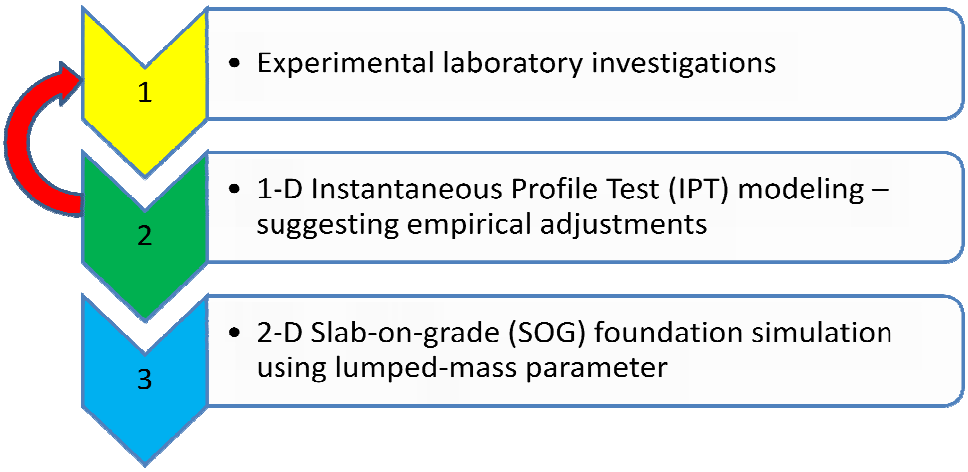

Figure 5.30. Relationship between numerical modeling and experimental investigation of this study

The results from 1-D modeling showed that the numerical solution is extremely sensitive to k_{unsat} function, while the sensitivity to the SWCC was limited. It was also concluded that for the subject problem, using best fit k_{unsat} and SWCC scenarios give the most reliable and realistic results.

The results from 2-D modeling in which the slab-on-grade foundation conditions were simulated revealed the fact that for San Diego soil with the imposed boundary conditions discussed earlier, both intact and cracked soils are expected to behave similar in terms of the flow properties beyond the AEV of the cracks. In fact, it was concluded that in conditions where the flow remains unsaturated and the matric suction of the soil is maintained higher than the estimated AEV of the cracks, both cracked and intact soils act more or less the

same. However, if the matric suction is allowed to drop under the AEV for the cracked soil, the extremely high saturated hydraulic conductivity of cracks will cause an excessive wetting under the slab which can potentially cause serious damage to the structure.

Chapter 6

SUMMARY AND CONCLUSION

To understand the effect of desiccation cracking on unsaturated and saturated flow properties of soils, accurate and systematic experimental investigation is required. An accurate estimation of the volume change characteristics of a cracked soil is also prerequisite for many engineering applications. The backbone of this study was based on an advanced geotechnical testing program that was tailored particularly to the study of the effect of soil cracking on some important saturated and unsaturated engineering properties of soils such hydraulic conductivity, volume change, and water retention characteristic. A numerical analysis was also performed to simulate the cracked soil conditions and results were validated based on previously determined laboratory test results. In the following section, key findings and conclusions are highlighted and recommendations are made for future research in this area.

6.1. Summary

To reach to the primary objectives of this research, three tasks were performed. These tasks are presented in chapters 3, 4, and 5. In chapter 3, the volume change effects of cracks were investigated by designing and performing a number of laboratory tests to measure the swell pressure and swell potential of cracked soil and a comparison of these soil behaviors to those of intact soil.

Different approaches were used to capture the effect of soil cracks on the unsaturated and saturated flow properties of soils. This is addressed in detail in chapter 4. First, the saturated hydraulic conductivity of the cracked and intact

soils were determined and compared by utilizing constant head flexible wall permeability tests performed in a triaxial apparatus. Second, the unsaturated hydraulic conductivity of both cracked and intact soils were estimated by conducting 7 unsaturated conductivity measurement tests, all based on the instantaneous profile method. Third, the soil water characteristic curve was determined for intact and cracked specimen using an oedometer-type pressure plate device (e.g. Fredlund SWCC cells manufactured by GCTS, Tempe, AZ). Finally, numerical analyses, solving Richards equation, were performed using a commercial finite element-based software, SVFlux, to: 1) simulate the unsaturated hydraulic conductivity tests and compare the numerical results with the laboratory findings and make any required empirical adjustments to the modeling properties, and 2) slab-on-ground foundations were modeled to study the effect of the cracked soil layer under the slab on the degree and extent of wetting for simulation of roof runoff ponded next to the slab during rainfall events.

6.2. Conclusion

Based on the results of this research, for the range of soils similar to the tested soil, the following conclusions are drawn:

1) Cracks reduce the swell pressure of soils, and the degree of reduction depends on the level (volume) of soil cracking.
2) Laboratory investigations on the test soil of this study showed that for the crack volumes that are considerably lower than the swell potential of soil, the cracks are more likely to be closed after wetting.

3) For the soil tested in this study, when the crack volume is large relative to swell potential, the cracks may appear to close, but still represent preferential flow paths for saturated flow.

4) The saturated hydraulic conductivity (k_{sat}) for cracks is dramatically higher than that for the intact matrix.

5) The unsaturated hydraulic conductivity of the tested soil was not substantially influenced by the cracks.

6) For most unsaturated soil engineering applications, it can be said that both cracked and intact soils behave the same in terms of the unsaturated hydraulic conductivity and for unsaturated flow conditions where the soil suction remains above the air entry value, AEV, of the cracks.

7) The soil-water characteristic curve (SWCC) for a cracked soil can be represented by a bimodal curve. But the position of the AEV for the cracks is extremely low for many if not most field cracking cases where cracks are visible.

8) The AEV of the cracks was found to be extremely low, around 0.1 kPa for the crack dimensions tested in this study. The crack size and volume used in this study represents approximately the smallest crack width for visible cracks reported in the literature, and the crack volume used was consistent with field observations obtained from a literature review. Larger cracks would exhibit lower AEV.

9) Dewatering of larger field cracks are expected to occur at tremendously low suction values (lower than 0.1 kPa), and perhaps to dewater under gravity alone.

10) The SWCC at higher suctions are essentially the same for cracked and intact specimens, which may support viewing a cracked soil as a continuum for unsaturated flow applications.

11) Instantaneous profile test (IPT) numerical modeling showed that the results of the model are highly sensitive to the imposed k_{unsat} function, but not very sensitive to variability in the SWCC function.

12) The performance of foundations built on expansive soils susceptible to cracking is not highly affected if the wetting condition is temporary (i.e. not relatively continuous ponding) and will result in unsaturated flow conditions.

13) However, if a cracked soil is subjected to a long-term wetting, such as extended ponding, which will result in driving the matric suction of the soil to the values lower than the AEV of the cracks, then the dramatic increase in hydraulic conductivity of the cracks can drive a significant amount of water underneath the slab which can potentially cause serious damage to the structure.

14) In terms of heave prediction, for a foundation built on a cracked soil, it is expected that the cracks partially accommodate some amount of total swell potential, which is favorable. However, this conclusion holds as long as the matric suction of the surrounding soil remains larger than the AEV

of the actual cracks. If pore water pressure becomes positive, the negative effects of rapid infiltration of water through the cracks may overshadow the ameliorating effect of reduction in swell pressure and heave resulting from presence of the cracks.

6.3. Recommendation for future work

Based on the findings of this study, the following research areas are recommended:

1) Different clay soil types with wide range of PI are recommended for future studies.
2) A wider range of initial crack volume should be studied to further assess the effect of crack size and volume on saturated and unsaturated properties of soils.
3) A wider range of initial crack volume should be studied to assess the effect on swell pressure and swell potential of expansive soils.
4) A discrete modeling approach, wherein the crack is modeled as a void within the intact material, can also be applied and examined to the cracked soil problems for modeling purposes.
5) Crack healing process and effects on saturated and unsaturated hydraulic conductivities requires further investigation, particular across a wider range of clay types (PI values).
6) A full-scale foundation test on cracked vs. intact soil can also improve the understanding of how cracks can affect the performance of foundations.

7) While studying the saturated hydraulic conductivity of a cracked soil from constant head permeability tests, consideration of the actual flow paths, using a solution of Laplace equations, may result in a more accurate quantitative estimation of the k_{sat} for the cracked soil.

8) 2-D Numerical modeling of the saturated flow for cracked and intact soils can also help to better understand the effect of soil cracks on the performance of foundations under excessive and continuous ponding conditions and for heavy landscape irrigation conditions, such as turf landscape.

REFERENCES

Abbaszadeh M. M., Houston S., Zapata C., Houston W., Welfert B., Walsh K. 2011. Laboratory determination of Soil Water Characteristic Curves for cracked soil. Unsaturated Soils – Alonso & Gens (eds). pp. 409-415.

Abdullah, W. S. 2002. Bidimensional swell effect on accuracy of footing heave prediction. Geotechnical Testing Journal, GTJODG, Vol. 25, No. 2, pp. 177-186.

Albrecht, B. A., and Benson, C. H. 2001. Effect of desiccation on compacted natural clays. J. Geotech. Geoenviron. Eng., 127(1): 67– 75.

Anderson, J.L. and Bouma, J., 1973. Relationships between hydraulic conductivity and morphometric data of an argillic horizon. Soil Sci. Soc. Am. Proc., 37: 408--413.

Arnold J. G., Potter K. N., King K. W. and Allen P. M., 2005. Estimation of soil cracking and the effect on surface runoff in a Texas Blackland Prairie watershed. Hydrol. Process. 19, 589–603-.

Ashayeri I., Yasrebi S. 2009. Free-Swell and Swelling Pressure of Unsaturated Compacted Clays; Experiments and Neural Networks Modeling. Geotech Geol Eng, 27:137–153.

Askar Azza and Jin Yee-Chung, 2000. Macroporous drainage of unsaturated swelling soil. Water Resources Research, Vol. 36, No. 5, 1189-1197.

ASTM Standard D2487. Standard practice for classification of soils for engineering purposes (Unified Soil Classification System). ASTM International, West Conshohocken, PA. DOI: 10.1520/D2487-00. www.astm.org.

ASTM Standard D422. Standard test method for particle size analysis of soils. ASTM International, West Conshohocken, PA. DOI: 10.1520/D422-63. www.astm.org.

ASTM Standard D4318. Standard test methods for liquid limit, plastic limit and plasticity index of soils. ASTM International, West Conshohocken, PA. DOI: 10.1520/D4318-00. www.astm.org.

ASTM Standard D4546. Standard test methods for one-dimensional swell or collapse of cohesive soils. ASTM International, West Conshohocken, PA. DOI: 10.1520/D4546-08. www.astm.org.

ASTM Standard D4829. Standard test method for expansion index of soils. ASTM International, West Conshohocken, PA. DOI: 10.1520/D4829-03. www.astm.org.

ASTM Standard D5298. Standard test method for measurement of soil potential (suction) using filter paper. ASTM International, West Conshohocken, PA. DOI: 10.1520/D5298-03. www.astm.org.

ASTM Standard D698. Standard test methods for laboratory compaction characteristics of soil using standard effort (12,400 ft-lbf/ft3). ASTM International, West Conshohocken, PA. DOI: 10.1520/D698-00a. www.astm.org.

Attom, M. F., Barakat, S. 2000. Investigation of three methods for evaluating swelling pressure of soils. Environmental & Engineering Geoscience, Vol. VI, No. 3, August 2000 (Summer), pp. 293-299.

Aubertin, G.M., 1971. Nature and extent of macropores iv~ forest soils and their influence on subsurface water movement. USDA For. Serv. Res. Pap., NE-192. For. Serv. USDA, 33 pp.

Bagge, G. 1985. Tension cracks in saturated clay cuttings. Proceedings, 11th International Conference on Soil Mechanics and Foundations Engineering, San Francisco, Vol. 2, pp. 393–395.

Baker, R. 1981. Tensile strength, tension cracks, and stability of slopes. Soils and Foundations, 21(2): 1–17.

Bandyopadbyay K, Mohanty P, Misra A, 2003. Influence of tillage practices and nutrient management on crack parameters in a vertisol of Central India. Soil & Tillage Research, 71(2): 133–142. DOI: 10.1016/S0167-1987(03)00043-6.

Bolt, G.H. 1956. Physico-chemical analysis of the compressibility of pure clays. Géotechnique, 6(2): 86–93.

Börgesson, Lennart 1985. Water flow and swelling pressure in non-saturated bentonite-based clay barriers. Engineering Geology, 21, pp 229-237.

Bouma J. and Dekker L.W.., 1978. A case study on infiltration into dry clay soil I. Morphological obesrvations. Geoderma, 20 (1978) 27—40.

Bouma J. and Wosten J.H.M., 1984. Characterizing ponded infiltration in a dry cracked clay soil. Journal of Hydrology, 69 (1984) 297-304.

Bouma, J., 1980. Field measurement of soil hydraulic properties characterizing water movement through swelling clay soils. J. Hydrol., 45: 149-158.

Bouma, J., Jongerius A., Boersma O., Jager A., and Schoonderbeek D. 1977. The function of different types of macropores during saturated flow through four swelling soil horizons, Soil Sci. Soc. Am. J. 41, 945-950.

Brian A. Albrecht, Craig H. Benson, 2001. Effect of desiccation on compacted natural clays. Journal of Geotechnical and Geoenvironmental Engineering / January. Vol. 127, No. 1, 67-75.

Bronswijk .J.B., 1988. Modeling of water balance, cracking and subsidence of clay soils. Journal of Hydrology, 97, Pages 199-212.

Carman P.C., 1939. Permeability of saturated sands, soils and clays. J Agric Sci 29:262–273

Chapman, D.L. 1913. A contribution to the theory of electrocapillarity. Philosophical Magazine, 25: 475–481.

Chen, F.H., 1988. Foundations on expansive soils. Development in Geotechnical Engineering. Elsevier, New York.

Chen-Wuing Liu, Shih-Wei Cheng, Wen-Sheng Yu, Shih-Kai Chen (2003); Water infiltration rate in cracked paddy soil. Geoderma 117. 169–181.

Chertkov V. Y. 2002. Modeling cracking stages of saturated soils as they dry and shrink. European Journal of Soil Science, March, 53,105-118.

Chertkov V. Y. and Ravina I., 1999. Analysis of the Geometrical Characteristics of Vertical and Horizontal Shrinkage Cracks. J. agric. Engng Res. 74, 13-19.

Chertkov V. Y. and Ravina I., 2002. Combined effect of interblock and interaggregate capillary cracks on the hydraulic conductivity of swelling clay soils. Water Resources Research, VOL. 38, NO. 8, 1157.

Cokca, E., 2000. Comparison of suction and oedometer methods for the measurement of swell pressure. Quarterly Journal of Engineering Geology and Hudrogeology, 33, 141-147.

Corser, P., Cranston, 1991. Observations on long-term performance of composite clay liners and covers. Proceedings of the conference on Geosynthetics Design and Performance. Vancouver Geotechnical Society, Vancouver, Canada.

Corte, A., Higashi, A., 1960. Experimental research on desiccation cracks in soil. Corps of Engineers, Research 66. US Army Snow Ice and Permafrost Research Establishment.

Das S. K., Samui P., Sabat A. K., and Sitharam T. G., 2010. Prediction of swelling pressure of soil using artificial intelligence techniques. Environ Earth Sci. 61:393–403.

Dasog G. S., Shashidhara G. B., 1993. Dimension and volume of cracks in a vertisol under different crop covers. Soil Science, Vol. 156, No. 6, 424-428.

Davidson Malcolm R., 1984. A green-ampt model of infiltration in a cracked soil. Water Resources Research, VOL. 20, NO. 11, PAGES 1685-1690, NOVEMBER 1984.

Davidson Malcolm R., 1985. Numerical calculation of saturated-unsaturated infiltration in a cracked soil. Water Resources Research, Vol. 21, No. 5, Pages 709-714.

Diiwu J. Y., Rudra R. P., Dickinson W. T., Wall G. J., 2001. Two-component Transfer Function Modeling of Flow through Macroporous Soil. J. agric. Engng Res. 80 (2): 223-231.

Dye H. B., Houston S. L., Welfert B. D. 2011a. Influence of Unsaturated Soil Properties Uncertainty on Moisture Flow Modeling. Geotech Geol Eng (2011) 29:161–169.

Ebrahimi-B, N., Gitirana Jr., G.F.N., Fredlund, D.G., Fredlund, M.D., and Samarasekera, L. 2006. A lower limit for the water permeability coefficient. 57th Canadian Geotechnical Conference. Session 5E, 12-19.

Ehlers, W., 1975. Observations on earthworm channels and infiltration on tilled and untilled loess soil, Soil Sce., 119, 242-249.

Elias, E.A., Salih, A.A., and Alaily, F., 2001. Cracking patterns in the Vertisols of the Sudan Gezira at the end of dry season. Int. Agrophysics, 15, 151-155.

Erzin Yusuf, and Ero Orhan, 2007. Swell pressure prediction by suction methods. Engineering Geology 92, 133–145.

Evans, R.G. Smith, C.J., Mitchell, P.D. and Newton, P.J., 1990. Furrow infiltration on nontilled beds with cracking soils. Journal of Irrigation and Drainage Engineering, Vol. 116, No. 5, September/October, 1990.

Favre F., Boivin P., Wopereis M.C.S., 1997. Water movement and soil swelling in a dry, cracked Vertisol. Geoderma 78 113-123.

Flury M., Fluhler H., Jury W. A., Leuenberger J., 1994. Susceptibility of soils to preferential flow of water: A field study. Water resources research, Vol. 30, No. 7, Pages 1945-1954, July 1994.

Forchheimer, P. 1914. Hydrolik, Tuebner, Leipzig, Berlin, 116–118.

Fredlund D. 2006. Unsaturated soil mechanics in engineering practice. Journal of Geotechnical and Geoenvironmental Engineering, Vol. 132, No. 3, March 1, 2006. ASCE, ISSN 1090-0241/ 2006/3-286–321.

Fredlund Delwyn G., Houston Sandra L., Nguyen Quan, Fredlund Murray D. 2010. Moisture movement through cracked clay soil profiles. Geotech Geol Eng (2010) 28:865–888.

Ghodrati , M., F. F. Ernst, and W. A. Jury 1990. Automated spray system for application of solutes to small field plots. Soil Sci. Soc. Am. J., 54, 287-290.

Gouy, G. 1910. Electric charge on the surface of an electrolyte. Journal of Physics, 4(9): 457.

Greve A., Andersen M.S., Acworth R.I., 2010. Investigations of soil cracking and preferential flow in a weighing lysimeter filled with cracking clay soil. Journal of Hydrology 393 (2010) 105–113.

Groisman A., Kaplan E., 1994. An experimental study of cracking induced by desiccation. Europhys. Lett., 25 (6), pp. 415-420.

Hallet P. D., Newson T. A., 2005. Describing soil crack formation using elastic-plastic fracture mechanics. European Journal of Soil Science, February 2005, 56, 31–38.

Hewitt, P. & Phillip, L. 1999. Problems of clay desiccation in composite lining systems. Engineering Geology, 53, 107–113.

Hilf, W. 1956. An investigation of pore-water pressure in compacted cohesive soils. Ph.D. dissertation, Tech. Memo. No. 654, U.S. Dep. of the Interior, Bureau of Reclamation, Design and Construction Div., Denver, CO, 654 pp.

Hu L, Peron H, Hueckel T, Laloui L., 2006. Numerical and phenomenological study of desiccation of soil. In: Advances in Unsaturated Soil, Seepage, and Environmental Geotechnics. ASCE geotechnical special publication 148; 2006. p. 166–73

Hung Q. Vu and Delwyn G. Fredlund 2004. The prediction of one-, two-, and three-dimensional heave in expansive soils. Can. Geotech. J. 41: 713–737.

Işık Yilmaz 2009. Swell potential and shear strength estimation of clays. Applied Clay Science 46. pp 376–384.

Jacquemin, S., 2011. Laboratory determination of hydraulic conductivity functions for unsaturated cracked fine grained soil. Thesis for Master of Science. Arizona State University.

Kayabali, K. and Demir, S., 2011. Measurement of swelling pressure: direct method versus indirect methods. Can. Geotech. J. 48: 354–364.

Kazemi, H., 1969. Pressure transient analysis of naturally fractured reservoirs with uniform fracture distribution. Soc. Pet. Eng. J., 451-62. Trans., AIME, 246.

Kazemi, H., 1979. Numerical simulation of water imbibition in fractured cores, Soc. Pet. Eng. J. 323- 330.

Kissel, D.E., Ritchie, J.T. and Burnett, E., 1973. Chloride movement in undisturbed clay soil. Soil Sci. Soc. Am. Proc., 37: 21--24.

Kodikara J., Barbour S. L., and Fredlund D.G. 1998. An idealized framework for the analysis of cohesive soils undergoing desiccation: Discussion Can. Geotech. J. 35: 1112–1114 (1998).

Kodikara, J.K., Barbour, S.L. and Fredlund, D.G., 2000. Desiccation cracking of soil layers. In Proceedings of Asian Conference on Unsaturated Soils: From Theory to Practice (edited by H. Rahardjo, D.G. Toll and E.C. Leong), A.A. Balkema, pp. 693–698.

Köhne J.M., Köhne S., Gerke H.H., 2002. Estimating the hydraulic functions of dual-permeability models from bulk soil data. Water Resour Res 38(7):1121–1132

Konrad J. M., Ayad R., 1997. Desiccation of a sensitive clay: field experimental observations.. Can. Geotech. J. 34: 929–942 (1997).

Kozeny J. 1927. Ueber Kapillare Leitung des Wassers im Boden. Wien AkadWiss 136(2a):271.

Kutilek, M., 1996. Water relations and water management of vertisols. In: Ahmed, N., Mermut, M. (Eds.), Vertisols and Technologies for Their Management. Developments in Soil Science. Elsevier, Amsterdam, The Netherlands.

Lachenbruch, A. H., 1962. Mechanics of thermal contraction cracks and ice-wedge polygons in permafrost, Special Paper No. 70, The Geological Society of America, New York.

Lau, L.T.K., 1987. Desiccation crack of clay soils. MSc Thesis, Department of Civil Engineering, University of Saskatchewan, Canada.

Lehmann F., Ackerer PH. 1998. Comparison of iterative methods for improved solutions of the fluid flow equation in partially saturated porous media. Transport in Porous Media 31: 275–292.

Li J.H., Zhang L.M., Wang Y., and Fredlund D.G. 2009. Permeability tensor and representative elementary volume of saturated cracked soil. Can. Geotech. J. 46: 928–942.

Liu Chen-Wuing, Chen Shih-Kai, and Jang Cheng-Shin, 2004. Modelling water infiltration in cracked paddy field soil. Hydrol. Process. 18, 2503–2513.

Longwell, C.R. 1928. Three common types of desert mud cracks. America Journal of Soil Science, 5th Series. XV: 136-145.

Lu N., Likos W. J., 2004. Unsaturated soil mechanics (2004). Published by John Wiley & Sons, Inc., Hoboken, New Jersey.

Lytton, R.L., 1977a. The characterization of expansive soils in engineering, Presentation at the Symposium on Water Movement and Equilibrium in Swelling Soils. American Geophysical Union, San Francisco, CA.

Lytton, R.L., 1977b. Foundation on expansive soils. In: C.S. Desai and J.T. Christian (Editors), numerical methods in geotechnical engineering. McGraw-Hill, New York, pp. 427-458.

Lytton, R.L., 1994. Prediction of movement in expansive clays, In Proceedings of Vertical and Horizontal Deformations of Foundations and Embankments. Geotechnical Special Publication No. 40, ASCE, New York, pp. 1827–1845.

Mallant D., Tseng P.H., Torde N., Timmerman A., Feyen J. 1997. Evaluation of multimodal hydraulic function in charactering a heterogeneous field soil. J Hydrol 195:172–199

McKeen, R.G., 1981. Design of airport pavements on expansive soils. Report No. FAARD- 81-25, Federal Aviation Administrafion, Washington, DC.

Melchoir, S. 1997. In-situ studies of the performance of landfill caps (compacted soil liners, geomembranes, geosynthetic clay liners and capillary barriers). Land Contamination and Remediation, 5, 209–216.

Miller C.J., Mi H., Yesiller N., 1998. Experimental analysis of desiccation crack propagation in clay liners. Journal of the American water resources association, vol. 34, no.3, 677-686.

Mitchell, J.K. and Soga, K. 2005. Fundamentals of soil behavior. Hoboken, NJ. John Wiley and Sons, Inc.

Montgomery, C.W. 1997. Environmental geology. McGraw-Hill, Boston, MA.

Morris, P.H., Graham, J., and Williams, D.J. 1992. Cracking in drying soils. Canadian Geotechnical Journal. 29: 263–277.

Mosleh A. AI-Shamrani and Abdullah I. AI-Mhaidib, 1999. Prediction of potential vertical swell of expansive soils using a triaxial stress path cell. Quarterly Journal of Engineering Geology, 32, 45 54.

Mualem Y., 1976. A new model for predicting the hydraulic conductivity of unsaturated porous media. Water Resour Res 12:593–622

Nagaraj, H. B., Munnas, M.Mohammed, and Sirdharan, A. 2009. Critical evaluation of determining swelling pressure by swell-load method and constand volume method. Geotechnical Testing Journal, Vol. 32, No. 4, pp. 305-314.

Nimmo, J. R. and Akstin, K. C., 1988, Hydraulic conductivity of a saturated soil at low water content after compaction by various methods: Soil Science Society of America Journal, v. 52, p. 303-310.

Nimmo, J. R., Rubin, J., and Hammermeister, D. P., 1987, ‘‘Unsaturated flow in a centrifugal field: Measurement of hydraulic conductivity and testing of Darcy’s law,’’ Water Resources Research, 23(1), 124–134.

Nimmo, J., Akstin, K., and Mello, K., 1992, ‘‘Improved apparatus for measuring hydraulic conductivity at low water content,’’ Soil Science Society of America Journal, 56, 1758–1761.

Nova´k V., Simunek J., and van Genuchten M. Th., 2000. Infiltration of water into soil with cracks. Journal of Irrigation and Drainage Engineering, 126(1) January/February: 41-47.

Novak V., 1999. Soil-crack characteristics estimation methods applied to heavy soils in the NOPEX area”, Agricultural and Forest Meteorology. 501-507.

Novak V., Simunek J., and Van Genuchten MTh. 2000. Infiltration into soil with fractures. J Irrig Drain Eng 126(1): 41-47.

Perrier, E, Mullon, C., Rieu, M., and De Marsily, G., 1995. Computer construction of fractal soil structures: Simulation of their hydraulic and shrinkage properties. Water Resources Research, 31(12): 2927-2943.

Philip L.K., Shimell H., Hewitt P.J. and Ellard H.T., 2002. Field-based test cell examining clay desiccation in landfill liners. Quarterly Journal of Engineering Geology and Hydrogeology, 35: 345–354.

Preston, S., Griffiths, B.S. and Young I.M., 1997. An investigation into sources of soil crack heterogeneity using fractal geometry. European Journal of Soil Science,48: 31-37.

Pruess, K., and Narasimhan, T.N., 1985. A practical method for modeling fluid and heat flow in fractured porous media, Soc. Pet. Eng. J., 25, 14-26.

Rao A.S., Phanikumar B.R. & Sharma R.S., 2004. Prediction of swelling characteristics of remoulded and compacted expansive soils using free swell index. Quarterly Journal of Engineering Geology and Hydrogeology, 37, 217–226.

Rao B. Hanumantha, Venkataramana K., and Singh D.N. (2011). Studies on the determination of swelling properties of soils from suction measurements. Can. Geotech. J. 48: 375–387.

Rayhani M.H.T, Yanful, E.K., Fakher A., 2007. Desiccation induced cracking and its effect on the hydraulic conductivity of clayey soils from Iran. Can Geotech. J. 44:276-283.

Remson, I., G. M. Hornberger, and F. J. Molz, 1971. Numerical methods in subsurface hydrology, 389 pp., Wiley-Interscience, New York.

Ritchie, J. T., Kissel D. E., and Burnett E., 1972. Water movement in undisturbed swelling clay soil, Soil Sci. Soc. Am. Proc., 36, 874–879.

Rollings, M.P. and Rollings, R.S., 1996. Geotechnical materials in construction. McGraw0Hill. New York, NY.

Romkens M.J.M., Prasad S.N., 2006. Rain Infiltration into swelling/shrinking/cracking soils. Agricultural water management 86, 196–205.

Ruy S., Di Pietro L., Cabidoche Y.M., 1999. Numerical modelling of water infiltration into the three components of porosity of a vertisol from Guadeloupe. Journal of Hydrology 221, pages 1–19.

Sadek S., Ghanimeh S., El-Fadel M. 2007. Predicted performance of clay-barrier landfill covers in arid and semi-arid environments. Waste Management 27. 572–583.

Saffigna, P. G., Tanner C. B., and Keeney D. R., 1976. Non-uniform infiltration under potato canopies caused by interception, stemflow, and hilling, Agron, J. 68, 337-342.

Savandis, S. and Mallwitz, K., 1997. Self-sealing behavior with regard to permeability of mineral sealing material in disturbed landfill liners/liner systems. In: August, H., Holzlöhner, U. & Meggyes, T. (eds) Advanced Landfill Systems. Thomas Telford, 182–192.

Scott G. J. T., Webster R. and Nortcliff S., 1986. An analysis of crack patter in clay soil: its density and orientation. Journal of Soil Science, 37, 653-668.

Sherard, J.L. 1973. Embankment dam cracking. In Embankment-dam engineering (Casagrande Volume). John Wiley & Sons, New York, pp. 271–353.

Silvestri, V., Sarkis, G., Bekkouche, N., and Soulié, M., 1992. Evapotranspiration, trees and damage to foundations in sensitive clays. Canadian Geotechnical Conference, Vol. II, pp. 533–538.

Singhal S., 2010. Expansive soil behavior: property measurement techniques and heave prediction methods. PhD Dissertation, Arizona State University, Department of Civil and Environmental Engineering.

Snow, D.T. 1969. Anisotropic permeability of fractured media. Water Resources Research, 5(6): 1273–1289.

Snow, D.T., 1965. A parallel plate model of fractured permeable media, Ph.D. Dissertation, 331. pp., University of California, Berkeley.

Spencer, E., 1968. Effect of tension crack on stability of embankments. Proc. ASCE, J. Soil Mech. Found. Div., Vol. 94, SM5, pp. 1159-1173.

Sridharan Asuri, Rao A. Sreepada, Sivapullaiah Puvvadi V., 1986. Swelling pressure of clays. Geotechnical Testing Journal. 9 (1): 24– 33.

Stapledon, D. H., 1970. Changes and structural effects developed in some South Australian clays, and their engineering consequences. Proceedings of a Symposium on Soils and Earth Structures in Arid Climates, Adelaide, pp. 62-71.

Stirk, G., 1954. Some aspects of soil shrinkage and the effect of cracking upon water entry into the soil. Aus. J. Agric. Res. 5, 279-290.

Stothoff, S. and Or D., 2000. A discrete-fracture boundary integral approach to simulating coupled energy and moisture transport in a fractured porous medium, “Dynamics of Fluids in Fractured Rocks, Concepts and Recent Advances”, Edited by B. Faybishenko, P. A. Witherspoon and S. M. Benson, AGU Geophysical Monograph 122, American Geophysical Union, Washington, DC, 269–279.

Sun J C, Wang G Q, Sun Q C. 2009. Crack spacing of unsaturated soils in the critical state. Chinese Sci Bull, 54: 2008-2012, doi: 10.1007/s11434- 009-0319-8

T. Windal, I. Shahrour, 2002. Study of the swelling behavior of a compacted soil using flexible odometer. Mechanics Research Communications 29. pp 375–382.

Tay Y. Y., Stewart D. I., Cousens, T. W., Shrinkage and desiccation cracking in bentonite-sand landfill liners. Engineering Geology 60, 2001. 263-274.

Topp, G.C. and Davis, J.L., 1981. Detecting infiltration of water through soil cracks by time-domain reflectometry. Geoderma, 26: 13-23.

van Genuchten M. Th., 1980. A closed form equation for predicting the hydraulic conductivity of unsaturated soils. Soil Sci Soc Am J 44:892–898

Warren, J.E., and Root P.J., 1963. The behavior of naturally fractured reservoirs, Soc. Pet. Eng. J., pp. 245-255, Trans., AIME, 228.

Wells Tony, Fityus Stephen, and Smith David W., 2007. Use of in situ air flow measurements to study permeability in cracked clay soils. Journal of geotechnical and geoenvironmental engineering, ASCE / December 2007. Pp 1577-1586.

Wells, T., Fityus, S., Smith, D. W., and Moe, H. 2006. The indirect estimation of hydraulic conductivity of soils using measurements of gas permeability. I: Laboratory testing with dry granular soils. Australian J. Soil Research, 44, 719–725.

Wu, Y. S, Haukwa C., and Bodvarsson G. S., 1999. A site- scale model for fluid and heat flow in the unsaturated zone of yucca mountain, nevada. Journal of Contaminant Hydrology. 38 (1-3), 185-217.

Wu, Y. S., Pruess, K., 2005. A physically based numerical approach for modeling fracture-matrix interaction in fractured reservoirs. In: Proceedings world geothermal congress 2005, Antalya, Turkey, 24-29 April, pp 1-8.

Wu, Y.S., 2000. On the effective continuum method for modeling multiphase flow, multi-component transport and heat transfer in fractured rock, “Dynamics of Fluids in Fractured Rocks, Concepts and Recent Advances”, Edited by B. Faybishenko, P. A. Witherspoon and S. M. Benson, AGU Geophysical Monograph 122, American Geophysical Union, Washington, DC, 299–312.

Xiong Donghong, Zhou Hongyi, Du Changjiang et al., 2006. A review on soil crack study. Soil, 38(3): 249–255. (In Chinese)

Yesiller N., Miller C.J., Inci G., Yaldo K. 2000. Desiccation and cracking behavior of three compacted landfill liner soils. Engineering Geology 57, 105–121.

Zapata C.E., 1999. Uncertainty in soil-water characteristic curve and impact on unsaturated shear strength predictions. Ph.D. Dissertation, Arizona State University, Tempe.

Zapata, C.E., Houston, S.L., Houston, W.N., and Dye, H. (2006). Expansion Index and Its Relationship with Other Index Properties. Unsaturated Soils. Geotechnical Special Publication No. 147. Also in Miller, et al. (eds.), Proceedings of the Fourth International Conference on Unsaturated Soils, April 2-6, Carefree, AZ. pp. 2133-2137.

Zein El Abedine A., and Robinson, G.H., 1971. A study on cracking in some Vertisols of the Sudan. Geoderma, 5: 229-241.

Zhan Tony L. T., Charles W. W. Ng, and Fredlund D. G., 2006. Instrumentation of an unsaturated expansive soil slope, Geotechnical Testing Journal, Vol. 30, No. 2.

Zhan Tony L. T., Charles W. W. Ng, and Fredlund D. G., 2007. Field study of rainfall infiltration into a grassed unsaturated expansive soil slope. Can. Geotech. J. 44: 392–408.

Zhang L, Fredlund D.G., 2004. Characteristics of water characteristic curves for unsaturated fractured rocks. In: The second Asian conference on unsaturated soils, Unsat-Asia, Osaka, Japan, pp 425–428

Zhang, L.M., Li, J.H., Fredlund, D.G., 2011. Unsaturated conductivity function for unsaturated cracked soil. Unsaturated soils: 993-999.

Zhang, Z., 2004. Consolidation theories for saturated-unsaturated soils and numerical simulation of residential buildings on expansive soils. PhD thesis Thesis, Texas A&M University, College Station, TX, USA.

APPENDIX A

SAMPLE CALCULATION OF SATURATED HYDRAULIC CONDUCTIVITY

The test procedure was kept the same as previous tests. The only change was that the new membrane was used for the second and third test (3rd and 4th cracked). Also, due to the leakage, all the Volume Change Device (VCD) valves' were replaced to prevent the leakage. Like before, after the sample was saturated over 90%, I decreased the bottom back pressure to 600 kPa, while the other two pressures were kept constant (Top back pressure: 630 kPa, Cell Pressure: 650 kPa). Following, there is an example of my calculations for k:

$$k = \frac{QL}{hAt}$$

Where, k = hydraulic conductivity, m/s

Q = total discharge volume, m3, in time t, s

A = cross sectional area of soil sample, m2

L = depth of the soil sample, m2

h = head gradient between the top and the bottom of the soil sample, m

As my first reading, I observed the water level increased as much as 10 mm in a 0.704 cm^2 tube after 30 seconds. With these numbers, we will calculate the k as follows:

$$k = \frac{(0.01m \times 0.704cm^2) \times (0.02806m)}{(3m) \times (39.48cm^2) \times (0.5 \times 60s)} = 5.55956 \times 10^{-8} m/s = 5.55956 \times 10^{-6} cm/s$$

Table A-1 shows the results for the first cracked sample, and Tables A-2 to A-4 are summarizing the new results.

Table A-1: Hydraulic conductivity measurements for the first cracked sample

	Q(m3)	L(m)	Δh(m)	A(m2)	t(s)	k (m/s)
1	2.11E-06	0.0285	3	0.003948	45	1.12935E-07
2	6.34E-07	0.0285	3	0.003948	15	1.01641E-07
3	1.2E-06	0.0285	3	0.003948	45	6.39964E-08
4	1.27E-06	0.0285	3	0.003948	120	2.54103E-08
5	1.06E-06	0.0285	3	0.003948	150	1.69402E-08
6	1.06E-06	0.0285	3	0.003948	180	1.41169E-08
7	2.11E-06	0.0285	3	0.003948	240	2.11753E-08
8	2.11E-06	0.0285	3	0.003948	260	1.95464E-08
9	1.34E-06	0.0285	3	0.003948	300	1.07288E-08
10	9.5E-07	0.0285	3	0.003948	330	6.93009E-09
11	9.5E-07	0.0285	3	0.003948	360	6.35258E-09
12	9.86E-07	0.0285	3	0.003948	390	6.08111E-09
13	9.5E-07	0.0285	3	0.003948	420	5.44507E-09
14	2.78E-06	0.0285	3	0.003948	510	1.31204E-08
15	2.25E-06	0.0285	3	0.003948	60	9.01313E-08
16	2.91E-06	0.0285	3	0.003948	90	7.77603E-08
17	4.89E-06	0.0285	3	0.003948	150	7.84672E-08
18	4.49E-06	0.0285	3	0.003948	150	7.2105E-08
19	3.7E-06	0.0285	3	0.003948	120	7.42258E-08
20	1.06E-05	0.0285	3	0.003948	390	6.52534E-08
21	1.07E-05	0.0285	3	0.003948	420	6.13499E-08
					Average k =	4.49 E-08 m/s

Table A-2: Hydraulic conductivity measurements for the second cracked sample

	Q(m3)	L(m)	Δh(m)	A(m2)	t(s)	k (m/s)
1	7.04E-07	0.02806	3	0.003948	30	5.55956E-08
2	6.336E-07	0.02806	3	0.003948	30	5.00361E-08
3	1.408E-06	0.02806	3	0.003948	60	5.55956E-08
4	1.1264E-06	0.02806	3	0.003948	60	4.44765E-08
5	5.984E-07	0.02806	3	0.003948	30	4.72563E-08
6	5.28E-07	0.02806	3	0.003948	30	4.16967E-08
7	7.2512E-07	0.02806	3	0.003948	45	3.81757E-08
8	2.6048E-07	0.02806	3	0.003948	15	4.11408E-08
9	9.504E-07	0.02806	3	0.003948	60	3.75271E-08
10	3.168E-07	0.02806	3	0.003948	20	3.75271E-08
11	5.984E-07	0.02806	3	0.003948	40	3.54422E-08
12	1.7952E-06	0.02806	3	0.003948	120	3.54422E-08
13	8.448E-07	0.02806	3	0.003948	60	3.33574E-08
14	4.224E-07	0.02806	3	0.003948	30	3.33574E-08
15	6.336E-07	0.02806	3	0.003948	45	3.33574E-08
16	6.336E-07	0.02806	3	0.003948	45	3.33574E-08
17	1.584E-06	0.02806	3	0.003948	120	3.12725E-08
18	8.096E-07	0.02806	3	0.003948	60	3.19675E-08
19	4.224E-07	0.02806	3	0.003948	30	3.33574E-08
				Average K =		3.94705E-08 m/s

Table A-3: Hydraulic conductivity measurements for the third cracked sample

	Q(m3)	L(m)	Δh(m)	A(m2)	t(s)	k (m/s)
1	5.632E-07	0.0274	3	0.003959	60	2.16549E-08
2	0.000000352	0.0274	3	0.003959	30	2.70686E-08
3	5.632E-07	0.0274	3	0.003959	60	2.16549E-08
4	2.816E-07	0.0274	3	0.003959	30	2.16549E-08
5	4.224E-07	0.0274	3	0.003959	45	2.16549E-08
6	4.928E-07	0.0274	3	0.003959	45	2.5264E-08
7	4.576E-07	0.0274	3	0.003959	60	1.75946E-08
8	1.0208E-06	0.0274	3	0.003959	120	1.96247E-08
9	2.816E-07	0.0274	3	0.003959	30	2.16549E-08
10	0.000000352	0.0274	3	0.003959	45	1.80457E-08
11	3.872E-07	0.0274	3	0.003959	45	1.98503E-08
12	1.4432E-06	0.0274	3	0.003959	180	1.84969E-08
13	4.928E-07	0.0274	3	0.003959	60	1.8948E-08
14	2.112E-07	0.0274	3	0.003959	30	1.62411E-08
15	9.504E-07	0.0274	3	0.003959	120	1.82713E-08
16	0.000000176	0.0274	3	0.003959	30	1.35343E-08
17	2.1824E-06	0.0274	3	0.003959	300	1.67825E-08
18	3.966E-07	0.0274	3	0.003959	60	1.52491E-08
19	2.30028E-06	0.0274	3	0.003959	300	1.7689E-08
20	3.91312E-06	0.0274	3	0.003959	540	1.67176E-08
					Average k =	1.9382E-08 m/s

Table A-4: Hydraulic conductivity measurements for the third cracked sample

	Q(m3)	L(m)	Δh(m)	A(m2)	t(s)	k (m/s)
1	2.816E-07	0.02825	3	0.003959	30	2.23266E-08
2	4.576E-07	0.02825	3	0.003959	120	9.07019E-09
3	5.28E-07	0.02825	3	0.003959	180	6.97707E-09
4	4.9984E-06	0.02825	3	0.003959	3270	3.63576E-09
5	7.04E-08	0.02825	3	0.003959	30	5.58166E-09
6	7.04E-08	0.02825	3	0.003959	45	3.7211E-09
7	7.04E-08	0.02825	3	0.003959	45	3.7211E-09
8	7.04E-08	0.02825	3	0.003959	60	2.79083E-09
9	2.816E-07	0.02825	3	0.003959	180	3.7211E-09
10	7.04E-08	0.02825	3	0.003959	60	2.79083E-09
11	1.408E-07	0.02825	3	0.003959	90	3.7211E-09
12	3.52E-08	0.02825	3	0.003959	30	2.79083E-09
13	2.464E-07	0.02825	3	0.003959	240	2.44197E-09
					Average k =	5.6377E-09 m/s

APPENDIX B

DIFFERENT METHODS OF MEASURING THE UNSATURATED HYDRAULIC CONDUCTIVITY OF SOILS

Steady state methods

Constant head method

This method is one of the oldest techniques for measuring the hydraulic conductivity of an unsaturated soil. This method is based on applying a constant hydraulic head across the unsaturated soil specimen, while the soil suction is also kept constant often times by using axis translation technique. The steady state flow through the specimen is then measured and the unsaturated hydraulic conductivity can be measured using Darcy's law.

Constant flow method

This method is very similar to constant head method, except in this method the flow rate will be controlled rather than being measured. One of the advantages of this method comparing with the constant head method is that very low flow rates, which are often difficult to measure with constant head method, can be applied to the specimen using the advanced motorized flow pumps. In this method, the sample is seated inside a conventional confining cell and isolated from the cell fluid using a latex membrane. From air pore pressure to the water pore pressure and the confining pressure, everything can be controlled. First the sample is saturated using backpressure technique. Then, a flow pump is used to withdraw a known amount of water from the specimen. This way, by knowing both pore air pressure and pore water pressure of the specimen, the suction of the soil is known. Flow is then reintroduced through the specimen and the steady-state head loss is measured.

Centrifuge method

The steady-state centrifugation method (SSCM) is a laboratory test in which a spinning centrifuge is utilized to rapidly establish steady-state fluid flow through an unsaturated specimen. Hydraulic conductivity is calculated by measuring steady-state flow under the elevated gravitational gradient. This method is appropriate for measuring conductivity of materials with relatively low permeability or low degree of saturation. Employing centrifuge technique reduces the amount of time required for steady state to be reached. Detailed descriptions of various experimental setups and an analysis of the general governing principles are provided by Nimmo et al. (1987, 1992) and Nimmo and Akstin (1988).

Transient (unsteady state) methods

Horizontal infiltration method

This method was originally developed by Bruce and Klute (1952). Later, it has been modified by different other researchers. This method involves measuring and analyzing the water content changes along a horizontal soil column while one side of the column is allowed to saturate. This technique is primarily applicable for relatively coarse-grained soils due to the time constrains associated with applying this method for fine-grained soil.

Outflow method

An axis-translation type equipment such as Fredlund cell or Tempe cell are required to perform an outflow test. The hydraulic diffusivity of the sample can be determined by measuring the water flow rate of a sample subjected to suction increments.

Transient (unsteady state) methods

Horizontal infiltration method

This method was originally developed by Bruce and Klute (1952). Later, it has been modified by different other researchers. This method involves measuring and analyzing the water content changes along a horizontal soil column while one side of the column is allowed to saturate. This technique is primarily applicable for relatively coarse-grained soils due to the time constrains associated with applying this method for fine-grained soil.

APPENDIX C

THEORETICAL RELATIONSHIP BETWEEN WIDTH OF CRACK AND CAPILLARY RISE IN A CRACK

Should one idealize a soil crack as a capillary, there would always be a relationship between the width and depth of cracks which are capable of holding water inside of them. If the crack is too deep or too wide, the water cannot develop enough tension to overcome the self-weight of the water inside it, and as a result, the water will flow out of the crack, assuming the water pressure at the base of the crack is essentially zero.

First, the relationship will be derived between height of capillary rise, h_c, which will be assumed to be the crack depth, and the crack width, w_c. A continuous rectangular section throughout the crack depth is assumed, which is equivalent to saying the crack has a constant width from top to bottom, as shown in Figure C-1. This assumption is of interest because cracks of this shape were generated in the laboratory.

Assuming the meniscus is fully developed and tangent to the side wall of the crack, the surface tension forces can be assumed to be vertical at the crack walls (Fig. C-2) and equal to:

$$\text{Upward forces} = T_s \times 2 \text{ cm} \quad \text{(C-1)}$$

Where, T_s = surface tension force per unit of length (73×10^{-5} N/cm); and 2 cm is the total length over which surface tension acts, for a 1 cm segment.

The downward forces are equal to the weight of water and therefore, equal to the volume times the unit weight of water :

$$\text{Downward forces} = h_c \times w_c \times 1 \text{ cm} \times \gamma_w \quad \text{(C-2)}$$

Where, h_c = crack height; w_c = crack width; 1 cm = 1 unit length of crack; and γ_w = specific weight of water (9.807×10^{-3} N/cm^3).

For equilibrium in the vertical direction, upward forces are equal to the downward forces:

$$T_s \times 2\text{ cm} = h_c \times w_c \times 1\text{ cm} \times 9.807 \times 10^{-3} \quad \text{(C-3)}$$

Solving for h_c (with h_c and w_c in cm):

$$h_c = \frac{0.149}{w_c} \approx \frac{0.15}{w_c} \quad \text{(C-4)}$$

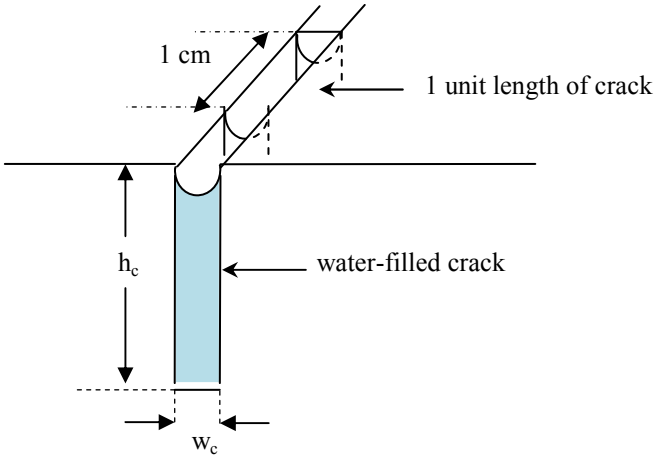

Figure C-1 Schematic of constant width crack

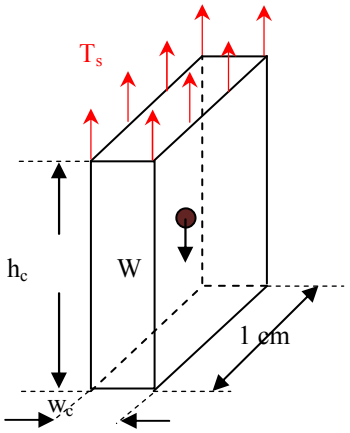

Figure C-2 Free body diagram (FBD) of unit length water element in crack

It should be noted that Equation C-1 is based on several simplifying assumptions which are at variance with actual field conditions, but it is

nevertheless potentially useful as a rough guide in estimating the AEV of the cracks.

Equation C-4 was used to generate the results shown in Table C-1, wherein the depth of crack ranges from 7 mm to 13 mm. This range in crack depth was chosen because, for this type of soil, naturally formed cracks, formed in laboratory condition, were about 10 mm deep, or slightly more. For each crack depth shown, it is assumed that the crack is full of water, the meniscus is fully developed and the surface tension at the top of the crack is just sufficient to balance the weight of water in the crack.

Table C-1 Depth of crack and corresponding suction for which cracks of various widths will just start to dewater due to gravity alone

Depth of crack, h_c		Corresponding suction = $h_c \times \gamma_w$	Width of crack that dewaters due to gravity alone	
cm	mm	kPa	cm	mm
0.7	7.0	0.069	0.21	2.1
1.0	10.0	0.098	0.15	1.5
1.3	13.0	0.127	0.11	1.1

Because the suction is given by u_a-u_w and the pre-ceding derivation was made for the case of u_a=0, the only component of suction is the water tension, u_w. Thus, the "corresponding suction" column in Table C-1 can be thought of an equivalent AEV. At the suction shown, the dewatering is just commencing and air is starting to enter the crack.

At crack sizes smaller than those shown in Table C-1, the capillary model would predict that dewatering due to gravity alone would not occur. However, if u_a were elevated to a value above zero, then u_a would generate an additional

downward force which, together with the weight, could be made to overcome the surface tension forces. The derivation can be repeated along the same lines as before, but a new force due to u_a must be added to the free body diagram (Fig C-3).

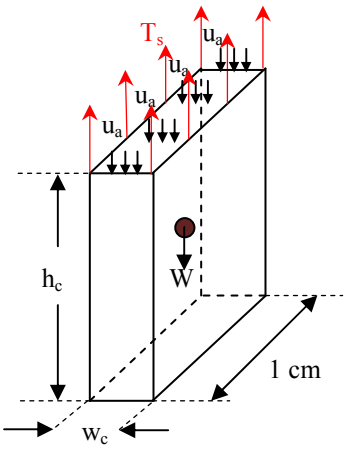

Figure C-3 FBD including downward forces due to u_a

Again, for a unit length of crack, Equation C-1 re-mains unchanged, but Equation C-2 can be rewritten as follows:

$$\text{Downward forces} = h_c \times w_c \times 1\text{cm} \times \gamma_w + u_a\,(w_c \times 1\text{cm}) \qquad \text{(C-5)}$$

For equilibrium in the vertical direction, and solving for u_a (with h_c and w_c in cm) we get:

$$u_a = \frac{1.46\times10^{-3}}{w_c} - 9.807\times10^{-3}\times h_c \qquad \text{(C-6)}$$

Note that h_c controls u_w, which is given by $u_w = h_c \times \gamma_w$. Also, h_c controls the volume and weight of water in the crack. Due to these compensating effects, $u_a - u_w$ is insensitive to h_c, as shown in Tables C-2a, C-2b, and C-2c. Figure C-4 shows that u_a is also somewhat insensitive to h_c.

Table C-2a Relationship between h_c, w_c, and u_a for commencement of crack dewatering based on Equation C-6, for h_c = 0.7 cm

w_c		u_a		$u_w=h_c\times\gamma_w$	Suction(u_a-u_w)
cm	mm	N/cm^2	kPa	kPa	kPa
0.2	2.0	0.00044	0.0044	-0.0686	0.073
0.15	1.5	0.0029	0.029	-0.0686	0.098
0.1	1.0	0.0077	0.077	-0.0686	0.146
0.075	0.75	0.0126	0.126	-0.0686	0.195
0.05	0.50	0.022	0.22	-0.0686	0.289
0.01	0.10	0.139	1.39	-0.0686	1.459

Table C-2b Relationship between h_c, w_c, and u_a for commencement of crack dewatering based on Equation C-6, for h_c = 1.0 cm

w_c		u_a		$u_w=h_c\times\gamma_w$	Suction(u_a-u_w)
cm	mm	N/cm^2	kPa	kPa	kPa
0.15	1.5	0.0	0.0	-0.098	0.098
0.1	1.0	0.0048	0.048	-0.098	0.146
0.075	0.75	0.00967	0.0967	-0.098	0.195
0.05	0.50	0.0194	0.194	-0.098	0.292
0.01	0.10	0.1362	1.362	-0.098	1.46

Table C-2c Relationship between h_c, w_c, and u_a for commencement of crack dewatering based on Equation C-6, for h_c = 1.3 cm

w_c		u_a		$u_w=h_c\times\gamma_w$	Suction(u_a-u_w)
cm	mm	N/cm^2	kPa	kPa	kPa
0.1	1.0	0.0018	0.018	-0.128	0.146
0.075	0.75	0.0067	0.067	-0.128	0.195
0.05	0.50	0.0164	0.164	-0.128	0.292
0.01	0.10	0.133	1.33	-0.128	1.46

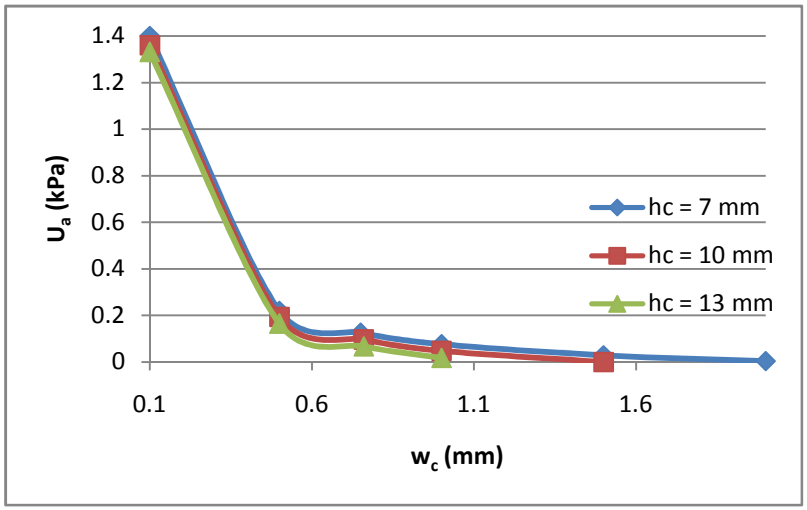

Figure C-4 Relationship between h_c, w_c, and u_a for commencement of crack dewatering

Now that different derivations were obtained for constant width crack, the same procedure can be used to derive new relationships for any shape of crack. For instance, in case of a V-shape crack, the analysis remains the same, except the volume of the unit length of water becomes one half of that obtained in the case shown above.